Environmental contamination associated with artisanal gold mining in Guyana

A thesis submitted to the Committee on Graduate Studies in partial fulfilment of the requirements for the degree of Doctor of Philosophy in the Faculty of Arts and Science

Trent University

Peterborough, Ontario, Canada

Environmental and Life Sciences Ph.D. Graduate Program

May 2025

Abstract

Environmental contamination associated with artisanal gold mining in Guyana

Chetwynd Osborne

A meta-analysis revealed that while there is often a greater degree of contamination of soils and sediments with metals, contamination by mercury (Hg) is a large concern owing to its toxicity at low concentrations. The case study in Guyana characterized Hg and concentrations of other metals (As, Cd, Co, Cu, Mn, Ni, Pb, and Zn) in soil and sediment within gold mined areas. Metal concentrations were low in soil and sediment of sampled gold mines, while the concentrations of Hg were much higher in soil and sediment and contamination was not localized to the mine site. Moss bags and Hg passive air samplers (*Mer*PAS) were deployed to measure atmospheric Hg around a gold mine in Mahdia, Guyana over a 90-day period as well as a 2-day period that encompassed a periodic burn (typically 2-hr). Mercury in moss and *Mer*PAS were positively correlated over both deployment periods, but Hg concentrations measured during the 2-day event were several-fold higher in both moss and *Mer*PAS compared with the 90-day exposure demonstrating that most of the Hg sorbed to both moss and passive samplers is lost during periods of inactivity. Using the 2-day deployment as a conservative estimate of atmospheric Hg exposure, Hg air concentrations around the burning station exceeded 100,000 ng m^{-3} averaged over a 48-hr period, and moss Hg concentrations were greater than 250,000 ng g^{-1} around the burning station, although Hg concentrations in both media decreased rapidly with distance. Mercury concentration in soil and sediment was strongly related to organic matter content, which tended to be higher away from the mine site. These controls of organic matter (carbon; C) cycling on Hg distribution and movement are clear at sites

exposed to high atmospheric Hg and exist at the global scale, although Hg:C ratios in environmental media are greatly elevated at the gold mine site compared with the global average. Locally sourced biochar did not sufficiently improve physical properties (porosity) in overburden soil, which showed the worse plant response, possibly due to the high clay content that contributes to the “baked” condition of these soils and restrict root growth.

Keywords**:** Gold mining, Environmental contamination, Mercury, Metals, Organic matter, Biochar

Authorship statement

I conceptualized the research, developed the research methodology, research questions and its scientific grounding in consultation with my supervisor and supervisory committee. I led the collection of all field data and processed and analyzed all samples. I delineated the research questions, described how it fits in with the current scientific literature and described its potential environmental and policy impact. I revised the text, after comments from my supervisors and committee. I conducted the literature search and wrote the general introduction and remaining chapters of this thesis. During the whole process I asked for and implemented input and feedback from my supervisory team.

Acknowledgements

I would like to thank my thesis supervisor Dr. Shaun Watmough and my committee members Dr. Catherine Eimers and Dr. Holger Hintelmann for their tremendous support, guidance, and insight. Throughout this experience, you all helped me demystify ideas, overcome challenges, and encouraged me to stay motivated.

I express gratitude to Soyini Mc Pherson, the Guyana Geology and Mines Commission, Hopkinson gold mining operation and staff, Obermuller gold mining operation and staff, Shelby Conquer, Ed Smith, Patrick Levasseur, Kaylen Foley, Kevin Adkinson, Victor Bewsh, Dr. Huy Dang, and Adelheid Willsie for their logistical, field, and laboratory support that went into this thesis. Many hands contributed to this project and that is largely thanks to you all. I acknowledge the wonderful people I have met along the way at Trent University and thank you to the environmental geoscience research group. Grateful for the Sustainable Guyana Program, a partnership between Trent University and the University of Guyana funded by CGX Energy Inc. and Frontera Energy Corporation.

Gratitude is expressed to my wonderful family and friends who have supported me throughout my entire academic journey. Thank you to my fiancée and mother for their unwavering support, inspiration, and love.

Table of Contents

List of figures

List of tables

List of abbreviations

Abbreviation	*Meaning*
AGM	Artisanal gold mining
As	Arsenic
Cd	Cadmium
C	Carbon
Co	Cobalt
Cu	Copper
CCME	Canadian Council of Ministers of the Environment
CoC	Contaminants of concern
DOC	Dissolved organic carbon
EPA	Environmental Protection Agency
GEM	Gaseous elemental mercury
GGMC	Guyana Geology and Mines Commission
Hg	Mercury
Mn	Manganese
Ni	Nickle
OM	Organic matter
Pb	Lead
PCA	Principal Component Analysis
SDG	Sustainable Development Goal
UNCCD	United Nations Convention to Combat Desertification
WHO	World Health Organization

Zn	Zinc

1.0 General introduction

Artisanal gold mining (small and medium scale) has historically been an important livelihood option for many rural communities in the Global South, but mining practices can contaminate the environment with various contaminants of concern (CoC) (Delgado Jiménez et al., 2022). Guyana has witnessed an upsurge in economic activities, which has led to the expansion in gold mining over the last few years, and this is anticipated to continue given the heavy dependence of Guyana's economy on gold (GLSC, 2017). Previous studies that assessed environmental contamination associated with artisanal gold mining in Guyana, only focused on soil and sediment contamination (Howard et al., 2011; Howard, 2006; Kalamandeen et al., 2020) and atmospheric contamination near gold shops (Brown et al., 2020), rather than a holistic assessment across various environmental media. This study presents the first comprehensive assessment in Guyana to better understand environmental contamination associated with artisanal gold mining. The findings from this research are expected to inform policy frameworks, monitoring plans, and provide baseline information for national guidelines within the gold mining sector of Guyana.

1.1 Environmental contamination associated with artisanal gold mining in South America: A meta-analysis

Globally, artisanal gold mining serves as the principal source of income for 30 million miners in developing countries. With approximately 12% of gold production globally being derived from illegal mining practices, which benefits miners economically. Despite the provision of livelihood options, the environment suffers as a result of land degradation, sedimentation of water source, degradation of soil, deforestation, and chemical

contamination with mercury (Hg) and other metals (Gafur et al., 2018; Martín et al., 2020; Ogola et al., 2002; UNIDO & Green Industry, 2011). Gold mining has been identified as a strong driver of land degradation (Tankari Dan-Badjo et al., 2019), given the extractive nature, which entails the removal of large expanses of forest cover and top soil to retrieve the gold bearing ore. Such practices disturb the landscape in a significant way and have ripple effects on terrestrial and aquatic ecosystems over the short, medium and long term (Batsaikhan et al., 2016). The release of CoC (As, Cd, Co, Cu, Hg, Mn, Ni, Pb, Zn) that are typically associated with artisanal gold mining negatively affects ecosystem functioning when present above threshold limits in soil and sediment (Fashola et al., 2016).

Synthesis studies related to the impact of gold mining on the environment have been done in other regions such as North America (Asif & Chen, 2016; Cheney et al., 2024), Africa (Edwards et al., 2014; Laker, 2023; Mencho, 2022; Mimba et al., 2023; Tibane & Mamba, 2022) and Asia (Soe et al., 2022; Zhao & Xing, 2024), but not on a continental scale in South America. This thesis undertook a meta-analysis to provide a comprehensive assessment of available studies (n=34) on Hg and metals contamination in environmental media (soil and sediment) near artisanal gold mines across South America (11 countries). This meta-analysis revealed that gold mining has contributed to the contamination of nearby soil and sediment, creating potential ecological risks in the vicinity of the mining area. Although the degree of contamination of soil and sediments by several metals was greater than Hg, contamination by Hg often exceeded guidelines, especially in sediments owing to its toxicity at low concentrations. Rapid measures are needed to remediate contaminated soils, restore the landscape of gold mining areas, and carry out environmentally protected gold mining of undisturbed deposits to transition from

the exploitation of natural resources to more sustainable usage as enshrined within the adoption of the 17 sustainable development goals (SDGs) (Keesstra et al., 2018). In the quest to achieve the SDGs related to climate, food, water, and health, pressures on land are expected to increase. Therefore, the avoidance of further land degradation poses a challenge, which warrants a paradigm shift to achieve a balance between losses and gains (Keesstra et al., 2018). Combatting land degradation has been an international duty since 1992 under the auspices of the United Nations Convention to Combat Desertification (UNCCD) and this has been further realized through SDG Target 15.3, which seeks to restore degraded lands by 2030 (UNCCD, 2018; Wijitkosum, 2021). In the quest to achieve this goal, the need exists for an analysis of current problems, future environmental trends, and vulnerability.

1.2 Characterizing Hg and other metal concentrations in soil and sediment within gold mined areas of Guyana

As evidence by the meta-analysis, artisanal gold mining significantly alters the mineral and chemical composition of soil due to the accumulation of large quantities of sulfide-rich tailing materials (Adekiya et al., 2024). Enriched metals (As, Cd, Co, Cu, Mn, Ni, Pb, and Zn) in the gold-bearing ore could be a source of environmental contamination after the gold is separated and the remaining materials are discharged as tailings (Barcelos et al., 2020). The addition of Hg to amalgamate the gold further compounds the issue. A focus on the impact of gold mining at the small and medium scale on environmental media, has gained momentum over the last few decades, given the potential threats posed to the terrestrial and aquatic environment (soil, water resources, sediment, flora, fauna)

(Rakotondrabe et al., 2018). The impacts of gold mining are not limited to soils and vegetation on mine sites. Sediments are also affected and show longer-term loadings. Discharge of contaminants threatens the ecological goods and services offered by sediments – provision of nutrients for benthic life and habitat for various species (Ali et al., 2018; Islam et al., 2015; Jiang et al., 2013; Kumar et al., 2021; Macdonald et al., 2015; Pejman et al., 2015). These contaminants potentially accumulate in sediments, thereby worsening the water quality and pose threats to the wider aquatic environment (Caballero-Gallardo et al., 2020; Kumar et al., 2021; Pejman et al., 2015). Elevated Hg in sediment poses high environmental risk since it can be converted to methylmercury in sediments through methylation of inorganic Hg by microorganisms under anaerobic conditions. Methylmercury is the more toxic form because it biomagnifies along the food chain, resulting in greater environmental and human health concerns (Helmrich et al., 2021; Wang et al., 2024).

The meta-analysis across South America identified gold mining as a major cause of contamination of nearby soil and sediment. The degree of contamination associated with artisanal gold mines in Guyana have not been characterized. This thesis characterized Hg and metals (As, Cd, Co, Cu, Mn, Ni, Pb, and Zn) contamination in soils and sediments collected from two gold mines in Guyana (Frenchman and Mahdia, Potaro Mining District) to better understand the degree of contamination locally. The localized study found that gold mining leads to high levels of Hg deposition to terrestrial and aquatic ecosystems. However, other metals were not a concern given the low concentrations (below threshold limits) measured in the soil and sediment of sampled gold mines compared with other

studies across South America. The elevated levels of Hg (exceed guidelines) suggest much higher contamination in soil and sediment that is not localized to the mine site.

1.3 Atmospheric Hg monitoring using passive samplers and moss bags within gold mined areas of Guyana

Mercury (primary oxidation states Hg^0 and Hg^{2+}) is emitted into the environment from natural (*e.g.*, soil, volcano, ocean) and from anthropogenic sources (*e.g.*, gold mining) (Corredor et al., 2021; Antía Gómez-Armesto et al., 2020; Grigal, 2002; Niane et al., 2019). The relatively long atmospheric lifespan (0.5 to 2 years) of gaseous elemental Hg released from the burning of gold amalgam, facilitates spatial transport across the mining operation and even to sites farther away from the gold mine before redisposition onto the surface of soil and vegetation (Buck et al., 2019; De Simone et al., 2014; Slemr et al., 2011). These characteristics of Hg coupled with its persistent and non-biodegradable nature, strong enrichment, and toxicity negatively affects the environment and human health (Buck et al., 2019). Surges in gold prices and associated socio-economic factors could lead to an increase in small and medium scale gold mining, which drives the emission of large quantities of Hg (ca. 675 – 1000 tonnes per year) into the atmosphere (Gerson et al., 2022).

However, little is known about the levels of atmospheric Hg emissions and accumulation across small and medium scale gold mines in Guyana. Therefore, monitoring of atmospheric Hg within gold mining sites in Guyana is key to understanding local cycling and fate of Hg. Passive air sampling is a low-cost no-power approach to monitoring atmospheric Hg (Jeon et al., 2020). Mercury passive air samplers (*Mer*PAS® from Tekran) are useful for monitoring of atmospheric Hg within gold mining areas, given the ability to

provide time-averaged concentrations of Hg over the timescale of days to months (McLagan et al., 2016; Naccarato et al., 2021). These passive air samplers could also be supplemented with inexpensive active moss biomonitoring, which is a technique based on the direct uptake of atmospheric Hg or the oxidation of Hg^0 to Hg^{2+} into the tissue of moss (Bargagli, 2016; Lodenius, 1998). Continuous monitoring of atmospheric Hg in remote gold mines of Guyana can be expensive. Therefore, active moss biomonitoring and passive air sampling offers an efficient, cost-effective, and simple approach to evaluating patterns in atmospheric Hg deposition within gold mines. Based on the elevated levels of Hg in soil and sediment of the sampled gold mines, atmospheric Hg assessment was done in this study around a gold mining area using moss and passive samplers over a longer term (90 days) and a short-term (2 days) period during which a burn occurred. Mercury in moss and *Mer*PAS were positively correlated over both deployment periods, but Hg concentrations measured during the 2-day event were several-fold higher in both moss and *Mer*PAS compared with the 90-day exposure demonstrating that most of the Hg sorbed to both moss and passive samplers is lost during periods of inactivity. Using the 2-day deployment as a conservative estimate of atmospheric Hg exposure, Hg air concentrations around the burning station exceeded 100,000 ng m^{-3} averaged over a 48-hr period, and moss Hg concentrations were greater than 250,000 ng g^{-1} around the burning station, although Hg concentrations in both media decreased rapidly with distance. Moss and passive samplers may be useful for measuring atmospheric Hg but should only be deployed for short periods to minimize Hg loss to the atmosphere. There was no relationship with Hg concentration in soil and sediment with either distance from the burning station or Hg measured in the

deployed moss bags. Instead, Hg concentration in soils and sediment were strongly related to organic matter (OM) content, which tended to be higher away from the mine site.

1.4 Contrasting Hg/C relationship in environmental media near artisanal gold mining sites in Guyana with those observed at the global scale

Elevated concentrations of Hg released into the atmosphere due to artisanal gold mining, leads to increased Hg exposure to adjacent forest canopies (Gerson et al., 2022). Terrestrial ecosystems act as large storage pools for atmospheric Hg deposition that accumulates in surface litter and soil (Grigal, 2003; Pokharel & Obrist, 2011). Leaf litter with direct soil contact may function as a temporary pool for soil Hg, which may be important for risk assessments since this can aid the dispersal of contaminants through leaf litter translocation. As litter decompose, OM enters soil, which is the largest terrestrial carbon (C) pool that accumulates via continuous plant C inputs. Carbon in soil can be transported from terrestrial ecosystems (soil, plant materials, and wetlands) to freshwater ecosystems through various flow paths (Franco-Cisterna et al., 2024). The quality and quantity of C is an important factor that controls sorption with inorganic Hg, which is likely to sink rapidly to the bottom where it is buried in sediment (Eckley et al., 2021). Given the affinity between Hg and C, these relationships could track the movement of Hg in environmental media, which may differ between gold mining sites and remote sites that are not influenced by gold mining.

Although Hg movement and C within the biosphere are connected, it is unclear how these patterns may differ in areas exposed to high levels of Hg compared with regions remote from pollution sources. This study presented the first demonstration of Hg/C

patterns in environmental media (foliage, leaf litter, soil, water, sediment) near artisanal gold mining sites in Guyana relative to those observed globally to provide a greater understanding of Hg movement within the biosphere. The results of this study showed strong positive relationships between soil C and Hg for regions close and distant from point source, with Hg/C ratios being much lower in sites farther away from emission source compared with those observed near artisanal gold mines. The processes and patterns of Hg/C ratios in environmental media were similar in Guyana and globally synthesized studies, with much higher values at contaminated sites compared with clean sites. It was evident that Hg/C ratios were lowest in foliage, with increases during decomposition due to continued accumulation from the atmosphere, while mineral soil Hg/C ratios decreased indicating greater losses of C relative to Hg or dilution by C inputs from below ground biomass. Surface water ratios reflected inputs from dominant flow paths (surface soils and wetlands), while sediment sample ratios were closer to mineral soils due to a greater contribution of erosional losses.

1.5 Evaluation of biochar on plant growth on waste spoils from artisanal gold mines in Guyana.

The operating life of gold mining sites in Guyana can vary from a few years to a few decades, with the main aim of achieving return on investment. Generally, these sites are actively mined for one to five years in the case of small and medium scale mines, and five to 20 years in the case of large-scale mines. The duration of active mine operation is dependent on factors such as location, gold demand and world price, production cost and rate, quantity and quality of gold (grade), and ground condition (Mining Information

Toolkit for Guyana, 2012). Artisanal miners tend to abandon sites following gold exploitation without implementing measures to reclaim degraded land post-mining (Nacishali Nteranya & Mukulia, 2023). Reclamation practices post-mining is important for biodiversity conservation and these practices may vary based on intensity of artisanal gold mining. Generally, large scale mines tend to have better reclamation given the available financial and human resources as well as expertise to reclaim land to high standards. However, the requirement for adequate reclamation pose immense challenges for small and medium scale mines given their limited capacity and finances (Toy & Griffith, 2001).

Understanding litter dynamics (decomposition) and the interaction between C and Hg provides insights into the reclamation of degraded soil since this determines the supply rate of C to soil and the reactivation of nutrient cycling. In Guyana, gold mine spoils are not adequately characterized prior to reclamation and in the absence of such critical scientific data, *Acacia mangium* (invasive species) is predominantly being used for reclamation of mined out sites due to its ability to tolerate infertile soils and extract soil contaminants (Garbisu & Alkorta, 2001; Majid et al., 2012). Waste spoils from gold mines exhibit biological, chemical, mechanical, and physical deficiencies due to low nutrient and OM content, instability and limited cohesion, and elevated levels of Hg and metals (Adekiya et al., 2024). Few studies in Guyana have evaluated how soil amendments may be used to improved soil quality and plant performance (Moonilall et al., 2020; Persaud et al., 2018; Whyte et al., 2024). Soil properties and reclamation could be enhanced through the application of biochar, which is a stable carbon-rich derivative from pyrolysis of plant material (Ahmad et al., 2014). *Chlorocardium rodiei* (greenheart) is a readily available wood species in Guyana (Kekem et al., 1996) that could be subjected to pyrolysis to

produce biochar. This type of biochar is locally sourced in Guyana and may enhance nutrient availability (calcium, nitrogen, phosphorus, potassium) and improve physical properties (porosity and water holding capacity) of soil to support plant growth (Festin et al., 2019). This study evaluated the effect of a locally sourced soil amendment (*Chlorocardium rodiei* biochar) on *Poa pratensis* (Kentucky bluegrass) growth on waste spoils from artisanal gold mines in Guyana to provide some insights into the enhancement of soil physicochemical properties to support reclamation. The growth chamber study (under laboratory conditions that approximate conditions in Guyana) showed that plant response was worse at overburden sites, but did not improve with the addition of biochar (10 t ha^{-1}), likely because soil physical properties (porosity) were not sufficiently improved, and the "baked" conditions of clay-rich soil led to more compaction and possible restriction of root growth.

1.6 Research objectives

The work presented in this thesis aimed to contribute to the understanding of Hg contamination relative to other metals as outputs of artisanal gold mines. The five chapters appended to the thesis address interconnected issues regarding Hg and metals contamination of the environment due to artisanal gold mining (Figure 1.1). The main objectives of the studies were to:

a. Assess environmental contamination associated with artisanal gold mining in South America through a meta-analysis.
b. Characterize Hg and other metal concentrations in soil and sediment within gold mined areas of Guyana

c. Monitor atmospheric Hg using passive samplers and moss bags within gold mined areas of Guyana
d. Contrast Hg/C relationship in environmental media near artisanal gold mining sites in Guyana with those observed at the global scale
e. Evaluate biochar effects on plant growth on waste spoils from artisanal gold mines in Guyana

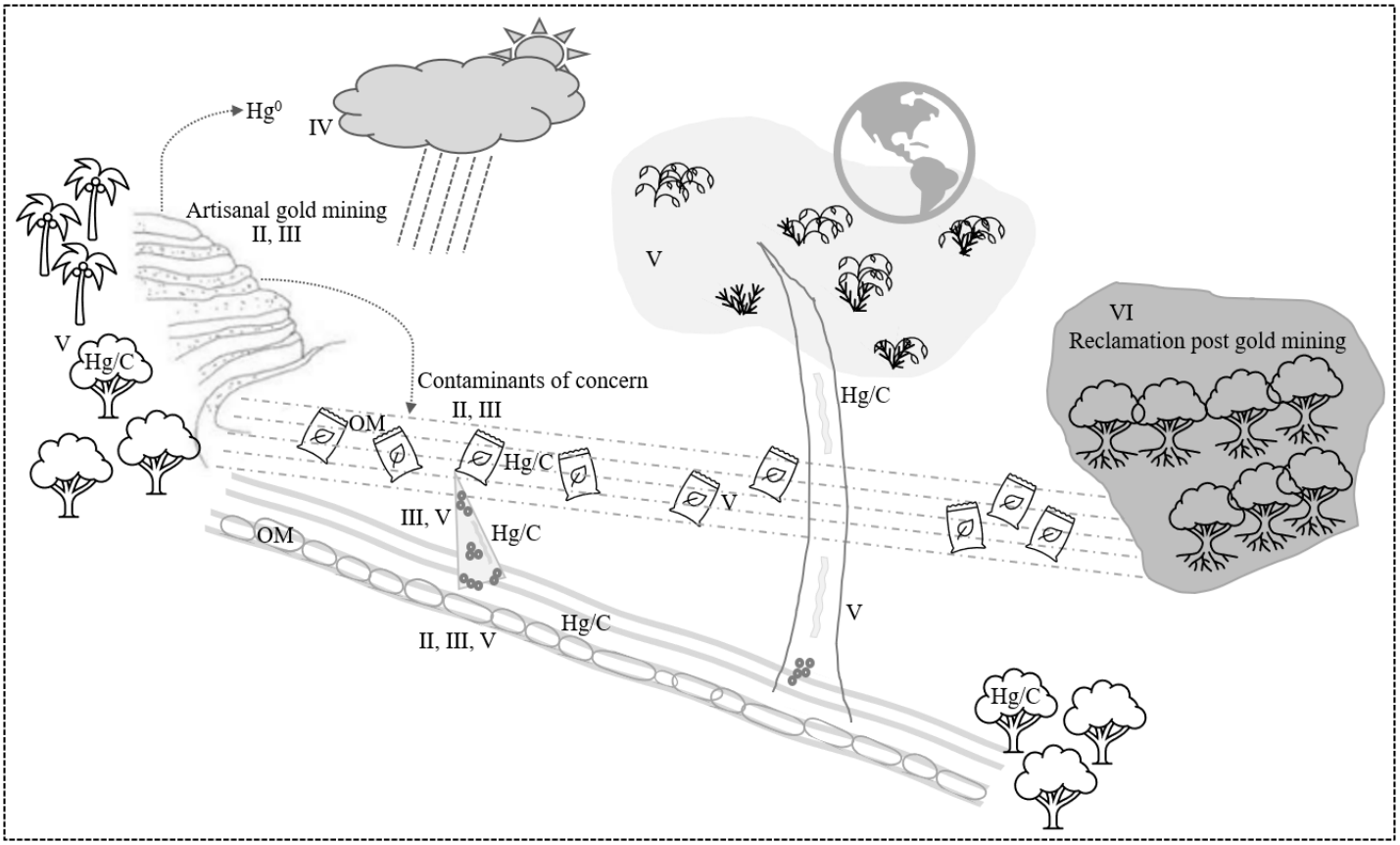

Figure 1. 1. Schematic representation of artisanal gold mining environmental contamination addressed in chapters appended to this thesis: (II) Environmental contamination associated with artisanal gold mining in South America: A meta-analysis; (III) Characterizing Hg and other metal concentrations in soil and sediment within gold mined areas of Guyana; (IV) Atmospheric Hg monitoring using passive samplers and moss bags within gold mined areas of Guyana; (V) Contrasting Hg/C relationship in environmental media near artisanal gold mining sites in Guyana with those observed at the global scale; and (VI) Evaluation of biochar on plant growth on waste spoils from artisanal gold mines in Guyana.

2.0 Environmental contamination associated with artisanal gold mining in South America: A meta-analysis

2.1 Introduction

Artisanal gold mining (small and medium scale) is a fundamental sector for most of the South American economies, but is also a large source of pollution (Chen et al., 2022; Hou et al., 2023). Small scale gold mining practices typically involve small groups of individuals from rural and immigrant communities who extract ore deposits in small areas (illegal in some cases) using rudimentary tools (diggers, pans, spades, sluice boxes, and shovels). Medium scale gold mining practices are more structured with more individuals for greater division of labor and semi-mechanized approaches (excavators, heavy engines, heavy duty trucks, and gold washing plants) are used to extract larger ore deposits (Timsina et al., 2022). Both small and medium scale gold mining result in hydrocarbon spills that contaminate soil and sediment, but the environmental pollution is usually worse for small scale mining due to its unregulated and informal nature (Rakotondrabe et al., 2018).

Given the value of gold and its superior application prospects, gold mining is widely practiced in many mining-rich countries across South America (Argentina, Bolivia, Brazil, Chile, Colombia, Ecuador, Guyana, French Guiana, Peru, Suriname, and Venezuela) (Qian et al., 2019). Gold mining is a popular occupation in these countries due to its higher earning potential compared with agriculture, forestry, and fishing (Wongsasuluk et al., 2021). According to recent data, gold production across South America reached a maximum of 441,295 metric tons in 2022 (Jaganmohan, 2024). However, the increasing demand for gold has highlighted the environmental risks of its

expansion (Barcelos et al., 2020). The methods used to extract gold could dictate the impact of gold mining on the environment (Veiga et al., 2022). Studies related to the impact of gold mining on the environment have been done in other regions such as North America (Asif & Chen, 2016; Cheney et al., 2024), Africa (Edwards et al., 2014; Laker, 2023; Mencho, 2022; Mimba et al., 2023; Tibane & Mamba, 2022) and Asia (Soe et al., 2022; Zhao & Xing, 2024), but not on a continental scale across South America. Therefore, an examination of documented gold mining practices in literature across South America could provide insights into the degree of environmental contamination within the region.

Artisanal gold mining leads to widespread pollution in soil and sediment, but concentrations of arsenic (As), cobalt (Co), copper (Cu), cadmium (Cd), lead (Pb), zinc (Zn), manganese (Mn), and nickel (Ni) are much higher close to point sources due to their existence in particulate rather than gaseous form (Poikolainen et al., 2004). Gold mining activities such as excavation and processing of the gold bearing ore are done by sluicing and panning (gravity concentration methods) which require the use of water that is later discharged into nearby streams and rivers or stored onsite in small ponds. The unregulated disposal of tailing materials and wastewater can result in varying levels of contamination of soil and sediment (Mimba et al., 2023). Although metals are present in small quantities naturally in bedrock and soil, gold mining activities substantially increase the concentration of these contaminants of concern (CoC's) in soil and sediment through direct disposal, leaks, spills, and other pathways (Kabir et al., 2012; Poikolainen et al., 2004; Pratte et al., 2013). The presence of As, Cd, Co, Cu, Mn, Ni, Pb, and Zn at levels above recommended quality guidelines for soil and sediment are a concern due to their ability to accumulate in food chains and toxicity to most organisms (Poikolainen et al., 2004). These CoC's have

substantial and long lasting effects on the local environment and human health and are often viewed as representative toxic metals that are indicative of environmental pollution (Kabir et al., 2012). This sort of human health threat coupled with the non-degradable nature of these CoC's results in substantial and extended effects on the environment and organisms despite remediation efforts (Kabir et al., 2012; Tian et al., 2015).

The introduction of mercury (Hg) through the gold-amalgamation process to recover free gold from the primary ores further compounds environmental issues related to gold mining (Miserendino et al., 2018; Velásquez-López et al., 2010). Mercury is encountered on the surface of the Earth in chemical forms such as elemental Hg^0, divalent inorganic Hg^{2+}, and organometallic methylmercury (MeHg) (Niane et al., 2019). Although countries across South America have signed the *Minamata Convention on Mercury* (UNEP, 2013) to safeguard human health and the environment, some countries still utilize Hg in small and medium scale gold mining (Canuel et al., 2009). This method of gold extraction is applied extensively since it is cheaper than many of the alternative measures, is simple and quick, and can be applied independently by one person. In contrast to other metals, Hg tends to be emitted in a gaseous form (Hg^0) and as a result, Hg deposition tends to be less clearly associated with points sources since it can be transported over long distances – from the arctic to the tropics (Costa et al., 2012; Durnford et al., 2010; Lacerda et al., 2020; Pacyna et al., 2010). During the Hg-gold amalgamation process, large quantities of elemental Hg could also be lost directly to soil and sediment based on total mass (Guédron et al., 2018). Once deposited, Hg can be found in soil as Hg^0 droplets or as Hg^{2+} bound with organic matter (Niane et al., 2019). High levels of Hg can cause severe human health problems (neurological, cardiovascular, immunological, and renal disorders)

and contaminate ecosystems (disrupt species function and behavior) (Nkuba et al., 2019; Santos-Lima et al., 2020; Yan et al., 2019). Mercury from gold mine sites can be transported to aquatic ecosystems via soil and riverbank sediment erosion and Hg methylation is favored in the anoxic environments of sediment (Niane et al., 2019). Methylmercury is the more toxic form of elemental Hg, since it can accumulate in organisms and biomagnify in trophic food chains even at low concentrations, posing increased health risk to humans (Bravo et al., 2018; Chen et al., 2020).

Soils and sediments provide essential functions in the terrestrial and marine ecosystems given their vital role in ecological stability, agricultural production and provision of habitats (Chen et al., 2022). However, contamination of soils and sediments by Hg and metals is becoming an increasingly severe environmental problem regionally (Chen et al., 2022). With the release of excess amounts of Hg and metals into the environment, soil and sediment quality decreases, leading to a reduction in ecological stability and food security (Chen et al., 2022). Mining activities are considered one of the most significant sources of Hg and metals found in soil and sediment, with various studies reporting contamination by Hg and other metals near gold mines (Bempah & Ewusi, 2016; Chen et al., 2022; Duan et al., 2018; Hadzi et al., 2019; Odukoya et al., 2022).

Meta-analysis methods have been used to comprehensively analyze contamination near gold mining areas (Chen et al., 2022; De Miguel et al., 2014; Hou et al., 2023; Hu et al., 2021; Lavoie et al., 2019). Previous studies have used meta-analysis based on different effect size metrics to estimate the health effects of Hg emission from gold mining (Hu et al., 2021; Taux et al., 2022). This method is applicable in efficiently addressing environmental questions on the impact of artisanal gold mining through a large-scale study.

Comprehensive studies on Hg and metals contamination in environmental media near artisanal gold mines on a continental scale are yet to be carried out. The main objective of this study is to assess the degree of contamination in soil and sediment near artisanal gold mines and explain variation by mining practices (small versus medium scale) across South America. Small scale gold mines are expected to show higher effects for CoC in soil and sediment compared with medium scale gold mines. Contaminants of concern that are directly associated with gold ore are expected to have a larger effect than Hg. Because atmospheric Hg is mostly gaseous and not part of the ore, it is expected to have a broader distribution compared with other metals that are part of the ore and associated with particles. This meta-analysis is expected to provide a sound scientific basis for future policies to control toxic element pollution and reduce the ecological risks in South America and by extension, globally.

2.2 Methods

2.2.1 Study selection and guiding questions for meta-analysis

The meta-analysis was based on available data published from 2008 to 2023 to represent the last 15 years of scientific studies related to artisanal gold mining in South America. Studies were selected from Argentina, Bolivia, Brazil, Chile, Colombia, Ecuador, Guyana, French Guiana, Peru, Suriname, and Venezuela (Figure 2.1). These countries were selected based on available data of environmental contamination associated with artisanal gold mining practices and no data was available for Paraguay and Uruguay, hence their exclusion from the meta-analysis. This study focused on nine CoC's that are commonly associated with artisanal gold mining, namely, As, Cd, Co, Cu, Hg, Mn, Ni, Pb, and Zn.

To objectively identify and process relevant studies for analysis, a comprehensive systematic literature search was conducted. Online databases such as *Google Scholar, Science Direct, Web of Science, Springer, and American Chemical Society* were searched for peer-reviewed articles using simultaneously the keywords “artisanal gold mining” and “environmental impact”. Variants of these terms were included – metal contamination, soil, sediment, gold mine, toxic element pollution, and environmental media. Inclusion and exclusion of literature was based on the criteria outlined in Figure 2.2. Following the literature selection and screening process, 34 articles were selected for a comprehensive analysis. The meta-analysis was primarily guided by the question – how does contamination of soils and sediments by COC’s vary by artisanal gold mining practices across South America?

Figure 2. 1. Map of focus countries and location of study sites.

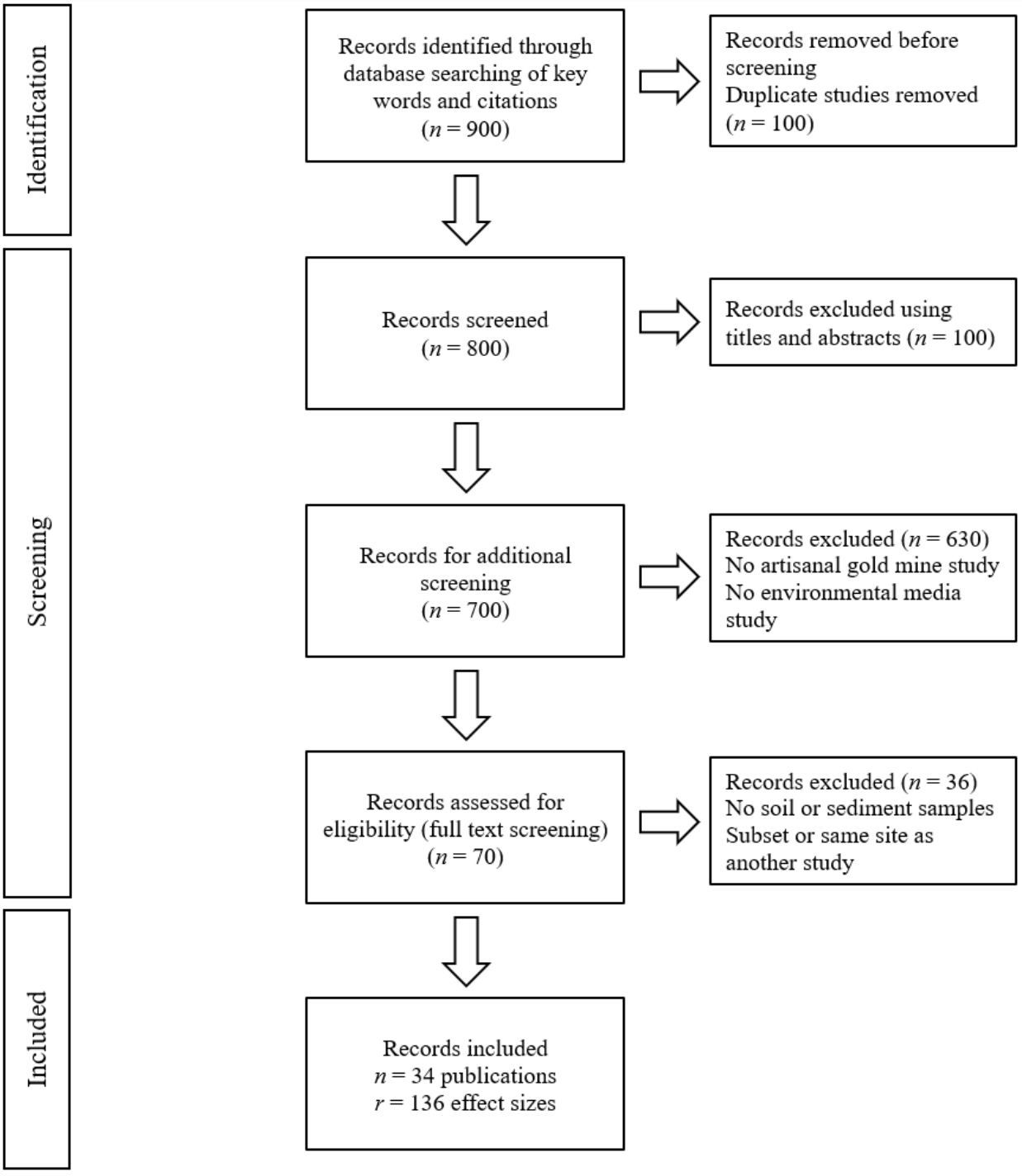

Figure 2. 2. Flow chart of literature selection and screening process.

2.2.2 Collection of soil and sediment for meta-analysis

Soil results from these studies were reported by depth integral and mineral soil data at a depth of 0 – 20 cm were used in this meta-analysis. At this depth, CoC are usually more concentrated and provide better and consistent estimates of the degree of environmental contamination associated with artisanal gold mining. Sediment results came from both rivers and lakes, since gold mines influenced river sediment in some studies and lake sediment in others. Water depth for sediment collection was not mentioned in screened studies, but some studies indicated that surface sediments (0 – 10 cm) were collected.

2.2.3 Statistical analysis

The spatial distribution of studies across focus countries of South America was mapped in ArcGIS Pro 2.9.0 (Esri, 2021), utilizing GPS coordinates from each study (Figure 2.1). For studies without GPS coordinates, site locations were extracted from Google Earth Pro (Google, 2024), based on the specified locations of the study. In the absence of local guidelines for soil and sediment quality across South America, guidelines recommended by the Canadian Council of Ministers of the Environment (CCME) and Environmental Protection Agency (EPA) were used (Table 2.1).

Studies that reported CoC concentrations in soil and sediment from impacted and unimpacted areas close to small and medium scale gold mines were extracted from the published data. Hierarchical analysis was first done on all data according to soil and sediment and then separated by small and medium scale gold mines. For this study, gold mines with informal approach, labor-intensive, and rudimentary techniques were classified as small scale, while those with a more organized approach, greater division of labor, and

semi-mechanized techniques were classified as medium scale. Estimating the effect size (*i.e.*, the magnitude and direction of the experimental effect) for each independent experiment is a core principle of meta-analysis (Reid & Watmough, 2014). Effect size estimates were pooled for summary purposes by comparing parameter metrics (CoC concentrations) from individual studies across South America using random-effects models. A conditionally applied argument was included to exclude studies from the random effects model when studies that reported CoC were less than three to ensure reliable estimation of random effect component and accurately capture heterogeneity. Random-effects models control nonindependence in ecological meta-analysis by accounting for variation within a study and between various studies. The I^2 statistic was used to quantify heterogeneity among studies (Higgins & Thompson, 2002; Hu et al., 2021; Veroniki et al., 2016).

2.3 Results

2.3.1 Results of the search

Data were extracted from 34 published articles (Table S2.1), which measured concentrations for the nine CoC (As, Cd, Co, Cu, Hg, Mn, Ni, Pb, and Zn) in soil and sediment. Among these studies, 18 measured CoC in soil and 22 measured CoC in sediment. Here, 136 effect size (*r*) values were extracted for the CoC from 11 countries across South America.

2.3.2 Degree of soil and sediment contamination

Contaminants of concern surpassed guideline values (Table 2.1) in 18 % of reported soil results and 40 % of reported sediment results. Some CoC concentrations in soil (As, Co, Cu, Hg, Mn, Pb, and Zn) and sediment (As, Cd, Cu, Hg, Mn, Ni, Pb, and Zn) exceeded CCME and EPA guidelines. The studies showed a larger exceedance for As (64 %) in soil and Cu (100 %) and Hg (71 %) in sediment (Figure 2.3). The exceptions were Cd and Ni, which were always below recommended guidelines in soil (Figure 2.3).

The random effects model for CoC in soils and sediments showed a summary effect size of 344.16 and 793.66 respectively, with heterogeneity (I^2) among studies (Figure 2.4). These positive effect sizes indicate an average increase in concentrations for CoC in soils and sediments of areas affected by gold mining compared with unimpacted areas. The average increase in effect size in soil was statistically significant (p = 0.02) since the confidence interval produced by the random effects model does not include 0 (CI = 54.08, 634.23). However, the average increase in sediment effect size was not statistically significant (p = 0.12) since the confidence interval produced by the random effects model included 0 (CI = -207.75, 1795.07) (Figure 2.4). Some CoC exhibited much larger effect sizes in soil (*e.g.*, As, Co, Hg, Mn, and Pb) or sediment (*e.g.*, Cd, Cu, Ni, and Zn) and sediment results were not always consistent with soils. For example, the effect sizes for As and Mn were much larger in soil, while in sediment the effect size for Cu was far greater than observed in soils. Generally, CoC such as As, Cu, Mn, Pb, and Zn showed a larger effect than Hg in soil and sediment (Figure 2.4). However, these larger effect sizes do not necessarily reflect the exceedance values and hence potential environmental risk, since Hg

concentrations exceeded sediment guidelines for 71 % of studies, despite a small effect size (Figure 2.3).

Table 2. 1. Contaminants of concern recommended guidelines for soil (industrial) and sediment (freshwater) quality (CCME, 2024; US EPA, 2000, 2002).

Element	**Soil (dry weight)**	**Sediment (dry weight)**
As (mg kg^{-1})	12[a]	5.9[a]
Cd (mg kg^{-1})	22[a]	0.6[a]
Co (mg kg^{-1})	300[a]	-
Cu (mg kg^{-1})	91[a]	35.7[a]
Hg (ng g^{-1})	100[b]	100[b]
Mn (mg kg^{-1})	450[b]	300[b]
Ni (mg kg^{-1})	89[a]	20[b]
Pb (mg kg^{-1})	600[a]	35[a]
Zn (mg kg^{-1})	410[a]	123[a]

- no reported guideline, [a] CCME guideline, [b] EPA guideline

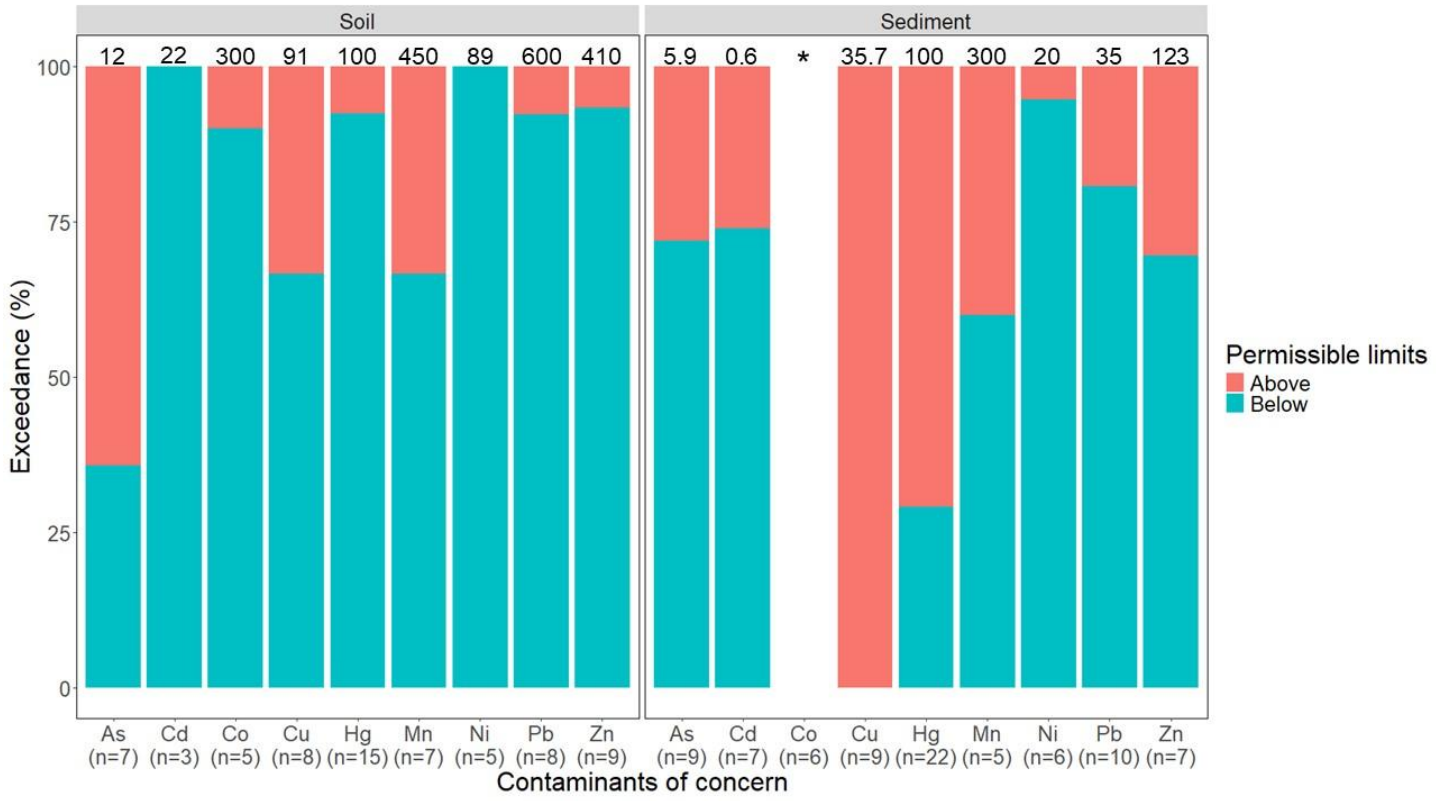

Figure 2. 3. Contaminants of concern across South America according to CCME and EPA guidelines for soil and sediment quality. Values above bars indicate permissible limits – Hg measured in ng g^{-1} and other CoC (As, Cd, Co, Cu, Mn, Ni, Pb, and Zn) measured in mg kg^{-1}, *no reported limit, n = number of studies.

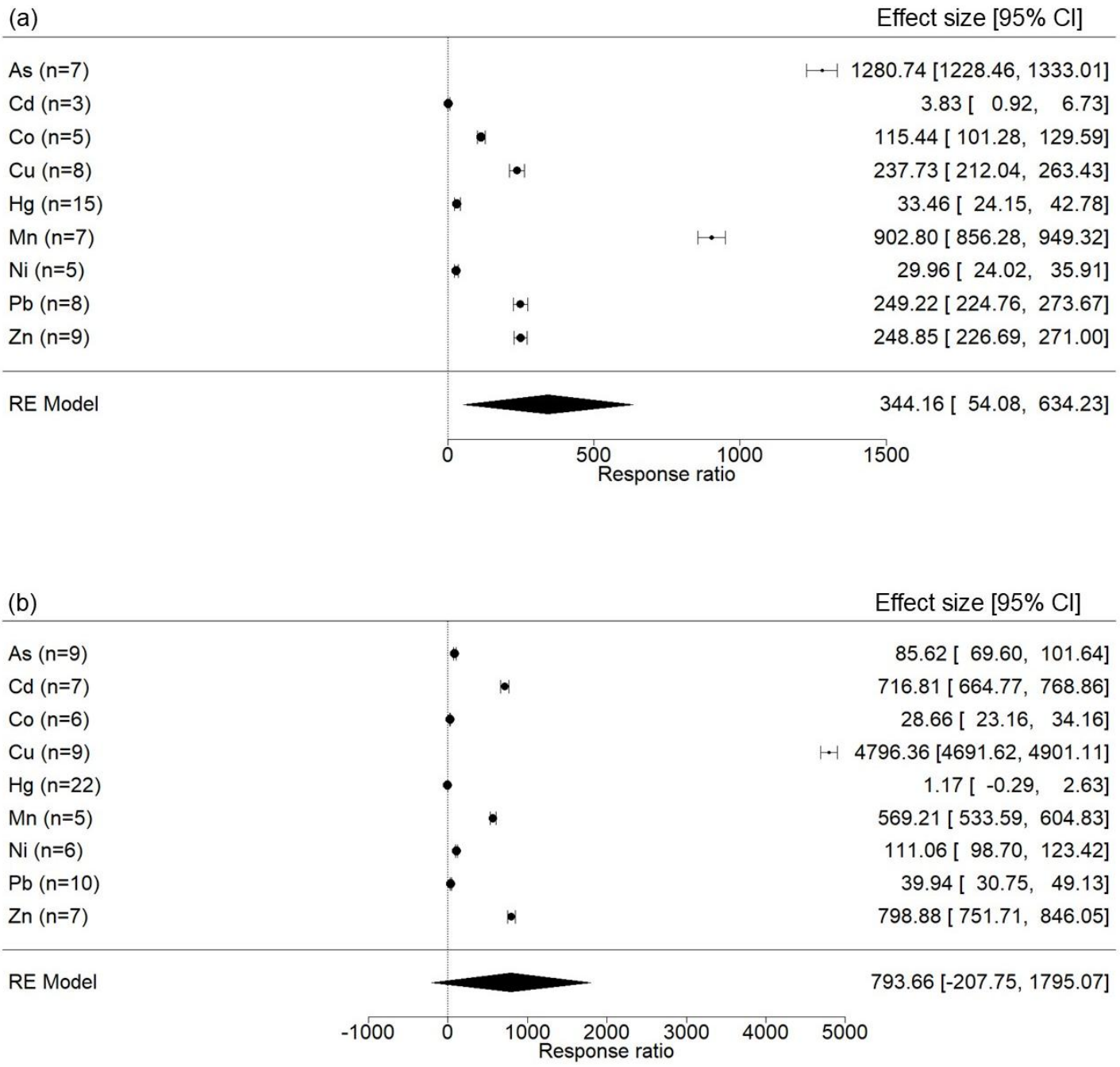

Figure 2. 4. Summary forest plot of CoC displaying the results of random effects meta-analysis for (a) soils and (b) sediments across South America. CI = confidence interval; n = number of studies.

2.3.3 Effect of mine size

Artisanal gold mining practices as described in each study from surveyed countries in South America were grouped according to small and medium scale mines, with 62% of the studies related to small scale gold mines while 38% were medium scale gold mines. The random effects model for CoC in soils according to small and medium scale gold mines showed a summary effect size of 230.09 and 391.26 respectively, with heterogeneity (I^2) among studies (Figure 2.5). The average increase in effect size in soil was statistically significant for small scale (p = 0.02, CI = 36.03, 424.15) and medium scale (p = 0.03, CI = 37.50, 745.02) (Figure 2.5). The positive effect size for soils indicates an average increase in concentrations for CoC at small and medium scale gold mines. These differences as a group were also evident among individual CoC effect size in soil at small and medium scale gold mines. For example, some CoC in soil have a larger effect at small scale gold mines (*e.g.*, Co, Cu, and Ni) while other COC's have higher effect sizes at medium scale gold mines (*e.g.*, As, Cd, Mn, Pb and Zn). The effect size of Hg in soil was almost identical at small and medium scale gold mines. Contaminants of concern such as Co, Cu, and Mn showed high variability in soils at small scale gold mines, while As, Pb, and Zn were highly variable in soils at medium scale gold mines.

River and lake sediments influenced by small and medium scale gold mines showed a summary effect size of 653.89 and 178.06 respectively, with heterogeneity (I^2) among studies (Figure 2.6). However, the average increase in effect size in sediment at small scale (p = 0.09, CI = -100.58, 1408.37) and medium scale (p = 0.06, CI = -8.29, 364.41) were not statistically significant but individually there are significant effect sizes (Figure 2.6). The positive effect sizes for sediments indicate an average increase in concentrations for

CoC at small and medium scale gold mines, with greater effect at the small scale. For example, the effect sizes for As, Pb, and Zn in sediment were much larger at the small scale compared with medium scale. Overall, the CoC's in sediments were not as variable as in soils, where only Cd showed high variability at small scale gold mines and Cu and Zn were highly variable at medium scale gold mines. The effect size of Hg was only significant at small scale gold mines.

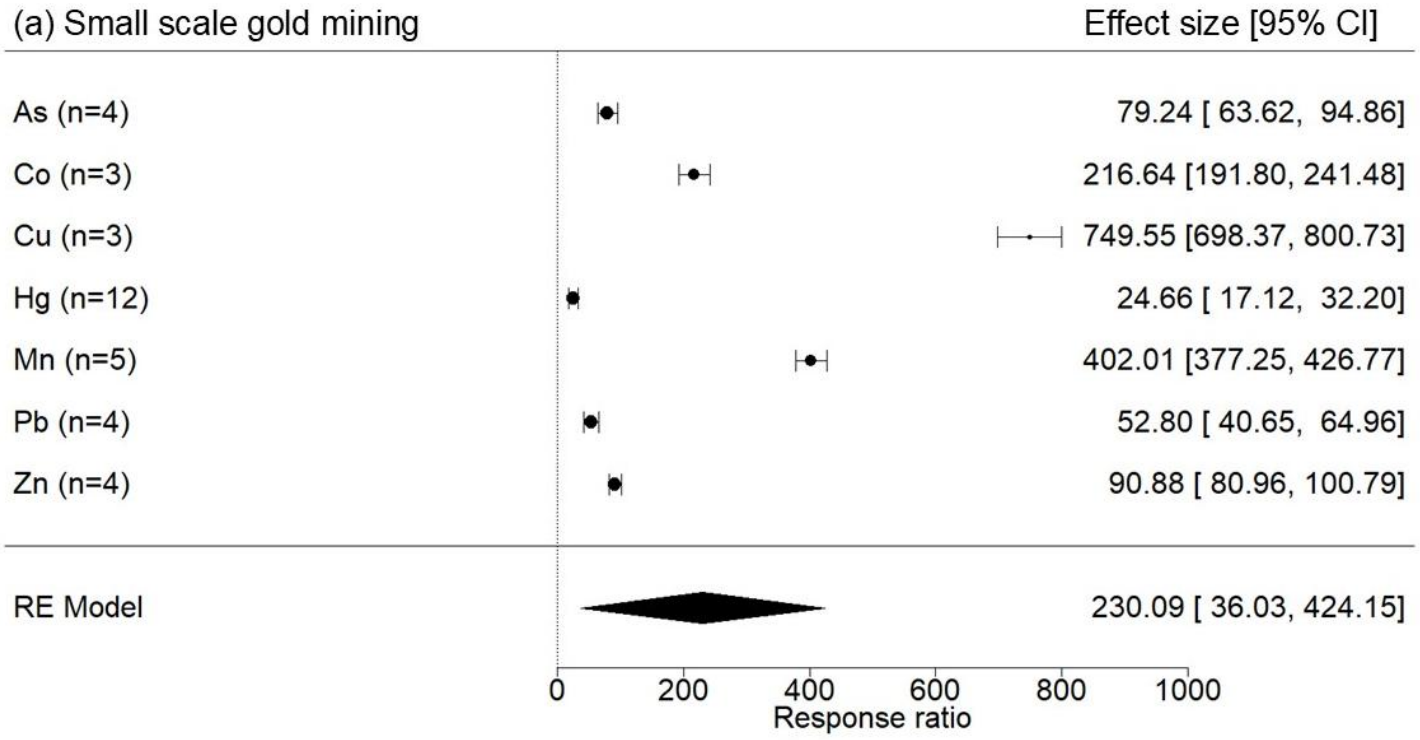

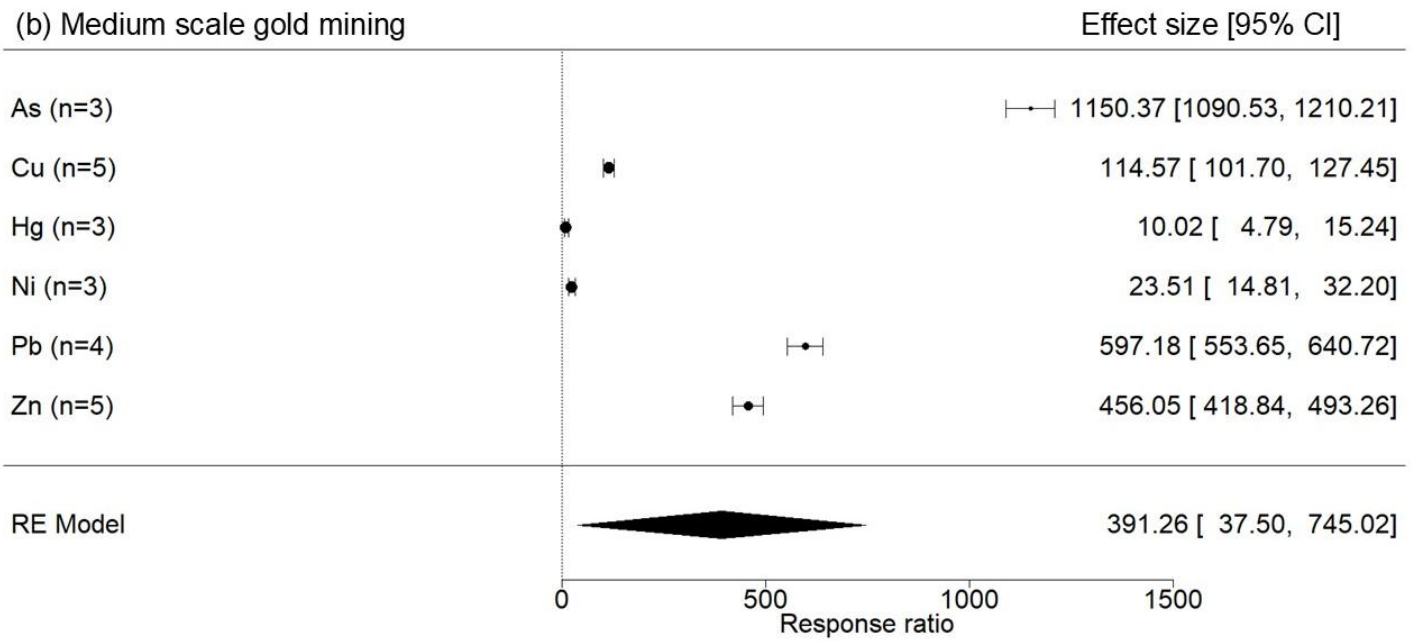

Figure 2. 5. Summary forest plot of soil CoC displaying the results of random effects meta-analysis for (a) small scale gold mining and (b) medium scale gold mining across South America. CI = confidence interval; n = number of studies.

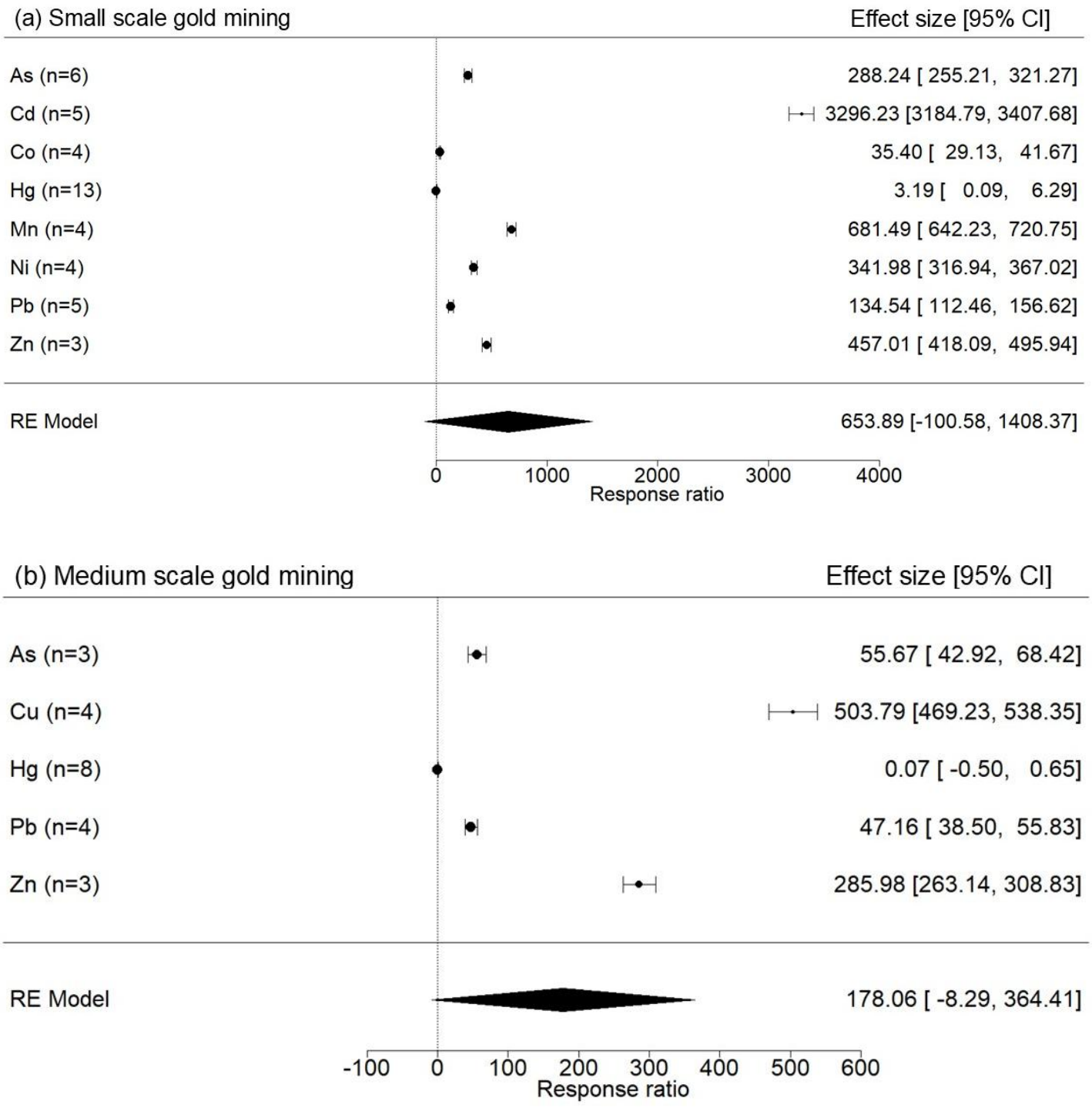

Figure 2. 6. Summary forest plot of sediment CoC displaying the results of random effects meta-analysis for (a) small scale gold mining and (b) medium scale gold mining across South America. CI = confidence interval; n = number of studies.

2.4 Discussion

2.4.1 Contaminants of concern in soils and sediments

This study shows that there is widespread metal contamination of soil and sediments associated with small and medium scale gold mining in South America. The degree of impact varies by metal and between soil and sediment and there are differences between impacts associated with small scale mining relative to medium scale mining. Additionally, the extent of contamination does not necessarily equate to environmental risk as almost 75 % of studies show Hg exceeds EPA guidelines in sediment yet it shows a very modest effect size. This suggests some influence of gold mining activities where Hg is added during the gold recovery process, with direct lost into sediment.

Gold mining generates large amounts of waste during the separation of gold from the ore. The remaining materials are disposed of as tailings and contain high levels of As, Cd, Cu, Mn, Pb, and Zn, which could contaminate nearby soils and sediments (Barcelos et al., 2020; Chen et al., 2023). The variability of metals in soil and sediment may be due to different ore minerology, differences in extraction procedures (small versus medium scale), waste management differences or differences in mine spoils age across South America. For example, the high levels of As and Mn in soil near gold mines could be attributed to the rich As and Mn content in mineralized waste rocks after separation of gold from ore, which may enter soil through poor and uncontrolled management of mine tailings (Abdul-Wahab & Marikar, 2012; Mensah et al., 2020). The leaching of tailing materials into streams and the presence of Cu-bearing minerals such as chalcopyrite could explain the high levels in sediment (Weleabzgi et al., 2021). The pattern of CoC in sediment differed from soil due to heterogeneity among studies used, which indicates variability in patterns of

environmental contamination from gold mining across different study sites. Armah et al. (2014) reported that the heterogeneity among studies applies to data collection procedures, preparation of metals for analysis, and sample storage, which may influence the magnitude and comparability of metal concentrations. The extraction procedures applied by small and medium scale mines differ, where medium scale mines extract and process larger ore deposits through semi-mechanized approaches by a team of 20+ people compared with small scale mines which are more labor intensive and done by one to five people. Such extractions disturb large quantities of earth materials that mix with mine spoils and alter the quality of soil and sediment at varying degrees. Mine spoil age could also influence metals concentrations due to the presence of residual contaminants from previous mining activities as well as mining-enhanced weathering and deposition from geogenic sources (Mensah et al., 2023). Additionally, metals from exposed waste rock piles and tailings could be mobilized in solution and spread to surrounding areas by erosion if waste is not properly managed. Once these metals enter adjacent water bodies, interaction with sediment is possible (Awotwi et al., 2021; Hammond et al., 2007; Mimba et al., 2023; Seki et al., 2022).

The differences in percentage of studies exceeding quality guidelines for soil and sediment suggest varying degrees of environmental contamination across studies. The high exceedance of As in soil and Cu and Hg in sediment indicates high environmental risk compared with other CoC. This high As exposure in soil could restrict plant growth, soil fertility, and disrupt the food chain due to its toxicity and persistence in nature over a long period (Gupta et al., 2022). Copper is acutely toxic to biota when present above threshold concentration in sediment and directly affects the functionality of primary producers and

decomposers in freshwater ecosystems (Beghelli et al., 2016; Gardham et al., 2015). Elevated concentrations of Hg in sediments can be transformed into methylmercury, which is the more toxic and bioaccumulative form of Hg, through microbial activity (Eckley et al., 2021; Wang et al., 2015). Arsenic and Cu showed a larger effect than Hg in soil and sediment due to the direct association of these contaminants with gold ore. Mercury is not a part of the ore, but is added during the amalgamation process to separate the gold from the ore. Fashola et al. (2020) and Carling et al. (2013) reported elevated concentrations that exceed recommended guidelines for As and Cu in soil and sediment influenced by artisanal gold mining.

The findings reported in this meta-analysis are similar to what was reported by Hou et al. (2023) meta-analysis of contamination in soils near gold mines at a global scale (24 countries on six continents), where the average levels of potentially toxic elements (As, Co, Cu, Hg, Mn, Pb, and Zn) in soils near gold mines exceeded background values and presented varying levels of contamination due to gold mining activities. Rajaee et al. (2015) integrated assessment of artisanal and small-scale gold mining reported Hg levels lower than guideline values in soil, but sediment Hg levels surpassed guideline values in 64 % of the studies.

2.4.2 Small versus medium scale gold mining

Small and medium scale gold mining practices employ different numbers of people, use different mining techniques, and the environmental contamination differs. Based on the low number of studies (n=34), the overall effect size in soil was higher at medium scale gold mines possibly due to the larger volume of ore being processed. Typically, >500 to

500,000 tonnes of ore per year could be processed by medium scale gold mines, leading to the generation of more waste (Hammond et al., 2007). Such high volumes of mine waste often contain various metals (As, Pb, Zn) at elevated concentrations, contaminating soil. Although medium scale gold mining is more mechanized and formalized, significant environmental contamination is still possible in the absence of proper regulations and waste management techniques (Timsina et al., 2022; van Straaten, 2000). The higher effect size in sediment at small scale gold mines may be associated with the unregulated and informal nature of small-scale mines, which results in unabated export of contaminated mine spoils and tailings to streams due to poor waste management techniques and lack of reclamation post-mining. Zinc could be leached from mine tailings and migrate with surface runoff before adsorption by the matrix components of sediment (Wang et al., 2019). Li et al. (2024) reported that surface runoff primarily controlled the release of Zn from mine tailings to sediment. Differences in the geology of the waste rocks which constitute small and medium scale mines may influence the degree of contamination in soil and sediment. This is associated with the weathering processes of these rocks over time that could lead to the release of contaminants into nearby soil and sediment where they accumulate and negatively affect the ecosystem (Navarro et al., 2008). The differences in mining practices could explain the degree of contamination at small and medium-scale gold mines. Small and medium scale gold mining practices remove soil and vegetation to access the gold-bearing ore, generating large volumes of waste with various CoC that are released into the surrounding environment. Improper disposal of waste generated from small and medium scale gold mines could lead to widespread contamination of soil and sediment in the absence of proper regulations (Akoto et al., 2023). Poor management of tailing materials

from gold mining could lead to uncontrolled acid mine drainage, which negatively impacts the surrounding environment. This acidity is formed through the oxidation of pyrite rich gold-bearing ores when it encounters oxygen from the atmosphere in the oxidized zone of tailings (Laker, 2023).

In contrast to other metals Hg has a gaseous phase (Hg^0) so it can travel over long distances and cause both local and regional contamination. Therefore, the release of Hg at the emission source could be transported far away given the high atmospheric mobility and long lifespan. The transformation of Hg to MeHg is also a main concern since it is more toxic than inorganic Hg and bioaccumulates and magnifies like no other metal. The low effect size of Hg at small and medium scale mines compared with other CoC could be associated with the limited use of Hg by some mines and effective recovery techniques with the use of properly designed retorts to limit Hg emission. However, the bioaccumulation potential and toxicity of Hg render it as problematic even with small increases. Increases in Hg effect size in soil and sediment were greater at small scale gold mines, indicating higher emission or application due to the absence of a retort (which aids in Hg recovery) during the process of gold amalgamation. Compared to other CoC in soil and sediment, Hg is not part of the ore but is added during gold extraction and is emitted to the atmosphere during burning. Small scale gold mines are normally engaged in open flame burning of gold amalgam which result in direct release of large amounts of Hg into the atmosphere through volatilization (Green et al., 2019). Gravity separation methods are applied as the step to produce concentrates with more than 20% gold (acceptable level of purity for the smelting process). However, if the desired gold purity is not met Hg amalgamation is done, where Hg forms an alloy (amalgam) with gold, separating it from

other minerals (Timsina et al., 2022). Amalgamation with Hg is widely used in small scale operations rather than cyanidation because it is cheap, accessible, and simple to apply (Fashola et al., 2016). Mercury remains in soil for a relatively long period due to constant recycling between the atmosphere and surface environment (Gworek et al., 2020). This long lifespan in soil could result in the transport of Hg-bound particles to sediment through surface runoff, leading to the formation of methylmercury which is more toxic (De Simone et al., 2014; Driscoll et al., 2013; Slemr et al., 2011). González-Carrasco et al. (2011) reported that Hg concentrations in the air of Portovelo, Ecuador near gold mining processing plants were elevated following amalgam burning. Carranza-Lopez et al. (2019) also reported extremely high Hg levels (exceeding international guidelines) in the air around mines and gold-processing shops in Colombia. These elevated levels of atmospheric Hg above natural background concentration for the global south (> 1 ng m^{-3}) (Sprovieri et al., 2016) exposes people to Hg vapors through breathing and pollute soil and sediment.

Small and medium scale gold mining afford many low-skilled workers the opportunity to lift themselves out of poverty. However, the operation of this industry with minimal to no pollution controls pose major environment and human health challenges (Pavilonis et al., 2017). Although policy instruments exist across South America to regulate artisanal gold mines (Table S2.2), enforcement is still a challenge given the sporadic and remote nature of these gold mines. The isolated occurrence of many small cooperative mines and the lack of enforcement and infrastructure, contributes to the development of the present critical environmental conditions in South America (Acosta et al., 2011). For example, Colombia lacks specific regulations (Table S2.2) to guide the closure and

remediation of mines. In the absence of such regulations, the obligation to close and remediate mines are outlined in the environmental license and on a case-by-case basis, based on the type of mine, mineral and location (Zapata et al., 2017). This could negatively affect post mining activities that are intended to safeguard the environment.

There were some inherent limitations in conducting this meta-analysis of studies related to artisanal gold mining environmental contamination across South America. A high degree of heterogeneity existed among the studies included due to inconsistencies in CoC measurements, exposure levels, study design, and method of analysis. Also, limited studies (n=34) related to soil and sediment contamination due to artisanal gold mining were available across South America for inclusion in this meta-analysis.

2.5 Conclusion

A comprehensive analysis of studies on contamination in soils and sediments near artisanal gold mines from 2008 to 2023 was conducted. The results highlight the variability of CoC's in soils and sediments based on 34 studies from 11 countries across South America. Although effect sizes indicated the extent of contamination, environmental risk was not always the same, since many studies showed Hg beyond threshold limits in sediments relative to a very small effect size. Gold mining has caused contamination of nearby soil and sediment, creating potential ecological risks in the vicinity of the mining area. Rapid measures should be taken to remediate contaminated soils, restore the landscape of gold mining areas, and carry out environmentally protected gold mining of undisturbed deposits to avoid the release of contaminants into the environment which could have lasting effects on ecosystems.

3.0 Characterizing Hg and other metal concentrations in soil and sediment within gold mined areas of Guyana

3.1 Introduction

Artisanal gold mining plays a key role in the livelihood of rural communities and the socioeconomic development of various countries across South America, including Guyana (Harlow et al., 2019). In recent decades, consecutive surges in gold price on the global market has led to the expansion of gold mining operations in South America (Timsina et al., 2022). However, the large amounts of waste generated from gold mining activities contaminate the environment and little efforts with respect to reclamation post small and medium scale gold mining (López-Blanco et al., 2015). Small and medium scale gold mining operations in Guyana involve removal of forest cover, land dredging, and separation of low-grade gold-bearing ore with high-pressured water supply. The gold-bearing ore is collected in a sluice box and gold is recovered through mercury (Hg)-gold amalgamation (Howard et al., 2011). Such practices of gold mining introduce contaminants (As, Cd, Co, Cu, Mn, Ni, Pb, and Zn) to environmental media and the addition of Hg further compounds the issue. The meta-analysis in chapter 2 of this thesis revealed high variability of contaminants of concern (As, Cd, Co, Cu, Hg, Mn, Ni, Pb, and Zn) in soils and sediments based on 34 studies from 11 countries across South America. Here, the varying contamination of soils and sediments were associated with ore minerology, extraction procedures (small versus medium scale), seasonality, waste management, and mine spoils age. Interestingly, the effect size of contaminants in soil and sediment (greater effect for metals) does not necessarily equate to environmental risk, since contaminants could still

exceed threshold limits despite a small effect size. The presence of contaminants at elevated concentrations pose potential threats to biota and human health. Tankari Dan-Badjo et al. (2019) and Xiao et al. (2017) found soils of artisanal gold mining sites were contaminated with As, Cd, Cr, Ni, Pb, and Zn above the World Health Organization (WHO) recommended limits. The degree of metal contamination however is highly variable and is largely due to differences in the composition of the ore (Fontboté et al., 2017). For example, Fashola et al. (2016) reported that Cd and Zn occur in the form of sphalerite in gold ore while Pb occur in the form of galena when the concentration of sulfide in ore is high. Arsenic occur in gold ore as arsenopyrite and pyrite (Chen et al., 2023; Iatan, 2021) and elevated levels of As have been reported in several studies across South America since gold mine ore-bearing particles serve as a major source of As (Dias et al., 2022; López-Blanco et al., 2015; Pavilonis et al., 2017; Fernando Santos-Francés et al., 2017; Tume et al., 2018).

Contamination of soils and sediments with Hg associated with artisanal gold mining is due to the addition of Hg in the extraction process. In South America, Hg emissions from gold mining constitutes ca. 70% of South America total emissions (UN Environment, 2019). This was supported by the meta-analysis in South America (as reported in chapter 2 of this thesis) which showed small effect sizes for Hg, but large exceedance of Environmental Protection Agency (EPA) guidelines (100 ng g^{-1}) owing to gold mining activities and direct loss of Hg during the gold recovery process, especially in sediments. In contrast to other metals, emissions of Hg into the atmosphere may be deposited on surfaces in proximity to the gold mining site and farther away. Akoto et al. (2023) and Danala Danga et al. (2024) reported that there was considerable variability in soil contamination for gold mining areas, which ranged from moderate to heavy (2,100 –

12,400 ng g^{-1}) contamination with Hg. The higher concentrations of Hg were found in soils from the mining area compared with adjacent sites due to direct elemental Hg spills during the amalgamation of gold after washing. Similarly, a study in Senegal found soils contaminated with elemental Hg concentrations up to 3,900 ng g^{-1} near artisanal and small-scale gold mines, which eventually travels to downstream aquatic ecosystems where oxidation and methylation takes place (Niane et al., 2019). Such transport or retention of Hg is influenced by soil properties. Soil particle size and organic matter (OM) content affects the behavior of Hg and metals in soil, where finer particle size and higher OM are typically associated with higher concentrations of Hg and metals (Gong et al., 2023; Qin et al., 2023). Velásquez Ramírez et al. (2021) found that Hg levels for gold mine spoil soils were below the upper permissible limits stipulated by British, Canadian and Peruvian environmental quality standards. Here, soil OM, clay content, pH, and vegetation cover were important predictors of variations in soil Hg levels.

Localized impacts of gold mining are not limited to soils and vegetation on mine sites. Sediments are also affected and show longer-term loadings. Mercury and metals enter aquatic ecosystems through atmospheric deposition, surface runoff, and rock weathering (Koskey et al., 2020). The lack of vegetation at gold mining sites may also lead to erosion of soils and overburden (Fitri, 2018; Macháček, 2020; Mencho, 2022). Howard et al. (2011) reported that sediments in rivers at gold mine sites in Mathew's Ridge and Port Kaituma, Guyana were contaminated by Hg from gold mining activities. Here, sediment concentrations showed extremely high variability, ranging from 29 to 1,200 ng g^{-1} with a mean value of 229 ± 223 ng g^{-1}. Metals fixed in sediments can be dissolved into the water again through changes in OM, oxidation-reduction potential, and salinity (Han et al., 2017).

Such changes in environmental conditions can pose high biological and ecological risks due to the reactivation of legacy metals. For example, Rudd et al. (2018) reported that methylation of legacy Hg trapped in sediment maintains elevated Hg in biota following 50 years of Hg discharge in Penobscot Estuary.

In sediments, the surface to volume ratio, OM, and grain size can influence Hg and metals levels, with grain size being the main parameter (Koskey et al., 2020; Maslennikova et al., 2012; Xu et al., 2017). Yao et al. (2015) reported that finer fraction of sediments contained a higher concentration of heavy metals compared with the coarse fraction. This was partly due to the high clay content and the greater surface area per unit of mass of the fine particles, thereby increasing this fraction adsorption capacity. However, studies by Maslennikova et al. (2012) indicated that coarse fraction of sediments absorbed high levels of heavy metals compared with the fine fraction. This was possibly linked to the residence time of coarser particles and accumulation conditions, specifically, the reservoir ecological state and climatic parameters. The grain size of sediments is also associated with the availability of contaminants, where fine fraction of sediments tends to be higher in clay content, with higher levels of OM (Koskey et al., 2020).

The impact of small and medium scale gold mining on soil and sediment, has gained momentum over the last few decades, given the potential threats posed to the terrestrial and aquatic environment (Rakotondrabe et al., 2018). Small and medium scale gold mining operations in Guyana continues to utilize rudimentary tools (diggers, spades, sluice boxes, and shovels) and semi-mechanized approaches (excavators, heavy engines, heavy duty trucks, and gold washing plants), which has the potential to alter soil and sediment chemistry to varying degrees. Alteration of soil chemistry due to Hg and other metals

contamination may vary inside and outside mining sites, given the complex nature of mining sites. These mining sites are partitioned into: (a) the pit – areas with mixture of material remaining after gold has been separated from the ore and high intensity of disturbance, (b) overburden – areas overlying the gold ore, including topsoil, which are displaced during the mining process, and (c) adjacent sites – areas without deposits of material from the mining process (Kalamandeen et al., 2020). To date, no study in Guyana has characterized the extent of metal and Hg contamination in soils and sediments. The purpose of this study was to assess the contents of contaminants of concern (As, Cd, Co, Cu, Hg, Mn, Ni, Pb, and Zn) in soil and sediment of gold mined areas and evaluate physiochemical properties that are related to their variability in the environment. It is hypothesized that Hg and metals will exhibit different spatial patterns with metals being enriched at the mine sites, while Hg will be elevated at sites more distant from the mine and more closely associated with OM.

3.2 Methodology

3.2.1 Study area

The study area in Guyana was in the mining district of Potaro (5° 18’ 36” N to 5° 18’ 12” N and 59° 18’ 16” W to 58° 54’ 14” W). The Potaro mining district (ca. 3.5 million acres of land area) is characterized by many small and medium scale gold mines. The Essequibo river which is approximately 960 km long passes through the Potaro mining district before discharging into the Atlantic ocean (Howard et al., 2011; Pasha et al., 2017). The Essequibo and Potaro rivers form the catchment for this mining district. Samples were collected from gold mines in Mahdia and Frenchman (Figure 3.1). The Mahdia zone is larger than the

Frenchman zone and currently has more gold mining activities. Sampling sites were accessed by means of trails and a land cruiser. During the sampling periods, active gold mining was evident at the Mahdia location, while the Frenchman location was inactive due to excess flooding of pits.

The study area is characterized by lowland montane forest and dry to moist forests, which sits on laterite soil, clay and alluvial soil, lithosols soil and latosols soil. Annual precipitation varies from 2,200 to 4,000 mm and mean annual temperature ranges between 23 to 32 ℃ (GLSC, 2013). In recent years, the study area experienced an upsurge in small and medium scale gold mining activities. Based on the mining legislation of Guyana, small scale gold mines have a fixed land claim size of 27.5 acres and medium scale gold mines have a land claim size that range from 150 to 1,200 acres (Hilson & Vieira, 2007).

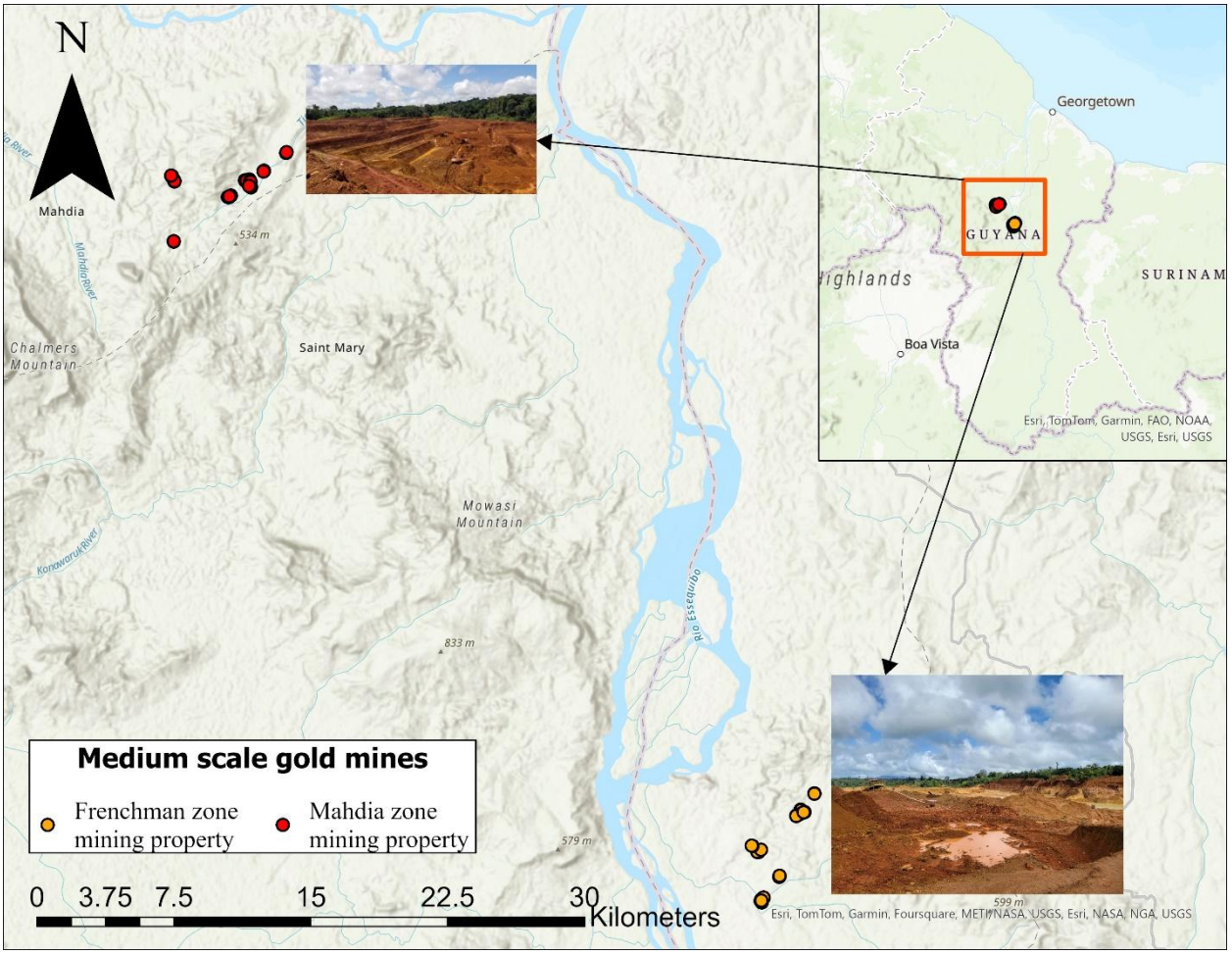

Figure 3. 1. Map of study area.

3.2.2 Soil sample collection

Soil samples were collected from two active gold mines in Mahdia (Hopkinson medium scale operation) and Frenchman (Obermuller medium scale operation) (Figure 3.1). These gold mining operations employed semi-mechanized approaches (excavators and bulldozers) and in some cases water was being recycled from tailings facility. Each sample location was separated into four zones: distant site (2 – 4 km from source of gold mining with vegetation), adjacent site (1 – 2 km from source of gold mining with vegetation), overburden, and pit. Surface (0 – 10 cm) soil samples (n = 80) were taken randomly in each

zone (10 samples in each zone). These samples (each weighing ca. 100 g) were collected with a small trowel from five sample points at regular 10 m spacing over a period of 4 days from 8 to 11 July 2022. When present, vegetation and forest floor was removed to take soil samples at forested sites (distant and adjacent). The trowel was cleaned after each sample collection to avoid cross-contamination. Soils were placed in labelled Ziploc® bags and stored in a cooler for transport to the University of Guyana Agriculture laboratory to be oven-dried. Soil samples were air-dried for 10 days at 105℃ in an oven (Thermo Scientific, Freas 645) and stored in sealed and labelled Ziploc® bags. These samples were packaged into another Ziploc® bag for storage at 4℃ to avoid any contamination until transport to Trent University Environmental Geoscience laboratory for analysis. A small amount of Hg may also have been lost during the drying procedure as Hojdová et al. (2015) reported that the loss of Hg in samples dried at 105℃ was 3 % compared with freeze dried samples.

3.2.3 Sediment sample collection

Sediment sampling was done in the dry season (July 2022, 2023, 2024) at Mahdia across the major stream channel (width of ca. 30 – 50 cm and depth of ca. 15 cm) that drained the mining area (Figure 3.2). The stream had pH of 5.81 ± 0.10, turbidity of 104.31 ± 15.74 NTU, and dissolved oxygen of 7.76 ± 0.05 mg L^{-1} at the time of sampling. Grab samples of sediment (ca. 50 g) were collected with a stainless-steel trowel at depth of 0 – 10 cm to capture upper sediment contamination. These samples were collected in triplicates (n = 72) from within the mining operation and downstream of the mine in Mahdia over a distance of 2 – 4 km. Collected sediments were placed in labelled Ziploc® bags and stored in a

cooler for transport to the University of Guyana Agriculture laboratory to be oven-dried (105℃, Thermo Scientific, Freas 645).

Figure 3. 2. Stream channel passing through Mahdia gold mining area.

3.2.4 Soil and sediment chemistry analysis

Dried soil samples were crushed to homogenize the samples and sieved (2 mm) to remove stones and roots. To determine soil pH, a sub-sample of soil (5.0 g) was added to each 50 ml conical centrifuge tube, followed by 25 ml of 0.01 M $CaCl_2$. The suspension was subjected to a shaking process (Shaker Table, Eberbach) for 60 minutes, then allowed to sit for another 60 minutes for soil particles to settle prior to measurement with a pH meter (Oakton, pH 510 Series). (Muddarisna & Siahaan, 2014).

Soil and sediment organic matter (%OM) was measured by loss-on-ignition (Equation 1). After oven-drying (24 hours at 105℃) of soil and sediment (5 g) to constant weight, organic matter was ignited at 400℃ for 10 hours (Heiri et al., 2001).

$$\%OM = \left(\frac{W_1 - W_2}{W_1 - C_w} \right) \times 100 \qquad \text{Equation 1}$$

Where, W_1 = weight pre ignition, W_2 = weight post ignition, and C_w = crucible weight.

Total Hg concentration in soil and sediment was measured with a Direct Mercury Analyzer (DMA-80) by thermal decomposition, amalgamation, and atomic absorption spectrometry. Sub-samples of dried soil and sediment (0.05 g) were heated to 900℃ to reduce Hg species to elemental Hg, which was loaded onto an amalgamator. Subsequent heating of the amalgamator resulted in the release of Hg vapors into a single bean, fixed wavelength atomic absorption spectrophotometer. Quality control of Hg measurements was assured by the inclusion of blanks and certified reference materials (*Enviro*MAT™ SS-1) at the start of each experimental run (40 samples) and recovery ≥ 93 % was considered acceptable.

Contaminants of concern (As, Cd, Co, Cu, Mn, Ni, Pb, and Zn) associated with artisanal gold mining as identified in the meta-analysis (chapter 2) were subjected to an acid digestion (HNO_3) process, which is not a total digest (unlike perchloric acid) to measure concentrations in soil and sediment. This acid digestion method was used to solubilize and extract metals from soil and sediment matrix for measurement. A sub-sample of dried soil and sediment (0.2 g) was added to each 100 ml polypropylene acid resistant digestion tube, followed by 2.5 ml of concentrated HNO_3. Tubes were swirled gently to ensure complete mixing with HNO_3 and closed loosely. Tubes were placed in a block-digester and hot plate (Cole-Parmer®) for 16 hours (8 hours cold and 8 hours hot). Following the completion of acid digestion, cooled samples were subjected to a filtration process (Fisherbrand® Filter Paper Qualitative P8 Grade). The volume of the filtered sample was adjusted to 25 ml with BPURE water and transferred to a 50 ml conical centrifuge tube for storage at 4℃. This was followed by the pipetting of 10 ml of digested sample into a 15 ml conical centrifuge tube and stored at 4℃ until analysis with inductively coupled plasma-optical emission spectrometry (ICP-OES). Blank reagents and digested standard reference material (*Enviro*MAT™ SS-1) were run with each batch of samples to ensure quality control and recovery of 80 – 120 % was considered acceptable.

Particle size analysis of soil and sediment samples was measured with a laser scattering particle size distribution analyzer (LA-950V2, Horiba) to determine clay, silt, and sand composition. Calgon (Sodium Hexametaphosphate) solution was prepared by mixing 30 g of Calgon with 1L of reverse osmosis (RO) water on a stir plate (VWR Stirrer) at 800 rpm for 30 minutes. A sub-sample of soil and sediment (2.0 g) remaining after the loss-on-ignition process, was added to each 50 ml conical centrifuge tube, followed by 2.5

ml of Calgon solution. The suspension was subjected to a shaking process (Shaker Table, Eberbach) at low speed for 8 hours. Particle size was determined for each sample by adding 3 drops of the suspension to the Horiba LA-950V2 and all measurements were taken in triplicates.

3.2.5 Surface leaching experiment

In order to evaluate whether the amount of Hg associated with dissolved organic carbon (DOC) could be potentially leached into sediments, soil extraction experiments (Ott, 2021) were conducted with surface soil (dried and sieved) collected from each of the four locations in Mahdia (5 surface x 4 zones = 20 samples). The leaching experiment used 30 ml syringes to create leaching columns that mimic surface runoff mechanisms. Each syringe with the plunger removed was packed with 0.25g of virgin polyester fill (avoid collection of larger soil particles with the leachate) and 10g of soil above. The plunger was used to ensure soil was packed to a consistent density within the syringe. Approximately 40 ml of BPURE water (maintain consistency in extracts) was added to each syringe and ca. 25 ml and 15 ml leachate was collected for DOC and total Hg analysis, respectively. Samples were filtered (0.45 µm filter) into 20 ml glass vials and covered with parafilm and caps until analysis. Dissolved organic carbon in filtered leachate samples was measured with a Total Carbon Analyzer (Shimadzu). Blanks and quality assurance solutions (total inorganic carbon and total organic carbon standards) were run with each batch of samples to ensure quality control.

Total Hg concentration in leachate samples was measured with a Tekran 2600-CVAFS Mercury Analysis System by cold vapor atomic fluorescence spectrometry. A sub-

sample of filtered leachate (15 ml) was added to each 40 ml glass vial, followed by 0.1 ml of 0.2 M BrCl and swirled gently to ensure complete mixing. Vials were allowed to sit overnight in the dark to form a pale-yellow solution. Calibration standards of 0 pg, 25 pg, 50 pg, 100 pg, 250 pg, 500 pg, and 1000 pg were prepared with 1 ng ml^{-1} diluted Hg standard. Samples were diluted to desired concentration and 60 µl of 20 % Sn_2Cl in 10 % HCl was added to each vial (final volume of 25 ml) for analysis. Vials were capped with septa caps and shaken before loading the autosampler. Water blank (no reagent), blank reagent, and standard reference material (*Enviro*MAT™ SS-1) were run with each batch of samples to ensure quality control and recovery ≥ 95 % was considered acceptable.

3.2.6 Statistical analysis

Statistical analysis was conducted with R version 4.0.4 (R Core Team, 2021), at an acceptable α-level of 0.05. Descriptive statistical analysis was conducted with R statistical package to assess range, mean and standard error of soil and sediment physicochemical properties (pH, OM, texture). Data was subjected to Shapiro-Wilk normality test to assess normal distribution.

Spearman correlation heat map was used to determine if soil and sediment Hg and metals are related to physicochemical parameters (pH, OM, texture). The conventional conversion factor of 0.58 was used to convert soil OM to soil C (Jensen et al., 2018). Linear regression analysis was done to assess the effect of OM on soil and sediment Hg and metals concentrations. The nonparametric Kruskal-Wallis test was used to compare physiochemical properties and Hg/DOC and metals concentrations among sampling zones.

When the Kruskal-Wallis indicated significance, Dunn test was used to determine the levels of the independent variable that differ from each other level (Zar, 2010).

3.2.6.1 PCA with missing values

Principal component analysis (PCA) assessed association between physicochemical parameters and Hg and metals and exploration of probable clusters in surface soil and sediment (Baran et al., 2019). Data from sampled soils and sediments are included, however samples with missing values for any parameter were treated with an iterative algorithm. This PCA algorithm is based on an imputation method that enables the estimation of principal axes and components despite the presence of missing values (skipping of missing values) (Osborne et al., 2024). The imputation is executed with the R package *miss*MDA, by simultaneously considering the similarities between individuals and the relationships between variables (Josse et al., 2011; Josse & Husson, 2016).

3.3 Results

3.3.1 Physicochemical characteristics of soil and sediment

Across the sample sites, soils were acidic ranging from 3.56 – 5.28 and pH was approximately half a unit lower in the two forest sites (distant and adjacent) (3.86 – 4.36) compared with overburden and pit sites (4.47 – 4.64) (Table 3.1). Soil organic matter (%OM) content across all sites was highly variable, ranging from 1.35 – 19.43% and soil OM content was about 3-fold higher in distant and adjacent sites (8.69 – 17.00%) compared with overburden and pit sites (2.53 – 5.28%). The exception was the reference site at Frenchman that had lower OM (2.84%) compared with the overburden site (Table 3.1).

The OM content of the stream sediment at Mahdia ranged between 4.13 and 17.15% and OM was very similar in the mining operation zone (8.52 ± 0.43%) and downstream (7.14 ± 0.41%) (Table 3.2).

Soil and sediment samples were dominated by the sand fraction across all sampled zones and this fraction differed significantly among sampled zones (Table 3.1 and 3.2). The mining operation zone, which is primarily overburden materials and mine wastes, contained higher clay particles compared with the other sample zones (Table 3.1 and 3.2).

3.3.2 Mercury and metals in surface soils

High variability in surface soil Hg concentration was evident across the two gold mines, with both Mahdia (22.12 – 970 ng g^{-1}) and Frenchman (8.16 – 424 ng g^{-1}) demonstrating variability by a factor of approximately 50 (Figure 3.3). Soil Hg concentrations showed no obvious patterns associated with distance to gold mining activities. The mean concentration of Hg across the sampled gold mine in Mahdia was highest at the adjacent site (614 ± 54 ng g^{-1}), followed by the distant site (501 ± 26 ng g^{-1}), pit (322 ± 105 ng g^{-1}), and overburden (180 ± 50 ng g^{-1}). While at Frenchman, the adjacent site (332 ± 16 ng g^{-1}) showed the highest mean concentration of Hg, followed by pit (232 ± 30 ng g^{-1}), overburden (118 ± 21 ng g^{-1}), and distant site (19 ± 4 ng g^{-1}) (Figure 3.3).

Most other metals (Co, Cu, Mn, Ni, and Zn) exhibited higher concentrations in the overburden and pit zones compared with the two forest sites (Figure 3.4). Soil Pb concentrations at the forest site adjacent to the mine were notably elevated and had concentrations similar to those measured in the overburden and pit (8.63 ± 0.30 mg kg^{-1}) at Mahdia. However, concentrations of all metals except Hg were below levels of concern.

Additionally, the minimum detection limits of As and Cd were 0.01 and 0.02 mg kg^{-1}, respectively and these metals were not detected in soil across the sampled gold mining sites of Mahdia and Frenchman, which contrast to some other studies around gold mines in South America.

Table 3. 1. Summary statistics of Mahdia and Frenchman goldmine soils. Different letters indicate statistically significant differences ($p < 0.05$) using Dunn's test between sample zones.

	Distant					Adjacent					Overburden					Pit				
	pH	OM (%)	Clay (%)	Silt (%)	Sand (%)	pH	OM (%)	Clay (%)	Silt (%)	Sand (%)	pH	OM (%)	Clay (%)	Silt (%)	Sand (%)	pH	OM (%)	Clay (%)	Silt (%)	Sand (%)
									Mahdia (n = 40)											
Mean	3.89^{a}	17.00^{a}	13.37^{ab}	7.16^{a}	79.60^{ab}	4.36^{b}	12.27^{b}	11.67^{a}	5.31^{a}	82.65^{a}	4.51^{b}	5.25^{c}	15.88^{ab}	8.00^{a}	75.57^{ab}	4.47^{b}	5.28^{d}	15.34^{b}	6.16^{a}	77.50^{b}
SE	0.09	0.61	0.33	0.33	0.54	0.16	0.55	0.48	0.23	0.62	0.07	0.66	0.33	0.33	0.66	0.10	0.59	0.17	0.17	0.38
Min	3.63	13.57	13.04	6.82	78.51	3.92	9.56	8.81	4.10	79.80	4.22	1.35	15.54	7.57	75.00	4.11	3.28	14.48	5.15	75.00
Max	4.44	19.43	14.04	7.82	80.14	5.28	14.40	13.48	6.72	85.22	4.88	8.12	16.54	8.60	76.89	5.05	8.36	16.00	7.00	78.89
									Frenchman (n = 40)											
Mean	4.22^{a}	2.84^{a}	-	-	99.66^{a}	3.86^{b}	8.69^{b}	2.72^{a}	1.36^{a}	94.25^{a}	4.53^{c}	3.84^{c}	27.56^{b}	11.00^{b}	60.84^{bc}	4.64^{d}	2.53^{d}	11.47^{b}	8.26^{b}	78.86^{b}
SE	0.06	0.23	-	-	0.33	0.10	0.15	0.23	0.15	1.00	0.05	0.34	0.58	0.33	1.00	0.06	0.17	0.67	0.60	0.62
Min	3.95	1.60	-	-	99.00	3.56	7.87	1.69	0.49	86.34	4.31	2.43	26.56	10.64	59.87	4.44	1.43	9.30	6.54	74.29
Max	4.58	3.73	-	-	100.00	4.34	9.35	3.76	2.14	96.55	4.87	5.30	28.70	11.64	62.80	5.01	3.03	17.00	12.22	80.82

OM – organic matter, SE – standard error, Min – minimum, Max – maximum, - not detected

Table 3. 2. Summary statistics of Mahdia goldmine sediments. Different letters indicate statistically significant differences ($p < 0.05$) using Dunn's test between sample zones.

	Mining Operation (n = 36)				Downstream (n = 36)			
	OM (%)	Clay (%)	Silt (%)	Sand (%)	OM (%)	Clay (%)	Silt (%)	Sand (%)
Mean	8.52[a]	5.46[a]	2.53[a]	87.17[a]	7.14[b]	4.34[a]	1.54[a]	91.77[b]
SE	0.43	1.13	0.85	2.00	0.41	0.46	0.16	0.77
Min	4.13	1.00	0.00	52.55	4.13	1.78	0.87	79.34
Max	13.12	23.26	18.83	94.48	17.15	10.71	4.31	96.00

OM – organic matter, SE – standard error, Min – minimum, Max – maximum

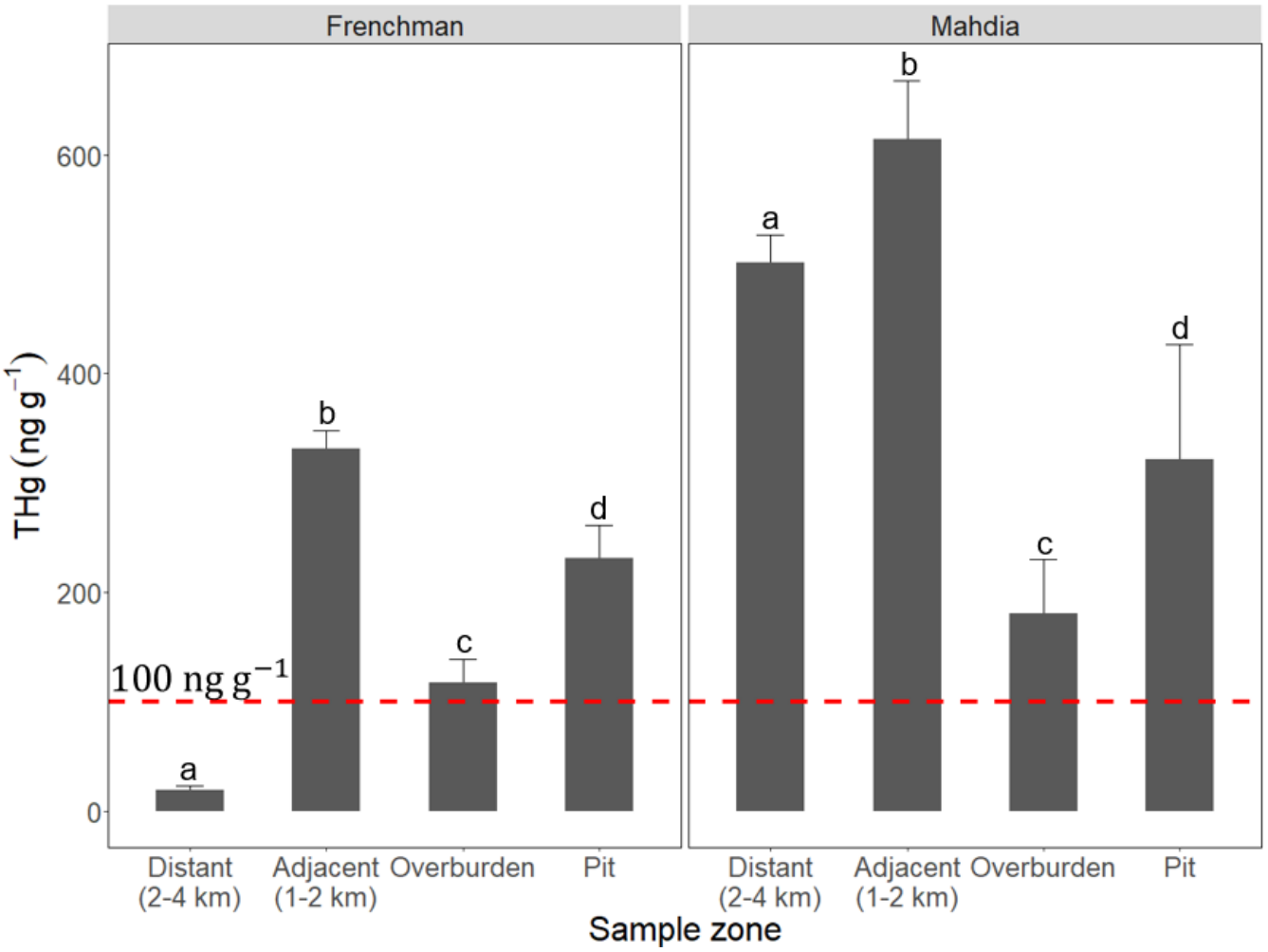

Figure 3. 3. Barplot of Hg in soil according to zone of sampling across Mahdia and Frenchman. Different letters indicate statistically significant differences ($p < 0.05$) using Dunn's test between sample zones. Broken red line indicates EPA recommended guideline for Hg in soil (100 ng g^{-1}). Values in bracket below distant and adjacent sites indicate distance from gold mine.

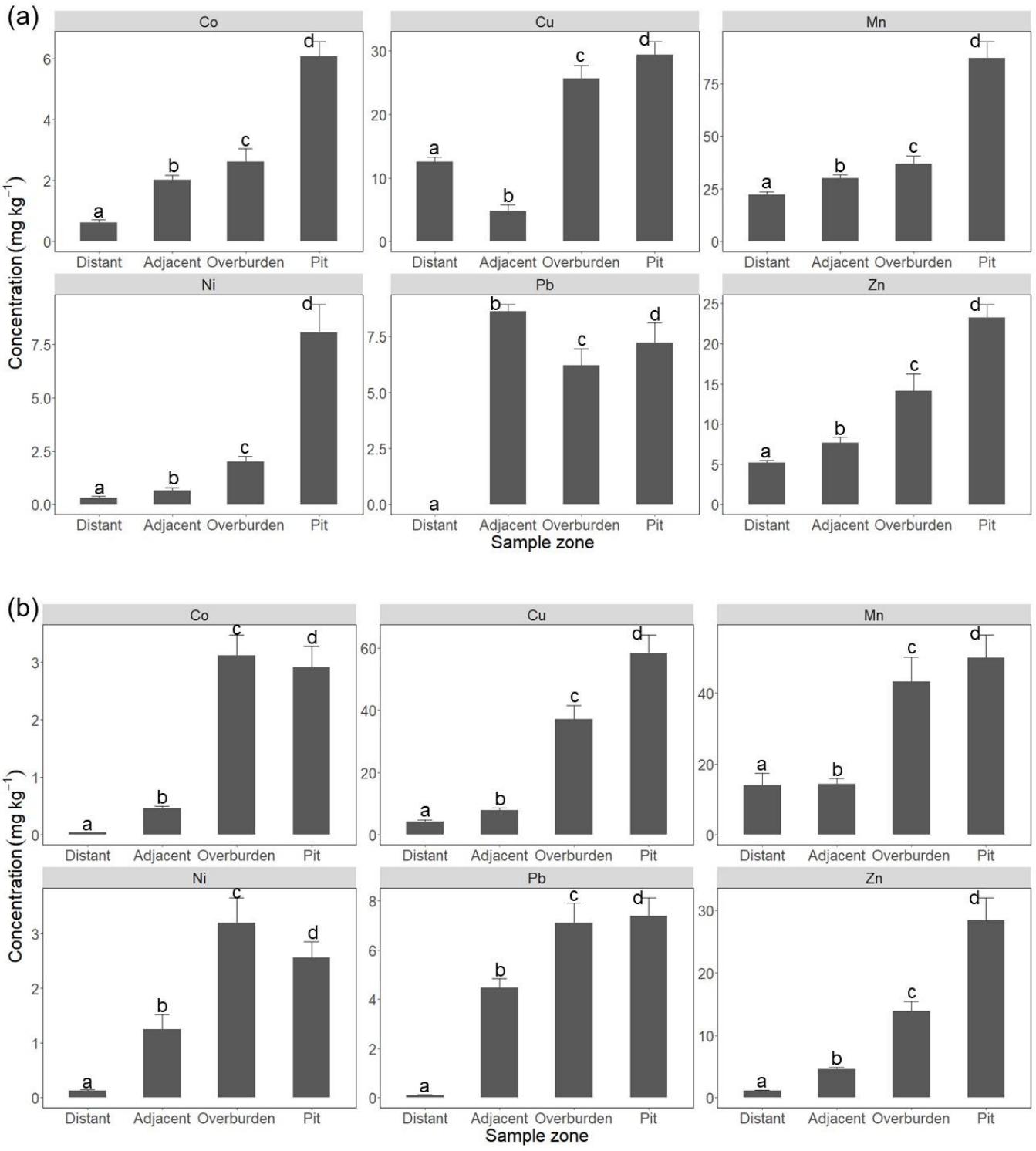

Figure 3. 4. Barplot of metals in soil according to zone of sampling across (a) Mahdia and (b) Frenchman. Different letters indicate statistically significant differences ($p < 0.05$) using Dunn's test between sample zones.

3.3.3 Mercury and metals in surface sediments

Surface sediment Hg concentration from the stream in Mahdia was also highly variable and ranged from 25.17 – 5305 ng g^{-1} and the mean concentration of Hg downstream (1398 ± 292 ng g^{-1}) was similar ($p > 0.05$, Kruskal-Wallis test) to the average concentration measured from within the mining operation zone (1233 ± 223 ng g^{-1}) (Figure 3.5).

Generally, metals (Co, Cu, Mn, Ni, and Zn) were not elevated at the mining operation exposure zone relative to downstream sediment and mean concentrations were often higher downstream (Figure 3.6). The only exception was Pb that had a higher concentration at the mining operation zone compared with downstream. Similar to soil, metal concentrations in stream sediment were low compared with several other studies impacted by gold mining in South America. Arsenic and Cd concentrations in Mahdia stream sediment were also below detection limits (0.01 and 0.02 mg kg^{-1}, respectively).

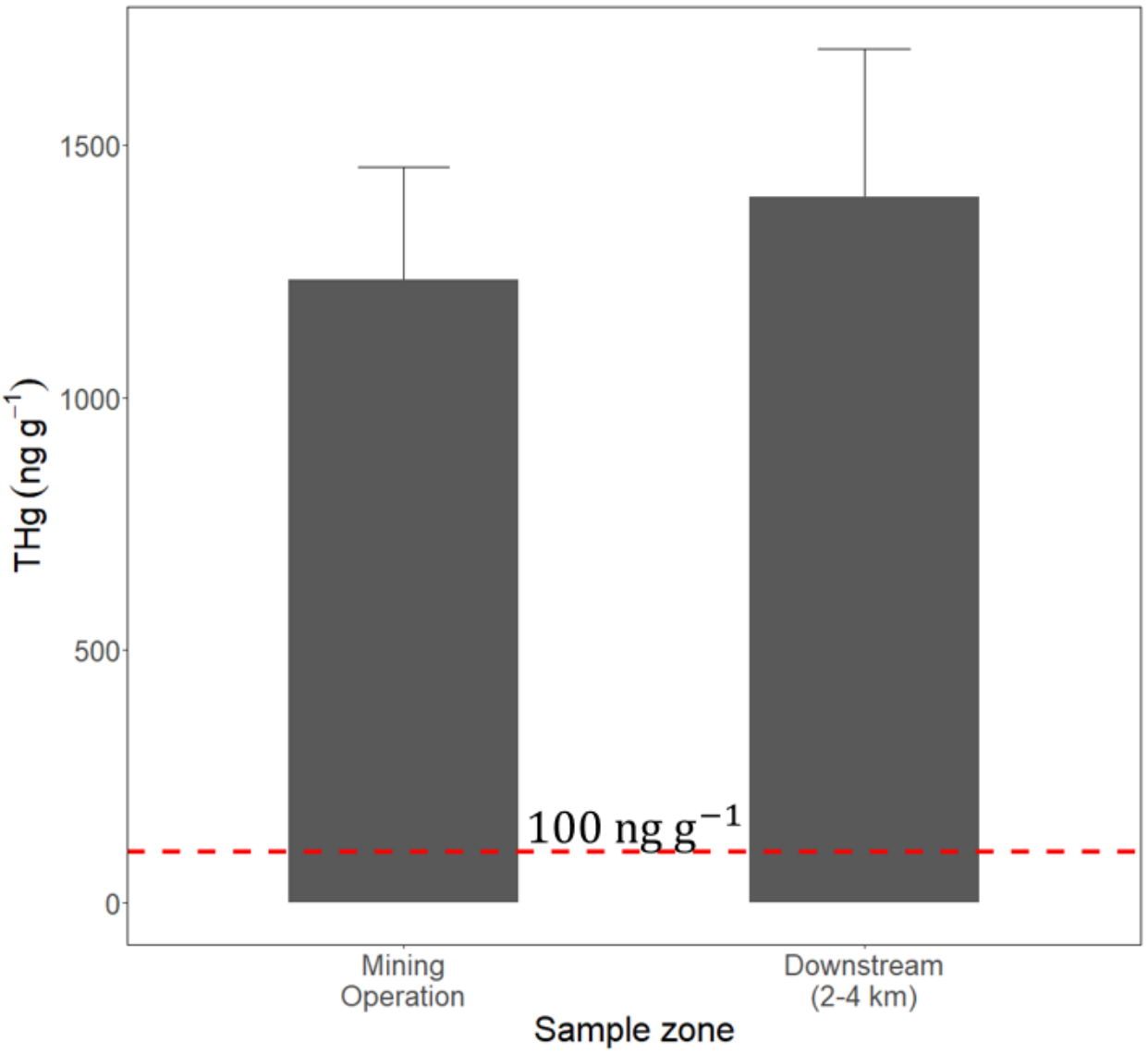

Figure 3. 5. Barplot of Hg in sediment according to zone of sampling across Mahdia. Broken red line indicates EPA recommended guideline for Hg in sediment (100 ng g^{-1}). Value in bracket below downstream site indicate distance from gold mine.

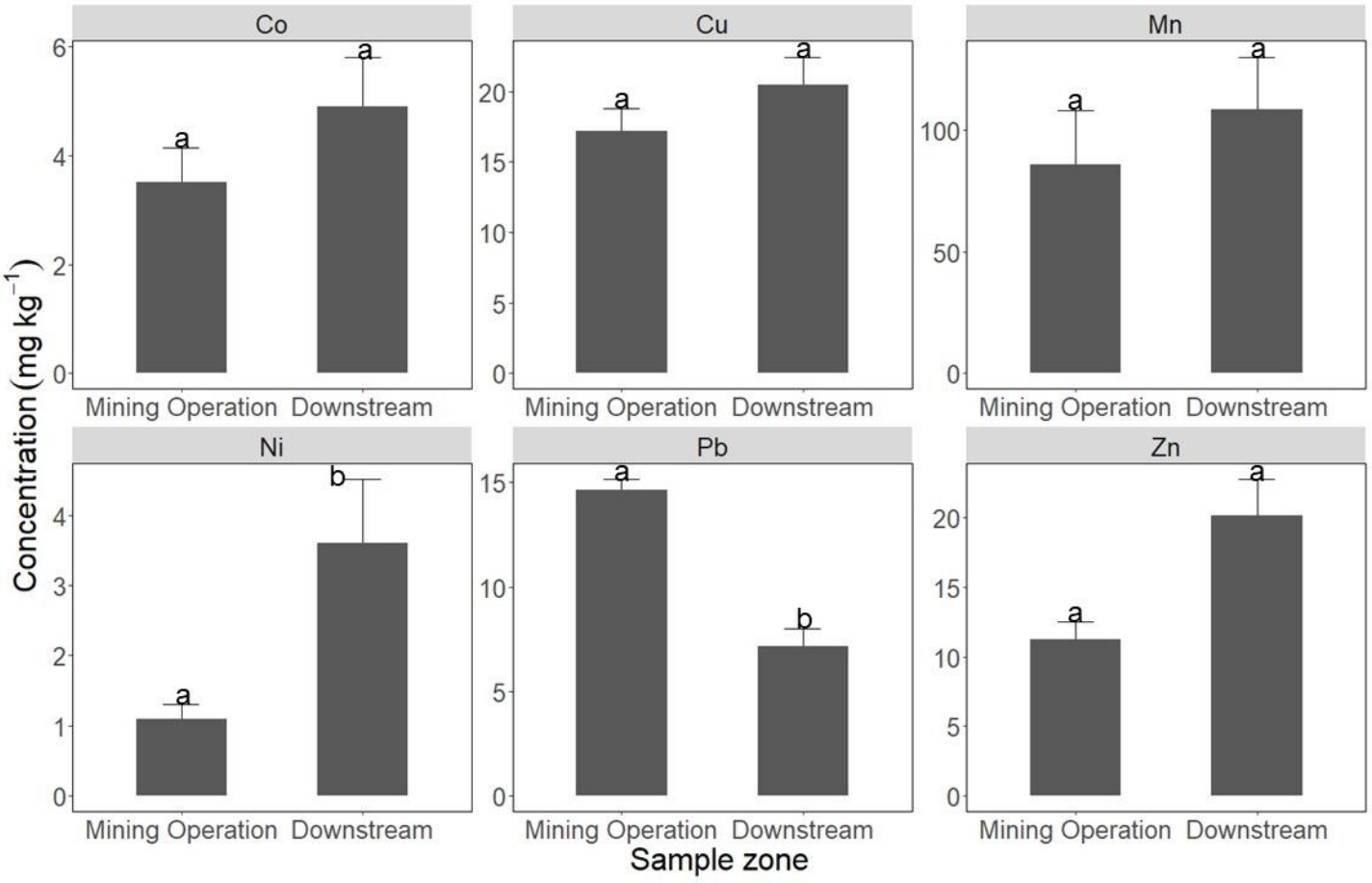

Figure 3. 6. Barplot of metals in sediment according to zone of sampling across Mahdia. Different letters indicate statistically significant differences ($p < 0.05$) using Dunn's test between sample zones.

3.3.4 Relationship among metals and physicochemical properties of soil

The distribution of Hg in soil was very different to the other metals that were more strongly associated with mineral size while Hg was more strongly associated with OM. The PCA analyses of surface soil accounted for ca. 90% of the total variance within the first four axes of data. PC1 was negatively loaded by Co, Cu, Mn, Ni, Pb, Zn, and pH and accounted for 46.49% of the total variance. PC2 accounted for 23.04% of the total variance, with

negative loading on Hg, OM (%), clay (%), silt (%) and positive loading on sand (%) (Figure 3.7). Metals (Co, Cu, Mn, Ni, Pb, Zn) generally positively correlated with each other, soil pH and finer soil fractions (clay and silt), while Hg was more strongly positively related to soil OM (Figure 3.8 and 3.9).

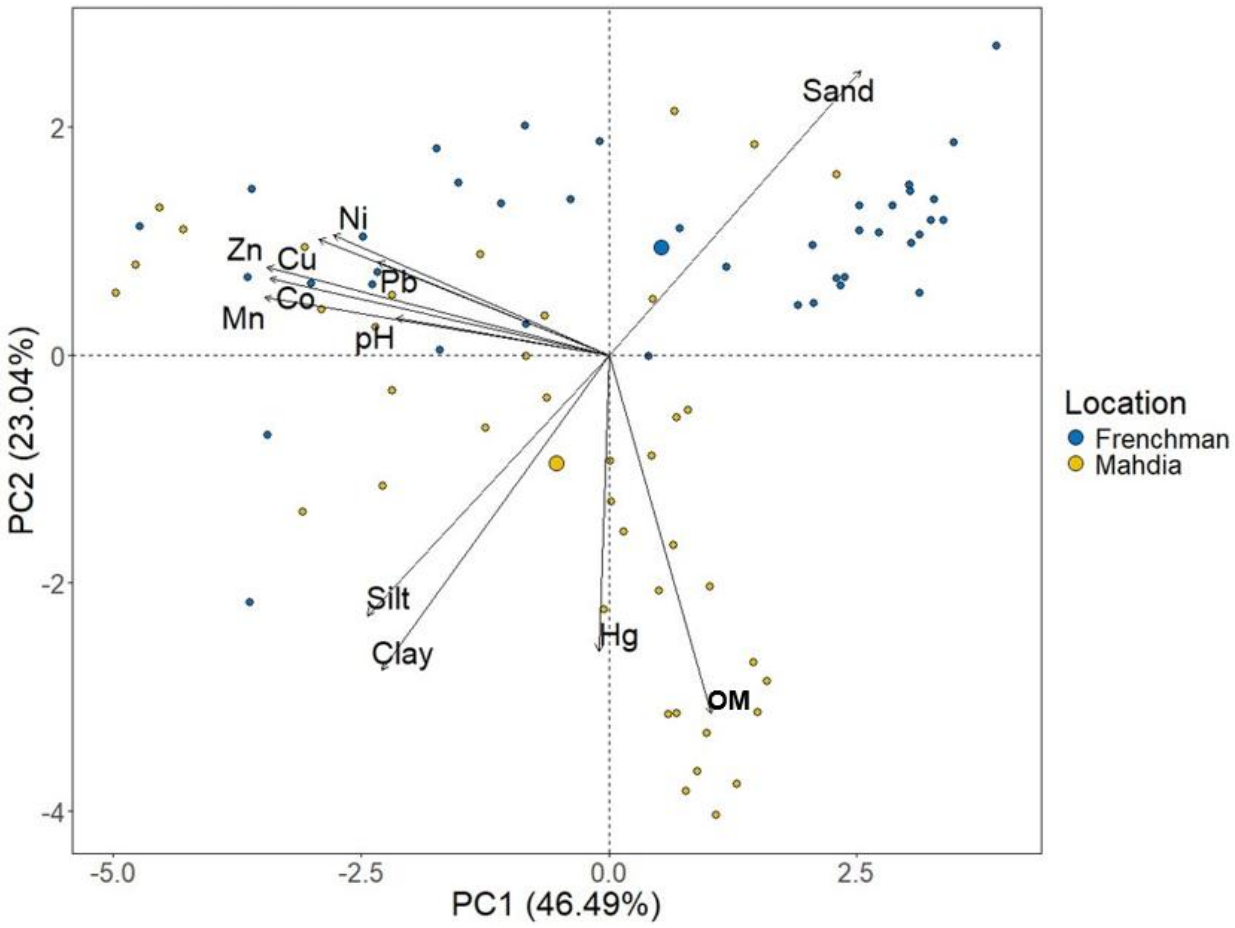

Figure 3. 7. Multivariate statistical representation of Hg and metals in surface soil sampled in Mahdia and Frenchman and loadings on two principal axes (PC1 and PC2), with standardized OM (%), clay (%), silt (%), sand (%), and pH values. Arrows show the scale and direction of correlation vectors for parameters.

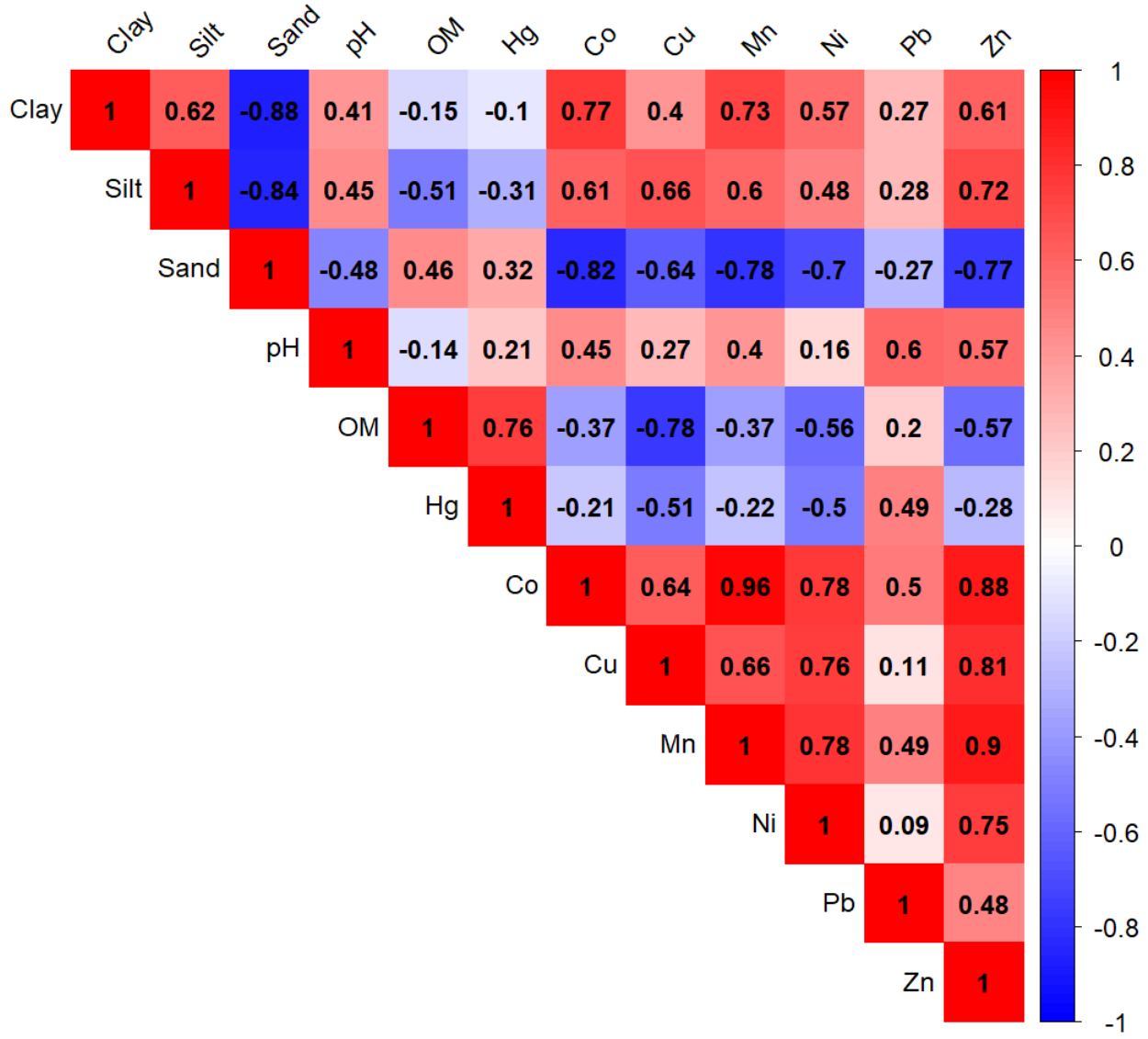

Figure 3. 8. Correlations between soil physicochemical parameters and soil Hg and metals.

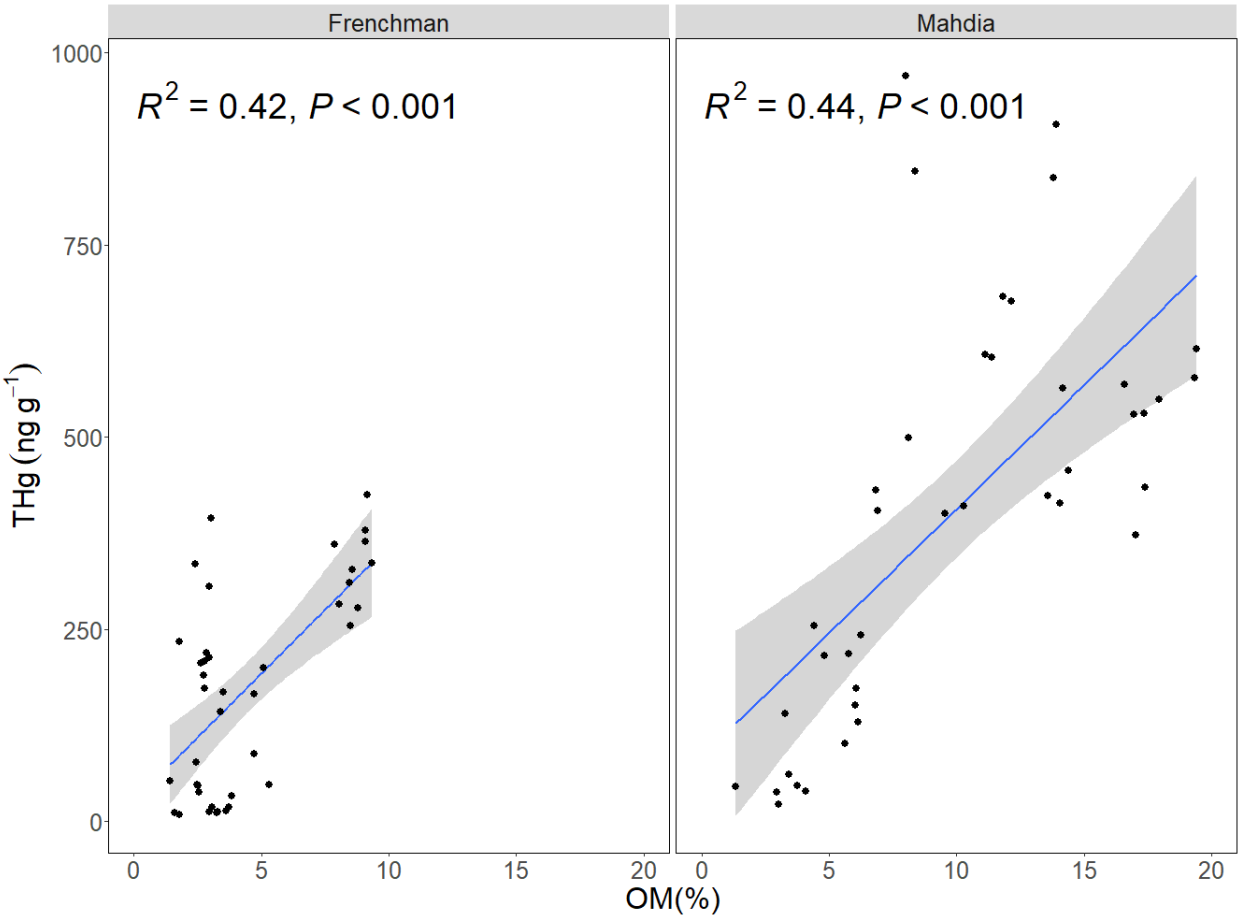

Figure 3. 9. Scatter plot and linear regression between soil OM and soil Hg. The gray shaded area around the solid regression line (blue) represents the 95% confidence interval.

3.3.5 Relationship among metals and physicochemical properties of sediment

The distribution of Hg in sediment was also very different to metals, where Hg was strongly associated with OM. The PCA analyses of Hg and metals in surface sediment accounted for ca. 85% of the total variance within the first four axes of data. PC1 was positively loaded by Co, Cu, Mn, Ni, and Zn and accounted for 38.82% of the total variance. PC2 accounted for 24.73% of the total variance and was negatively loaded by OM (%), Hg, and

sand (%) and positively loaded by clay (%), silt (%), and Pb (Figure 3.10). Mercury was strongly correlated with OM and clay, while metals (Co, Cu, Mn, Ni, Zn) generally correlated with each other but also other physiochemical properties (Figure 3.11).

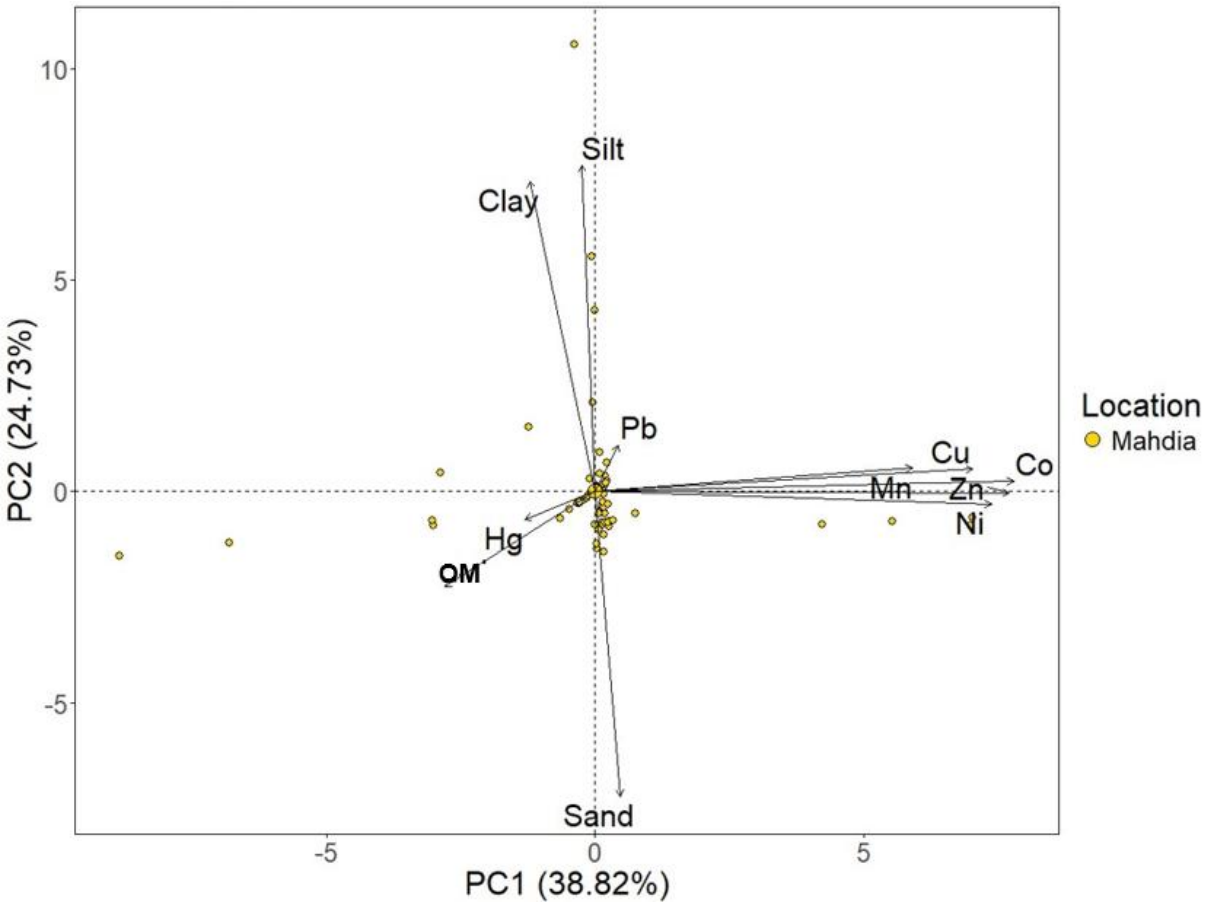

Figure 3. 10. Multivariate statistical representation of Hg and metals in surface sediment sampled in Mahdia and loadings on two principal axes (PC1 and PC2), with standardized OM (%), clay (%), silt (%), and sand (%). Arrows show the scale and direction of correlation vectors for parameters.

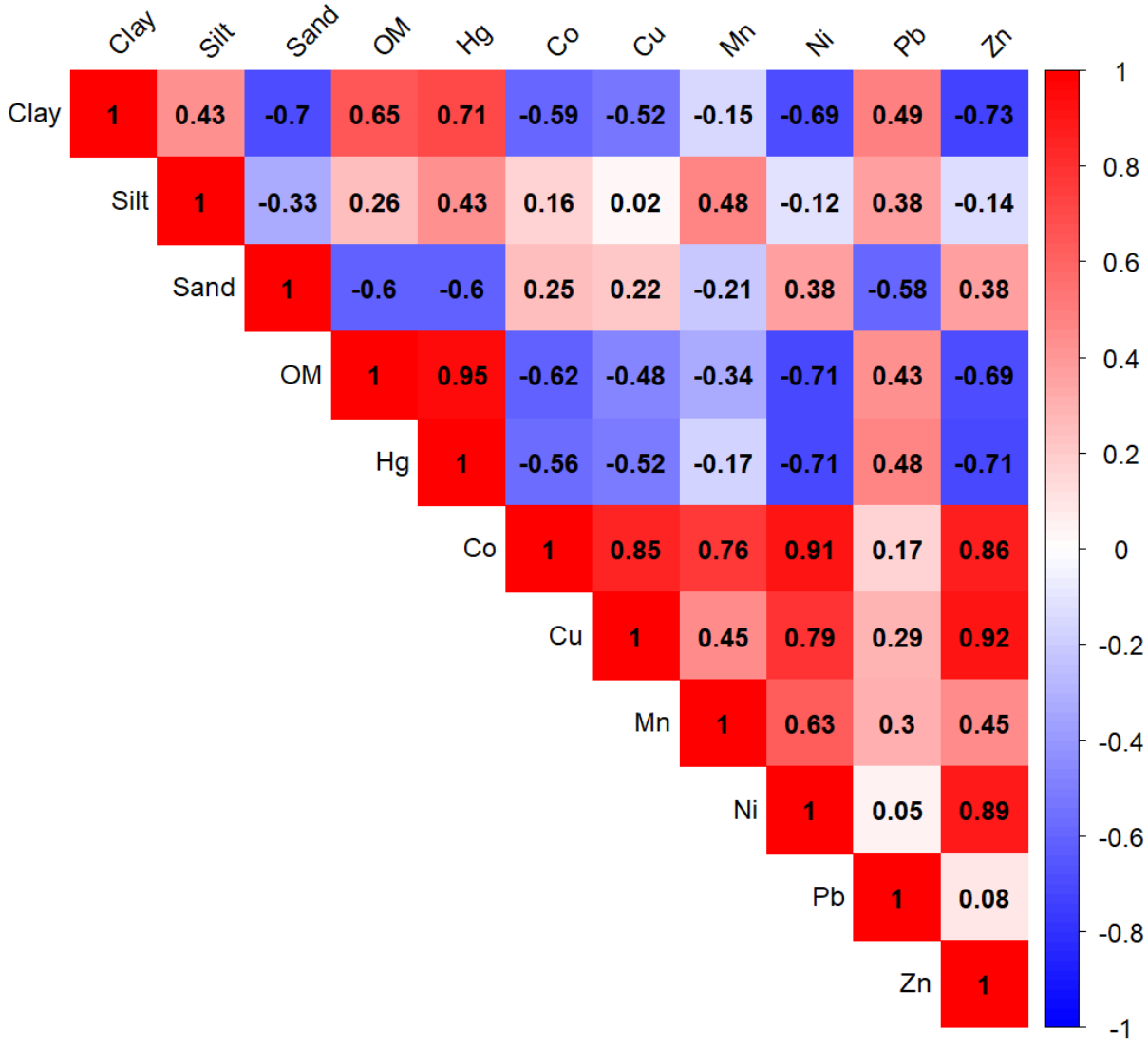

Figure 3. 11. Correlations between sediment physicochemical parameters and sediment Hg and metals.

3.3.6 Sediment Hg:OM relationships

Within the mining area there was a strong positive relationship between Hg and sediment OM (Figure 3.12). Downstream from the mining area (2 – 4 km) sediment Hg was highly variable but was unrelated to sediment OM (Figure 3.12). Leaching experiments showed

that concentrations of Hg released from the overburden, adjacent site and distant site were high (Figure 3.13b) and very similar to each other. In contrast, Hg released from the pit soil was significantly lower. Conversely, dissolved organic carbon (DOC) leached from these soils was much higher at the distant site compared with the 3 other locations, and as a result the Hg/DOC ratio from the overburden zone (104 ± 39 ng mg^{-1}) and adjacent site (73 ± 30 ng mg^{-1}) were about 3 to 8 times significantly higher than the pit (21 ± 6 ng mg^{-1}) and distant site (13 ± 2 ng mg^{-1}) (Figure 3.13).

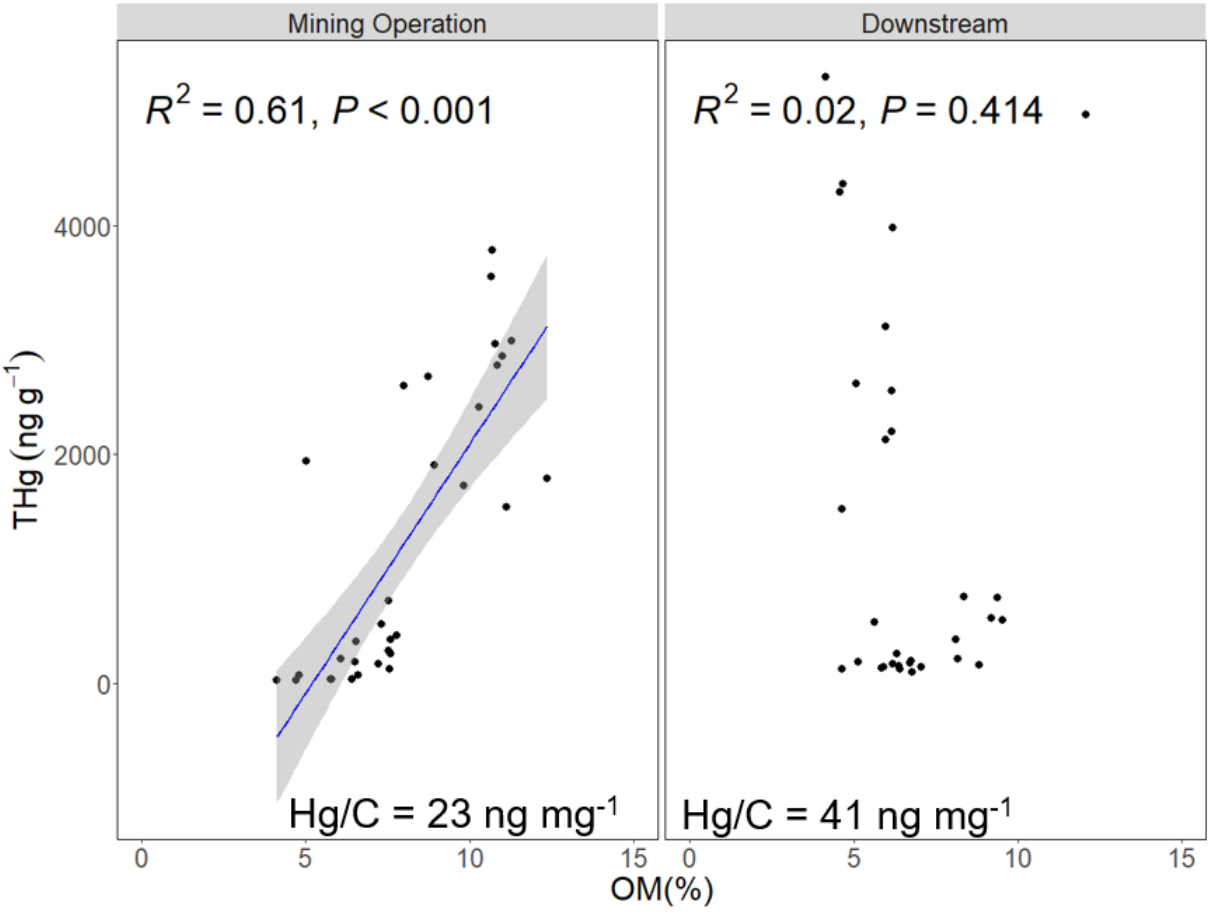

Figure 3. 12. Scatter plot and linear regression between sediment OM and sediment Hg according to exposure zone across Mahdia. The gray shaded area around the solid regression line (blue) represents the 95% confidence interval.

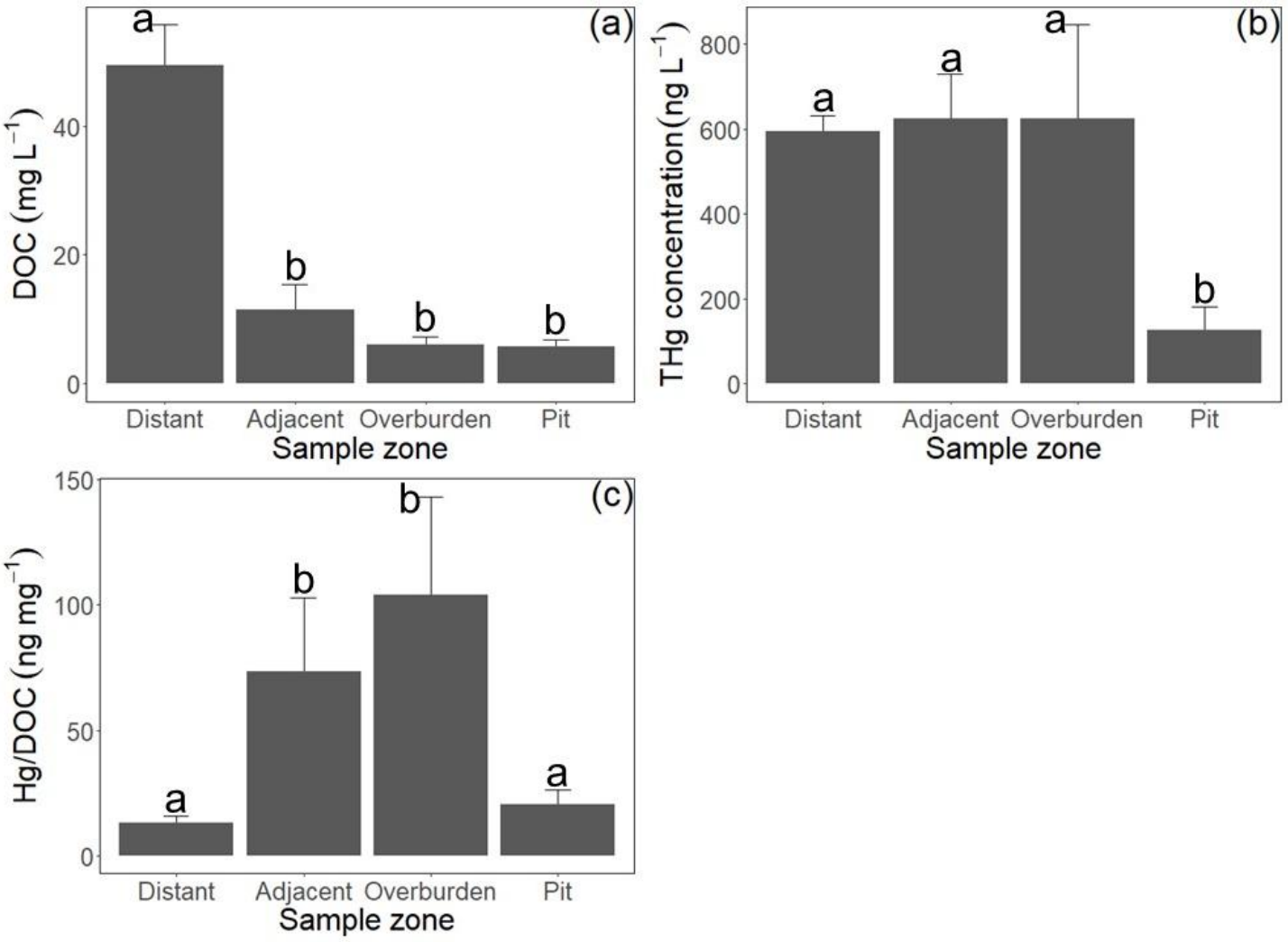

Figure 3. 13. Barplot of (a) DOC, (b) Hg, and (c) Hg to DOC ratio in surface soil runoff according to zone of sampling in Mahdia. Different letters indicate statistically significant differences ($p < 0.05$) using Dunn's test between sample zones.

3.4 Discussion

3.4.1 Mercury and metal concentrations in soil

Concentrations of metals and Hg in soils at the two mine sites were highly variable and exhibited different spatial patterns. Most metals (Co, Cu, Mn, Ni, and Zn) were strongly correlated in soils and were generally significantly higher in pits and overburden compared with distant and adjacent soils, which had lower pH and higher OM. Metals tend to exhibit higher concentrations close to point source since they have different atmospheric behavior in particulate form rather than gaseous form (Poikolainen et al., 2004). The one exception was Pb, which showed elevated concentration in the forest site adjacent to the mine. Notably, the concentrations of these metals fell below the established recommended levels outlined by the Environmental Protection Agency (EPA) and Canadian Council of Ministers of the Environment (CCME). Metals were associated with mined ores and higher clay content that characterizes the mined soils.

Generally, metals that exhibit strong correlation may have the same origin and under specific physicochemical circumstances such as high clay content, similar behaviors are evident (Chen et al., 2023; Tang et al., 2021). The association between metals and higher clay content could be explained by the strong adsorptive sites created by fine particles with larger surface area for metals, which allows soil to immobilize introduced metal ions (Adekiya et al., 2024; Deng et al., 2018; Haghighizadeh et al., 2024). Open-pit gold mining practices in Guyana removes large amounts of topsoil, overburden, and barren rock to get to the ore. Such removal produces large amounts of waste that contain high concentrations of Co, Cu, Ni, Pb, and Zn, which disrupts the natural geochemical cycle in soil (Fashola et al., 2016; Iatan, 2021). The meta-analysis in chapter 2 showed that metal

concentrations in small and medium scale gold mines varied across South America, with some studies showing higher concentrations (Dias et al., 2022; López-Blanco et al., 2015; Pavilonis et al., 2017; Santos-Francés et al., 2017; Teixeira et al., 2018) compared with others (Calabró et al., 2022; Covre et al., 2022; Tume et al., 2018). The levels of metal contamination were much lower than generally observed in South America and were localized to the extent that surrounding soils were largely unaffected. Enriched metals in the gold-bearing ore could be a source of environmental contamination after the gold is separated and the remaining materials are discharged as tailings (Barcelos et al., 2020). However, the sampled pit had limited tailing materials, which explains the lower range of metal concentrations. Metal levels in the overburden were relatively low and this could be attributed to the composition of materials here, which is predominantly topsoil stripped and removed during the mining process without any ore materials. The presence of Pb in the adjacent forest site may be attributed to the combustion of leaded gasoline that is used in trucks, generators, and other machinery at the mine site. Trucks traverse the forested adjacent sites regularly to transport goods and fuel to the mine site. Therefore, fuel spills and combustion of leaded gasoline are likely inputs of Pb in soil at the adjacent sites. Olowoyo et al. (2022) found pollution of Pb in soil taken from sites associated with high traffic and industrial activities were linked to the combustion of leaded gasoline.

Mercury exhibits a different spatial pattern to the other metals in soil and in contrast to other metals it is most strongly related to OM. This is because Hg is not part of the ore but is added during gold extraction and is emitted to the atmosphere during burning. Guédron et al. (2013) reported that Hg concentrations in soil were mainly related to atmospheric inputs from Hg-gold amalgamation. The presence of atmospheric Hg above

natural background levels for the global south (> 1 ng m^{-3}) (Sprovieri et al., 2016) as reported in chapter four (atmospheric Hg monitoring using passive samplers and moss bags within gold mined areas of Guyana) is predominantly received in soil through atmospheric wet or dry deposition and strongly bound to reduced sulfur (S) groups of OM (Biester et al., 2012; O'Connor et al., 2019). Soil Hg concentrations at all sites were very high (exceeding regional background of the Amazon, 100 ng g^{-1}) (Santos-Francés et al., 2011) compared with other studies (Covre et al., 2022; Guédron et al., 2018; Kroonenberg et al., 2022; Miserendino et al., 2018; Velásquez Ramírez et al., 2021). Even at the distant sites Hg was elevated and the higher OM at these sites allowed Hg to accumulate. The meta-analysis (chapter 2) showed small effect sizes for Hg in soil as much of the Hg emitted during the burning of gold can be transported far from the gold mine due to its gaseous form. The atmospheric transport of Hg coupled with its affinity for OM introduced through litter decomposition may explain elevated levels of Hg at distant sites. De Simone et al. (2014) and Slemr et al. (2011) reported that the relatively long lifespan (0.5 to 2 years) of gaseous elemental Hg in the atmosphere results in transport from emission sources, impacting soil at distant locations. Although soil serves as a Hg sink, other factors such as vegetation type influence Hg accumulation in soil (Gruba et al., 2019; Obrist et al., 2018; Xue et al., 2019). Mercury reacts with foliage and enters soils and the patchiness of OM to some degree explains the high variability in soil Hg. Velásquez Ramírez et al. (2021) reported that vegetation cover and soil OM were among the most vital variables contributing to variation of Hg levels in soil of alluvial gold mines in the Peruvian Amazon.

3.4.2 Mercury and metal concentrations in sediments

Metals, except for Pb, were not elevated in the stream sediment in the mining zone relative to the downstream zone. Additionally, metal concentrations were generally low and were not strongly related to physicochemical properties, suggesting that metals were not being exported from soils at the mined areas to the stream. Low metal concentrations were reported in other studies (Palacios-Torres et al., 2020; Zhao et al., 2021) because the soils were not greatly elevated and in contrast to soils, metals in sediments were not related to texture. In contrast, Hg was high in both locations and Hg was strongly positively correlated with OM and clay, but when separated only the mining zone demonstrated a relationship between Hg and OM. This suggests that Hg enters the stream with smaller organic rich particles within the mining zone. Sediment Hg loadings reported in this study are similar to previous studies of gold mining sites in Guyana, French Guiana, and Suriname that utilize Hg amalgamation methods (Howard et al., 2011; Laperche et al., 2014; Ouboter et al., 2012). The meta-analysis (chapter 2) also confirmed Hg concentration in sediment that exceeds EPA guidelines despite a small effect size. Elevated Hg in sediment poses high environmental risk since it can be converted to methylmercury in sediments through methylation of inorganic Hg by microorganisms under anaerobic conditions. Methylmercury is the more toxic form because it biomagnifies along the food chain, resulting in greater environmental and human health concerns (Helmrich et al., 2021; Wang et al., 2024). In most aquatic systems, Hg is predominantly associated with OM and the binding to OM in these natural systems appears to be by reduced sulfur (S) groups at concentrations high enough to bind all Hg (Eckley et al., 2021; Grigal, 2003; Koskey et al., 2020; Lavoie et al., 2019; Pinedo-Hernández et al., 2015; Skyllberg et al., 2000). The

findings reported here were also comparable to global studies across Colombia (Pinedo-Hernández et al., 2015), Ghana (Donkor et al., 2005), India (Chakraborty et al., 2015), Ontario (Coquery & Welbourn, 1995), and Brazil (Fragoso et al., 2018) that found significant positive relationships between Hg and sediment OM. Mercury concentrations reported in Colombia (524 ± 257 ng g^{-1}) and Ghana (265 ± 137 ng g^{-1}) exceeded natural background levels (100 ng g^{-1}) due to gold mining activities, which is a cause for concern given the high risk of environmental contamination. However, lower Hg concentrations were reported in India (65 ± 17 ng g^{-1}), Ontario (64 ± 19 ng g^{-1}), and Brazil (84 ± 9 ng g^{-1}), indicating limited anthropogenic influence.

Elevated Hg concentration downstream was consistent with the fact that Hg can be transported in the atmosphere due to its volatility in elemental form, which results in mobility. Sites farther away from the emission source may have higher soil OM which would bind Hg, but the amount of Hg bound to OM changes by location. For example, at the overburden and adjacent site Hg/DOC was significantly higher than the pit and distant site, reflecting elevated anthropogenic Hg inputs at these locations. The narrow range of DOC with elevated Hg concentration is due to direct excavation for gold mining activities that alters land cover, thereby removing OM from surface soil (Xue et al., 2019). Soil retrieved from gold mines experienced copious amounts of Hg released directly from gold amalgamation that tend to overwhelm the natural Hg/DOC relationship. Mercury bound to OM could also be transported within the stream and deposited further downstream given the direct influence of the overburden zone on the stream that drains the Mahdia mine site. As a consequence, the sediment at the downstream sites receives OM from multiple sources, each with likely varying Hg/C relationships which contrasts with the mine sites

where the relationship is likely more uniform. Also, the spatial distribution of sediment downstream (Figure S3.1) could be influenced by other stream channels that promote the mixing of contaminated and uncontaminated sediments. Surface runoff of Hg bound to soil OM has been suggested as an important input of Hg in sediment (Xue et al., 2019). The risk of Hg laden sediments from the mining zone to downstream is increased through runoff processes from gold mining sites (Donkor et al., 2005; Velásquez Ramírez et al., 2021).

Organic matter molecular weight and functional groups type and number affect its ability to bind Hg, where high molecular weight OM has fewer binding sites (Chen et al., 2022). Chakraborty et al. (2015) reported that the type of terrestrial OM and residence time in the stream, could modify OM. Mercury levels in Amazonian soils (which Guyana is apart) are high compared to temperate zones, primarily due to soil pedogenesis and high atmospheric depositions. Therefore, these soils constitute a vital reservoir of naturally accumulated Hg with the potential to be mobilized via anthropogenic (gold mining) or natural (deforestation) erosion. Such mobilization could lead to increased export of terrestrial Hg to aquatic ecosystems (Laperche et al., 2014). Factors such as Hg handling and practices during the gold recovery process could influence observed Hg loadings in sediments (Howard et al., 2011). The levels of terrestrial Hg (atmospheric deposition and concentration in soil) reported in this study could partially explain Hg found in studied sediments, given the export mechanism. These findings corroborates with that of Velásquez Ramírez et al. (2021) which reported the possible link of elevated Hg levels in sediments to the transport of Hg contaminated soil from stripped landscapes where gold mining occurs.

3.5 Conclusion

Gold mining has led to high levels of Hg deposition to terrestrial and aquatic ecosystems. Metals were not a concern given the low concentrations (below permissible limits) reported in the soil and sediment of sampled gold mines. The concentrations of Hg reported in this study suggest much higher contamination in soil and sediment that is not localized to the mine site. The correlation between Hg and OM in soil and sediment suggests that OM is a major factor affecting Hg accumulation. The elevated levels of Hg in sampled gold mines above regional background could be linked to the process of gold recovery, where the amalgam is burned, followed by wet and dry deposition of Hg from atmosphere which interacts with soil and sediment. The overburden and adjacent site Hg/DOC were significantly higher than the pit and distant site, indicating elevated anthropogenic Hg inputs at these locations and possible leaching to stream sediments.

4.0 Atmospheric Hg monitoring using passive samplers and moss bags within gold mined areas of Guyana

4.1 Introduction

Natural and anthropogenic emissions of mercury (Hg^0 and Hg^{2+}) into the environment have become a global concern. Most of the observations related to atmospheric Hg are gaseous elemental Hg (GEM) or total gaseous Hg, which are operationally defined fractions based on methods used. Gaseous elemental Hg (Hg^0) constitutes more than 95% of atmospheric Hg while the remaining fraction is made up of a mixture of oxidized/reactive gaseous Hg and particulate bound Hg species (Floreani et al., 2020; Vardè et al., 2022). The volatile nature of Hg^0 results in a residence time that falls between 0.5 and 2 years in the atmosphere. This extended lifetime of Hg in the atmosphere coupled with its ability of long range transport and settling on soil surfaces via dry and wet deposition, pose a major threat to ecosystems and human health (Buck et al., 2019; De Simone et al., 2014; Driscoll et al., 2013; Slemr et al., 2011; Tomiyasu et al., 2020). Therefore, understanding atmospheric transport is critical for understanding inputs of Hg to ecosystems. The adoption of the Minamata Convention by various country parties (including Guyana) to protect the environment and human health from Hg emissions, signals a global commitment to addressing concerns related to this toxic pollutant (UNEP, 2013). As a signatory to the convention, Guyana is guided by Article 22 of the convention, which requires formal assessment through *"comparable monitoring data on the presence and movement of mercury and mercury compounds in the environment"*. The importance of environmental monitoring is also highlighted by Article 19 of the convention (UNEP, 2013). Given the

strong emphasis placed on monitoring of Hg in the environment, the need exists for more research in Guyana to monitor atmospheric Hg emissions from gold mining, which serves as the largest emitter of Hg in Guyana.

The use of large amounts of Hg (ca. 675 – 1000 tonnes per year) in small and medium scale gold mining shifted the major emission source of atmospheric Hg from the Global North to the Global South (Gerson et al., 2022). However, little is known about the levels of atmospheric Hg emissions and accumulation across small and medium scale gold mines in Guyana. Guyana still utilizes Hg (10 – 25 tonnes per year) in small and medium scale gold mining (Canuel et al., 2009; Esdaile & Chalker, 2018). This method of gold extraction is applied extensively since it is cheaper than most of the alternative measures, is simple and quick, and can be applied independently by one person. However, most of that Hg is emitted to the atmosphere when amalgamation followed by burning is done in the absence of a retort (Gibb & O'Leary, 2014; Gyamfi et al., 2021). The retort is a condenser apparatus that cools the produced Hg vapor from amalgam heating, recovering Hg in its liquid form for reuse (Esdaile & Chalker, 2018). Gerson et al. (2022) reported elevated Hg (up to 10.9 ng m^{-3}) in the atmosphere for areas in the Peruvian Amazon adjacent (ca. 1 km away) to gold mines and this was attributed to Hg-gold amalgam burning.

The spatial distribution and dispersion of Hg can be influenced by anthropogenic emissions of Hg from small and medium scale gold mining activities (Casagrande et al., 2023). Gold mining activities in Guyana utilize metallic Hg, to separate gold particles from ore and other impurities, resulting in a visible Hg-gold amalgam. Periodic burning of the amalgam at the mining site occurs approximately every two weeks once enough ore has

been processed and these burns last for about 2 hours. This leads to direct evaporation of Hg into the atmosphere, dispersing into the environment (Casagrande et al., 2023). Around gold mining areas that are subject to such Hg contamination, elevated levels of Hg can be found in adjacent forests and nearby vegetation given the leaves large surface area that facilitates high adsorption of atmospheric Hg (Casagrande et al., 2023; Gerson et al., 2022). These large leaves are present in the upper forest strata such as arboreal, underwood, and herbaceous which continually receive atmospheric Hg due to numerous leaf crevices, trichomes, and cuticle surface area (Casagrande et al., 2023; Rea et al., 2001). Improved understanding of Hg transport and mechanisms of deposition to ecosystems requires accurate atmospheric monitoring, since the atmosphere is the main pathway for the distribution of Hg throughout different environmental media (Driscoll et al., 2013; Naccarato et al., 2021). In this context, atmospheric monitoring networks such as the Global Mercury Observation System (GMOS) was developed in the quest to establish a global atmospheric Hg measurement network, with several monitoring sites (>40) distributed globally. Following the launch of the GMOS, interest continues to grow for improved global Hg monitoring through increased spatial resolution of gaseous Hg data, particularly in remote locations and in developing countries (such as Guyana) to meet the objectives of the Minamata Convention (Naccarato et al., 2021; Pirrone et al., 2013).

Monitoring of atmospheric Hg within gold mining sites is key to understanding local cycling and fate of Hg. Passive air sampling is a low-cost no-power approach to monitoring atmospheric Hg (Jeon et al., 2020). Mercury passive air samplers (*Mer*PAS® from Tekran) are useful for monitoring of atmospheric Hg within gold mining areas, given the ability to provide time-averaged concentrations of Hg over the timescale of days to

months (Naccarato et al., 2021). The *Mer*PAS captures GEM by diffusive uptake and accumulation onto a sulfur-impregnated activated carbon sorbent within a protective shield and utilizes a diffusive barrier to control the sampling rate (Gačnik et al., 2024; Jeon et al., 2020; Mclagan et al., 2018; McLagan, et al., 2016). Air monitoring could also be supplemented with inexpensive active moss biomonitoring. The moss bag technique is based on the direct uptake of atmospheric Hg or the oxidation of Hg^0 to Hg^{2+} into the tissue of moss (Bargagli, 2016; Lodenius, 1998). The simple and cheap approach to Hg biomonitoring with mosses facilitates the identification of hotspots of anthropogenic emissions and assessment of spatial changes in patterns of Hg deposition (Bargagli, 2016). Mosses are widespread in nature and are used to evaluate regional patterns of atmospheric metal deposition, but some uncertainties exist when estimating deposition fluxes and concentrations of atmospheric Hg (Bargagli, 2016; Cowden & Aherne, 2019; Zhou et al., 2017). Therefore, caution must be exercised when estimating atmospheric Hg from moss samples, given the time needed for mosses to equilibrate elemental composition with changing atmospheric chemistry (Bargagli, 2016). Despite the challenges with moss biomonitoring estimates, the impact of different species and elevation of sampling locations, the pattern of Hg deposition derived from surveys with moss could provide a better measure of net supply of Hg to terrestrial ecosystems compared to data from wet deposition measures and model calculations (Schröder et al., 2010).

Continuous monitoring of atmospheric Hg in remote gold mines of Guyana can be expensive. Active moss biomonitoring and passive air sampling offers an efficient, cost-effective, and simple approach to evaluating patterns in atmospheric Hg deposition within gold mines. Brown et al. (2020) assessed Hg pollution from gold shops in Guyana using

portable Hg vapor monitor and lumex RA-915M spectrometer, but no study in Guyana has assessed Hg emissions from gold mining areas. The purpose of this study was to assess atmospheric Hg concentrations around a gold mining area using *Mer*PAS monitoring and active moss biomonitoring over a longer term (90 days) and a short-term (2 days) period during which a burn occurred. Additionally, the relationship of moss Hg to soil Hg was assessed. It is hypothesized that Hg concentration in active moss would be correlated to air concentrations obtained from passive samplers, the relationship between moss Hg and Hg air concentration would differ owing to Hg loss from moss during periods without burning and Hg release, and much higher Hg values measured during the 2 days compared with the 90 days exposure. It was also expected that soil Hg concentrations will be more closely associated with organic matter (OM) than moss Hg concentrations deployed at the same location.

4.2 Methodology

4.2.1 Study area

Atmospheric monitoring of Hg was done across Mahdia in the mining district of Potaro (5° 18’ 36” N and 59° 18’ 16” W) in Guyana (Figure 4.1). The Mahdia zone general wind direction is from the east and is characterized by many active small and medium scale gold mines. Annual precipitation varies from 2,200 to 4,000 mm and mean annual temperature ranges between 23 to 32 ℃ (GLSC, 2013). Sampling sites were accessed by means of trails and a land cruiser. The study area experienced an upsurge in small and medium scale gold mining activities in recent years (Laing et al., 2023).

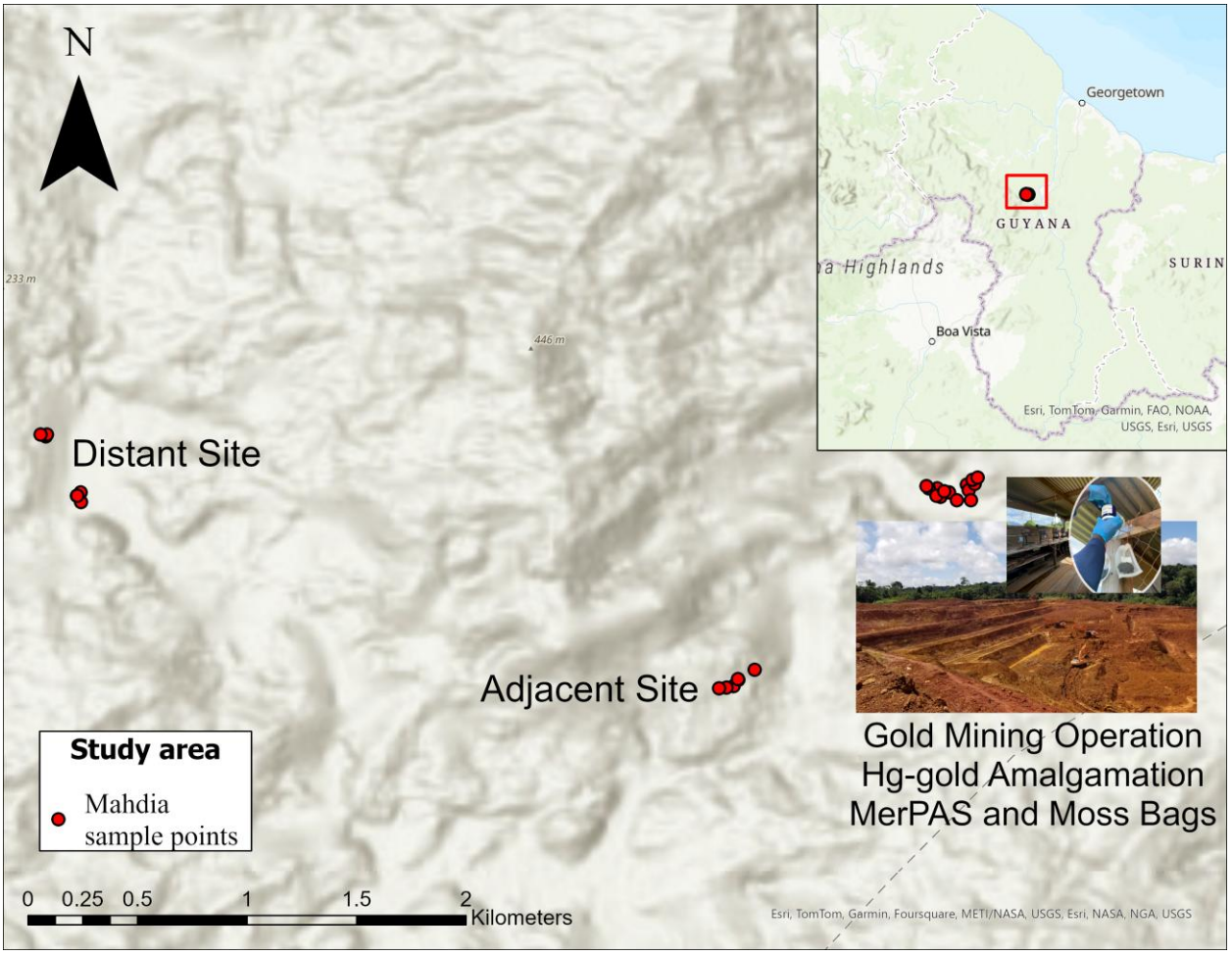

Figure 4. 1. Map of study area.

4.2.2 Preparation of moss bags and passive samplers

The moss *Ptychomitrium* spp. (greenest and youngest) was collected from an uncontaminated area that is isolated (200 km) from mining areas (6° 51’ 59.4” N and 58° 16’ 44.4” W). The use of one species of moss throughout aids in overcoming challenges of biomonitoring estimates with different species. Following the removal of other plant material, samples were triple-washed with distilled water while shaking to remove adhering particles (Lodenius, 2013). Each nylon mesh bag (15 x 10 cm, mesh size 1 mm) and Ziploc® bag (field blanks) received ca. 15 g (wet weight) of moss tissue. Pre-

assembled elemental Hg passive samplers (*Mer*PAS) came from Tekran Instruments Corporation (Toronto, Canada) for field application.

4.2.3 Atmospheric Hg sampling

Moss bags and *Mer*PAS were deployed across the gold mining site in Mahdia (Figure 4.1). The sample location was separated into three zones (mining operation, adjacent site (1 – 2 km from source of gold mining with vegetation), and distant site (2 – 4 km from source of gold mining with vegetation). Moss bags (n = 90) and *Mer*PAS (n = 11) were randomly deployed (suspended on nearby trees and buildings) in clusters for ca. 90 days (May to August 2023, long-term) and two days (July 2024, short-term) in each zone, taking into consideration wind direction. The short-term period (two days) of monitoring only focused on exposure near the burning station (ca. 150 m radius within mining operation zone) to capture emissions during the burning of gold. To better capture peak atmospheric Hg concentration during the burning of gold, short-term monitoring was done in the mining operation zone, since atmospheric Hg was expected to decline tremendously beyond 1 km of the mining operation zone. The mining operation zone received 70 moss bags and 7 *Mer*PAS and 10 moss bags and 2 *Mer*PAS at the adjacent and distant sites. Moss bags and *Mer*PAS (lost one to vandalism) were stored in sealed and labelled Ziploc® bags for transport to the laboratory for analysis. Surface (0 – 10 cm) soil samples (ca. 100 g, n = 25) were also taken at each moss bag location to gain some insights into possible redisposition and cycling of Hg. Moss samples were oven dried (Thermo Scientific, Freas 645) at 40°C for 70 hours and pulverized in a SPEX 8000D Mixer/Mill. Soil samples were oven-dried for 10 days at 105°C (Thermo Scientific, Freas 645), homogenized and sieved (2 mm). These samples were packaged into another Ziploc® bag for storage at 4°C to avoid any

contamination until transport to Trent University Environmental Geoscience laboratory for analysis. A small amount of Hg may also have been lost during the drying procedure as Hojdová et al. (2015) reported that the loss of Hg in samples dried at 105℃ was 3 % compared with freeze dried samples.

4.2.4 Analysis for atmospheric Hg concentration

The concentrations of other metals (As, Cd, Co, Cu, Mn, Ni, Pb, and Zn) in moss were measured by inductively coupled plasma-mass spectrometry (ICP-MS) following acid digestion (HNO_3, not a total digest). Metal concentrations in moss were low (Table S4.1), with no significant difference among location, confirming the findings of chapter 3 (characterizing Hg and other metal concentrations in soil and sediment within gold mined areas of Guyana), where metals were not elevated in sampled soils away from the mine. Therefore, Hg concentration in moss samples was the focus given the main use of Hg in gold amalgamation. Total Hg concentration in moss (retrieved from ca. 90 days exposure) and surface soil samples were measured with a Direct Mercury Analyzer (DMA-80) by thermal decomposition, amalgamation, and atomic absorption spectrometry. Sub-samples of dried moss and soil (0.05 g) were heated to 900℃ to reduce Hg species to elemental Hg, which was loaded onto an amalgamator. Subsequent heating of the amalgamator resulted in the release of Hg vapors into a single bean, fixed wavelength atomic absorption spectrophotometer. Quality control of Hg measurements was assured by the inclusion of blanks and apple leaves certified reference materials (NIST 1515) at the start of each experimental run (40 samples) and recovery ≥ 93 % was considered acceptable.

Soil organic matter (%OM) was measured by loss-on-ignition (Equation 1). After oven-drying (24 hours at 105℃) of soil (5 g) to constant weight, organic matter was ignited at 400℃ for 10 hours (Heiri et al., 2001).

$$\%OM = \left(\frac{W_1 - W_2}{W_1 - C_w} \right) \times 100 \qquad \text{Equation 2}$$

Where, W_1 = weight pre ignition, W_2 = weight post ignition, and C_w = crucible weight.

Total Hg concentration in moss samples retrieved from the two days deployment was measured with a Tekran 2600-CVAFS Mercury Analysis System by cold vapor atomic fluorescence spectrometry because initial runs using the DMA-80 were off-scale. Moss samples were subjected to an acid digestion (7 HNO_3: 3 H_2SO_4) process, which is a total digest. A sub-sample of dried moss (0.05 g) was added to each 40 ml glass vial, followed by 5 ml of digestion acid (HNO_3/H_2SO_4). Vials were swirled gently to ensure complete mixing with digestion acid. Vials with a clean marble on top were placed in a block-digester and hot plate (Fisherbrand®) for 14 hours hot at 110℃. Following the completion of acid digestion, the volume was adjusted to 25 ml with deionized water and allowed to cool. Digested samples were stored at room temperature in the dark until analysis. Calibration standards of 0 pg, 25 pg, 50 pg, 100 pg, 250 pg, 500 pg, and 1000 pg were prepared with 1 ng ml^{-1} diluted Hg standard. Digested samples were diluted to desired concentration and 60 µl of 20 % Sn_2Cl in 10 % HCl was added to each vial (final volume of 25 ml) for analysis. Vials were capped with septa caps and shaken before loading the autosampler. Water blank (no reagent), blank reagent, and digested apple leaves standard reference material (NIST 1515) were run with each batch of samples to ensure quality control and recovery ≥ 95 % was considered acceptable.

*Mer*PAS retrieved from the 90 days and two days exposure were measured by Tekran Instruments Corporation (Toronto, Canada) according to appropriate trace-clean procedures to avoid incidental contamination. The stainless-steel mesh screen containing the carbon sorbent was removed from the elemental Hg passive sampling body. *Mer*PAS retrieved from the 90 days deployment was measured by thermal combustion according to EPA Method 7473 on a Nippon MA-3000 Mercury Analyzer using cold vapor atomic absorption spectrometry to measure Hg. *Mer*PAS retrieved from the two days exposure was initially set up for thermal combustion according to EPA Method 7473 on a Nippon MA-3000 Mercury Analyzer using cold vapor atomic absorption spectrometry to measure Hg. However, similar to moss samples, the very high sample concentrations required a wet digestion process according to EPA Method 1631 on a Tekran 2600-IVS using cold vapor atomic fluorescence spectrometry to measure Hg. Quality control of Hg measurements was assured by the calibration of instrument against NIST 3133, calibration against certified reference materials NIST 2685C (bituminous coal matrix), inclusion of blanks, and recovery ≥ 95 % was considered acceptable. Due to the mass limitations of the analytical technique, the *Mer*PAS carbon was divided into multiple sample aliquots and the results summed to give the total Hg captured on each *Mer*PAS. The sampled air volume was determined based on the deployment interval and the white-bodied elemental Hg passive sampling rate of 0.111 m^3 day^{-1}.

4.2.5 Statistical analysis

Statistical analysis was conducted with R version 4.0.4 (R Core Team, 2021), at an acceptable α-level of 0.05. Descriptive statistical analysis was conducted with R statistical

package to assess Hg concentration range, mean, and standard error. Data was subjected to Shapiro-Wilk normality test to assess normal distribution.

Exponential models were used to evaluate the relationship significance between atmospheric Hg and distance from mining operation. Spearman correlation was used to determine if moss Hg concentration is related to gaseous elemental Hg concentration. Equations (slopes) of the relationship between gaseous elemental Hg concentration and moss Hg concentration over long-term (90 days) and short-term (two days) exposures were used to extrapolate Hg relationship between moss and *Mer*PAS based on the assumption of multiple burns over an extended period. Bayesian log empirical kriging with ArcGIS Pro 2.9.0 (Esri, 2021) was used to geospatially interpolate and map spatial variation of atmospheric Hg (derived from active moss biomonitoring) in the mining operation zone, which had the required density of samples relative to emission source over long-term (90 days) and short-term (two days) exposure. The experimental variogram model used to generate atmospheric Hg concentration maps was based on log transformed concentration data using Bayesian empirical kriging to enhance the visualization of concentrations spatial distributions (McLagan et al., 2021). Linear regression analysis was done to assess the effect of OM and moss Hg on soil Hg concentration.

4.3 Results

4.3.1 Active biomonitoring of Hg with moss and MerPAS monitoring

4.3.1.1 Long-term exposure (90 days)

Large variability in atmospheric Hg was evident across the sampled gold mine in Mahdia during the long-term exposure, with the mining operation zone demonstrating a higher

range of concentrations in moss (87.0 – 1963 ng g^{-1}) and *Mer*PAS (41.2 – 144 ng m^{-3}) compared with forested sites (adjacent and distant) (Table 4.1). Atmospheric Hg concentrations exceed natural background levels for the global south (1 ng m^{-3}) (Sprovieri et al., 2016) at all locations and show an obvious pattern of declining Hg with increasing distance from mining operation and source of burning (Figure 4.2). Atmospheric Hg was strongly associated with distance from emission source and both moss and *Mer*PAS showed a precipitous fall in Hg over a small distance of 0 – 1 km away from emission source (Figure 4.2a). The mean concentration of Hg in moss was highest at the mining operation (444 ± 135 ng g^{-1}), followed by the adjacent site (100 ± 12 ng g^{-1}), and distant site (77 ± 4 ng g^{-1}). Similarly, with *Mer*PAS, the mining operation (93 ± 51 ng m^{-3}) showed the highest mean concentration of Hg, followed by the adjacent site (3.69 ng m^{-3}, single value reported), and distant site (2.25 ± 0.19 ng m^{-3}) (Table 4.1). Notably, Hg concentration at the distant site was closer to the global southern hemisphere average background concentration of approximately 1 ng m^{-3}. In contrast, the mining zone was 20−71 times higher, with concentrations up to 144 ng m^{-3} averaged over a period of 90 days (long-term) (Table 4.1).

4.3.1.2 Short-term exposure (2 days)

Moss and *Mer*PAS exposed for just two days during a gold amalgamation period (burning of gold with Hg) exhibited Hg concentrations that were up to 100 times higher than concentrations measured over the long-term period (Table 4.1). Similar to the long-term exposure there was large variability in atmospheric Hg, with mean concentrations of 83,382 ± 14,672 ng g^{-1} in moss and 56,803 ± 14,759 ng m^{-3} in *Mer*PAS at the mining

operation zone (Table 4.1). Given the precipitous decline in atmospheric Hg beyond 1 km of the mining operation zone, the short-term period (two days) of monitoring only focused on exposure near the burning station (ca. 150 m radius within mining operation zone) to capture emissions during the gold amalgamation process. This short-term exposure also showed association between atmospheric Hg and distance from emission source and both moss and *Mer*PAS showed a precipitous fall in Hg over a small distance of 0 – 150 m away from the burning station (Figure 4.2b). The concentration of Hg with *Mer*PAS was about 3-fold higher at the burning station site (115,187 ng m^{-3}) compared with the site farther away at the fence line of the mining zone (34,251 ng m^{-3}). Similarly, with moss bags, Hg concentration was about 2-fold higher at the burning station (259,423 ng g^{-1}) compared with the site at the fence line of the mining zone (140,874 ng g^{-1}) (Table 4.1). The high atmospheric Hg concentration at the burning station exceeded permissible exposure limits recommended by the Occupational Safety and Health Administration (100,000 ng m^{-3}) and National Institute for Occupational Safety and Health (50,000 ng m^{-3}).

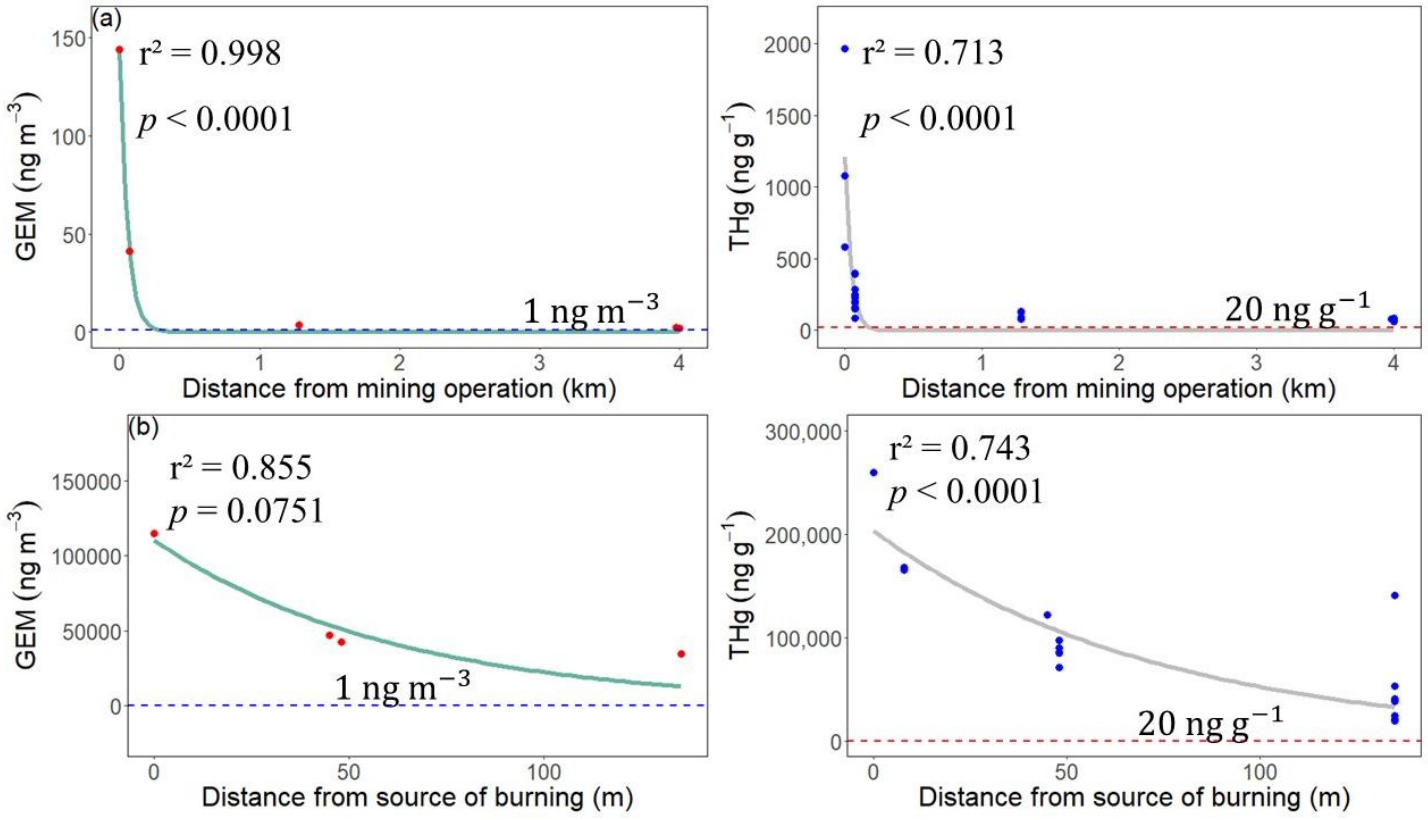

Figure 4. 2. Exponential relationship between atmospheric Hg and distance from Mahdia mining operation following (a) long-term (90 days) and (b) short-term (2 days) exposures. Blue and red dotted lines indicate natural background levels.

Table 4. 1. Total Hg concentrations (range, mean) in *Mer*PAS (ng m^{-3}) and mosses (ng g^{-1}) from Mahdia over long-term and short-term exposures.

Location	**Zone**	**M (moss) / *Mer*PAS**	**Hg (range)**	**Hg (mean ± SE)**
		Long-term (90 days exposure)		
Mahdia	Mining Operation	M (*Ptychomitrium* spp.)	87.0 – 1963	444 ± 135
	Adjacent	M (*Ptychomitrium* spp.)	76.8 – 131	100 ± 12
	Distant	M (*Ptychomitrium* spp.)	62.0 – 83	77 ± 4
	Mining Operation	*Mer*PAS	41.2 – 144	93 ± 51
	Adjacent	*Mer*PAS	3.69*	3.69*
	Distant	*Mer*PAS	2.06 – 2.43	2.25 ± 0.19
		Short-term (2 days exposure)		
Mahdia	Mining Operation	M (*Ptychomitrium* spp.)	19,306 – 25,9423	83,382 ± 14,672
	Mining Operation	*Mer*PAS	34,251 – 115,187	56,803 ± 14,759

**Single value*

4.3.2 Spatial variability of atmospheric Hg concentration

4.3.2.1 Long-term exposure (90 days)

Gaseous elemental mercury (GEM) was significantly positively correlated with Hg in moss samples measured during both sampling periods although the slope of the relationship was about 3 times higher than short-term exposure (Figure 4.3a). Moss left in the field for 2 days (during a burn) had about 100x higher Hg concentrations than moss left in the field for 90 days, clearly demonstrating that Hg is lost from moss during periods of inactivity with respect to burning. If Hg was lost from only moss and not *Mer*PAS the expected relationship between moss Hg and GEM obtained from *Mer*PAS would be much lower than observed (Figure 4.4). However, the majority of Hg captured by *Mer*PAS is also being lost as Hg content of the samplers were approximately 15-fold lower after long-term exposure near source (874 ± 485 ng/sample) compared with the two days exposure (12,033 ± 3,146 ng/sample) especially given the fact that multiple burns would have occurred during the 90 days exposure (Figure 4.4). While Hg concentrations in moss and *Mer*PAS deployed for 90 days are clearly grossly underestimating atmospheric Hg, the strong relationship between Hg in moss and *Mer*PAS, moss concentrations was used to predict the relative spatial pattern in GEM (ng m^{-3}) at the mining operation zone (normalized to 1.0 at the burning station where the highest Hg concentration was recorded). The relatively high concentration of atmospheric Hg localized to the mining operation zone varied spatially, reaching a peak concentration near the station of the Hg-gold amalgamation process and dramatically faded away in short distances (100 m or less) relative to the emission source (Figure 4.5).

4.3.2.2 Short-term exposure (2 days)

Similar to the long-term exposure, GEM was significantly positively correlated with Hg in moss with exceptionally high values measured in both moss and *Mer*PAS (Figure 4.3b). Based on this relationship, moss concentrations were used to predict spatial pattern in GEM (ng m^{-3}) at the mining operation zone. Although the short-term exposure could provide more reliable estimates of atmospheric Hg concentration during burning of gold, some Hg loss is still possible because *Mer*PAS were retrieved about 20 hours after the end of the 2-hour burn so these estimates should also be considered conservative. Atmospheric Hg concentration varied spatially around the burning station, reaching a peak concentration of 116,860 ng m^{-3} during the burning of gold and dramatically faded away over a short distance of 100 m or less (Figure 4.6).

4.3.2.3 Atmospheric Hg and soil Hg interactions

Despite greatly elevated Hg concentrations in the atmosphere there is no relationship between Hg measured in moss and soil Hg measured at the location of moss deployment (Figure 4.7). Instead, there was a strong association between soil Hg and OM (Figure 4.8).

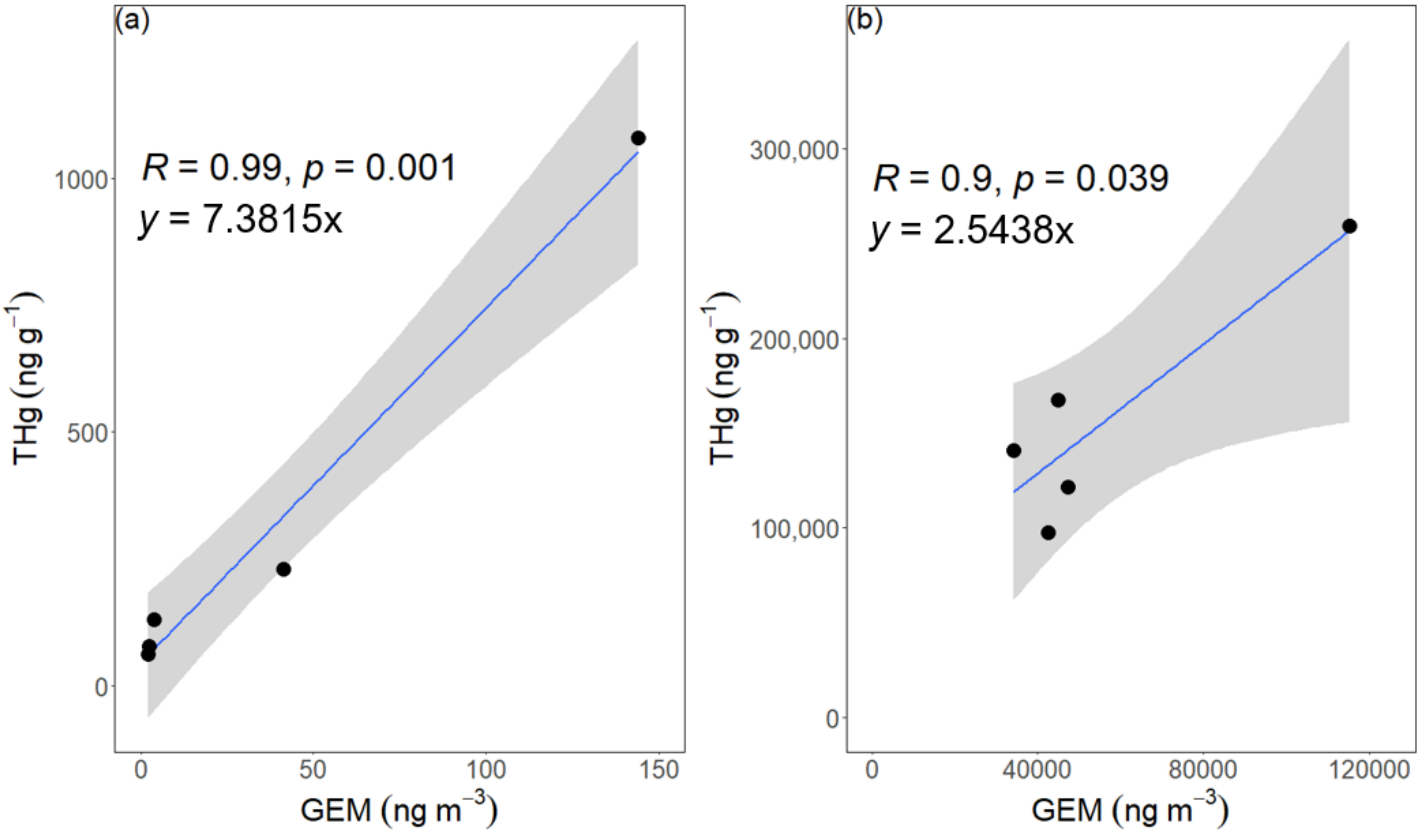

Figure 4. 3. Scatterplot of correlation between GEM and Hg concentration derived from moss bags in Mahdia mining operation following (a) long-term (90 days) and (b) short-term exposures. The gray shaded area around the solid regression line (blue) represents the 95% confidence interval.

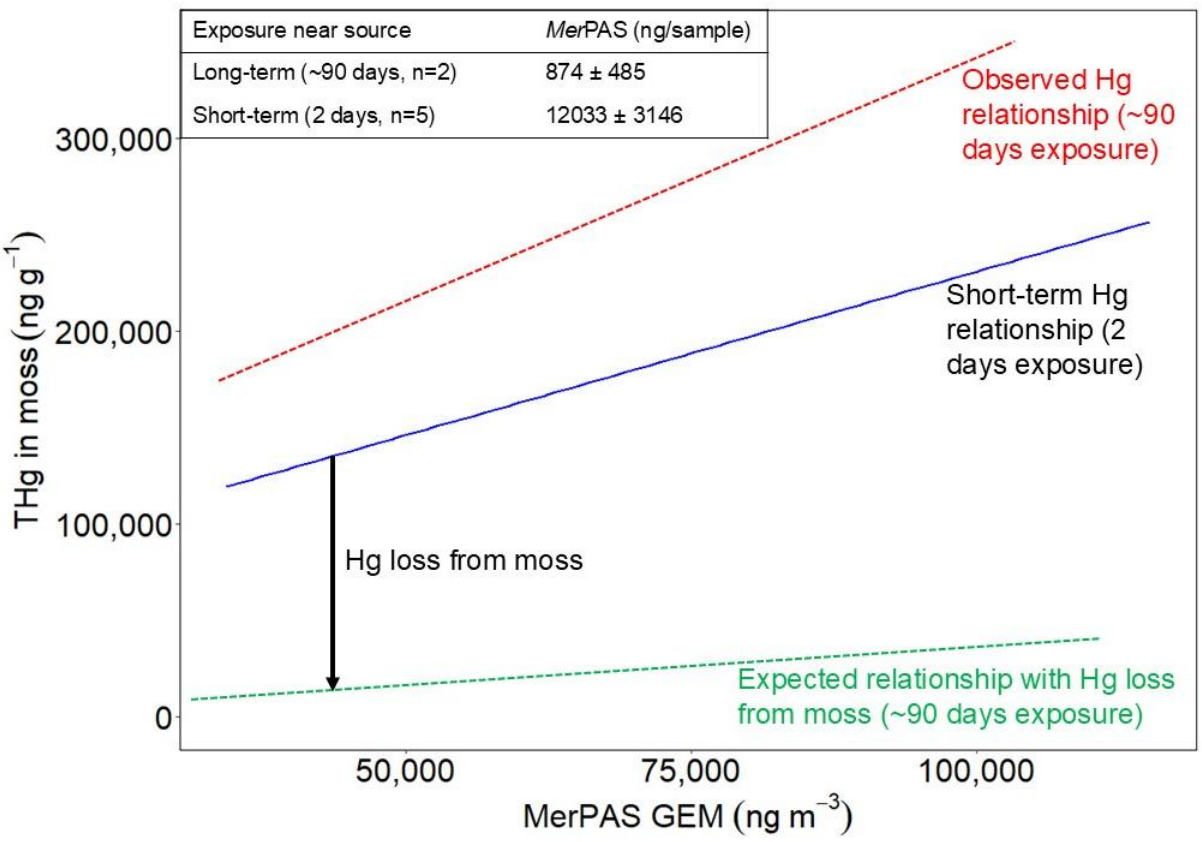

Figure 4. 4. Extrapolated conservative estimates of atmospheric Hg concentration relationship between moss and *Mer*PAS in Mahdia based on long-term (90 days) and short-term (two days) exposures.

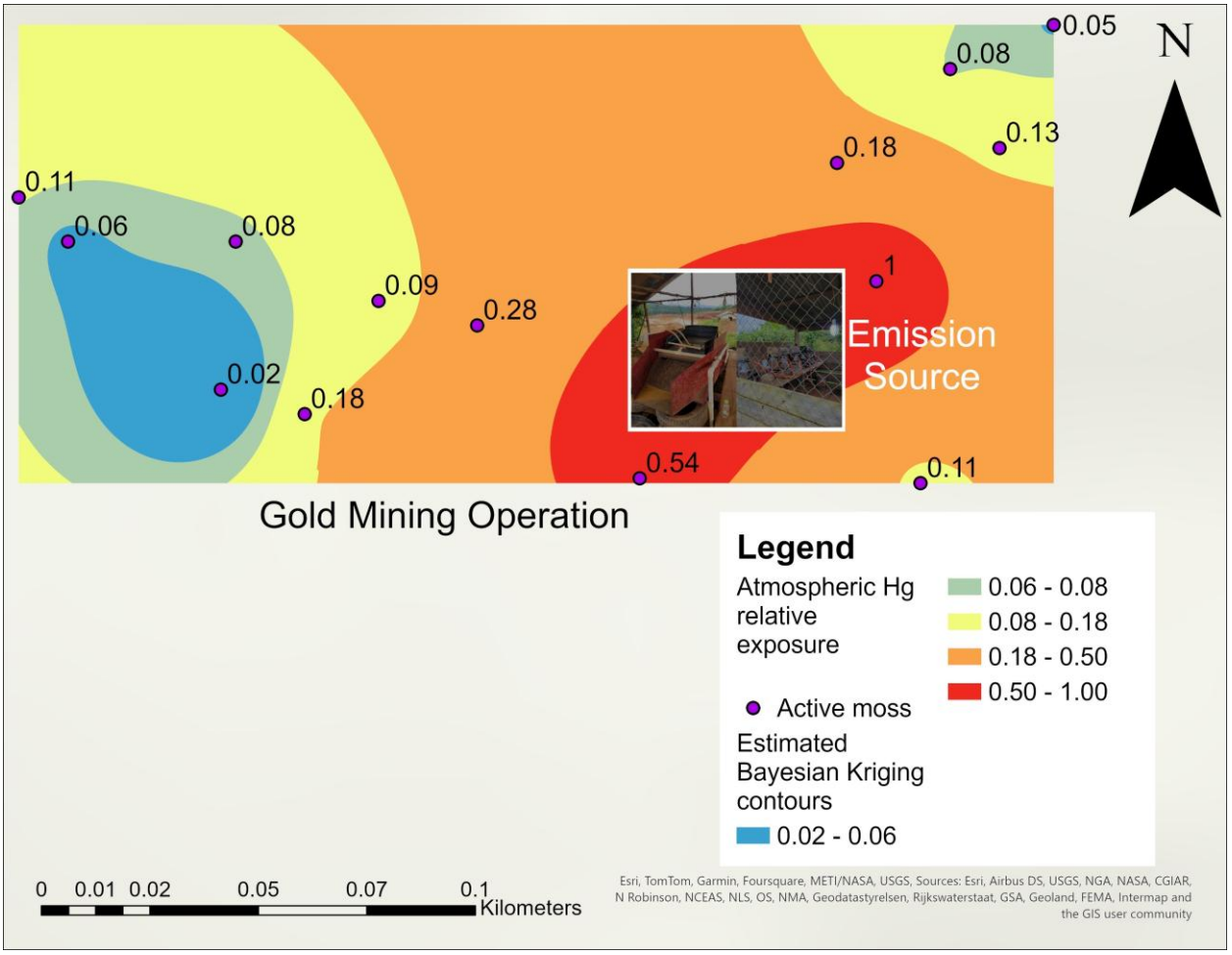

Figure 4. 5. Predicted (moss relative exposure) and geospatially interpolated (Bayesian log empirical kriging) atmospheric Hg concentration estimates across sampled mining operation (near emission source) in Mahdia following long-term exposure (90 days).

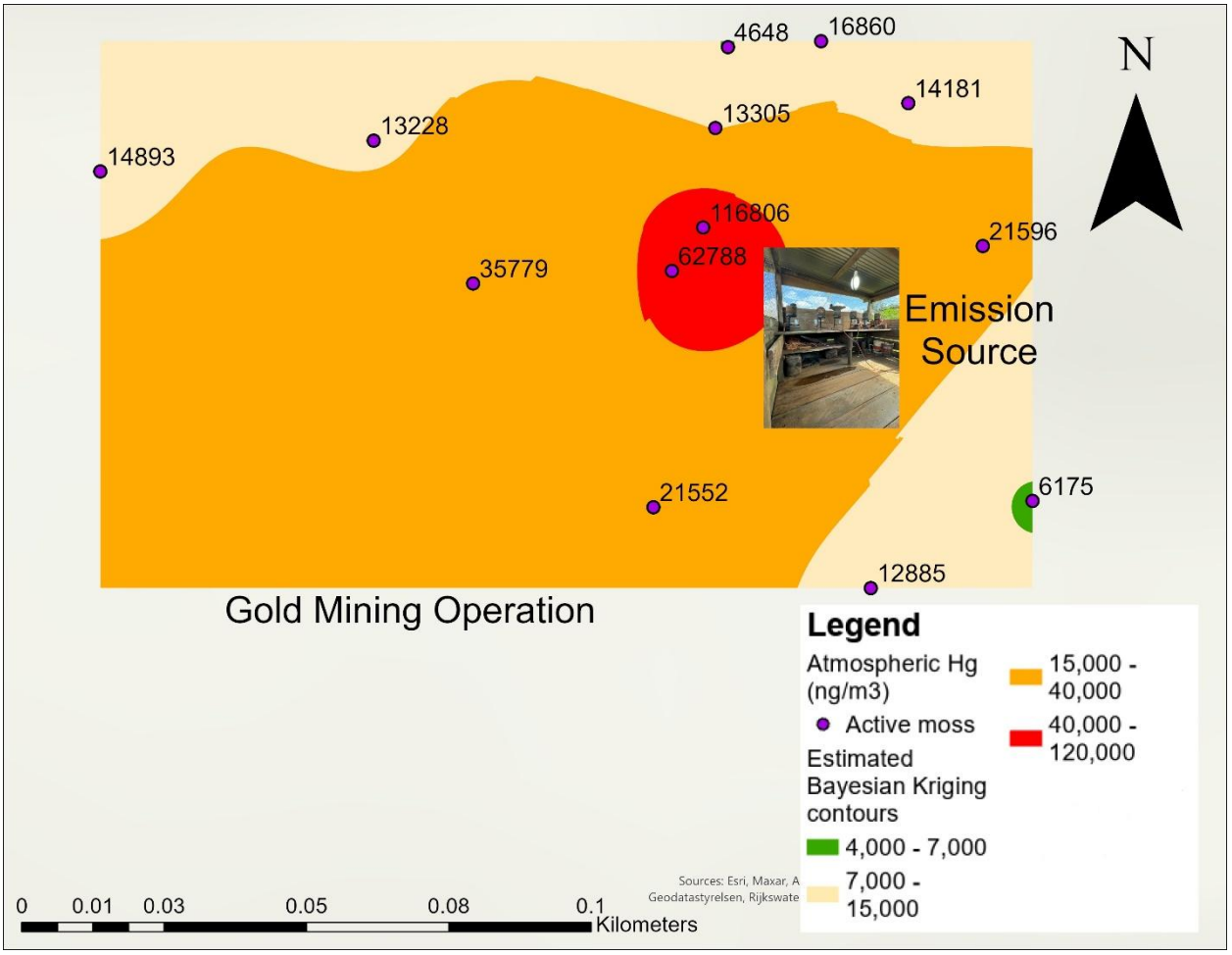

Figure 4. 6. Predicted (active moss biomonitoring) and geospatially interpolated (Bayesian log empirical kriging) atmospheric Hg concentration estimates across sampled mining operation (near emission source) in Mahdia following short-term exposure (two days).

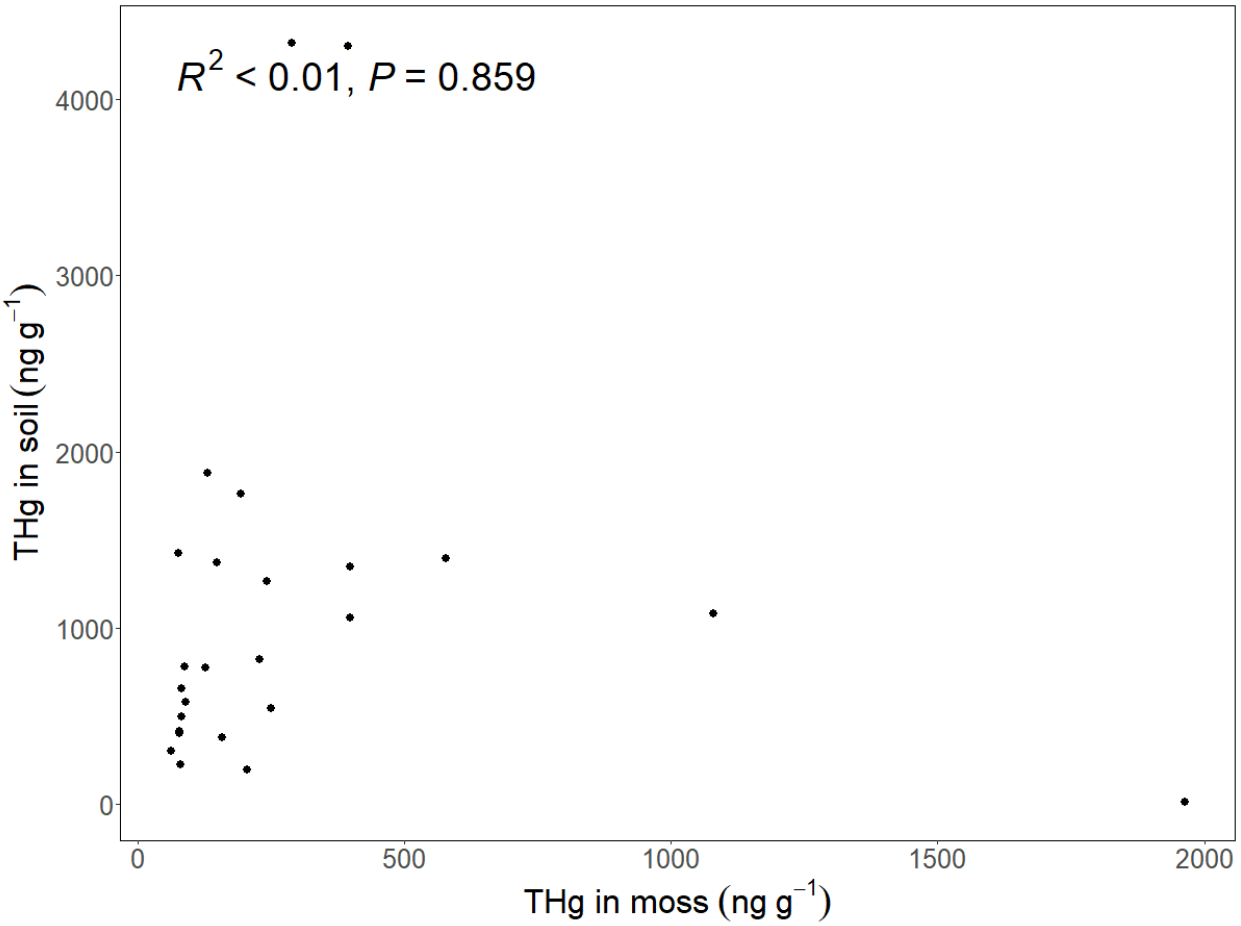

Figure 4. 7. Scatterplot of relationship between moss Hg and soil Hg in Mahdia.

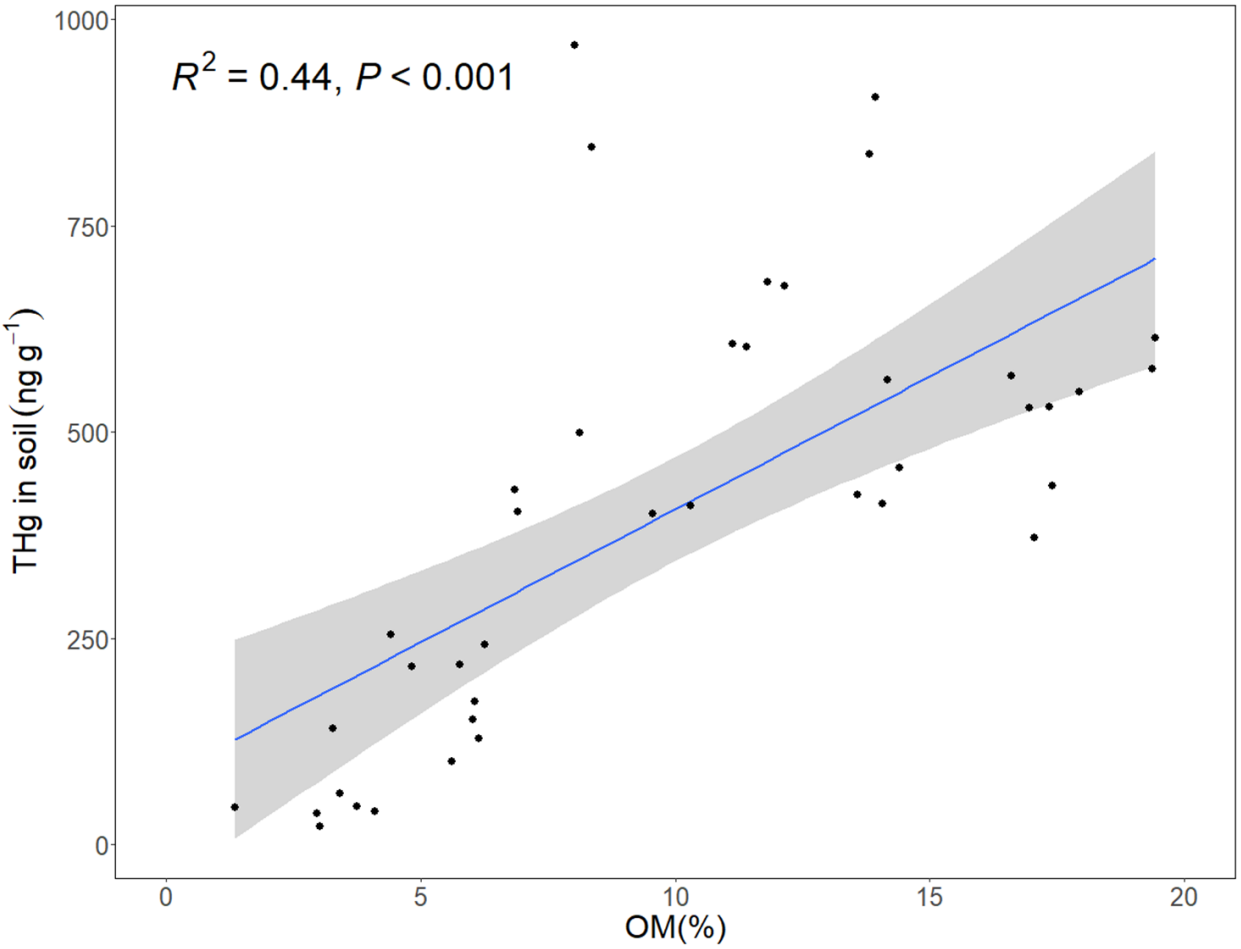

Figure 4. 8. Scatter plot and linear regression between soil OM and soil Hg in Mahdia. The gray shaded area around the solid regression line (blue) represents the 95% confidence interval.

4.4 Discussion

4.4.1 Monitoring of atmospheric Hg concentration

Atmospheric Hg was high (exceeded natural background levels for the global south, > 1 ng m^{-3}) (Sprovieri et al., 2016) in the vicinity of artisanal gold mining, but the 90 days exposure resulted in moss and *Mer*PAS values that were much lower than the two days exposure during a burn, by a factor of a 100. Moreover, the differences in moss Hg and *Mer*PAS concentrations between the two periods demonstrate that during periods without burning activities (and Hg emissions) much of the Hg sorbed to both moss and passive samplers is reemitted back to the atmosphere. Assuming the short-term exposure period is providing more reliable data, atmospheric Hg at the site can exceed 115,187 ng m^{-3}. Atmospheric Hg concentrations after two days of exposure followed the pattern of high values near the station where Hg-gold amalgams are burned and low values farther away. Notably, a steep drop in Hg was evident within a 100 m radius. This suggests dilution of the plume of contaminated air in a 50 m radius around the burning station due to high increases in air volume with distance from the burning area and greater dispersion into the atmosphere. Dilution of Hg contaminated air around the burning station is not linear since it depends on characteristics of dispersion in the atmosphere. These characteristics include turbulence, wind, and other atmospheric processes that disperse emitted Hg horizontally, vertically, and temporally (Cichowicz & Dobrzański, 2022). Gray et al. (2015) found that elevated atmospheric Hg at contaminated sites could be dispersed by persistent wind over a short distance of 300 m.

Although retorts are used at the sampled gold mine for amalgam heating, Hg emissions were still elevated, indicating some defects in the retort design and usage.

Esdaile and Chalker (2018) reported that the proper use and design of retorts could reduce the emission of Hg by recovering more than 90% of Hg. Even though there were few Hg measurements at artisanal gold mining sites to compare with, the extremely high GEM concentrations observed in the Mahdia gold-processing area are not unique to this area. Elevated GEM concentrations were also reported at mining sites in Indonesia (12,782 ng m^{-3}, at gold processing area), Italy (6,700 ng m^{-3}, 100 m radius of emission source), Ghana (900 ng m^{-3}, 150 m radius of emission source), USA (64 ng m^{-3}, within 300 m of emission source), and Peru (10.9 ng m^{-3}, 1 km away from emission source) (Gerson et al., 2022; Gray et al., 2015; McLagan et al., 2019; Nakazawa et al., 2016; Snow et al., 2021). Brown et al. (2020) also reported GEM concentrations greater than 300,000 ng m^{-3} inside gold shops in Guyana where amalgams and sponge gold are burned and purchased. This exceeds permissible exposure limits recommended by the Occupational Safety and Health Administration (100,000 ng m^{-3}) and National Institute for Occupational Safety and Health (50,000 ng m^{-3}) over an eight-hour work period. Also, GEM concentrations during Hg-gold amalgamation in the Mahdia gold mine exceeded these safety limits, which is a human health concern (damage to central nervous system). This suggests that people living in the mining camp where amalgam burning is taking place can be exposed to extremely high GEM concentrations. Therefore, personal protective equipment and proper use and design of retorts are needed to reduce exposure risk to Hg use in gold mines.

4.4.2 Moss and MerPAS Hg interactions

The fact that moss exposed for 90 days has Hg concentrations approximately 100 times lower than just two days of exposure demonstrates that during periods free from burning

Hg is released from moss to the atmosphere. Therefore, exposure over the longer term could surpass 200,000 ng m^{-3} at the mine site. Contrary to the expectation of greater accumulation of Hg in moss over long-term exposure, the two days monitoring showed higher Hg concentration. The elevated Hg in moss after two days could be associated with the Hg-gold amalgamation at the time of sampling, leading to adherence of Hg to mosses spongy structure (Meloni et al., 2025). Mosses physiology and their bioaccumulation of Hg may be influenced by environmental variables (temperature, humidity), affecting cell walls and membrane permeability and accessibility to cations binding sites for functional groups (Ciani et al., 2023). The rapid decline in Hg suggests mixing of clean air masses that dilutes atmospheric Hg concentrations (Berg et al., 2008). Giordano et al. (2009) indicated that long exposure time for moss (more than 6-week) may result in the release of absorbed Hg due to climatic and physiological changes. Bargagli (2016) reported the usefulness of moss Hg to estimate atmospheric Hg concentrations, but these estimates are not always reliable due to GEM exchanges between moss and air, and the time needed for moss to equilibrate elemental composition with changing atmospheric chemistry. Aboal et al. (2010) also reported that Hg concentrations in moss tissues do not accurately estimate the atmospheric deposition because environmental variables (temperature, radiation, precipitation) may modify the uptake kinetics of Hg in moss and alter final concentrations. This results in a state of unstable equilibrium between inputs and outputs of Hg in moss. The warm climate in Guyana coupled with high temperatures and solar radiation could increase vapor pressure and lead to Hg loss at these contaminated areas (McLagan et al., 2019). During a high degree of solar radiation photochemical oxidants such as O_3 could be formed and its reaction with elemental Hg leads to oxidation and transformation to Hg^{2+},

which is relatively short-lived in the atmosphere and deposition is more likely locally (Fernández et al., 2000). The concentrations of other metals (Co, Cu, Mn, Ni, Pb, and Zn) in moss showed no relationship to distance from mining operation, since they have different atmospheric behavior in particulate form rather than gaseous form (Poikolainen et al., 2004). Therefore, depositions of these metals are usually higher near point source compared with Hg which could be transported over long distances due to its high atmospheric mobility.

This study also showed that Hg is lost from the passives because the relationship between moss Hg and GEM Hg is much higher than would be expected if Hg was only being lost from the moss. Additionally, the Hg content (ng/sampler) of *Mer*PAS exposed for just 2 days had a 15-fold higher value than those exposed for 90 days. Using a conservative estimate of just 4 burns during the 90-day period, the Hg content in samplers would be expected to be 4 times higher suggesting that the majority of Hg sorbed during the burn is lost. Also, during the time of burning and collection of *Mer*PAS about 20 hours would have elapsed without burning activities. Therefore, Hg loss is possible and renders these values as conservative estimates during burning. Such loss of Hg from the passive sampling system may occur during transport from sampling site to laboratory and influence of air flow on sampling rate, which can vary with environmental conditions and lead to loss of Hg to sampler body (Huang & Gustin, 2015; Lyman et al., 2010).

4.4.3 Spatial variability of atmospheric Hg concentration

During both exposure periods there were significant linear relationships between moss Hg concentration and GEM obtained from *Mer*PAS, so moss data were used to provide an

assessment of spatial exposure during the two time periods (90 days and 2 days exposure) recognizing that the 90-day period represents relative exposure. Other studies (Božič et al., 2022; Monaci et al., 2022; Sutton et al., 2014) have shown positive relationships between moss and passive samplers. Relationships between biota Hg and GEM concentration are highly dependent on air temperature, wind fluxes, species of biota, and speciation of Hg (Lodenius, 2013). The dependence of biomonitoring on various factors results in the non-calibration of this method, while passive air samplers are calibrated taking into consideration the effect of meteorological parameters (wind speed and temperature) (Huang et al., 2014; McLagan et al., 2017, 2018). Gačnik et al. (2024) found that biomonitoring and passive monitoring can be used to effectively identify areas with high GEM concentrations, thereby increasing observational confidence. Bargagli (2016) emphasized the unique opportunities offered by mosses as Hg biomonitors in areas with scattered Hg sources such as geothermal fields, mineral deposits or volcanic activity. While, Jeon et al. (2020) and McLagan et al. (2016) reported that passive air samplers such as *Mer*PAS could provide long-term monitoring of GEM concentrations in developing countries (such as Guyana) and remote region, but still cost $400 – 500 per sample. Terrestrial ecosystems functioning includes complex interactions between abiotic and biotic components. Therefore, the monitoring of atmospheric Hg with moss can be a useful tool, providing that it is done according to established guidelines and protocols and the interpretation of results takes into consideration the eco-physiological factors that influence the accumulation of Hg (Bargagli, 2016). The combination of active moss biomonitoring and *Mer*PAS methods are probably best suited for short-term (<48 hours) studies comparing the periods of burning with periods of inactivity rather than longer term

deployment that at best will provide estimates of relative exposure. Additionally, it is recommended that shorter periods be assessed during gold amalgam burns owing to the very episodic nature of Hg release that occurs during a 2-hour period. Ideally these would be complimented with active measurements to demonstrate the effectiveness of passive samplers that are exposed to rapid and dramatic fluctuations in atmospheric Hg.

Bayesian log empirical kriging identified hotspots close to emission source (Hg-gold amalgamation station) within the mining operation zone, where atmospheric Hg concentrations reached 116,806 ng m^{-3} (over a period of two days, Figure 4.6). This suggests that localized effects of burning gold amalgam with Hg are strong drivers of Hg emission. Atmospheric Hg was higher than McLagan et al. (2021) who reported elevated GEM (10.8 – 37.4 ng m^{-3}) near an emission source (within 200 m radius). Vaselli et al. (2013) also found elevated atmospheric Hg concentrations from 200 to >10,000 ng m^{-3} and confirmed the sharp decline in the range of values at short distances (few 100 m away) from mining. Pockets of lower concentrations at points 100 to 200 m away from the emission source, may be attributed to rapid dilution of atmospheric Hg concentrations by clean air masses. Bargagli (2016) reported that the dilution of atmospheric Hg concentrations in moss by clean air masses is a common feature in mineralized areas. Here, Hg concentrations up to 4000 ng m^{-3} inside smelting plants dropped to ca. 2 ng m^{-3} over a short distance of approximately 300 m.

4.4.4 Atmospheric Hg and soil Hg interactions

While atmospheric Hg concentrations decrease rapidly with distance from the burning area there was no relationship between soil Hg and moss Hg. Instead, Hg was strongly

correlated with soil OM and often soil close to the burning area had very little OM. So, Hg contamination extends beyond the mine zone and is greatly affected by its interaction with vegetation (which in turn can lead to Hg contamination in sediments as reported in chapter 3). The low soil OM near the burning area is associated with the destructive nature of gold mining that clear cuts existing vegetation, which disrupts the natural biogeochemical degradation of plant materials. The results suggests that residence time and retention of Hg in soil and leaf litter as discussed in chapters 3 and 5 are more relevant to shaping patterns of Hg concentrations than direct interaction with atmospheric deposition (Obrist et al., 2011). Yu et al. (2014) observed no significant relationship between atmospheric Hg deposition and soil Hg concentration due to historical soil formation and disturbance, legacy Hg in soils, and the dynamics of soil OM to effectively bind Hg. The close relationship between soil OM and Hg is consistent with observations that Hg forms complexes with functional groups of OM, particularly those with reduced sulfur (Khwaja et al., 2006; Santos-Francés et al., 2011). Velásquez Ramírez et al. (2021) found a strong positive relationship between OM and soil Hg for areas impacted by gold mining in Peru. The quality and type of OM primarily controls the binding of Hg, where the formation of covalent bonds with available active sites of reduced sulfur could be attributed to the phenomenon of polarizability. Here, the rule of hard and soft acids and bases predicts that soft acids and soft bases interact strongly. This is due to sulfur containing thiol functional groups that act as a soft base to strongly bind Hg which is a polarizable soft acid (Mousavi, 2015; O'Connor et al., 2019; Reis et al., 2015).

4.5 Conclusion

Atmospheric Hg around artisanal gold mines can be very high (exceed natural background levels for the global south) but decrease rapidly with distance from the mine site. During periods of burning atmospheric Hg can exceed 115,187 ng m^{-3} and result in moss Hg concentrations greater than 259,423 ng g^{-1}. Moss Hg was correlated with GEM estimated by *Mer*PAS during both short-term and long-term exposures, although most of the Hg sorbed during the short-term is lost during periods of inactivity causing longer term estimates to be grossly underestimated. Moss and passive samplers may be useful to measure atmospheric Hg but should only be deployed for short periods to minimize loss to the atmosphere.

5.0 Contrasting Hg/C relationship in environmental media near artisanal gold mining sites in Guyana with those observed at the global scale

5.1 Introduction

Terrestrial ecosystems are receptors of mercury (Hg) and act as large storage pools for atmospheric Hg deposition that accumulates in surface litter and soil (Grigal, 2003; Pokharel & Obrist, 2011). The cycles of Hg and carbon (C) are strongly linked at the landscape and biogeochemical levels, with several studies globally showing a strong linear relationship between Hg and C in terrestrial ecosystems (Grigal, 2003; Olson et al., 2018; Różański et al., 2016; Wang et al., 2023; Watmough et al., 2019). Terrestrial vegetation is considered the missing sink in the global Hg mass balance and is estimated to absorb more than 1,000 tonnes of atmospheric Hg annually (Han et al., 2025). Studies have shown that atmospheric Hg is mainly absorbed by leaf stomata and that leaf litter constitutes 50 to 84% of litter biomass with higher Hg concentrations compared with other plant tissues such as root and stem (Ericksen et al., 2003). Therefore, fallen leaves are an important contributor to Hg fluxes to soil (Assad et al., 2016; Ericksen et al., 2003).

Mercury concentrations in decomposing leaf litter is often higher than leaves, possibly due to continued absorption of Hg from the atmosphere or transfer from soil (Ma et al., 2022). Accumulation of Hg in surface litter alone accounts for 30 to 60% of total atmospheric Hg inputs to soil, which is often greater than inputs through direct wet deposition (Pokharel & Obrist, 2011). Given the affinity between organic matter (OM) and Hg in leaf litter and soil, the mobility and behavior of Hg is also associated with the dynamics of C (Grigal, 2003; Pokharel & Obrist, 2011). Litterfall serves as a major source

of soil OM, where >50% of net primary production returns to soil through plant litter decomposition. Therefore, litter decomposition is an essential step in the C cycle and the product of decomposition normally becomes less available, thereby stabilizing soil OM and associated contaminants such as Hg (Frouz, 2018; He et al., 2019; Ndungu et al., 2016).

Soil OM serves as the largest terrestrial C pool that accumulates via continuous plant C inputs into soil. Carbon in soil can be transported from terrestrial ecosystems (soil, plant materials, and wetlands) to freshwater ecosystems through various flow paths (Franco-Cisterna et al., 2024). The quality and quantity of C is an important factor that controls sorption with inorganic Hg, which is likely to sink rapidly to the bottom where it is buried in sediment (Eckley et al., 2021). The anoxic condition of sediments facilitate the biotic methylation of inorganic Hg, leading to the formation of methylmercury which is the most toxic form of Hg (de Oliveira et al., 2015; Wang et al., 2024).

Gold mining practices at the small and medium scale results in the release of high concentrations of Hg into the atmosphere (as reported in chapters 2, 3, and 4 of this thesis), leading to elevated deposition into adjacent forest canopies (Gerson et al., 2022). While Hg movement and C within the biosphere are connected it is unclear how these patterns may differ in areas exposed to high levels of Hg compared with regions remote from pollution sources. Relationships between Hg and C have not been extrapolated across the biosphere, except for a few studies and primarily for freshwater who report a relatively consistent value of 0.25 ± 0.20 ng mg^{-1} in freshwaters (Grigal, 2002; Lavoie et al., 2019; Riscassi & Scanlon, 2011). However, the stoichiometry of the Hg/C relationship varies spatially in other environmental media such as plant tissues, litter, soil and sediments (Grigal, 2003; Gruba et al., 2019).

Comparing Hg/C patterns in environmental media surrounding gold mining sites with relationships observed globally could provide a greater understanding of Hg movement within the biosphere. This study presents the first demonstration of Hg/C relationships in the biosphere relative to gold mining sites in Guyana. The purpose of this study was to assess how Hg/C relationships in environmental media (foliage, leaf litter, soil, water, sediment) near artisanal gold mining sites in Guyana compares with Hg/C relationships observed globally synthesized from published studies. It is hypothesized that Hg/C ratios observed in environmental media (foliage, leaf litter, soil, water, sediment) near gold mining sites in Guyana will be higher compared with clean sites at the global scale.

5.2 Methodology

5.2.1 Gold mining case study

The gold mining area was in Mahdia (*in-situ*) (5° 16’ 54” N to 5° 17’ 3” N and 59° 3’ 32” W to 59° 5’ 46” W) (Figure 5.1). The mine area is typically separated into the mining zone (overburden and pit), adjacent site (1 – 2 km away from gold mine with forest), and distant site (2 – 4 km away from gold mine with forest). The *in-situ* study focused on sample collection at the forested site, 2 – 4 km from gold mine. The Mahdia zone general wind direction is from the east, annual precipitation varies from 2,200 to 4,000 mm, and mean annual temperature ranges between 23 to 32 ℃ (GLSC, 2013). The area with no mining (*ex-situ*) was in a northeastern region of Guyana (Anna Catherina, West Coast Demera) that is 197 km away (6° 51.991’ N and 58° 16.7381’ W) from the gold mining area in Mahdia (Figure 5.1). Here, the general wind direction is from the northeast, annual

precipitation varies from 2,200 to 2,800 mm, and mean annual temperature ranges between 25 to 28 ℃ (GLSC, 2013).

5.2.2 Field sampling

To evaluate how Hg and Hg/C relationships vary in soils with distance from the gold mine in Mahdia, surface (0 – 10 cm) soil samples (ca. 5 kg) were collected (July 2024) from an *in-situ* forested site (2 – 4 km away from the gold mine) (Figure 5.1). Since wetland sites were not present in the Mahdia area, soil extraction experiments were done with surface soils to simulate precipitation regimes and evaluate Hg and dissolved organic carbon (DOC) that could be potentially leached into sediments (as reported in chapter 3). Sediment samples downstream (2 – 4 km away) of the gold mine in Mahdia was at a similar distance away from the gold mine as the *in-situ* forested site, so Hg and C values (as reported in chapter 3) were extracted from this location.

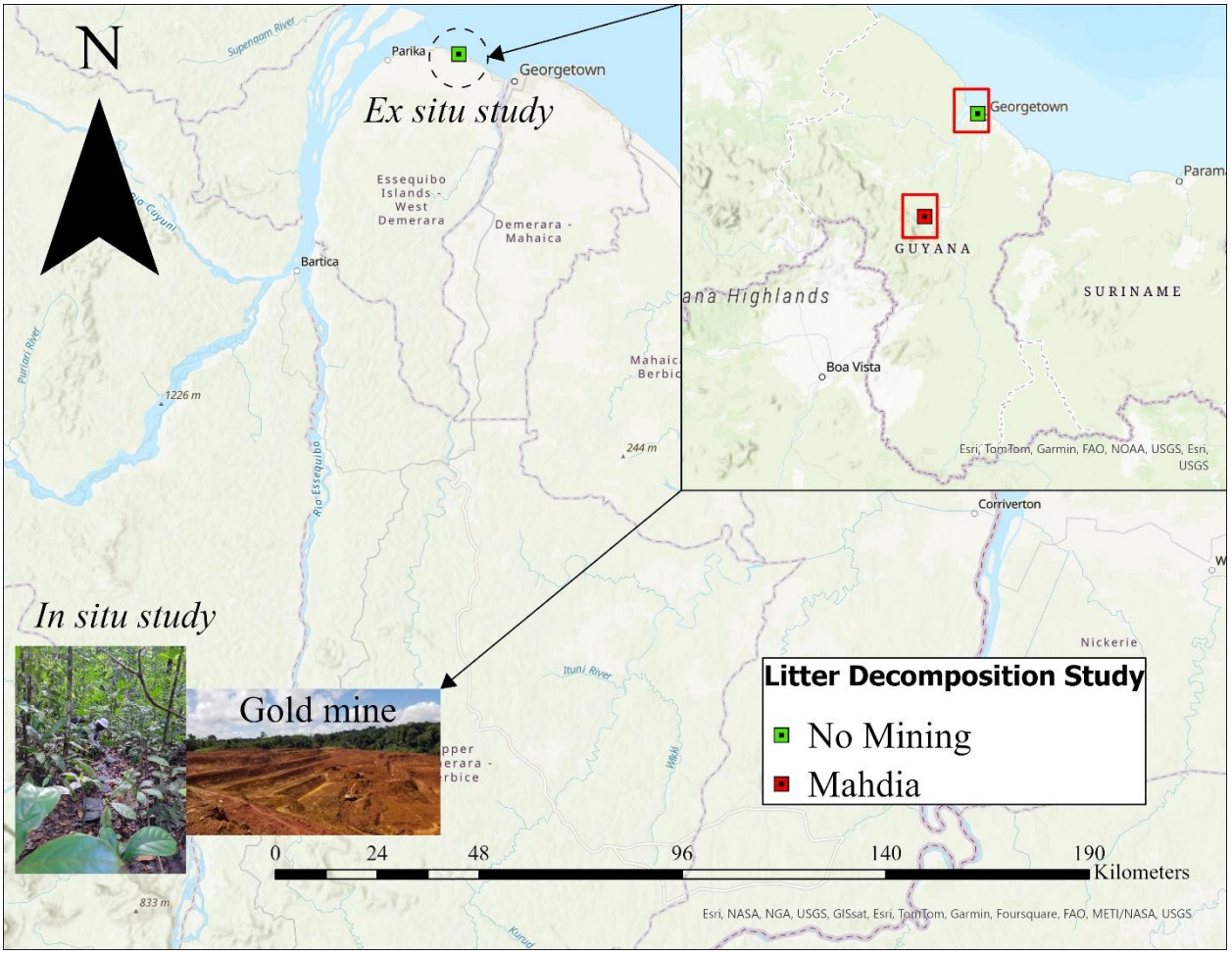

Figure 5. 1. Location of deployed litterbags.

5.2.3 Preparation of litterbags

Freshly fallen *Cecropia obtuse* leaves were collected from the *in-situ* forested site (same as soil collection) and oven dried (Thermo Scientific, Freas 645) at 35℃ to constant weight. Each litterbag (20 x 20 cm, mesh size 1 mm) received 15 g (dry weight) of leaf litter (Karberg et al., 2008; Scheid et al., 2009).

5.2.4 In-situ leaf litter decomposition experiment

Litterbags (n = 12) were deployed *in-situ* (same as leaf litter collection site) in Mahdia for 14 months between June 2023 and July 2024 to determine Hg concentration in leaf litter exposed to gold mining. Based on the atmospheric Hg measurements from chapter 4, values at the mine site exceeded 115,187 ng m^{-3} over a 48-hr period during the burning of gold amalgam, but longer-term estimates are not available due to loss of Hg from passive samplers during periods of inactivity (no burning). The *in-situ* site received 12 litterbags at random points in direct contact with the soil surface and secured with nails driven into the soil via the corners of the litterbags (Lecerf et al., 2021; Scheid et al., 2009). Litterbags were stored in sealed and labelled Ziploc® bags for transport to the laboratory for analysis. These litter samples were constituted as *in situ* soil + litter. Litterbags were cleaned to remove any moss and soil growing on the netting and litter samples were carefully cleaned by hand to remove extraneous material. Litter samples and baseline foliage were oven-dried at 35℃ to constant weight, weighed and ground to powder with an electric coffee mill (Black & Decker). These samples were packaged into another Ziploc® bag for storage at 4℃ to avoid any contamination until transport to Trent University Environmental Geoscience laboratory for analysis.

5.2.5 Ex-situ leaf litter decomposition experiment

Litterbags (n = 12) were deployed *ex-situ* for five months between July 2024 and December 2024 to distinguish soil versus atmosphere as a source of Hg to leaf litter. There was no local Hg source at the *ex-situ* location in Anna Catherina (6° 51.991’ N and 58° 16.7381’ W) so atmospheric Hg is expected to be around background levels (1 ng m^{-3}, global south

(Sprovieri et al., 2016)). Soil and litter samples collected from the *in-situ* location were separated into two 53 × 33 cm aluminum foil pans for the *ex-situ* experiment. Each pan received replicates of six litter bags, which were constituted as *ex situ* soil + litter. Litterbags were harvested per sample pan in December 2024 and cleaned. Litter samples and baseline foliage were oven-dried at 35℃ to constant weight, weighed and ground to powder with an electric coffee mill. These samples were packaged into another Ziploc® bag for storage at 4℃ to avoid any contamination until transport to Trent University Environmental Geoscience laboratory for analysis.

5.2.6 Foliage, leaf litter, and soil analysis

Carbon (C) content in leaf litter and foliage was measured with a CN analyzer (LECO, CN828). Dried sub-samples of foliage and leaf litter (0.08 g) were packed into 502-186 tin foil cup and twist sealed to minimize entrapped atmosphere. Each tin foil cup with sample was transferred to the appropriate position in the sample carousel to initiate analysis. Quality control of C measurements was assured by the inclusion of blanks and apple leaves certified reference materials (NIST 1515) at the start of each experimental run (30 samples) and recovery ≥ 95 % was considered acceptable.

Soil organic matter (%OM) was measured by loss-on-ignition (LOI) (Equation 1). After oven-drying (24 hours at 105℃) of soil (5 g) to constant weight, OM was ignited at 400℃ for 10 hours (Heiri et al., 2001). Organic matter content was converted to C using the conventional conversion factor of 0.58 (Equation 2) (Jensen et al., 2018). The obtained C (%) values were converted to mg g^{-1} C (1 mg g^{-1} C = 0.1% C) to ultimately derive Hg/C ratios in environmental media (foliage, leaf litter, soil, water, sediment) (Equation 3).

Foliage, leaf litter, and surface runoff samples were measured for C, while soil and sediment samples and samples from studies that reported OM as LOI were converted based on the above stated metrics to determine C content.

$$\%OM = \left(\frac{W_1 - W_2}{W_1 - C_w} \right) \times 100 \qquad \text{Equation 3}$$

Where, W_1 = weight pre ignition, W_2 = weight post ignition, and C_w = crucible weight.

$$C = 0.58 \times \%OM \qquad \text{Equation 4}$$

Where, *0.58* = conversion factor and *%OM* = percent organic matter (LOI).

$$Hg / C = \frac{Hg\ ng\ g^{-1}}{C\ mg\ g^{-1}} \qquad \text{Equation 5}$$

Where, *Hg* = mercury concentration and *C* = carbon content.

Total Hg concentration in foliage, leaf litter, and soil was measured with a Direct Mercury Analyzer (DMA-80) by thermal decomposition, amalgamation, and atomic absorption spectrometry. Sub-samples of dried foliage, leaf litter, and soil (0.05 g) were heated to 900°C to reduce Hg species to elemental Hg, which was loaded onto an amalgamator. Subsequent heating of the amalgamator resulted in the release of Hg vapors into a single bean, fixed wavelength atomic absorption spectrophotometer. Quality control of Hg measurements was assured by the inclusion of blanks and certified reference materials (NIST 1515 and *Enviro*MAT™ SS-1) at the start of each experimental run (40 samples) and recovery ≥ 93 % was considered acceptable.

Mercury and C values in foliage, leaf litter, mineral soil, surface runoff, and sediment for sites near the gold mine in Guyana were used to calculate mean Hg/C ratios to examine the movement of Hg through environmental media. For comparison, Hg and C values for the same environmental media were extracted from the literature from sites with no known local Hg source to calculate Hg/C ratios to track the movement of Hg at the global scale.

5.2.7 Data curation for Guyana Hg/C patterns

Measured C in foliage, leaf litter, and surface runoff (soil leachate), converted soil and sediment C values, and associated Hg concentrations were used to calculate Hg/C ratios in environmental media near the artisanal gold mine in Guyana.

5.2.8 Data curation for global Hg/C patterns

Foliage, leaf litter, wetland, mineral soil (0 – 20 cm), river, and sediment (lake and river) Hg and C (converted when studies report OM as LOI using equation 2) data were extracted from global studies for clean (Chakraborty et al., 2015; Coquery & Welbourn, 1995; Fragoso et al., 2018; Gómez-Armesto et al., 2020; Grigal, 2003; Juillerat et al., 2012; Lavoie et al., 2019; Luo et al., 2014; Ma et al., 2022; Obrist et al., 2009; Osborne et al., 2024; Różański et al., 2016; Sanei & Goodarzi, 2006; Watmough et al., 2019; Yang et al., 2018) and contaminated sites (Chakraborty et al., 2015; Donkor et al., 2005; Gerson et al., 2022; Guédron et al., 2018; Kongchum et al., 2011; Pinedo-Hernández et al., 2015; Ssenku et al., 2023; Tomiyasu et al., 2020). Data for the wetland studies were derived from 126 peat cores sampled in 16 countries across six continents (Africa, Asia, Europe, North

America, Oceania, and South America) (*Global Peatland Microbiome Project; Lamit and Lilleskov et al. unpublished*; Watmough et al., 2022). Soil Hg and C (converted when studies report OM as LOI using equation 2) data were extracted from global studies for clean (Grigal, 2003; Olson et al., 2018; Różański et al., 2016; Wang et al., 2023; Watmough et al., 2019) and contaminated (Tomiyasu et al., 2020) sites to examine changes in the slope of the Hg/C relationship based on exposure.

5.2.9 Statistical analysis

Mercury and C in mineral soil and leaf litter were subjected to Shapiro-Wilk normality test to assess normal distribution and all statistical analysis was done with R version 4.0.4 at an acceptable α-level of 0.05 (R Core Team, 2021). Linear regression analysis was done to evaluate the relationship between soil Hg and C at varying distances from emission source at a gold mining site in Guyana. Relationships between soil Hg and C at the global scale were compared with compiled datasets from the gold mine in Guyana and another gold mine influence site in Indonesia. The litter decomposition experimental data was grouped according to *in situ* and *ex situ* to distinguish soil versus atmosphere as a source of Hg to leaf litter. The nonparametric Kruskal-Wallis test was used to compare Hg concentration and Hg/C ratio in leaf litter. When the Kruskal-Wallis indicated significance, Dunn test was used to determine the levels of the independent variable that differ from each other level (Fragoso et al., 2018; Ma et al., 2022; Zar, 2010). Mean Hg/C ratios from environmental media (foliage, leaf litter, soil, water, sediment) near the gold mine were calculated and compared with mean Hg/C ratios for the same environmental media globally to provide insights into Hg movement within the biosphere.

5.3 Results

5.3.1 Hg:C relationships with distance in soil near a artisanal gold mine

High variability in surface soil Hg concentration was evident across the three zones, with the mining operation zone demonstrating a higher range (22.12 – 970 ng g^{-1}) in Hg concentration compared with the adjacent (400 – 906 ng g^{-1}) and distant (372 – 614 ng g^{-1}) sites (Figure 5.2). Soil Hg was linearly related to C, but the Hg/C ratios changed slightly and was lower at the distant site (Figure 5.2).

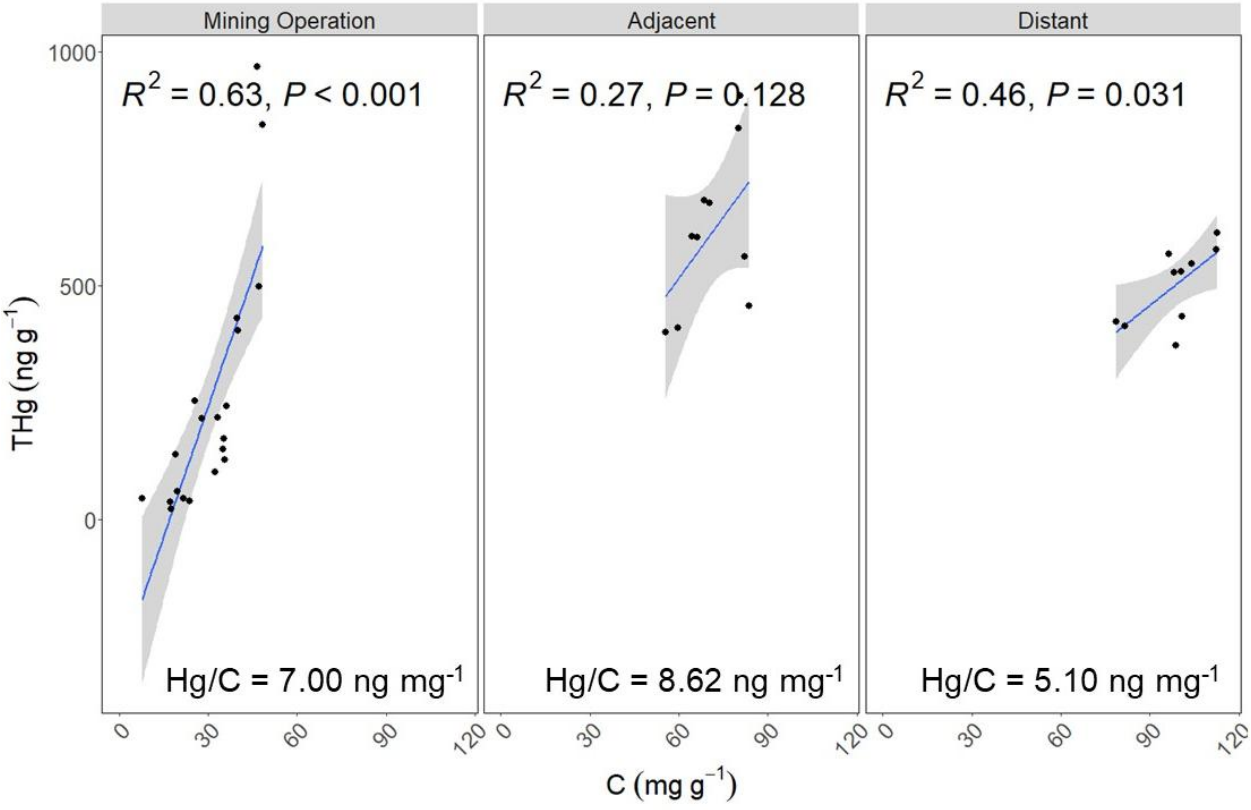

Figure 5. 2. Scatter plot and linear regression between soil C and soil Hg based on distance (km) from source of gold mining in Mahdia. Adjacent = 1 – 2 km away from gold mine and Distant = 2 – 4 km away from gold mine. The gray shaded area around the solid regression line (blue) represents the 95% confidence interval.

5.3.2 Contrasting soil Hg:C relationships in Guyana with global relationships

A strong positive relationship also exists between soil C and Hg and in regions distant from point source although Hg/C are much lower (Antarctica = 4.85 ng mg^{-1}, British Colombia = 1.03 ng mg^{-1}, Saskatchewan = 0.82 ng mg^{-1}, USA = 0.44 ng mg^{-1}, Norway = 0.50 ng mg^{-1}, and Sweden = 0.56 ng mg^{-1}) than those observed near the artisanal gold mine in Guyana (7 ng mg^{-1}) and other artisanal gold mining sites in Indonesia (63 ng mg^{-1}) (Figure 5.3).

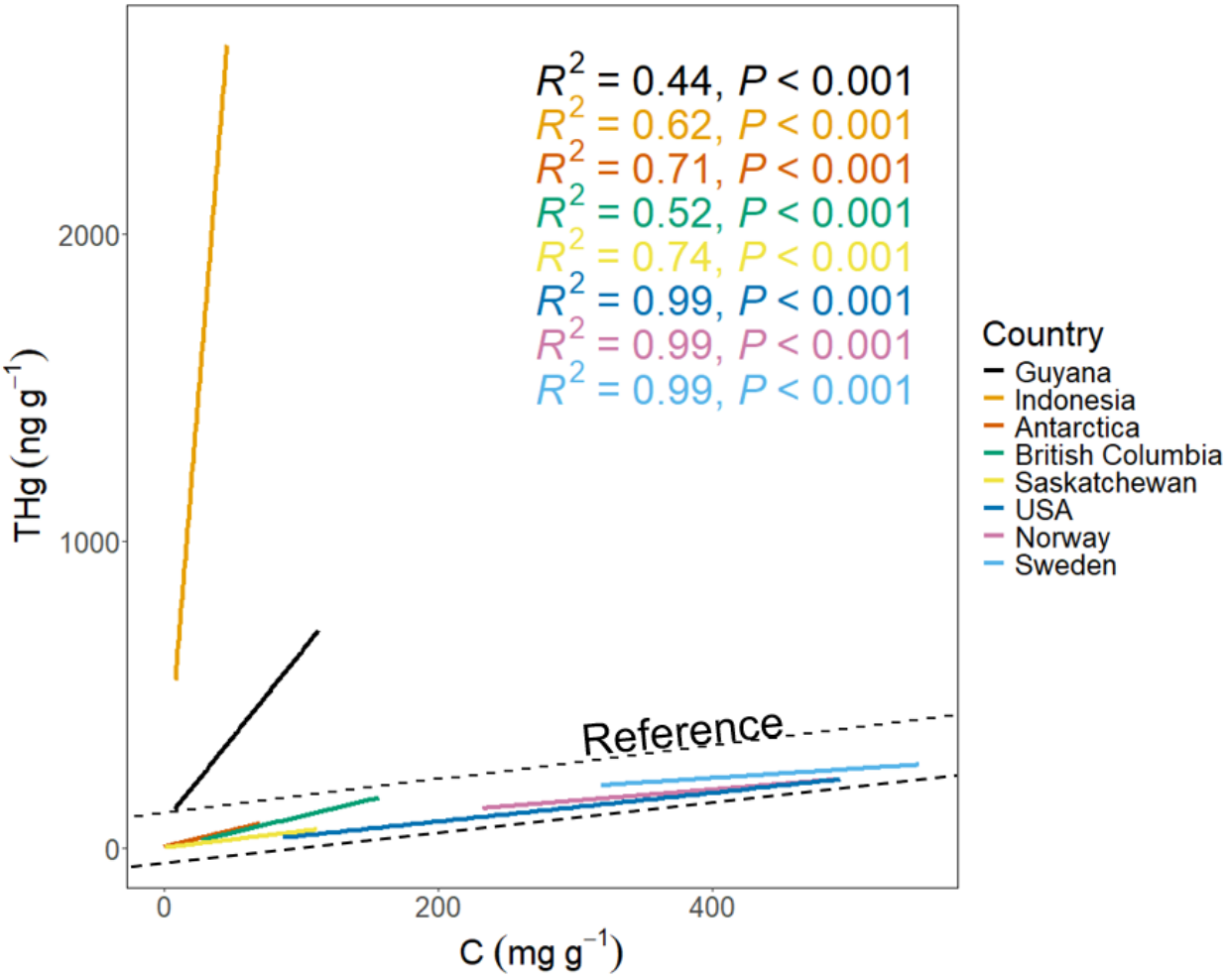

Figure 5. 3. Linear regression between soil C and soil Hg – Guyana vs global studies. The area between broken lines indicates no gold mining pollution.

5.3.3 Leaf litter decomposition and changes in Hg and Hg/C in-situ and ex-situ

Prior to the study, leaf litter Hg and Hg/C ratios in the *in-situ* and *ex-situ* studies were almost identical (Figure 5.4 a-b). However, in the *in-situ* study Hg increased about 4-fold in leaf litter (7235 ± 819 ng g^{-1}) after 14 months of decomposition compared with baseline Hg concentration (1625 ± 30 ng g^{-1}) (Figure 5.4a). The change in Hg levels following decomposition under *in-situ* conditions also resulted in an increase in Hg/C ratio (32 ± 3 ng mg^{-1}) (Figure 5.4b).

The *ex-situ* study was conducted using soil collected from the location of the *in-situ* study and soil Hg concentration at both sites was very similar ~ 500 ng g^{-1} (Figure 5.4c). However, in the *ex-situ* study Hg decreased about 30-fold in leaf litter (70 ± 9 ng g^{-1}) after 5 months of decomposition compared with baseline Hg concentration (2084 ± 162 ng g^{-1}) (Figure 5.4a). This amounts to a 100-fold difference in leaf litter Hg that is decomposed in the same soil under different atmospheric Hg exposures. The change in Hg levels after 5 months of decomposition under *ex-situ* conditions resulted in a large decrease in the Hg/C ratio (0.25 ± 0.03 ng mg^{-1}) that was also about 100-fold lower than the *in-situ* study (Figure 5.4b). The remaining leaf litter mass under *ex-situ* condition was 77 % of its initial mass after 5 months of decomposition, while *in-situ* it was 44 % of the initial mass after 14 months of decomposition, so the decrease observed *ex-situ* is not due to differences in leaf litter mass loss.

Mean Hg concentration was elevated in surface runoff (595 ± 37 ng L^{-1}) and sediment (365 ± 88 ng g^{-1}) relative to the leaf litter samples *in-situ* (Table 5.1). Soil water extracts (surface runoff) demonstrated a higher Hg/C ratio (13.23 ± 2.47 ng mg^{-1}) compared with sediment (7.32 ± 1.07 ng mg^{-1}) (Table 5.1).

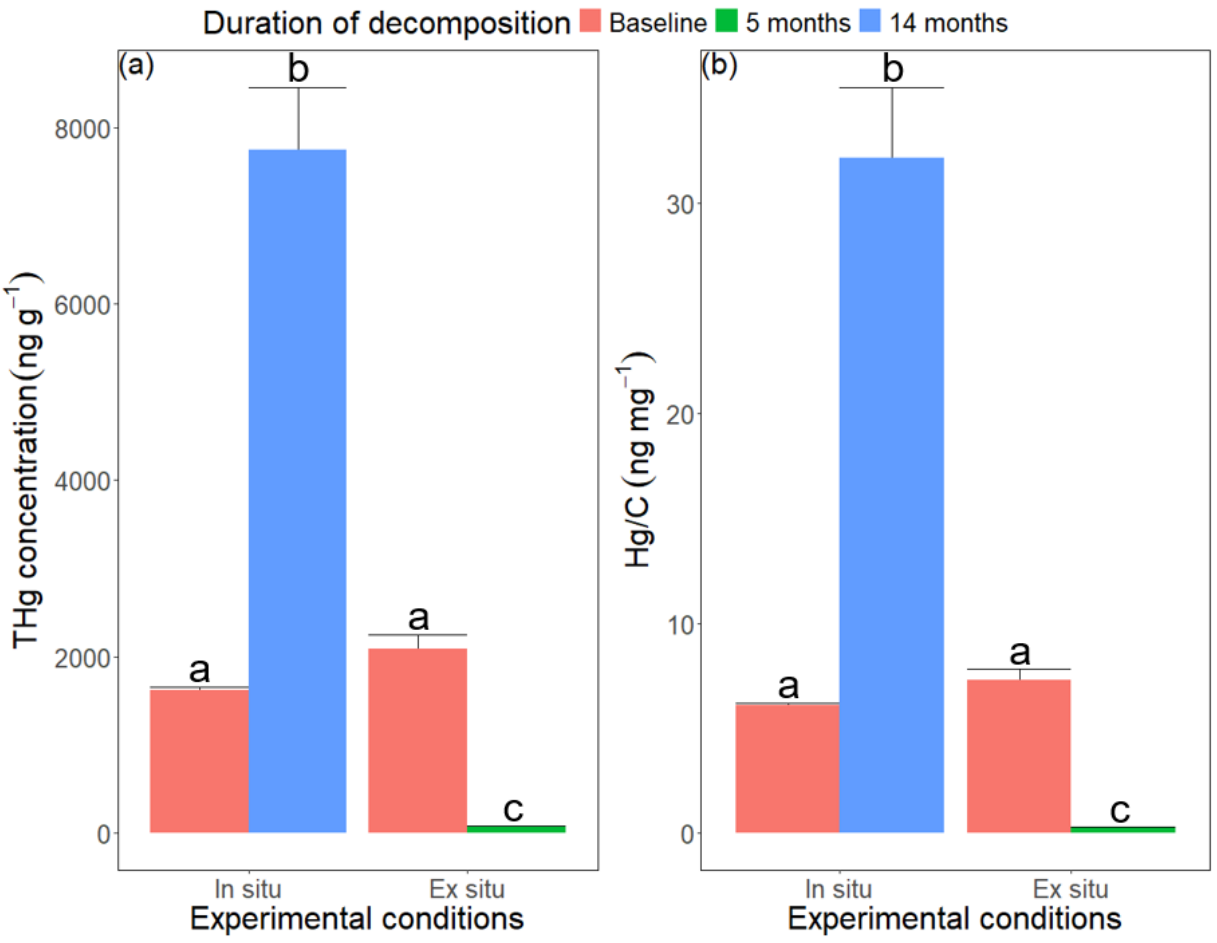

(c)

Experimental conditions	Soil pH	Soil OM (%)	Soil Hg (ng g^{-1})
In situ	3.89 ± 0.09	17.00 ± 0.61	501 ± 26
Ex situ	4.79 ± 0.10	14.63 ± 0.37	556 ± 50

Figure 5. 4. Concentrations of Hg in leaf litter after (a) *in situ* (14 months) and *ex situ* (5 months) decomposition experiments along with associated Hg/C relationships under (b) *in situ* and *ex situ* conditions. Corresponding Hg concentration in (c) soil underneath litter bags is also shown. Different letters indicate statistically significant differences ($p < 0.05$) using Dunn's test between each treatment per variable.

Table 5. 1. Mean extracted estimates for surface runoff and sediment relative to *in-situ* forested site.

Variable	Mean ± SE
Surface runoff (2 – 4 km from gold mine)	
Hg (ng L^{-1})	595 ± 37
DOC (mg L^{-1})	49 ± 6
Hg/C (ng mg^{-1})	13.23 ± 2.47
Downstream sediment (2 – 4 km from gold mine)	
Hg (ng g^{-1}**)**	365 ± 88
OM (%)	7.55 ± 0.57
C (%)	4.38 ± 0.33
C (mg g^{-1})	44 ± 3.31
Hg/C (ng mg^{-1})	7.32 ± 1.07

5.3.4 Comparison of Hg/C patterns of Guyana sites with global sites

The Hg:C values in other environmental media (foliage, leaf litter, mineral soil, wetlands, waters, and sediment) from global studies were compiled and compared to the study site in Guyana and other contaminated sites (Table 5.2). At the global scale, Hg/C ratios in foliage (0.14 ± 0.23 ng mg^{-1}) and soil (0.80 ± 0.42 ng mg^{-1}) were lower compared with Hg/C ratios in contaminated foliage (9.78 ± 1.56 ng mg^{-1}) and soil from a gold mine in Indonesia (63 ± 7 ng mg^{-1}) (Table 5.2).

Patterns of Hg/C relationships in various environmental media were similar in Guyana and globally synthesized studies, but with much higher Hg/C ratios occurring at

contaminated sites compared with clean sites (Figure 5.5). In Guyana, Hg/C in foliage is high (9.78 ± 1.56 ng mg^{-1}) and increases in leaf litter by about 3-fold (27.77 ± 2.24 ng mg^{-1}) reflecting continued accumulation in leaf litter from atmospheric exposure. In mineral soil Hg/C ratios decreased (5.10 ± 0.20 ng mg^{-1}) suggesting some Hg loss relative to the source leaf litter. Soil water extracts (surface runoff) Hg/C ratio was 13.23 ± 2.47 ng mg^{-1}, which reflects interaction between water and contaminated mineral soil and leaf litter through overland flow. The Hg/C ratio in sediment was 7.32 ± 1.07 ng mg^{-1} and similar to mineral soil suggesting erosional runoff with particulate Hg/C as a dominant contributor to Hg in sediment (Figure 5.5).

At the global scale, Hg/C in foliage is low (0.14 ± 0.23 ng mg^{-1}) and increases in leaf litter by about 6-fold (0.82 ± 0.15 ng mg^{-1}) suggesting continued accumulation in leaf litter similar to what is occurring at the Guyana site. The mineral soil Hg/C ratio (0.80 ± 0.42 ng mg^{-1}) was similar to leaf litter, whereas wetland soils had much lower Hg/C ratios (0.24 ± 0.22 ng mg^{-1}), which are almost identical to values reported in a global synthesis of Hg/C ratios in river (0.25 ± 0.20 ng mg^{-1}) (Lavoie et al., 2019), suggesting wetlands are the major contributor to Hg in freshwaters. Similar to the mine site, the Hg/C ratio in sediment (0.46 ± 0.41 ng mg^{-1}) falls between those observed in wetlands and mineral soils suggesting some erosional inputs from overland flow mixing of particulate Hg/C in leaf litter and mineral soil (Figure 5.5).

Table 5. 2. Guyana and global patterns of Hg/C (ng mg^{-1}).

Hg/C ratios (ng mg^{-1})		Source [Country]
Guyana and contaminated sites		
Foliage (n=30)	9.78 ± 1.56	This study
Foliage (n=72, global)	14.32 ± 5.17	(Gerson et al., 2022; Ssenku et al., 2023) [Peru, Uganda]
Leaf litter (n=20)	27.77 ± 2.24	This study
Leaf litter (n=41, global)	0.42 ± 0.10	(Guédron et al., 2018; Ssenku et al., 2023) [French Guiana, Uganda]
Mineral soil (n=10)	5.10 ± 0.20	This study
Mineral soil (n=19, global)	63 ± 7	(Tomiyasu et al., 2020) [Indonesia]
Surface runoff (n=5)	13.23 ± 2.47	This study
Sediment (n=21)	7.32 ± 1.07	This study
Sediment (n=92, global)	8.28 ± 0.78	(Chakraborty et al., 2015; Donkor et al., 2005; Kongchum et al., 2011; Pinedo-Hernández et al., 2015) [India, Ghana, USA, Colombia]
Global clean sites		
Foliage (n=70)	0.14 ± 0.23	(Ma et al., 2022; Yang et al., 2018) [China, USA]

Hg/C ratios (ng mg^{-1})		Source [Country]
Leaf litter (n=34)	0.82 ± 0.15	(Gómez-Armesto et al., 2020; Juillerat et al., 2012; Ma et al., 2022) [Spain, Portugal, USA, China]
Wetland (n=126)	0.24 ± 0.22	(Osborne et al., 2024) [global study across 16 countries]
Mineral soil (n=253)	0.80 ± 0.42	(Grigal, 2003; Luo et al., 2014; Obrist et al., 2009; Różański et al., 2016; Watmough et al., 2019) [Seden, Norway, USA, China, Poland, Canada]
River (n=3578)	0.25 ± 0.20	(Lavoie et al., 2019) [global study across 14 countries]
Sediment (n=100)	0.46 ± 0.41	(Chakraborty et al., 2015; Coquery & Welbourn, 1995; Fragoso et al., 2018; Sanei & Goodarzi, 2006) [India, Canada, Brazil]
n=number of samples		

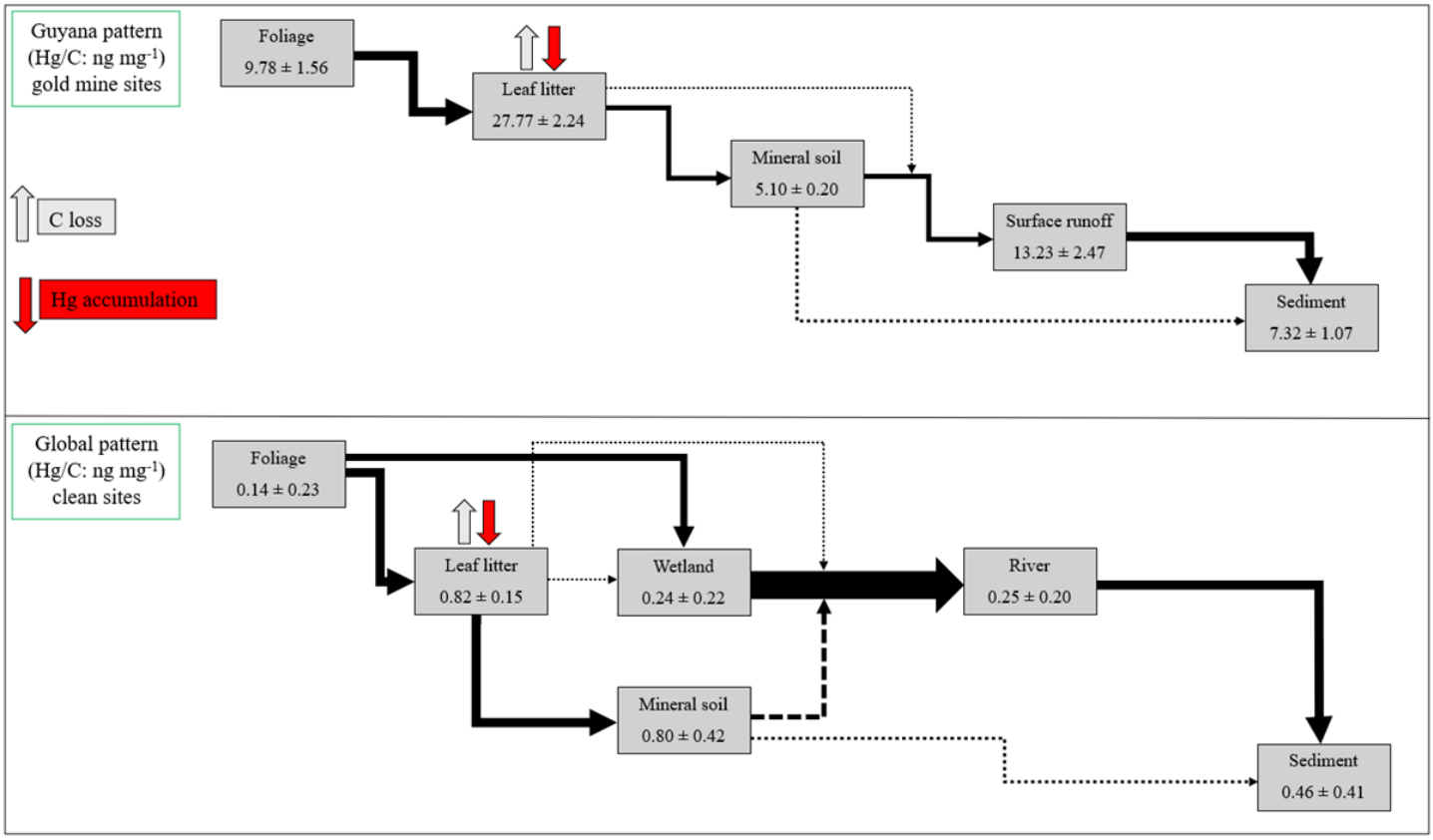

Figure 5. 5. Conceptual model of Hg/C ratio in environmental media at sites near artisanal gold mining in Guyana versus global clean sites. Grey boxes indicate Hg/C (ng mg^{-1}) in environmental media. Black arrows indicate the pathway of Hg and thickness of arrow indicate relative influence.

5.4 Discussion

5.4.1 Relationship between Hg and C in soil

Strong relationships between Hg and soil C were evident in Guyana although the slope of this relationship decreases slightly up to 4 km from the gold mine. This relationship also exists globally, but the slope of the relationship (and Hg/C ratio) are much lower than values observed in Guyana and at other gold mine sites in Indonesia. Atmospheric Hg is

volatilized through Hg-gold amalgamation and other sources such as deforestation, which is captured again by vegetation and incorporated in soil through litterfall and rainfall, where soil C binds Hg (Olson et al., 2018; Tomiyasu et al., 2020; Watmough et al., 2019). The higher slope of Hg/C observed near gold mining sites in Guyana and Indonesia suggests that Hg emissions associated with gold mining activities interact with vegetation and C, which is indicative of atmospheric Hg exposure. Close to gold mines, the periodic nature of burning gold amalgams likely results in large temporal changes in Hg/C ratios, with much higher values during a burn and much lower values occurring during intermittent periods. Moss bags placed around the gold mine for example, showed elevated Hg (259,423 ng g^{-1}) during a burn and 100 times lower Hg values during intermittent periods (chapter 4).

In Guyana, the semi-mechanized approach (excavators, heavy engines, heavy duty trucks and gold washing plants) to medium scale gold mining results in the removal of forest cover and forest floor (rich above-ground OM layer) to extract gold. Such extractive processes contribute to the loss of soil C, which could explain the low range of soil C in this study and available to bind Hg. Despite the uncertainties surrounding the impact of C quantity and quality on the transport and availability of Hg for binding in soil (Eckley et al., 2021), consistent relationships between soil Hg and C were evident. Humification leads to a reorganization of organic compounds during the decomposition of OM, while mineralization leads to intense mass loss. Studies have shown that up to 90% of the initial mass of fallen leaves is lost through decomposition due to the release of CO_2, with another 50% of the remaining OM being lost through further decomposition under reducing conditions, predominately as CH_4. During this process, OM also traps and accumulates

deposited Hg (Biester et al., 2012; Kuhry & Vitt, 1996; Tomiyasu et al., 2020). The relationship between soil C and Hg in this study is consistent with observations that ionic Hg is largely complexed to reduced S groups that is abundant in organic molecules, in the organic horizon (Cheng et al., 2020; Obrist et al., 2009; Yang et al., 2007; Yu et al., 2014). Conditions such as climate, land-use change, and landscape disturbance affects the dynamics of soil C, which drives the spatial patterns of Hg concentrations in soil (Yu et al., 2014). The linear range between soil C and Hg is also a possible indication of the migration of Hg with organic compounds (Tomiyasu et al., 2020). Such migration can partially explain Hg found at sites farther away from the gold mine.

5.4.2 Leaf litter decomposition and relationship with Hg

Leaf litter Hg collected from a forested area close to an artisanal gold mine in Guyana increases *in-situ* but decreases *ex-situ* resulting in a 100-fold difference in Hg and Hg/C ratios even though decomposition took place in soil with similar Hg concentrations (~500 ng g^{-1}). Accumulation of Hg from the atmosphere must be the main contributor to leaf litter *in-situ* due to gold mining activities. The elevated atmospheric Hg concentration (>115,187 ng m^{-3} over a 48-hr period during the burning of gold amalgam as documented in chapter 4) within the gold mining environment is absorbed to the surface of the decaying leaf litter; hence increased Hg concentration (Pokharel & Obrist, 2011). In chapter 4, moss data also showed elevated Hg (259,423 ng g^{-1}) during a short-term gold amalgam burning period (48-hr), but when left for the season with large periods (90 days) of inactivity (no burning) Hg values were 100 times lower. Wet and dry deposition of atmospheric Hg to decaying leaf litter is an important cause of Hg increase (Demers et al., 2007; Li et al., 2022; Pokharel

& Obrist, 2011). Zhou et al. (2018) emphasized the importance of throughfall input including gaseous oxidized Hg or particulate bound Hg to enhance increased Hg in decomposing litter. Yuan et al. (2020) reported that the porous nature of decomposing leaf litter and the rich OM are favorable to the uptake of atmospheric Hg that is oxidized by organic S functional groups in humic substances. However, the high levels of gaseous elemental Hg emitted at the sampled gold mine in Guyana may saturate available functional groups and only a fraction of emitted gaseous elemental Hg may react. Also, the increase could be attributed to the rate of nutrient elements loss being much higher than the rate of Hg loss during leaf litter decomposition, which leads to Hg being concentrated in the decaying leaf litter given the distinct leaf litter mass decrease (Li et al., 2022; Pokharel & Obrist, 2011). Studies by Zhou et al. (2018) and Demers et al. (2007) reported increased concentrations of Hg and decreased litter mass following one year and two years of leaf litter decomposition, respectively. It appears that Hg accumulation in leaf litter might be accounted for by absorption from the atmosphere. The accumulation of Hg in leaf litter on the forest floor may be a combination of new (atmospheric Hg recently emitted from anthropogenic and natural sources), recycled, and old Hg (previously deposited and bound to vegetation) (Demers et al., 2007; Hintelmann et al., 2002).

Under *ex-situ* conditions atmospheric Hg concentration is expected to be much closer to natural background levels for the global south (1 ng m^{-3}) (Sprovieri et al., 2016) given the absence of gold mines. The loss of Hg during leaf litter decomposition could be explained by microbe and OM induced mineralization of C and gaseous elemental Hg volatilization directly from litter surface (Li et al., 2022; Obrist et al., 2010; Pokharel & Obrist, 2011). Therefore, with C mineralization loss, Hg losses by emission to the

atmosphere are also possible under *ex-situ* conditions without mining as confirmed by the low Hg/C ratio (Zhou et al., 2018). Obrist et al. (2010) reported that C losses during decomposition processes may be accompanied by corresponding losses of Hg via gaseous evasion and runoff processes. The warm climate in the *ex-situ* location coupled with high temperatures (25 to 28℃) and solar radiation could increase vapor pressure and lead to Hg loss (McLagan et al., 2019). In addition, Hg leaching with newly formed DOC through surface runoff could also contribute to Hg loss from litter (Li et al., 2022; Wang et al., 2019). This was supported by the findings of chapter three of this thesis which showed decreased Hg/DOC ratios for sites farther away from the emission source (13 ± 2 ng mg^{-1}) compared with sites closer to the emission source (104 ± 39 ng mg^{-1}). Tsui et al. (2008) also suggested that water chemistry (DOC, pH, suspended solid, dissolved sulfate) and terrestrial leaf litter characteristics are vital factors controlling Hg release during the decomposition of litter.

5.4.3 Guyana versus global Hg/C patterns in environmental media

The patterns of Hg/C relationships in various environmental media were similar in Guyana and globally synthesized studies, but with much higher values at contaminated sites compared with clean sites. Therefore, the cycling of Hg and C are intrinsically linked at both contaminated sites and clean sites observed globally. In Guyana and at the global scale, Hg/C ratios were lowest in foliage, with increases during decomposition, and surface water ratios reflected inputs from dominant flow paths (surface soils and wetlands), while sediment sample ratios were closer to mineral soils due to a greater contribution of erosional losses.

Mercury is absorbed by living and dead OM given the strong sorption capacity between C and Hg (Galloway et al., 2024), but this can exchange rapidly between burning and non-burning periods of gold amalgam in Guyana. Leaf litter has longer exposure time than foliage, allowing continuous Hg accumulation from the atmosphere during burning periods which increase Hg/C ratios in litter (Ma et al., 2022). Pan et al. (2023) reported higher Hg concentration in litter exposed to industrial zones (50 ng g^{-1}) compared with areas less affected by anthropogenic activities (28 ng g^{-1}). Therefore, increased atmospheric Hg exposure from contaminated sites could significantly increase the Hg/C ratio in litter. Litterfall adds Hg into soil and once buried in soil (no longer exposed to the atmosphere) dilution by belowground C inputs from fine roots lower the Hg/C ratio (Demers et al., 2007; Grigal, 2003; Hall & St Louis, 2004; McCormack et al., 2015). Obrist et al. (2010) found that most of the Hg associated with soil C is not lost to the atmosphere during respiration, but it is possibly retained in the soils or subjected to other loss pathways such as runoff and mobilization. The presence of dead roots and various organic C and N rich materials released as rhizodeposition (low molecular mass and polymeric exudates, mucilage, and sloughed-off cells) from living roots contributes to higher total C supply and greater efficiency in C retention, which may lower Hg/C ratios in soil (Kögel-Knabner, 2017; Sokol et al., 2019; Sokol & Bradford, 2019). Mercury is transported to surface water during rain events predominantly through surface flow paths resulting in a higher Hg/C ratio. This transport mechanism is linked to the dominant influence of soil C on the enrichment behavior and movement of Hg, leading to a significant portion of soil-bound Hg being transferred into surface water (Zheng et al., 2016). Sediment Hg/C ratio was closer to soil than surface runoff, indicating erosion and particulate C may be a greater

component. Soil erosion during rainfall-runoff events can introduce particulate bound Hg into sediment and extend the environmental risk from soils to aquatic ecosystems. During soil erosion and overland flow, surface runoff could be enriched by Hg that was deposited from the source litter (Navarro et al., 2008). Therefore, when rainwater reaches mineral soil, Hg is adsorbed and/or precipitated and move with the soil particles into sediments.

At the global scale, Hg/C ratios were much lower in environmental media of these clean sites compared with contaminated sites, but transfer of Hg through the biosphere appears to operate similar to that adjacent to the artisanal gold mine in Guyana. Foliage Hg/C ratios were much lower than Guyana possible due to species composition, seasonality as well as location. Han et al. (2025) reported elevated Hg concentration for deciduous leaf species due to larger leaf area, higher number of stomata, and higher stomatal conductance compared with coniferous leaf species. These factors could enhance atmospheric Hg absorbance by leaves and dictate associated Hg/C ratios. Seasonal variation could also influence Hg/C ratios in foliage, with summer periods showing lower values compared with winter-early spring periods (Tabaja et al., 2023). Here, the seasonal changes were associated with seasonal variations in tree physiology such as Hg accumulation in leaves following stomatal uptake. During winter-early spring periods water is available and there is no limitation to photosynthetic activity, so both Hg and CO_2 diffuse through opened stomata in foliage. However, the low Hg in foliage during the summer is a possible indication of declined Hg uptake due to reduced stomatal conductance (minimal photosynthetic activity) during these dry conditions (low precipitations) and high temperatures (> 25°C) (Tabaja et al., 2023). Foliage from remote locations tends to show much lower Hg/C ratios than sites near artisanal gold mines due to the absence of Hg

emission source (Du et al., 2019; Ma et al., 2022). Foliage is also recognized as an important interceptor of wet and dry deposition of atmospheric Hg. Foliage temporarily captures Hg during precipitation and subsequently deposit it as throughfall and litterfall (wet deposition), while in the absence of precipitation, dry deposition proceeds with the Hg deposited onto the surface of leaves (Choi et al., 2008; Miller et al., 2005). Similar to Guyana Hg/C ratio in litter increases presumably also caused by continued adsorption of Hg from the atmosphere although some studies (Demers et al., 2007; Ericksen et al., 2003) suggest uptake of Hg from soil may be important. The accumulation of Hg in fallen litter from soil may be complexed during soil contact or translocated from soil below and likely represent old Hg fluxes (Demers et al., 2007). Studies have shown that different leaf litter species are subject to different rates of decomposition and distribution pattern of Hg. For instance, Hall and St Louis (2004) and Ma et al. (2022) found that deciduous leaf litter decomposed faster than coniferous leaf litter, while Demers et al. (2007) reported the opposite. This notion could influence Hg/C ratios within litter depending on the rate of Hg inputs. Pokharel and Obrist (2011) reported a significant increase in *Populus tremuloides* litter Hg concentration (>24% of original concentration) after 18 months of decomposition compared with other leaf litter species which remained close to starting levels. Here, *P. tremuloides* litter showed a lower fraction of Hg loss which is consistent with increased Hg concentration in time. Soil Hg/C values were similar to litter but there is a lot of variability likely attributable to soil depth, location, OM, and age. Mercury deposited into soil could be retained and sequestered due to the strong affinity between Hg and soil C, but evidence has shown that Hg concentration declines with soil depth along with declining soil C (Obrist et al., 2010). Morosini et al. (2021) reported high Hg concentrations in surface soil

(0 – 40 cm) where C content is generally higher, and Hg concentrations declined sharply with increasing depth (100 cm). Elevated atmospheric Hg concentrations near emission source may lead to an increase in Hg deposition (wet and dry deposition), which has a strong influence on distribution patterns of Hg in soil on a regional scale due to the ability of soil C to bind with Hg (Ma et al., 2022). Interactions such as physicochemical fractioning of OM between the dissolved and adsorbed phases could account for the transport of Hg to soils (Demers et al., 2013). The degree of decomposition is also related to C/N ratios in soil, where lower C/N ratios are generally indicative of older decomposed fractions (Obrist et al., 2009). Ma et al. (2022) reported a significantly negative correlation between Hg/C and C/N ratios, suggesting that older and highly decomposed soils contain elevated levels of Hg.

In contrast to Guyana, wetlands are prevalent at the global scale and the mean Hg/C ratio measured in 126 peat samples from 16 countries across six continents (Africa, Asia, Europe, North America, Oceania, and South America) (*Global Peatland Microbiome Project; Lamit and Lilleskov et al. unpublished*; Watmough et al., 2022) were almost identical to the ratios obtained from an analysis of 3,578 surface water samples from 14 countries across four continents (Asia, Europe, North America, and South America) (Lavoie et al., 2019), suggesting that transport of C associated with Hg from wetlands is the primary source of Hg to surface waters globally. Organic rich wetland ecosystems are important sources and sinks of Hg and the transport of Hg to river is mainly driven by DOC given its affinity for Hg (Adediran et al., 2019; Aksentov & Sattarova, 2020; Grigal, 2003). The coarse matrix of mineral material within peatland that is enriched in DOC and associated Hg may be more hydrologically mobile for transport to stream channel than Hg

retained in podzolized mineral soil (Demers et al., 2013). Similar to Guyana, Hg/C ratios in global sediments were higher than surface waters and closer to soil Hg/C ratios suggesting that inputs of Hg associated with mineral soil C from erosional processes are important contributors to sediment Hg. Selvendiran et al. (2008) reported elevated Hg concentration and DOC during high runoff periods due to wetting events, which interact with sediment. This pattern reflects DOC control on Hg due to flushing of DOC associated with elevated flow regimes. Demers et al. (2013) also reported that the transport of legacy Hg from soils to aquatic systems possibly depends upon hydrologic flow paths and decomposition dynamics.

5.5 Conclusion

Organic matter return rate through litterfall depends on various factors that influence the process of decomposition and Hg movement through environmental media. A strong positive relationship exists between soil C and Hg for regions close and distant from point source, with Hg/C ratios being much lower in sites farther away from emission source compared with those observed near artisanal gold mines. The results of this study show that Hg concentration and Hg/C ratios increased in leaf litter by 100-fold for sites exposed to mining (*in-situ*) compared with sites without mining (*ex-situ*). Leaf litter with direct soil contact may function as a temporary pool for soil Hg, which may be important for risk assessments since this can aid the dispersal of contaminants through leaf litter translocation. Processes and patterns of Hg/C ratios in various environmental media were similar in Guyana and globally synthesized studies, with much higher values at contaminated sites compared with clean sites. Here, Hg/C ratios were lowest in foliage,

with increases during decomposition, and surface water ratios reflected inputs from dominant flow paths (surface soils and wetlands), while sediment sample ratios were closer to mineral soils due to a greater contribution of erosional losses. The outcomes of this study contribute to a greater understanding of the movement of Hg through environmental media. Understanding litter dynamics (decomposition) and the interaction between C and Hg provides insights into the reclamation of degraded soil since this determines the supply rate of C to soil and the reactivation of nutrient cycling. Further study should focus on the source and loss of Hg during the decomposition of leaf litter.

6.0 Evaluation of biochar on plant growth on waste spoils from artisanal gold mines in Guyana

6.1 Introduction

Anthropogenic activities such as artisanal gold mining has led to the contamination of soil with elements that are potentially toxic, and this has become a global concern due to impacts on environmental and human health (Durante-Yánez et al., 2022). Artisanal gold mining serves as a source of income for 30 million miners in developing countries (inclusive of Guyana), however, gold mining has historically been associated with the large production of solid wastes (Akoto & Anning, 2021; Costa et al., 2012; Driscoll et al., 2013; Martín et al., 2020). Gold mining, particularly at the small and medium scale results in soil degradation and deforestation, production of overburden/development wastes and tailings, and release of mercury (Hg) due to rudimentary techniques being employed to amalgamate gold ore with Hg (Akoto & Anning, 2021; Aram et al., 2021; Gafur et al., 2018; Ogola et al., 2002). In the quest to mitigate these potential threats, gold mining operations and regulators continue to pursue greener and efficient technologies coupled with stringent regulations and enforcement to replace rudimentary and traditional extraction methods and regulations (Akoto & Anning, 2021). Even with these efforts, small and medium scale gold mining operations in Guyana are still faced with waste spoils issues, which require informed management to effectively reclaim mined out sites.

The soil chemistry of gold mine spoils tends to undergo alterations due to Hg and metal contamination. This alteration is not always consistent since the Hg added to the ore may not be present in the overburden. Abandoned gold mines could be left to recover

vegetation naturally, but this process is slow due to the inhospitable environment (Chambi-Legoas et al., 2021). Therefore, reclamation efforts are needed to accelerate the revegetation of mined sites. Waste spoils from artisanal gold mines generally have low organic matter (OM), that can affect nutrient availability as well as physical props (poor cohesion) to facilitate plant growth (Festin et al., 2019; Lewis et al., 2020; Timsina et al., 2022). These waste spoils have also lost soil layer profile, soil compaction, and suffer from a decrease in soil microbial population (Gusmini et al., 2021). In developing countries like Guyana, gold mine spoils are not adequately characterized prior to reclamation. In the absence of such critical scientific data, *Acacia mangium* (fast growing woody fabaceous species), which has shown invasive characteristics owing to long viability in soil, abundant production of seed and dispersal efficiency over large scales (Bento et al., 2012; Cipriani et al., 2013; Majid et al., 2012), is predominantly being used for reclamation of mined out sites. The low cost phytoreclamation approach to cleaning up metal pollution in soil is an alternative to the more expensive chemical and physical processes (Ansari et al., 2009; Garbisu & Alkorta, 2001; Majid et al., 2012). However, few studies in Guyana have evaluated how soil amendments may be used to improved soil quality and plant performance (Moonilall et al., 2020; Persaud et al., 2018; Whyte et al., 2024).

Soil fertility and reclamation could be enhanced through the application of biochar, which is a stable carbon-rich derivative from pyrolysis of plant material (Ahmad et al., 2014). *Chlorocardium rodiei* (greenheart) is a readily available wood species in Guyana (Kekem et al., 1996) that could be subjected to pyrolysis to produce biochar. This type of biochar is locally sourced in Guyana and may enhance nutrient availability (calcium (Ca), nitrogen (N), phosphorus (P), potassium (K)) and improve physical properties (porosity

and water holding capacity) of soil to support plant growth (Festin et al., 2019). Research by Boraah et al. (2023) reported the excellent potential of wood-based biochar for soil improvement and rich carbon content of 50-70 %. Such improvements of the soil are linked to biochar's ability to enhance soil OM content and soil moisture (Musei et al., 2024).

Gold mining sites are commonly partitioned into: (a) the pit – areas with mixture of material remaining after gold has been separated from the ore and high intensity of disturbance, (b) overburden – areas overlying the gold ore, including topsoil, which are displaced during the mining process, and (c) adjacent sites – areas without deposits of material from the mining process (Kalamandeen et al., 2020). Soil materials of the overburden zone are primarily used for backfilling to commence reclamation; therefore, it is important to understand how well these soils could support growth to better inform exposure risks analysis. The purpose of this study was to assess the growth performance of *Poa pratensis* (seed germination capacity, seedling height, and root and shoot dry biomass) on gold mine spoils compared with nearby vegetated soils. The effect of treatment with biochar and without biochar on growth performance of *P. pratensis* was discussed, given the role of biochar (organic amendment) as a growth stimulant. It is hypothesized that *P. pratensis* growth performance will be higher in distant sites and biochar treated sites compared with overburden. The findings can potentially aid in the formulation of target specific recommendations for the reclamation of mined out sites, given the existing gaps in understanding the exposure risks.

6.2 Methodology

6.2.1 Field sampling

Soil samples were collected (May 2023) from two active gold mines in Mahdia (Hopkinson medium scale operation, 5° 16’ 76” N and 59° 5’ 40” W) and Frenchman (Obermuller medium scale operation, 4° 57’ 5” N and 58° 48’ 25” W). The Mahdia mine site is larger than the Frenchman mine site and currently has more gold mining activities. At each gold mine, surface (0 – 10 cm) soil samples (ca. 2 kg) were taken in triplicates from distant site (forested with limited anthropogenic activities and 2 – 4 km from the mining process) and the overburden zone (soil materials from this zone are used for backfilling to commence reclamation) (Figure 6.1). Soils were placed in labelled Ziploc® bags and stored in a cooler for transport to the University of Guyana Agriculture laboratory to be oven-dried (10 days at 105℃, Thermo Scientific, Freas 645). A small amount of Hg may also have been lost during the drying procedure as Hojdová et al. (2015) reported that the loss of Hg in samples dried at 105℃ was 3 % compared with freeze dried samples.

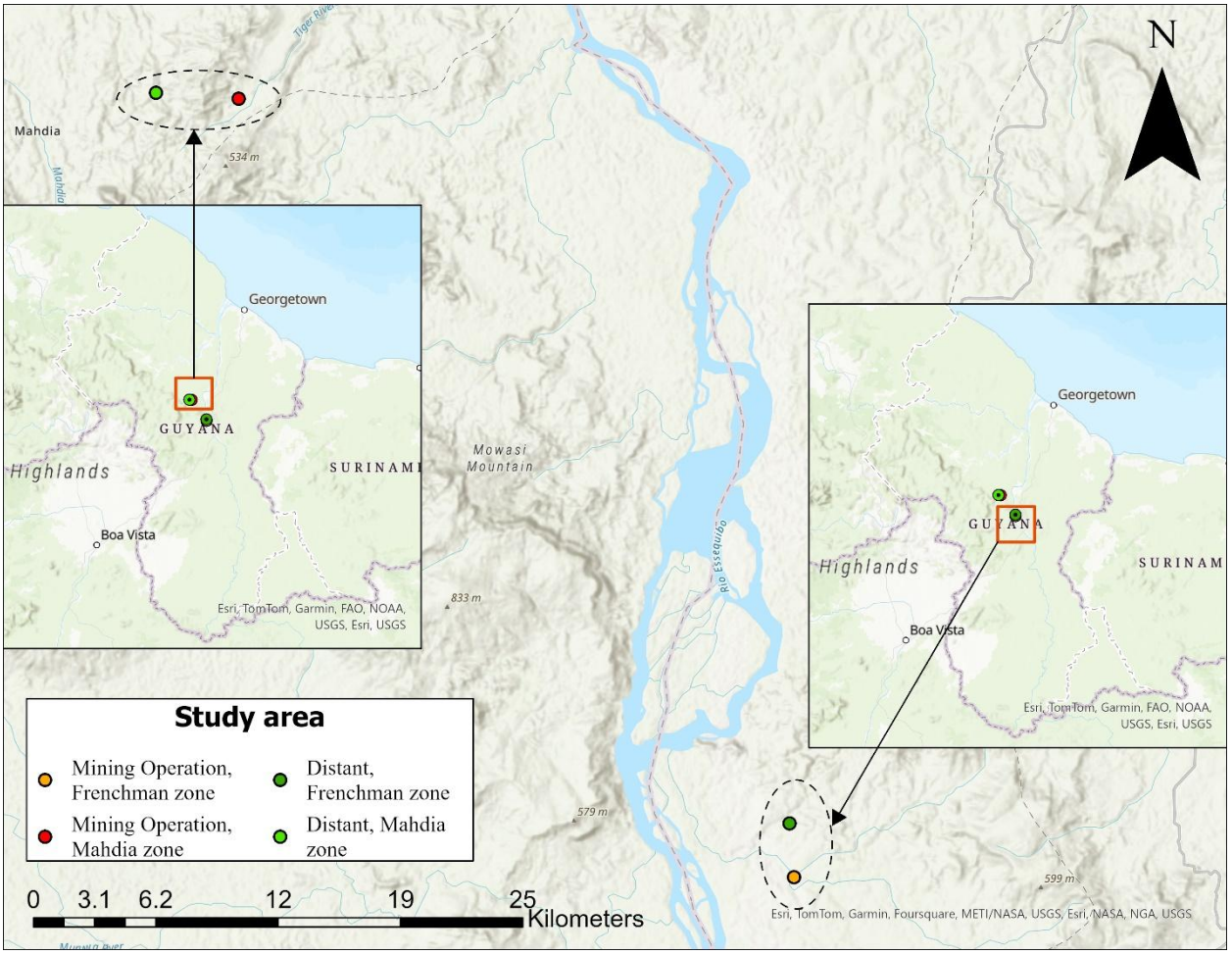

Figure 6. 1. Location of sample collection.

6.2.2 Biochar preparation and physicochemical properties

Biochar used for this study was generated from *Chlorocardium rodiei* (greenheart sawdust) that was collected from a local sawmill in Parika (Guyana) (France et al., 2024). The biochar was produced using pyrolysis at a temperature of 400°C for 4 hours in *Andrew Vreugdenhil Lab*. The biochar material is characterized by 68.8 % C; 2.49 % N; and total concentrations of 181 mg kg^{-1} P; 1215 mg kg^{-1} K; 183 mg kg^{-1} sodium (Na); 920 mg kg^{-1} Ca; 419 mg kg^{-1} magnesium (Mg); 0.05 mg kg^{-1} cobalt (Co); 2.23 mg kg^{-1} copper (Cu); 79 mg kg^{-1} manganese (Mn); and 9.61 mg kg^{-1} zinc (Zn). Metals such as arsenic (As),

cadmium (Cd), nickel (Ni), and lead (Pb) were not detected in the biochar material used. The minimum detection limits of As, Cd, Ni, and Pb were 0.01, 0.02, 0.04, and 0.02 mg kg^{-1}, respectively. Metals were not a concern in biochar given their relatively low concentrations, which were all below the recommended threshold limits set by the International Biochar Initiative for safe use in soil (International Biochar Initiative, 2015).

6.2.3 Experimental design and growth chamber trial

A randomized block design with dried, homogenized, and sieved (2 mm) soil samples from the overburden zone, the distant site, and soils with organic amendments (biochar + overburden and biochar + distant site) were set up in sets of 5 for a total of 40 pot experimental units. Biochar was applied to soil at a rate of 2.5 g (10 t ha^{-1}) per pot and mixed before being allowed to acclimate for four months (May to August 2024) prior to sowing seeds (Guo, 2020). A seed germination test was used to measure *P. pratensis* (Kentucky bluegrass) seed viability prior to sowing seeds. Fifteen seeds were placed into a container of water to sit for 15 minutes. Seeds that sink were considered viable, while those that float were removed, since they may not sprout.

Experimental units were randomly arranged to facilitate uniform illumination (Durante-Yánez et al., 2022; Guo et al., 2019). Each randomly arranged experimental unit (5 cm layer of soil packed in 5 cm diameter plastic pot) received 15 seeds and growth performance was monitored over a period of four weeks under laboratory conditions that approximate conditions in Guyana (temperature of 25℃ and relative humidity of 50 %), with the aid of daily 12-hour artificial lighting and appropriate watering. Every five days seedling height was measured (in mm) for each cultivar (n = 75) to assess growth rate on

the 5th, 10th, 15th, 20th, 25th, and 30th day from sowing. After a period of four weeks, seed germination capacity (% seed germination over an extended period) was assessed (Gawryluk et al., 2022; Hong et al., 2009). Dry biomass was assessed by dividing plant tissues into shoot and root (Figure 6.2) and taking the dry weight of each tissue after oven-drying (24 hours at 105℃).

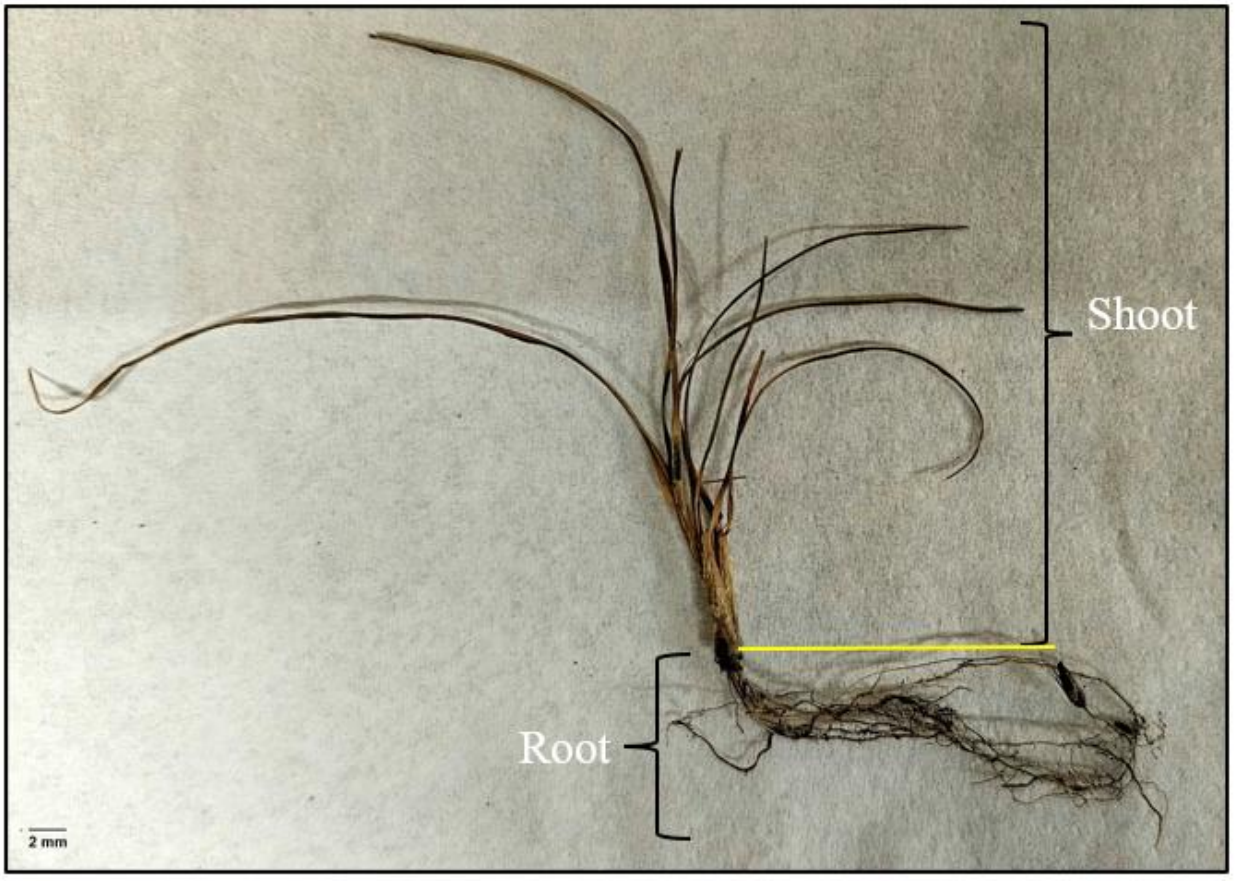

Figure 6. 2. *Poa pratensis* shoot and root anatomy.

6.2.4 Soil chemistry analysis

Dried soil samples were crushed to homogenize the samples and sieved (2 mm) to remove stones and roots. To determine soil pH, a sub-sample of soil (5.0 g) was added to each 50

ml conical centrifuge tube, followed by 25 ml of 0.01 M $CaCl_2$. The suspension was subjected to a shaking process (Shaker Table, Eberbach) for 60 minutes, then allowed to sit for another 60 minutes for soil particles to settle prior to measurement with a pH meter (Oakton, pH 510 Series). (Muddarisna & Siahaan, 2014).

Soil organic matter (%OM) was measured by loss-on-ignition (Equation 1). After oven-drying (24 hours at 105°C) of soil (5 g) to constant weight, organic matter was ignited at 400°C for 10 hours (Heiri et al., 2001).

$$\%OM = \left(\frac{W_1 - W_2}{W_1 - C_w} \right) \times 100 \qquad \text{Equation 6}$$

Where, W_1 = weight pre ignition, W_2 = weight post ignition, and C_w = crucible weight.

Total Hg concentration in soil was measured with a Direct Mercury Analyzer (DMA-80) by thermal decomposition, amalgamation, and atomic absorption spectrometry. Sub-samples of dried soil (0.05 g) were heated to 900°C to reduce Hg species to elemental Hg, which was loaded onto an amalgamator. Subsequent heating of the amalgamator resulted in the release of Hg vapors into a single bean, fixed wavelength atomic absorption spectrophotometer. Quality control of Hg measurements was assured by the inclusion of blanks and certified reference materials (*Enviro*MAT™ SS-1) at the start of each experimental run (40 samples) and recovery ≥ 93 % was considered acceptable.

The total nutrient (Ca, K, Mg, Na, P) and metal content (As, Cd, Co, Cu, Mn, Ni, Pb, Zn) in soil that may influence plant growth were subjected to an acid digestion (HNO_3) process, which is not a total digest (unlike perchloric acid) to measure concentrations in soil. A sub-sample of dried soil (0.2 g) was added to each 100 ml polypropylene acid resistant digestion tube, followed by 2.5 ml of concentrated HNO_3. Tubes were swirled

gently to ensure complete mixing with HNO_3 and closed loosely. Tubes were placed in a block-digester and hot plate (Cole-Parmer®) for 16 hours (8 hours cold and 8 hours hot). Following the completion of acid digestion, cooled samples were subjected to a filtration process (Fisherbrand® Filter Paper Qualitative P8 Grade). The volume of the filtered sample was adjusted to 25 ml with BPURE water and transferred to a 50 ml conical centrifuge tube for storage at 4°C. This was followed by the pipetting of 10 ml of digested sample into a 15 ml conical centrifuge tube and stored at 4°C until analysis with inductively coupled plasma-optical emission spectrometry (ICP-OES). Blank reagents and digested standard reference material (*Enviro*MAT™ SS-1) were run with each batch of samples to ensure quality control and recovery of 80 – 120 % was considered acceptable.

Particle size analysis of soil samples was measured with a laser scattering particle size distribution analyzer (LA-950V2, Horiba) to determine clay, silt, and sand composition. Calgon (Sodium Hexametaphosphate) solution was prepared by mixing 30 g of Calgon with 1L of reverse osmosis (RO) water on a stir plate (VWR Stirrer) at 800 rpm for 30 minutes. A sub-sample of soil (2.0 g) remaining after the loss-on-ignition process, was added to each 50 ml conical centrifuge tube, followed by 2.5 ml of Calgon solution. The suspension was subjected to a shaking process (Shaker Table, Eberbach) at low speed for 8 hours. Particle size was determined for each sample by adding 3 drops of the soil-Calgon solution to the Horiba LA-950V2 and all measurements were taken in triplicates. The chemistry of the seedlings (<0.2 g per pot) were not analyzed due to limited growth of grass at the end of the growth experiment (4 weeks).

6.2.5 Statistical analysis

Statistical analysis was conducted with R version 4.0.4 (R Core Team, 2021), at an acceptable α-level of 0.05. Descriptive statistical analysis was conducted with R statistical package to assess range, mean, and standard error of soil physicochemical properties (pH, OM, texture) and total nutrient (Ca, K, Mg, Na, P), Hg and metal content (Co, Cu, Mn, Ni, Pb, Zn) in soil. Data were subjected to Shapiro-Wilk normality test to assess normal distribution, and results were expressed as the mean ± standard error of the replicate measurements.

Using data that satisfy the normality assumptions, pH, OM, texture, seed germination capacity, seedling height, root and shoot dry biomass, and nutrient, Hg and metal content in soil were compared using one-way and two-way repeated measures ANOVA to test significant differences among applied treatments. When the ANOVA indicated significant treatment effects, mean values were separated using Tukey's Multiple Range Test and emmeans pairwise comparison (Durante-Yánez et al., 2022; Gawryluk et al., 2022; Hong et al., 2009; Marrugo-Negrete et al., 2016).

6.3 Results

6.3.1 Physicochemical characteristics of soil

Soils at all sites were acidic, ranging from 4.14 to 5.63 and the application of biochar significantly decreased soil pH to 4.71, except at the distant site at Mahdia that had the lowest pH (4.28) prior to amendment and the biochar increased it to 4.50 (Table 6.1). Soil organic matter (% OM) content at all sites ranged from 1.32 to 18 % and the addition of biochar significantly increased OM by approximately 8 % resulting in OM levels between

10.50 and 23.65 % (Table 6.1). The distant site at Frenchman was almost pure sand, whereas the overburden at both locations as well as the distant site at Mahdia had much higher quantities of clay and silt (Table 6.1).

Table 6. 1. Properties of soil samples from Frenchman and Mahdia. Different letters indicate statistically significant differences ($p < 0.05$) using Tukey's test between each treatment per variable.

Treatment	pH Mean ± SE (Range)	Organic matter (%) Mean ± SE (Range)	Clay (%) Mean ± SE (Range)	Silt (%) Mean ± SE (Range)	Sand (%) Mean ± SE (Range)
			Frenchman		
Distant	5.12 ± 0.12^{ab} (4.99 – 5.31)	2.00 ± 0.16^{c} (1.32 – 2.30)	-	-	99.66 ± 0.33^{a} (99 – 100)
Overburden	5.31 ± 0.10^{b} (5.00 – 5.55)	2.38 ± 0.07^{c} (2.21 – 2.53)	27.56 ± 0.58^{b} (26.56 – 28.70)	11.00 ± 0.33^{b} (10.64 – 11.64)	60.84 ± 1.00^{b} (59.87 – 62.80)
Biochar + Distant	4.70 ± 0.14^{a} (4.37 – 5.14)	10.50 ± 0.23^{b} (9.64 – 11.00)			
Biochar + Overburden	4.72 ± 0.14^{a} (4.45 – 5.20)	11.81 ± 0.28^{a} (11.00 – 12.42)			
			Mahdia		

Treatment	pH Mean ± SE (Range)	Organic matter (%) Mean ± SE (Range)	Clay (%) Mean ± SE (Range)	Silt (%) Mean ± SE (Range)	Sand (%) Mean ± SE (Range)
Distant	4.28 ± 0.05^{b} (4.14 – 4.42)	16.04 ± 0.50^{d} (15.15 – 18.00)	13.37 ± 0.33^{a} (13.04 – 14.04)	7.16 ± 0.33^{a} (6.82 – 7.82)	79.60 ± 0.54^{a} (78.51 – 80.14)
Overburden	5.37 ± 0.06^{c} (5.29 – 5.63)	5.56 ± 0.06^{c} (5.32 – 5.64)	15.88 ± 0.33^{a} (15.54 – 16.54)	8.00 ± 0.33^{a} (7.57 – 8.60)	75.57 ± 0.66^{a} (75.00 – 76.89)
Biochar + Distant	4.50 ± 0.07^{ab} (4.36 – 4.72)	23.65 ± 0.32^{b} (22.89 – 24.78)			
Biochar + Overburden	4.71 ± 0.06^{a} (4.61 – 4.95)	13.55 ± 0.63^{a} (12.07 – 15.25)			

- not detected

6.3.2 Biochar influence on soil chemistry

The application of biochar did not significantly increase the concentrations of Ca, Mg, Na, and P in any soil, but K increased slightly in the distant site and overburden zone at Frenchman following biochar application. Similarly, the addition of biochar to soil at Mahdia resulted in slight increases in the concentrations of Ca, Mg, and Na at the distant site and overburden, but these were not statistically significant (Table 6.2). Notably, the distant site and overburden zone at Mahdia showed significant increases in K with the addition of biochar (Table 6.2).

Concentrations of all metals except Hg were below levels of concern. Mercury concentrations in distant and overburden soils were highly variable, with higher range of concentrations at Mahdia (95 – 604 ng g^{-1}) compared with Frenchman (6 – 57 ng g^{-1}). The application of biochar had no effect on soil Hg at both locations (Table 6.3). Metal concentrations in the overburden and distant soils were low but were generally higher in overburden compared with distant sites at both locations (Table 6.3). Concentrations of most metals (Co, Cu, Mn, Ni, and Zn) decreased significantly with the addition of biochar in the overburden zone at Frenchman (Table 6.3). At Mahdia, the concentrations of Co, Cu, and Zn decreased slightly in distant and overburden soils, but this was not significant (Table 6.3). Additionally, the minimum detection limits of As and Cd were 0.01 and 0.02 mg kg^{-1}, respectively and these metals were not detected in soil at the distant site and overburden zone of Frenchman and Mahdia. Also, Pb (minimum detection limit of 0.02 mg kg^{-1}) was not detected in the distant site and overburden zone at Mahdia.

Table 6. 2. Total concentrations of nutrients in untreated soils and soils treated with Biochar. Different letters indicate statistically significant differences ($p < 0.05$) using Tukey's test between each treatment per variable.

Treatment	Element Mean ± SE (Range)				
	Ca (mg kg^{-1})	K (mg kg^{-1})	Mg (mg kg^{-1})	Na (mg kg^{-1})	P (mg kg^{-1})
	Frenchman				
Distant	349 ± 99[a] (131 – 594)	16.64 ± 5.00[a] (5.75 – 34.00)	42.22 ± 10.23[a] (15.15 – 68.29)	50.15 ± 18.43[a] (15.23 – 102)	15.27 ± 2.81[a] (9.22 – 24.56)
Overburden	134 ± 28[ab] (68.29 – 238)	28.49 ± 3.74[ab] (15.00 – 36.75)	104 ± 18.30[b] (32.84 – 131)	124 ± 13.81[b] (82.52 – 165)	84.05 ± 3.67[b] (75.00 – 92.48)
Biochar + Distant	321 ± 38.57[ab] (216 – 430)	17.12 ± 3.30[a] (9.77 – 27.19)	27.19 ± 3.87[a] (14.56 – 35.23)	34.54 ± 9.27[a] (18.08 – 50.17)	9.65 ± 2.20[a] (2.86 – 16.00)
Biochar + Overburden	114 ± 16.08[b] (82.71 – 171)	44.33 ± 7.18[b] (21.77 – 66.27)	28.88 ± 3.31[a] (19.58 – 35.20)	85.84 ± 16.50[ab] (34.69 – 134)	26.54 ± 10.26[a] (11.40 – 67.04)
	Mahdia				
Distant	178 ± 19.24[ab]	42.78 ± 5.00[ac]	56.67 ± 8.14[ac]	168 ± 13.86[a]	29.73 ± 3.84[a]

	(123 – 221)	(26.60 – 54.40)	(28.09 – 78.19)	(123 – 206)	(23.52 – 39.77)
Overburden	126 ± 12.57[b] (81.73 – 150)	22.10 ± 2.36[a] (18.86 – 31.48)	22.03 ± 3.39[b] (13.88 – 28.24)	87.85 ± 14.88[b] (33.79 – 110)	98.40 ± 16.88[b] (52.07 – 144)
Biochar + Distant	278 ± 64.61[a] (146 – 500)	89.00 ± 8.88[b] (76.55 – 124)	78.00 ± 8.87[a] (47.85 – 92.00)	181 ± 16.47[a] (124 – 225)	29.75 ± 4.60[a] (15.00 – 42.66)
Biochar + Overburden	153 ± 15.08[ab] (112 – 197)	60.07 ± 5.11[c] (49.79 – 74.47)	38.55 ± 4.70[bc] (26.68 – 51.70)	130 ± 7.74[ab] (115 – 160)	87.46 ± 7.80[b] (67.02 – 106)

Table 6. 3. Acid (HNO_3) extractable concentrations of Hg and other metals in untreated soils and soils treated with Biochar. Different letters indicate statistically significant differences ($p < 0.05$) using Tukey's test between each treatment per variable.

Treatment	Element Mean ± SE (Range)						
	Hg (ng g^{-1})	Co (mg kg^{-1})	Cu (mg kg^{-1})	Mn (mg kg^{-1})	Ni (mg kg^{-1})	Pb (mg kg^{-1})	Zn (mg kg^{-1})
			Frenchman				
Distant	15.33 ± 4.00[a] (6.00 – 26.48)	0.04 ± 0.01[a] (0.02 – 0.06)	4.30 ± 0.85[a] (3.33 – 7.68)	14.09 ± 5.07[a] (5.00 – 28.08)	0.13 ± 0.02[a] (0.06 – 0.19)	0.06 ± 0.03[a] (0.04 – 0.14)	1.10 ± 0.21[a] (0.54 – 1.80)

Overburden	44.25 ± 5.15[b] (30.42 – 56.68)	10.55 ± 2.39[b] (1.10 – 14.00)	23.76 ± 2.66[b] (14.10 – 30.10)	365 ± 6.77[b] (353 – 377)	7.83 ± 1.84[b] (0.49 – 9.89)	0.63 ± 0.57[a] (0.02 – 2.92)	17.50 ± 0.48[b] (16.09 – 18.13)
Biochar + Distant	14.20 ± 1.58[a] (11.41 – 20.35)	0.04 ± 0.01[a] (0.02 – 0.04)	2.07 ± 0.48[a] (0.57 – 3.41)	19.76 ± 2.30[a] (12.04 – 28.61)	0.08 ± 0.02[a] (0.08 – 0.11)	0.50 ± 0.45[a] (0.02 – 2.31)	1.33 ± 0.40[a] (0.00 – 2.39)
Biochar + Overburden	72.25 ± 7.22[b] (62.73 – 93.59)	1.00 ± 0.14[a] (0.62 – 1.39)	13.94 ± 2.46[c] (8.45 – 21.80)	77.00 ± 20.53[c] (24.00 – 129)	0.51 ± 0.07[a] (0.38 – 0.77)	0.43 ± 0.38[a] (0.22 – 1.92)	4.19 ± 0.86[c] (2.32 – 7.42)
			Mahdia				
Distant	453 ± 52.78[a] (316 – 604)	0.62 ± 0.14[a] (0.40 – 1.14)	12.58 ± 1.01[a] (11.00 – 16.54)	22.17 ± 2.24[a] (15.42 – 28.59)	0.31 ± 0.11[a] (0.06 – 0.69)	-	5.16 ± 0.51[a] (3.58 – 6.72)
Overburden	145 ± 15.85[b] (95.61 – 185)	1.08 ± 0.14[a] (0.68 – 1.54)	25.76 ± 10.52[a] (9.02 – 67.29)	18.86 ± 2.34[a] (13.11 – 27.05)	0.73 ± 0.11[a] (0.39 – 1.05)	-	5.29 ± 0.68[a] (3.34 – 6.49)
Biochar + Distant	370 ± 57.16[ac] (272 – 574)	0.50 ± 0.12[a]	10.79 ± 1.13[a]	28.01 ± 5.25[a]	0.43 ± 0.13[a]	-	4.79 ± 0.43[a]

		(0.27 – 0.94)	(8.40 – 13.84)	(19.12 – 48.01)	(0.17 – 0.80)		(3.57 – 6.29)
Biochar + Overburden	230 ± 22.22[bc] (183 – 302)	0.85 ± 0.10[a] (0.57 – 1.14)	11.26 ± 1.57[a] (8.23 – 16.78)	18.13 ± 1.90[a] (12.42 – 23.12)	1.26 ± 0.64[a] (0.30 – 3.79)	-	4.43 ± 0.45[a] (3.15 – 5.71)

- not detected (Pb minimum detection limit = 0.02 mg kg^{-1})

6.3.3 Growth performance of Poa pratensis

Seed germination capacity was generally higher for distant sites (84 to 99 %) compared with overburden (55 to 85 %) (Figure 6.4). Some incremental increases (>4 %) in seed germination capacity were evident for treatments with biochar compared with other treatments, but this was not statistically significant ($p > 0.05$, ANOVA) (Figure 6.4).

The growth of *P. pratensis* was higher in distant sites compared with overburden at both locations, but growth did not improve significantly by the addition of biochar although seedling height tended to be higher in the biochar treatments, especially at the distant sites (Figure 6.5). Seedlings growing on the distant soil were approximately twice as tall as seedlings growing on overburden by the end of the 4-week period (Figure 6.5).

Root and shoot dry biomass were higher in distant sites compared with overburden at both locations, but plant tissue dry biomass did not improve significantly by the addition of biochar even though root and shoot dry biomass tended to be higher in the biochar treatments, particularly at distant sites (Figure 6.6). Plant tissue dry biomass in distant soils were about twice the weight of plant tissue dry biomass in overburden at Frenchman, while at Mahdia plant tissue dry biomass was similar in distant soil and overburden (Figure 6.6).

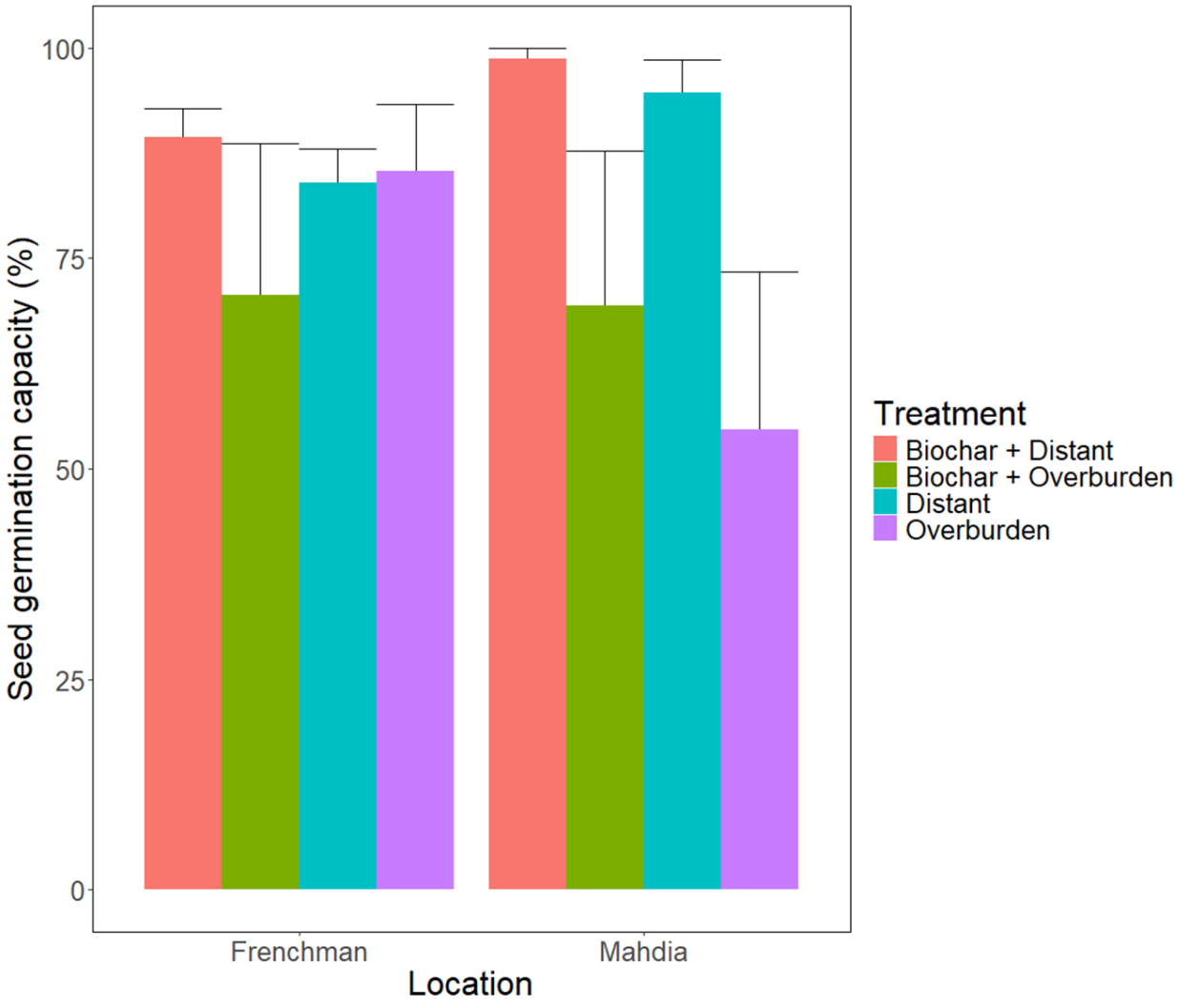

Figure 6. 3. Seed germination capacity of *P. pratensis* according to applied treatment.

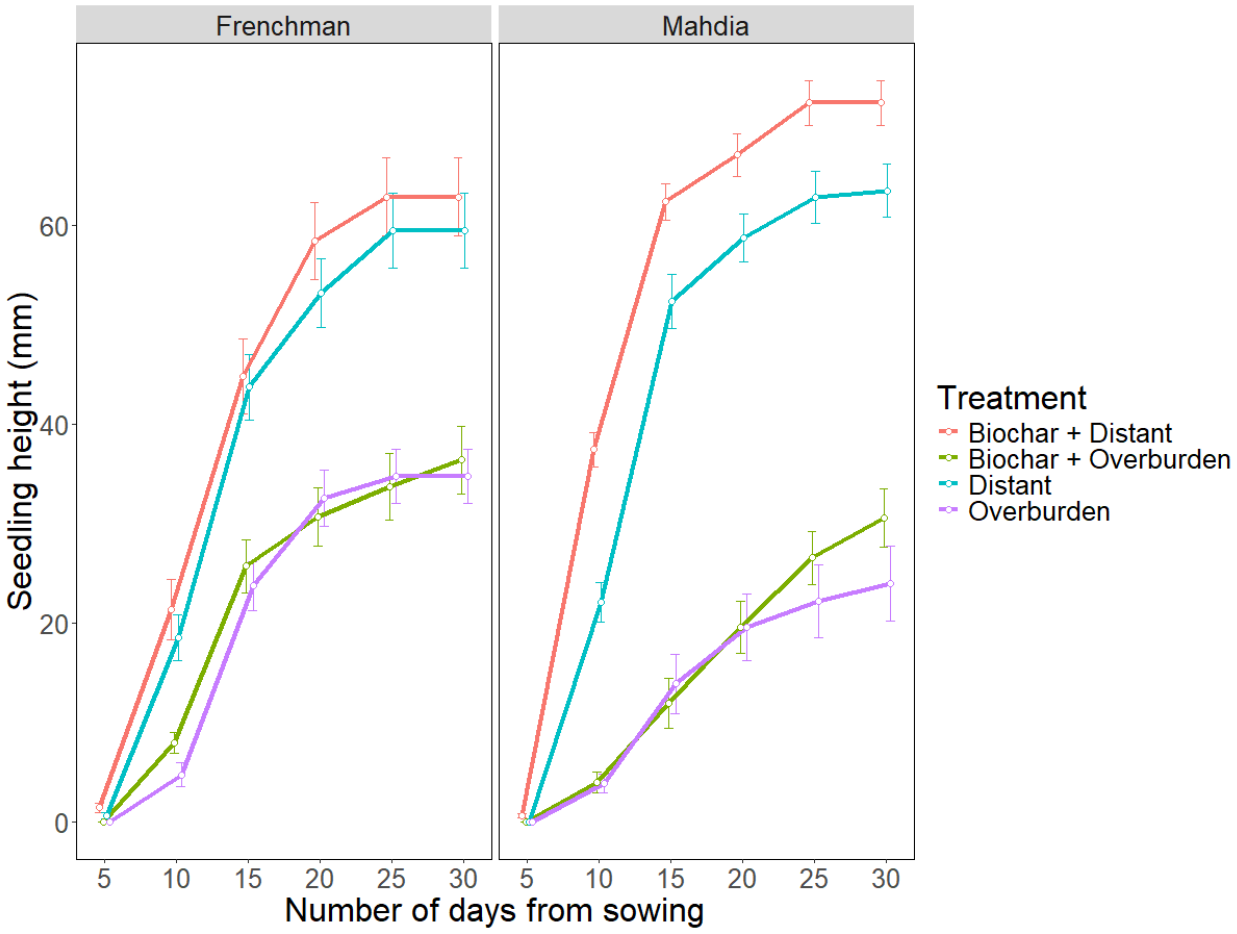

Figure 6. 4. Impact of number of days from sowing on cumulative seedling height (mm) of *P. pratensis* according to applied treatment.

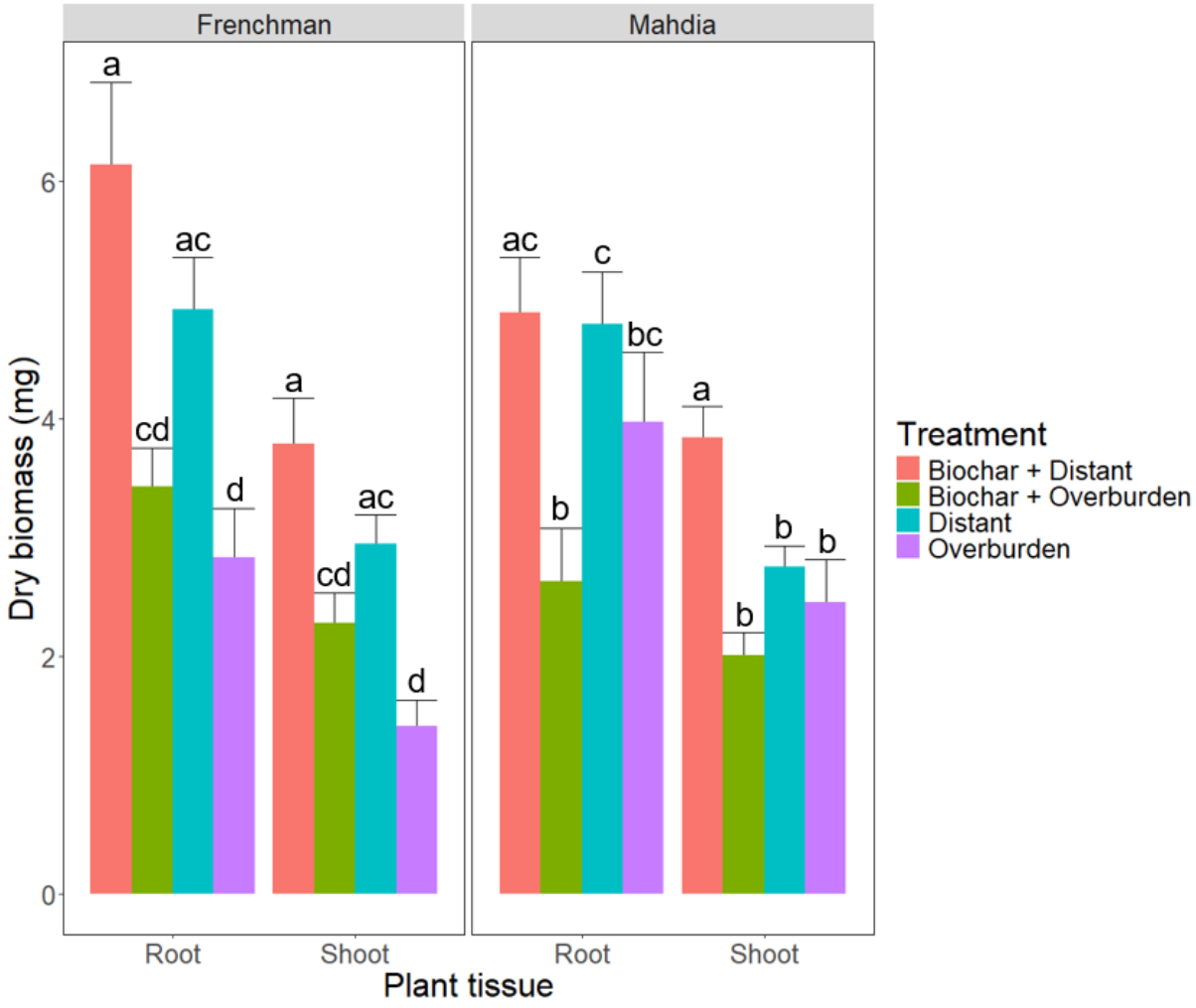

Figure 6. 5. *P. pratensis* dry biomass per tissue according to applied treatment, total dry biomass is the sum of tissues per applied treatment. Different letters indicate statistically significant differences ($p < 0.05$) using Tukey's test between each treatment per variable.

6.4 Discussion

Soils at the study sites were acidic and the overburden soils had very low OM content, but except for Hg, metal concentrations were only slightly higher in overburden compared with distant forest sites. The application of biochar significantly decreased soil pH and increased soil OM, but plant growth was much lower on overburden soils compared with distant sites and was not improved by the addition of biochar.

6.4.1 Soil physicochemical properties

The application of biochar lowered soil pH, except at the most acidic site, and increased soil OM content and these changes alter both metal and nutrient bioavailability (Barrow & Hartemink, 2023; Seshadri et al., 2015; Xu et al., 2022). At low pH, metals tend to be present as free ionic species or soluble organometals, which are more bioavailable (Marrugo-Negrete et al., 2015). Rhizosphere pH could be modified by the release of H^+ ions by roots, thereby increasing metal dissolution, since H^+ ions can displace metal cations absorbed on soil particles (Durante-Yánez et al., 2022; Salas-Moreno & Marrugo-Negrete, 2020). The evident increase in OM for soils with biochar tends to enhance the viability and vegetation of plants due to nutrient absorption (Durante-Yánez et al., 2022; Salas-Moreno & Marrugo-Negrete, 2020). Organic amendments such as biochar add OM plus nutrients to soil, which offers much more opportunities for improving soil biological, chemical, and physical properties that are vital for the success of reclamation initiatives (Larney & Angers, 2012). The local biochar material could be important for the reclamation of mine spoils due to inputs of high organic C content (68.8 % C) which provides an instant energy source to boost soil microbial activity and increased OM could improve poor physical

conditions of soil resulting from topsoil loss and compaction. Sun et al. (2024) reported that the addition of biochar (68.4 % C) produced from mixed feedstock of dominant tree species (*Quercus myrsinifolia*, *Pinus massoniana*, and *Lithocarpus glaber*) significantly increased soil OM, which promotes plant growth. Increased soil OM leads to increased organic acids, resulting in reduced pH and higher cations bioavailability. Therefore, metals tend to be less mobile in soil with acidic pH and high OM (Cruzado-Tafur et al., 2021; Marrugo-Negrete et al., 2015; Salas-Moreno & Marrugo-Negrete, 2020; Stefanowicz et al., 2020). Stefanowicz et al. (2020) found that OM rich soils could bind metals in acidic conditions, but the capacity for bonding is dependent on the metal.

Metal concentrations in soil from all sites were low and even though concentrations of most metals were higher in overburden they are unlikely to be impacting plant performance (seed germination capacity, seeding height, and root and shoot dry biomass). The exception was Hg, that was elevated at both distant and overburden soils owing to its release to the atmosphere during burning and subsequent interaction with OM (chapters 3 and 4). The elevated concentration of Hg (exceed background levels of 100 ng g^{-1} (Santos-Francés et al., 2011)) in soils is also supported by the findings of chapters 2, 3, 4, and 5, which showed high Hg concentrations in soil near artisanal gold mines. Gold mining, particularly at the small and medium scale in Guyana has led to the release of Hg into soil due to rudimentary techniques being employed to amalgamate gold ore with Hg. Studies have shown that the use of organic amendments in the reclamation of mine soil has the potential to accelerate the recovery process through the injection of copious amounts of OM that can adsorb Hg and reduce its bioavailability and alleviate physical limitations of soil (Larney & Angers, 2012; Salazar et al., 2009; Shipitalo & Bonta, 2008).

The application of biochar generally decreased metal concentration in overburden soils, which suggest dilution as the local biochar was low in metals. There was no evidence of differences in nutrients among sites, except K which increased with the addition of biochar in distant and overburden soil at Mahdia. The low concentrations of metals in soil could be attributed to the limited presence of ore materials and the composition of soils used, particularly in the overburden which is mostly topsoil stripped and removed during the mining process without any ore materials (as reported in chapter 3). The application of biochar could immobilize these metals resulting in reduced concentrations due to biochar relatively high cation exchange capacity and large surface area to adsorb and bind metal ions found in soil (Kadir Salam, 2023). Ali et al. (2017) found that the addition of bamboo biochar to mine contaminated soils immobilized metals such as Cd, Cu, Pb, and Zn due to the fixation of charged metals through ion exchange, physical entrapment on the large surface of biochar and soil chemistry changes to reduce phytotoxicity. Here, the bioavailable concentration of Cd, Cu, Pb, and Zn decreased by 23, 16, 11, and 14 % respectively following amendment with bamboo biochar.

Low OM concentrations in overburden soil along with high clay content suggest severe depletion of waste spoils due to the destructive nature of gold mining that strip topsoil (rich OM and nutrient layer) to extract gold. One of the distant sites (Frenchman, Table 6.1) also had low soil OM, but this soil was almost pure sand and therefore expected to have low OM (2.00 ± 0.16 %). The low OM in waste spoils results in limited capacity to retain moisture and nutrients even with the addition of local biochar material that contains higher concentrations of Ca (920 mg kg^{-1}), Mg (419 mg kg^{-1}), Na (183 mg kg^{-1}), and P (181 mg kg^{-1}). Compared with other studies (Sądej et al., 2020; Stefanowicz et al.,

2020) soil nutrient concentrations in this study was low. Low soil nutrient concentrations may also be associated with limited activities of soil microorganisms, resulting in a decline in OM decomposition and nutrient cycling (Chibuike & Obiora, 2014; Lehmann et al., 2011). Syuhada et al. (2016) reported low Ca (< 80 mg kg^{-1}) and Mg (< 70 mg kg^{-1}) concentrations in soil treated with biochar (produced from feedstock of oil palm) due to insufficient application rate to increase nutrients in degraded soils as well as limited period of the study to activate C oxidation, which tends to increase soil nutrients. The notable increase in K after the application of biochar may be attributed to the release of available K (1215 mg kg^{-1}) in biochar, which was about 30 times higher than the K concentration in soil prior to amendment. Liu et al. (2019) reported that the K concentration in raw materials is retained in the biochar during pyrolysis, and available K could be released into soil following amendment with biochar to supplement storage of K in soil.

6.4.2 Poa pratensis response to biochar

While there was little difference in *P. pratensis* germination among the treatments, plant growth over the 4-week period was significantly (~ 50%) lower in overburden soils compared with distant sites and the application of biochar did not significantly improve growth in any soil. As soil metal levels were low and nutrient concentrations were not consistently lower in untreated overburden soils it is unlikely that soil chemical factors are responsible for the poor growth on overburden soil. The only exception is the possibility that N may be limited owing to the low soil OM values, and the tree commonly planted at mine sites *Acacia mangium*, which is a N-fixing tree (Lewis et al., 2022; Nazeri et al., 2021; Vijayanathan et al., 2011). However, *P. pratensis* grew just as well at the distant sites

of Frenchman and Mahdia, even though Frenchman had OM levels similar to overburden a site that also had very low soil OM, indicating that soil nutrient levels are not the major factor limiting plant growth on overburden soils.

The high clay content in overburden soil contributed to the "crusting" of these soils and lower water infiltration rate during the 4-week growth chamber study (Figure S6. 1), which may have affected plant growth. The high clay content of soil could impede growth due to waterlogged conditions and compaction which restricts root development. It was expected that the application of biochar would also improve physical properties in overburden soil (Carlson et al., 2015). Soils with higher OM content could enhance aeriation of soils with high clay content, which reduces the probability of water logging and create more favorable conditions for root development and growth (Soinne et al., 2023). This positive effect of biochar on soil productivity is primarily linked to mechanisms such as: (a) biochar porous and spongy structure that enhances nutrient retention to facilitate constant supply of nutrients; (b) biochar enable sandy soil retention of more positively charged ions (including essential nutrients) and buffers the pH of soil to promote nutrient availability; (c) biochar improves soil aggregation, leading to the protection of OM from decomposition and promotion of soil organic C accumulation; and (d) biochar immobilize toxic elements to minimize potential harm to the environment (Ahmad et al., 2014; Ibrahim & Horton, 2021; Jeffery et al., 2011; Lehmann et al., 2011; Musei et al., 2024; Spokas et al., 2011).

However, beneficial responses to biochar are more commonly associated with sandy soils, whereas the overburden sites had a high clay/silt content. The high permeability of sandy soils results in low soil moisture content and nutrient retention,

leading to reduced soil productivity (Musei et al., 2024). Studies by Musei et al. (2024) found that biochar application as a sandy soil reclamation technology increased aboveground biomass by 67.4 %, soil moisture content by 17.3 %, and soil organic carbon by 74.2 %. It appears likely that the biochar rate used in the present study, although similar to values reported in other areas (Gusmini et al., 2021; Küçükyumuk et al., 2017; Prendergast-Miller et al., 2014; Sun et al., 2024; Zhang et al., 2012) may be insufficient to increase soil porosity and that the combined compaction and waterlogging experienced by seedlings on overburden soils was the primary factor impeding plant growth. The eroded conditions of overburden soil requires additional energy by *P. pratensis* to counteract stress to improve height and tissue dry biomass (Durante-Yánez et al., 2022; Marrugo-Negrete et al., 2015, 2016). Root development inhibition and nutrient transport and water imbalance impedes growth, damage the structure, decrease biochemical and physiological activities, which affects the production of biomass (Durante-Yánez et al., 2022; B. Kumar et al., 2017; Wu et al., 2018).

6.5 Conclusion

The application of biochar significantly decreased soil pH and increased soil OM. However, soil nutrients (Ca, K, Mg, Na, and P) were generally low, and did not improve significantly with the addition of biochar, except K. Mercury concentration was elevated in soil regardless of biochar amendment, while the other metals (Co, Cu, Ni, and Zn) exhibited low concentrations that were immobilized by biochar. Plant response was worse at overburden sites and did not improve with the addition of biochar, likely because soil physical properties (porosity) were not sufficiently improved, and pots were characterized

by alternating waterlogging during water additions with intermittent periods were soils "baked" becoming more compact and possibly restricting root growth.

The experiment was carried out for 30 days under growth chamber conditions, therefore longer-term studies should be carried out *in-situ* under various treatment application rates, long-term effectiveness measurements, and weather conditions, to determine the suitability of soil to support reclamation of mined out areas. As plants growing naturally in contaminated soil near an artisanal gold mine could exhibit different growth mechanisms, which may lead to better results compared with pot assay. Implementing these strategies will aid in improving efforts to mitigate ecological risks associated with Hg in the environment and expand the practical application of biochar in reclamation of mined out areas.

7 General conclusions

To have a better understanding of environmental contamination associated with artisanal gold mining, it is important to assess contaminants of concern in environmental media. Artisanal gold mining across South America has contributed to the contamination of nearby soil and sediment, leading to potential ecological risks in the vicinity of the mining area. Even though the degree of contamination of soils and sediments from sampled studies across South America were greater with metals, contamination by Hg is a large concern due to its toxicity at low concentrations. Metal concentrations were low (below recommended threshold limits) in soil and sediment of sampled gold mines in Guyana compared with other studies across South America. However, Hg concentrations were very high in soil and sediment and contamination was not localized to the mine site. Organic matter in soil and sediment was strongly related to Hg suggesting that OM is a major factor affecting Hg accumulation. Soil water extracts revealed high Hg/DOC ratios in overburden and adjacent soils, which suggests elevated Hg inputs at these locations and possible leaching to stream sediments. The burning of gold amalgam serves as the main source of atmospheric Hg in the gold mining area. Atmospheric Hg was very high (exceed natural background levels for the global south) around the gold mine but decrease rapidly with distance from the mine site. During periods of burning atmospheric Hg can exceed 100,000 ng m^{-3} and result in moss Hg concentrations greater than 250,000 ng g^{-1}. Mercury concentrations in moss and passive samplers were positively correlated, so these monitoring techniques may be useful to measure atmospheric Hg but should only be deployed for short periods to minimize Hg loss from both moss and passive samplers.

Organic matter return rate through litterfall depends on various factors that influence the process of decomposition and Hg movement through environmental media. The strong relationships between soil C and Hg held true for regions close and distant from point source, with Hg/C ratios being much lower in sites farther away from emission source compared with those observed near artisanal gold mines. The patterns of Hg/C ratios in various environmental media were similar in Guyana and globally synthesized studies, with much higher values at contaminated sites compared with clean sites. Understanding litter dynamics (decomposition) and the interaction between C and Hg provides insights into the reclamation of degraded soil since this determines the supply rate of C to soil and the reactivation of nutrient cycling. A locally produced biochar was applied at a rate of 10 t ha^{-1} during a 30-day growth chamber study to improve waste spoils physicochemical conditions to better support plant growth, but biochar amendment did not show any significant improvement since plant response was worse at overburden sites. This is likely due to soil physical properties (porosity) not sufficiently improved, and the "crusty" conditions of soil led to more compaction and possible restriction of root growth.

8 Future prospects

The overall aims of the studies were to contribute to a greater understanding of environmental contamination associated with artisanal gold mining in Guyana. Characterizing Hg and other metal concentrations in surface soil and sediment coupled with Hg/DOC ratios could be an important part of local monitoring and evaluation to understand the sources and processes leading to changes in Hg and metal input. Further study should focus on the source, speciation, and loss of Hg during the decomposition of leaf litter. Continued efforts are required to improve gold extraction techniques in Guyana, with the aim of reducing Hg emissions. Focusing on these gold mining areas within the framework of the Minamata Convention would achieve tremendous benefits. Since the Guyana Geology and Mines Commission (agency responsible for the gold mining sector in Guyana) has recognized the need for the development of national standards for the emission of GEM into the atmosphere, the data presented in this thesis may serve as a baseline for determining emissions limits. This may also assist in the generation of national air quality standards. A delicate balance is required between profits from gold mining and protecting environmental and human health.

Rapid measures should be taken to remediate contaminated soils, restore the landscape of gold mining areas, and carry out environmentally protected gold mining of undisturbed deposits to avoid the release of contaminants into the environment which could have lasting effects on ecosystems. The influence of biochar on the reclamation of degraded soil tends to vary with application rates and field management practices. The results of this research can make some novel contributions to understanding soil suitability to support reclamation of mined out areas and current knowledge of gold mine reclamation within

Guyana. The growth study experiment was carried out for 30 days under growth chamber conditions, therefore longer-term studies should be carried out *in-situ* under various treatment application rates, long-term effectiveness measurements, and weather conditions, to determine the suitability of soil to support reclamation of mined out areas. As plants growing naturally in contaminated soil near an artisanal gold mine could exhibit different growth mechanisms, which may lead to better results compared with pot assay. Implementing these strategies will aid in improving efforts to mitigate ecological risks associated with Hg in the environment and expand the practical application of biochar in reclamation of mined out areas.

References

Abdul-Wahab, S. A., & Marikar, F. A. (2012). The environmental impact of gold mines: pollution by heavy metals. *Central European Journal of Engineering*, *2*(2), 304–313. https://doi.org/10.2478/s13531-011-0052-3

Aboal, J. R., Fernández, J. A., Boquete, T., & Carballeira, A. (2010). Is it possible to estimate atmospheric deposition of heavy metals by analysis of terrestrial mosses? *Science of the Total Environment*, *408*, 6291–6297. https://doi.org/10.1016/j.scitotenv.2010.09.013

Acosta, J. A., Martínez-Martínez, S., Faz, A., Millán, R., Muñoz, M. A., Terán, T., & Vera, R. (2011). Characterization of the potential mercury contamination in the Apolobamba gold mining area, Bolivia. *Spanish Journal of Soil Science*, *1*(1), 86–99. https://doi.org/10.3232/SJSS.2011.V1.N1.06

Adediran, G. A., Liem-Nguyen, V., Song, Y., Schaefer, J. K., Skyllberg, U., & Björn, E. (2019). Microbial biosynthesis of thiol compounds: implications for speciation, cellular uptake, and methylation of Hg(II). *Environmental Science & Technology Technology*, *53*, 8187–8196. https://doi.org/10.1021/acs.est.9b01502

Adekiya, A. O., Oloruntoba, A., Ewulo, B. S., Ogunbode, T., & Sangoyomi, T. (2024). Heavy metal pollution in soils near Ilesha gold mining area, Nigeria. *The Open Agriculture Journal*, *18*, e18743315290216. https://doi.org/10.2174/0118743315290216240123111021

Aguilar, G., Valdés, A., Cabré, A., & Galdames, F. (2021). Flash floods controlling Cu, Pb, As and Hg variations in fluvial sediments of a river impacted by metal mining in the Atacama Desert. *Journal of South American Earth Sciences*, *109*, 103290. https://doi.org/10.1016/j.jsames.2021.103290

Ahmad, M., Rajapaksha, A. U., Lim, J. E., Zhang, M., Bolan, N., Mohan, D., Vithanage, M., Lee, S. S., & Ok, Y. S. (2014). Biochar as a sorbent for contaminant management in soil and water: A review. *Chemosphere*, *99*, 19–33. https://doi.org/10.1016/j.chemosphere.2013.10.071

Akoto, O., Yakubu, S., Ofori, L. A., Bortey-sam, N., Boadi, N. O., Horgah, J., & Sackey, L. N. A. (2023). Multivariate studies and heavy metal pollution in soil from gold mining area. *Heliyon*, *9*, e12661. https://doi.org/10.1016/j.heliyon.2022.e12661

Akoto, R., & Anning, A. K. (2021). Heavy metal enrichment and potential ecological risks from different solid mine wastes at a mine site in Ghana. *Environmental Advances*, *3*, 100028. https://doi.org/10.1016/j.envadv.2020.100028

Aksentov, K. I., & Sattarova, V. V. (2020). Mercury geochemistry of deep-sea sediment cores from the Kuril area, northwest Pacific. *Progress in Oceanography*, *180*, 102235. https://doi.org/10.1016/j.pocean.2019.102235

Ali, A., Guo, D., Zhang, Y., Sun, X., Jiang, S., Guo, Z., Huang, H., Liang, W., Li, R., & Zhang, Z. (2017). Using bamboo biochar with compost for the stabilization and phytotoxicity reduction of heavy metals in mine-contaminated soils of China. *Scientific Reports*, *7*, 2690. https://doi.org/10.1038/s41598-017-03045-9

Ali, M. M., Ali, M. L., Islam, M. S., & Rahman, M. Z. (2018). Assessment of toxic metals in water and sediment of Pasur River in Bangladesh. *Water Science and Technology*, *77*(5), 1418–1430. https://doi.org/10.2166/wst.2018.016

Ansari, M. K. A., Ahmad, A., Umar, S., & Iqbal, M. (2009). Mercury-induced changes in

growth variables and antioxidative enzyme activities in Indian mustard. *Journal of Plant Interactions*, *4*(2), 131–136. https://doi.org/10.1080/17429140802716713
Aram, S. A., Osei Lartey, P., Amoah, S. K., & Appiah, A. (2021). Gold eco-toxicology: Assessment of the knowledge gap on the environmental and health effects of mercury between artisanal small scale and medium scale gold miners in Ghana. *Resources Policy*, *72*, 102108. https://doi.org/10.1016/j.resourpol.2021.102108
Armah, F. A., Quansah, R., & Luginaah, I. (2014). A systematic review of heavy metals of anthropogenic origin in environmental media and biota in the context of gold mining in Ghana. *International Scholarly Research Notices*, *2014*, 252148. https://doi.org/10.1155/2014/252148
Asif, Z., & Chen, Z. (2016). Environmental management in North American mining sector. *Environmental Science and Pollution Research*, *23*, 167–179. https://doi.org/10.1007/s11356-015-5651-8
Assad, M. ., Parelle, J. ., Cazaux, D. ., Gimbert, F., Chalot, M. ., & Tatin-Froux, F. (2016). Mercury uptake into poplar leaves. *Chemosphere*, *146*, 1–7. https://doi.org/10.1016/j.chemosphere.2015.11.103
Awotwi, A., Anornu, G. K., Quaye-Ballard, J. A., Annor, T., Nti, I. K., Odai, S. N., Arhin, E., & Gyamfi, C. (2021). Impact of post- reclamation of soil by large-scale, small-scale and illegal mining on water balance components and sediment yield: Pra River Basin case study. *Soil and Tillage Research*, *211*, 105026. https://doi.org/10.1016/j.still.2021.105026
Baran, A., Mierzwa-Hersztek, M., Gondek, K., Tarnawski, M., Szara, M., Gorczyca, O., & Koniarz, T. (2019). The influence of the quantity and quality of sediment organic matter on the potential mobility and toxicity of trace elements in bottom sediment. *Environmental Geochemistry and Health*, *41*, 2893–2910. https://doi.org/10.1007/s10653-019-00359-7
Barcelos, D. A., Pontes, F. V. M., da Silva, F. A. N. G., Castro, D. C., dos Anjos, N. O. A., & Castilhos, Z. C. (2020). Gold mining tailing: Environmental availability of metals and human health risk assessment. *Journal of Hazardous Materials*, *397*, 122721. https://doi.org/10.1016/j.jhazmat.2020.122721
Bargagli, R. (2016). Moss and lichen biomonitoring of atmospheric mercury: A review. *Science of the Total Environment*, *572*, 216–231. https://doi.org/10.1016/j.scitotenv.2016.07.202
Barrow, N. J., & Hartemink, A. E. (2023). The effects of pH on nutrient availability depend on both soils and plants. *Plant and Soil*, *487*, 21–37. https://doi.org/10.1007/s11104-023-05960-5
Batsaikhan, B., Kwon, J. S., Kim, K. H., Lee, Y. J., Lee, J. H., Badarch, M., & Yun, S. T. (2016). Hydrochemical evaluation of the influences of mining activities on river water chemistry in central northern Mongolia. *Environmental Science and Pollution Research*. https://doi.org/10.1007/s11356-016-7895-3
Beal, S. A., Jackson, B. P., Kelly, M. A., Stroup, J. S., & Landis, J. D. (2013). Effects of historical and modern mining on mercury deposition in southeastern Peru. *Environmental Science and Technology*, *47*, 12715–12720. https://doi.org/10.1021/es402317x
Beghelli, F. G. S., Pompêo, M. L. M., Rosa, A. H., & Moschini-Carlos, V. (2016). Effects of copper in sediments on benthic macroinvertebrate communities in tropical

reservoirs. *Limnetica*, *35*(1), 103–116. https://doi.org/10.23818/limn.35.09
Bempah, C., & Ewusi, A. (2016). Heavy metals contamination and human health risk assessment around Obuasi gold mine in Ghana. *Environmental Monitoring and Assessment*, *188*(5), 261. https://doi.org/10.1007/s10661-016-5241-3
Bento, R. A., Saggin-Júnior, O. J., Pitard, R. M., Straliotto, R., Da Silva, E. M. R., De Lucena Tavares, S. R., De Landa, F. H. T. G., Martins, L. F., & Volpon, A. G. T. (2012). Selection of leguminous trees associated with symbiont microorganisms for phytoremediation of petroleum-contaminated soil. *Water, Air, and Soil Pollution*, *223*, 5659–5671. https://doi.org/10.1007/s11270-012-1305-3
Berg, T., Aspmo, K., & Steinnes, E. (2008). Transport of Hg from atmospheric mercury depletion events to the mainland of Norway and its possible influence on Hg deposition. *Geophysical Research Letters*, *35*, L09802. https://doi.org/10.1029/2008GL033586
Bertrand-Galindo, I., Barrueto, J. T., & Bertrand-Galindo, M. (2022). *Spotlight: Mining law in Chile*. https://www.lexology.com/library/detail.aspx?g=a6b9be96-78ce-41e1-8fb7-b8b1081e6cbb
Biester, H., Hermanns, Y. M., & Martinez Cortizas, A. (2012). The influence of organic matter decay on the distribution of major and trace elements in ombrotrophic mires - a case study from the Harz Mountains. *Geochimica et Cosmochimica Acta*, *84*, 126–136. https://doi.org/10.1016/j.gca.2012.01.003
Boraah, N., Chakma, S., & Kaushal, P. (2023). Optimum features of wood-based biochars: A characterization study. *Journal of Environmental Chemical Engineering*, *11*, 109976. https://doi.org/10.1016/j.jece.2023.109976
Božič, D., Živković, I., Hudobivnik, M. J., Kotnik, J., Amouroux, D., Štrok, M., & Horvat, M. (2022). Fractionation of mercury stable isotopes in lichens. *Chemosphere*, *309*, 136592. https://doi.org/10.1016/j.chemosphere.2022.136592
Bravo, A. G., Kothawala, D. N., Attermeyer, K., Tessier, E., Bodmer, P., Ledesma, J. L. J., Audet, J., Casas-Ruiz, J. P., Catalán, N., Cauvy-Fraunié, S., Colls, M., Deininger, A., Evtimova, V. V., Fonvielle, J. A., Fuß, T., Gilbert, P., Herrero Ortega, S., Liu, L., Mendoza-Lera, C., … Amouroux, D. (2018). The interplay between total mercury, methylmercury and dissolved organic matter in fluvial systems: A latitudinal study across Europe. *Water Research*, *144*, 172–182. https://doi.org/10.1016/j.watres.2018.06.064
Brown, S. T., Bandoo, L. L., Agard, S. S., Thom, S. T., Gilhuys, T. E., Mudireddy, G. K., Eechampati, A. V., Hasan, K. M., Loving, D. C., Seney, C. S., & Kiefer, A. M. (2020). A collaborative training program to assess mercury pollution from gold shops in Guyana's artisanal and small-scale gold mining sector. *Atmosphere*, *11*, 719. https://doi.org/10.3390/atmos11070719
Buck, D. G., Evers, D. C., Adams, E., DiGangi, J., Beeler, B., Samánek, J., Petrlik, J., Turnquist, M. A., Speranskaya, O., Regan, K., & Johnson, S. (2019). A global-scale assessment of fish mercury concentrations and the identification of biological hotspots. *Science of the Total Environment*, *687*, 956–966. https://doi.org/10.1016/j.scitotenv.2019.06.159
Caballero-Gallardo, K., Alcala-Orozco, M., Barraza-Quiroz, D., De la Rosa, J., & Olivero-Verbel, J. (2020). Environmental risks associated with trace elements in sediments from Cartagena Bay, an industrialized site at the Caribbean.

Chemosphere, *242*, 125173. https://doi.org/10.1016/j.chemosphere.2019.125173
Calabró, M. R., Roqueiro, G., Tapia, R., Crespo, D. C., Bargiela, M. F., & Young, B. J. (2022). Chronic toxicity, bioavailability and bioaccumulation of Zn, Cu and Pb in Lactuca sativa exposed to waste from an abandoned gold mine. *Chemosphere*, *307*, 135855. https://doi.org/10.1016/j.chemosphere.2022.135855
Calisto, R. B. (2019). Ecuador. In E. R. La Flèche (Ed.), *The mining law review* (8th ed., pp. 97–105). Law Business Research Ltd. www.TheLawReviews.co.uk
Canuel, R., Lucotte, M., & de Grosbois, S. B. (2009). Mercury cycling and human health concerns in remote ecosystems in the Americas. *S.A.P.I.EN.S*, *2*(1). http://journals.openedition.org/sapiens/766
Carling, G. T., Diaz, X., Ponce, M., Perez, L., Nasimba, L., Pazmino, E., Rudd, A., Merugu, S., Fernandez, D. P., Gale, B. K., & Johnson, W. P. (2013). Particulate and dissolved trace element concentrations in three southern Ecuador rivers impacted by artisanal gold mining. *Water, Air, and Soil Pollution*, *224*, 1415. https://doi.org/10.1007/s11270-012-1415-y
Carlson, J., Saxena, J., Basta, N., Hundal, L., Busalacchi, D., & Dick, R. P. (2015). Application of organic amendments to restore degraded soil: Effects on soil microbial properties. *Environmental Monitoring and Assessment*, *187*, 109. https://doi.org/10.1007/s10661-015-4293-0
Carranza-Lopez, L., Caballero-Gallardo, K., Cervantes-Ceballos, L., Turizo-Tapia, A., & Olivero-Verbel, J. (2019). Multicompartment Mercury Contamination in Major Gold Mining Districts at the Department of Bolivar, Colombia. *Archives of Environmental Contamination and Toxicology*, *76*, 640–649. https://doi.org/10.1007/s00244-019-00609-w
Casagrande, G. C. R., Dambros, J., de Andrade, E. A., Martello, F., Sobral-Souza, T., Moreno, M. I. C., Battirola, L. D., & de Andrade, R. L. T. (2023). Atmospheric mercury in forests: accumulation analysis in a gold mining area in the southern Amazon, Brazil. *Environmental Monitoring and Assessment*, *195*, 477. https://doi.org/10.1007/s10661-023-11063-6
CCME. (2024). *Canadian environmental quality guidelines*. https://ccme.ca/en/current-activities/canadian-environmental-quality-guidelines
Chakraborty, P., Sarkar, A., Vudamala, K., Naik, R., & Nath, B. N. (2015). Organic matter - A key factor in controlling mercury distribution in estuarine sediment. *Marine Chemistry*, *173*, 302–309. https://doi.org/10.1016/j.marchem.2014.10.005
Chambi-Legoas, R., Ortega Rodriguez, D. R., Figueiredo, F. de M. de, Peña Valdeiglesias, J., Zevallos Pollito, P. A., Marcelo-Peña, J. L., & Rother, D. C. (2021). Natural regeneration after gold mining in the Peruvian Amazon: Implications for restoration of tropical forests. *Frontiers in Forests and Global Change*, *4*, 594627. https://doi.org/10.3389/ffgc.2021.594627
Chen, C. F., Ju, Y. R., Lim, Y. C., Chen, C. W., Wu, C. H., Lin, Y. L., & Dong, C. Di. (2020). Dry and wet seasonal variation of total mercury, inorganic mercury, and methylmercury formation in estuary and harbor sediments. *Journal of Environmental Management*, *253*, 109683. https://doi.org/10.1016/j.jenvman.2019.109683
Chen, L., Wang, J., Guo, X., Wu, H., He, H., & Fang, L. (2022). Pollution characteristics and health risk assessment of potentially toxic elements in soils around China's gold

mines: a meta-analysis. *Environmental Geochemistry and Health*, *44*, 3765–3777. https://doi.org/10.1007/s10653-021-01175-8

Chen, S., Wu, P., Zha, X., Zhou, B., Liu, J., & Long, E. (2023). Arsenic and heavy metals in sediments affected by typical gold mining areas in Southwest China: Accumulation, sources and ecological risks. *International Journal of Environmental Research and Public Health*, *20*, 1432. https://doi.org/10.3390/ijerph20021432

Chen, X., Zheng, L., Sun, R., Liu, S., Li, C., Chen, Y., & Xu, Y. (2022). Mercury in sediment reflecting the intensive coal mining activities: Evidence from stable mercury isotopes and bayesian mixing model analysis. *Ecotoxicology and Environmental Safety*, *234*, 113392. https://doi.org/10.1016/j.ecoenv.2022.113392

Chen, Y., Liu, G., Zhou, C., Zhou, H., Wei, Y., & Liu, Y. (2023). The influence of gold mining wastes on the migration-transformation behavior and health risks of arsenic in the surrounding soil of mined-area. *Frontiers in Earth Science*, *10*, 1068763. https://doi.org/10.3389/feart.2022.1068763

Cheney, C. L., Eccles, K. M., Kimpe, L. E., Lehnherr, I., & Blais, J. M. (2024). Mercury deposition to lake sediments near historic gold mines in northern Canada. *Environmental Pollution*, *342*, 123038. https://doi.org/10.1016/j.envpol.2023.123038

Cheng, Z., Tang, Y., Li, E., Wu, Q., Wang, L., Liu, K., Wang, S., Huang, Y., & Duan, L. (2020). Mercury accumulation in soil from atmospheric deposition in temperate steppe of Inner Mongolia, China. *Environmental Pollution*, *258*, 113692. https://doi.org/10.1016/j.envpol.2019.113692

Chibuike, G. U., & Obiora, S. C. (2014). Heavy metal polluted soils: Effect on plants and bioremediation methods. *Applied and Environmental Soil Science*, 752708. https://doi.org/10.1155/2014/752708

Choi, H. D., Sharac, T. J., & Holsen, T. M. (2008). Mercury deposition in the Adirondacks: A comparison between precipitation and throughfall. *Atmospheric Environment*, *42*, 1818–1827. https://doi.org/10.1016/j.atmosenv.2007.11.036

Ciani, F., Fornasaro, S., Benesperi, R., Bianchi, E., Cabassi, J., Di Nuzzo, L., Grifoni, L., Venturi, S., Costagliola, P., & Rimondi, V. (2023). Mercury accumulation efficiency of different biomonitors in indoor environments: the case study of the Central Italian Herbarium (Florence, Italy). *Environmental Science and Pollution Research*, *30*, 124232–124244. https://doi.org/10.1007/s11356-023-31105-3

Cichowicz, R., & Dobrzański, M. (2022). 3D spatial dispersion of particulate matter and gaseous pollutants on a university campus in the center of an urban agglomeration. *Energy*, *259*, 125009. https://doi.org/10.1016/j.energy.2022.125009

Cipriani, H. N., Dias, L. E., Costa, M. D., Campos, N. V., Azevedo, A. A., Gomes, R. J., Fialho, I. F., & Amezquita, S. P. M. (2013). Arsenic toxicity in *Acacia mangium* Willd. and *Mimosa caesalpiniaefolia* Benth. seedlings. *Revista Brasileira de Ciencia Do Solo*, *37*, 1423–1430.

Coquery, M., & Welbourn, P. M. (1995). The relationship between metal concentration and organic matter in sediments and metal concentration in the aquatic macrophyte *Eriocaulon septangulare*. *Water Research*, *29*(9), 2094–2102. https://doi.org/10.1016/0043-1354(95)00015-D

Corredor, J. A. G., Perez, E. H., Figueroa, R., & Casas, A. F. (2021). Water quality of streams associated with artisanal gold mining; Suarez, Department of Cauca,

Colombia. *Heliyon*, *7*, e07047. https://doi.org/10.1016/j.heliyon.2021.e07047
Costa, M. F., Landing, W. M., Kehrig, H., Barletta, M., Holmes, C. D., Barrocas, P. R. G., Evers, D. C., Buck, D. G., Claudia Vasconcellos, A., Hacon, S. S., Moreira, J. C., & Malm, O. (2012). Mercury in tropical and subtropical coastal environments. *Environmental Research*, *119*, 88–100. https://doi.org/10.1016/j.envres.2012.07.008.
Covre, W. P., Ramos, S. J., da Silveira Pereira, W. V., de Souza, E. S., Martins, G. C., Teixeira, O. M. M., do Amarante, C. B., Dias, Y. N., & Fernandes, A. R. (2022). Impact of copper mining wastes in the Amazon: Properties and risks to environment and human health. *Journal of Hazardous Materials*, *421*, 126688. https://doi.org/10.1016/j.jhazmat.2021.126688
Cowden, P., & Aherne, J. (2019). Assessment of atmospheric metal deposition by moss biomonitoring in a region under the influence of a long standing active aluminium smelter. *Atmospheric Environment*, *201*, 84–91. https://doi.org/10.1016/j.atmosenv.2018.12.022
Cruzado-Tafur, E., Bierla, K., Torró, L., & Szpunar, J. (2021). Accumulation of As, Ag, Cd, Cu, Pb, and Zn by native plants growing in soils contaminated by mining environmental liabilities in the Peruvian Andes. *Plants*, *10*, 241. https://doi.org/10.3390/plants10020241
da Penha Rhodes, V., de Lena, J. C., Santolin, C. V. A., da Silva Pinto, T., Mendes, L. A., & Windmöller, C. C. (2018). Speciation and quantification of Hg in sediments contaminated by artisanal gold mining in the Gualaxo do Norte River, Minas Gerais, SE, Brazil. *Environmental Monitoring and Assessment*, *190*, 49. https://doi.org/10.1007/s10661-017-6394-4
Danala Danga, S., Ekengele Nga, L., Makhubela, T. V., Ibrahim, B., Bitom, D. L., & Kramers, J. D. (2024). Assessing soil contamination by potentially toxic elements in artisanal and small-scale gold mining sites of the Adamawa Region, Cameroon. *Geochemistry: Exploration, Environment, Analysis*, *24*. https://doi.org/10.1144/geochem2023-055
De Miguel, E., Clavijo, D., Ortega, M. F., & Gómez, A. (2014). Probabilistic meta-analysis of risk from the exposure to Hg in artisanal gold mining communities in Colombia. *Chemosphere*, *108*, 183–189. https://doi.org/10.1016/j.chemosphere.2014.01.035
de Oliveira, D. C. M., Correia, R. R. S., Marinho, C. C., & Guimarães, J. R. D. (2015). Mercury methylation in sediments of a Brazilian mangrove under different vegetation covers and salinities. *Chemosphere*, *127*, 214–221. https://doi.org/10.1016/j.chemosphere.2015.02.009
De Simone, F., Gencarelli, C. N., Hedgecock, I. M., & Pirrone, N. (2014). Global atmospheric cycle of mercury: A model study on the impact of oxidation mechanisms. *Environmental Science and Pollution Research*, *21*, 4110–4123. https://doi.org/10.1007/s11356-013-2451-x
Delgado Jiménez, A., Smith, N. M., & Holley, E. A. (2022). Capitals in artisanal and small-scale mining in Marmato, Colombia: Using the sustainable livelihoods framework to inform formalization. *Extractive Industries and Society*, *12*, 101157. https://doi.org/10.1016/j.exis.2022.101157
Demers, J. D., Driscoll, C. T., Fahey, T. J., & Yavitt, J. B. (2007). Mercury cycling in litter and soil in different forest types in the Adirondack region, New York, USA.

Ecological Applications, *17*(5), 1341–1351. https://doi.org/10.1890/06-1697.1
Demers, J. D., Yavitt, J. B., Driscoll, C. T., & Montesdeoca, M. R. (2013). Legacy mercury and stoichiometry with C, N, and S in soil, pore water, and stream water across the upland-wetland interface: The influence of hydrogeologic setting. *Journal of Geophysical Research: Biogeosciences*, *118*, 825–841. https://doi.org/10.1002/jgrg.20066
Deng, A., Wang, L., Chen, F., Li, Z., Liu, W., & Liu, Y. (2018). Soil aggregate-associated heavy metals subjected to different types of land use in subtropical China. *Global Ecology and Conservation*, *16*, e00465. https://doi.org/10.1016/j.gecco.2018.e00465
Dentons. (2022). *Doing mining in Argentina*.
Dias, Y. N., Pereira, W. V. da S., da Costa, M. V., de Souza, E. S., Ramos, S. J., do Amarante, C. B., Campos, W. E. O., & Fernandes, A. R. (2022). Biochar mitigates bioavailability and environmental risks of arsenic in gold mining tailings from the eastern Amazon. *Journal of Environmental Management*, *311*, 114840. https://doi.org/10.1016/j.jenvman.2022.114840
Donkor, A. K., Bonzongo, J. C. J., Nartey, V. K., & Adotey, D. K. (2005). Heavy metals in sediments of the gold mining impacted Pra River basin, Ghana, West Africa. *Soil and Sediment Contamination*, *14*(6), 479–503. https://doi.org/10.1080/15320380500263675
Driscoll, C. T., Mason, R. P., Chan, H. M., Jacob, D. J., & Pirrone, N. (2013). Mercury as a global pollutant: Sources, pathways, and effects. *Environmental Science & Technology*, *47*, 4967–4983. https://doi.org/10.1021/es305071v
Du, B., Zhou, J., Zhou, L., Fan, X., & Zhou, J. (2019). Mercury distribution in the foliage and soil profiles of a subtropical forest: Process for mercury retention in soils. *Journal of Geochemical Exploration*, *205*, 106337. https://doi.org/10.1016/j.gexplo.2019.106337
Duan, C., Fang, L., Yang, C., Chen, W., Cui, Y., & Li, S. (2018). Reveal the response of enzyme activities to heavy metals through in situ zymography. *Ecotoxicology and Environmental Safety*, *156*, 106–115. https://doi.org/10.1016/j.ecoenv.2018.03.015
Durante-Yánez, E. V., Martínez-Macea, M. A., Enamorado-Montes, G., Caballero, E. C., & Marrugo-Negrete, J. (2022). Phytoremediation of soils contaminated with heavy metals from gold mining activities using *Clidemia sericea* D. Don. *Plants*, *11*, 597. https://doi.org/10.3390/plants11050597
Durnford, D., Dastoor, A., Figueras-Nieto, D., & Ryjkov, A. (2010). Long range transport of mercury to the Arctic and across Canada. *Atmospheric Chemistry and Physics*, *10*, 6063–6086. https://doi.org/10.5194/acp-10-6063-2010
Eckley, C. S., Luxton, T. P., Stanfield, B., Baldwin, A., Holloway, J. A., McKernan, J., & Johnson, M. G. (2021). Effect of organic matter concentration and characteristics on mercury mobilization and methylmercury production at an abandoned mine site. *Environmental Pollution*, *271*, 116369. https://doi.org/10.1016/j.envpol.2020.116369
Eckley, C. S., Luxton, T. P., Stanfield, B., Baldwin, A., Holloway, J., Mckernan, J., & Johnson, M. G. (2021). Effect of organic matter concentration and characteristics on mercury mobilization and methylmercury production at an abandoned mine site. *Environmental Pollution*, *271*, 116369.

https://doi.org/10.1016/j.envpol.2020.116369
Edwards, D. P., Sloan, S., Weng, L., Dirks, P., Sayer, J., & Laurance, W. F. (2014). Mining and the African environment. *Conservation Letters*, *7*, 302–311. https://doi.org/10.1111/conl.12076
Environmental Protection (Amendment) Act, 20:05, 3 (2005).
Ericksen, J. A., Gustin, M. S., Schorran, D. E., Johnson, D. W., Lindberg, S. E., & Coleman, J. S. (2003). Accumulation of atmospheric mercury in forest foliage. *Atmospheric Environment*, *37*, 1613–1622. https://doi.org/10.1016/S1352-2310(03)00008-6
Esdaile, L. J., & Chalker, J. M. (2018). The mercury problem in artisanal and small-scale gold mining. *Chemistry - A European Journal*, *24*, 6905–6916. https://doi.org/10.1002/chem.201704840
Esri. (2021). *ArcGIS Pro for desktop* (2.9.0). Esri Inc. https://www.esri.com/en-us/arcgis/products/arcgis-pro/overview
Fashola, M. O., Ngole-Jeme, V. M., & Babalola, O. O. (2016). Heavy metal pollution from gold mines: Environmental effects and bacterial strategies for resistance. *International Journal of Environmental Research and Public Health*, *13*, 1047. https://doi.org/10.3390/ijerph13111047
Fashola, M. O., Ngole-Jeme, V. M., & Babalola, O. O. (2020). Physicochemical properties, heavy metals, and metal-tolerant bacteria profiles of abandoned gold mine tailings in Krugersdorp, South Africa. *Canadian Journal of Soil Science*, *100*, 217–233. https://doi.org/10.1139/cjss-2018-0161
Fernández, J. A., Aboal, J. R., & Carballeira, A. (2000). Use of native and transplanted mosses as complementary techniques for biomonitoring mercury around an industrial facility. *The Science of the Total Environment*, *256*, 151–161. https://doi.org/10.1016/S0048-9697(00)00478-2
Festin, E. S., Tigabu, M., Chileshe, M. N., Syampungani, S., & Odén, P. C. (2019). Progresses in restoration of post-mining landscape in Africa. *Journal of Forestry Research*, *30*(2), 381–396. https://doi.org/10.1007/s11676-018-0621-x
Fitri, M. (2018). The settlement morphology along Musi river: The influence of river characteristics. *DIMENSI - Journal of Architecture and Built Environment*, *45*(2), 133–140. https://doi.org/10.9744/dimensi.45.2.133-140
Floreani, F., Barago, N., Acquavita, A., Covelli, S., Skert, N., & Higueras, P. (2020). Spatial distribution and biomonitoring of atmospheric mercury concentrations over a contaminated coastal lagoon (Northern Adriatic, Italy). *Atmosphere*, *11*, 1280. https://doi.org/10.3390/atmos11121280
Fong-Sam, Y. (2022). *The mineral industry of Venezuela*. https://pubs.usgs.gov/myb/vol3/2017-18/myb3-2017-18-venezuela.pdf
Fontboté, L., Kouzmanov, K., Chiaradia, M., & Pokrovski, G. S. (2017). Sulfide minerals in hydrothermal deposits. *Elements*, *13*, 97–103. https://doi.org/10.2113/gselements.13.2.97
Fragoso, C. P., Bernini, E., Araújo, B. F., Almeida, M. G. de, & Rezende, C. E. de. (2018). Mercury in litterfall and sediment using elemental and isotopic composition of carbon and nitrogen in the mangrove of Southeastern Brazil. *Estuarine, Coastal and Shelf Science*, *202*, 30–39. https://doi.org/10.1016/j.ecss.2017.12.005
France, H. E., Strong, O. L. K., Scotland, K. M., Roy, T. M., & Vreugdenhil, A. J.

(2024). Pit-lake remediation by chemically activated *Chlorocardium rodiei*: Simultaneous metal ion removal from acidic waters. *Sustainable Chemistry for the Environment*, *6*, 100103. https://doi.org/10.1016/j.scenv.2024.100103

Franco-Cisterna, B., Drost, A. M., van Santvoort, V., Sarkis, S., & McGowan, S. (2024). Freshwater ecosystems: Carbon sequestration champions. *Frontiers for Young Minds*, *12*, 1302239. https://doi.org/10.3389/frym.2024.1302239

Frouz, J. (2018). Effects of soil macro- and mesofauna on litter decomposition and soil organic matter stabilization. *Geoderma*, *332*, 161–172. https://doi.org/10.1016/j.geoderma.2017.08.039

Gačnik, J., Živković, I., Kotnik, J., Božič, D., Tassone, A., Naccarato, A., Pirrone, N., Sprovieri, F., Steffen, A., & Horvat, M. (2024). Comparison of active measurements, lichen biomonitoring, and passive sampling for atmospheric mercury monitoring. *Environmental Science and Pollution Research*, *31*(24), 35800–35810. https://doi.org/10.1007/s11356-024-33582-6

Gafur, N. A., Sakakibara, M., Sano, S., & Sera, K. (2018). A case study of heavy metal pollution in water of Bone River by artisanal small-scale gold mine activities in eastern part of Gorontalo, Indonesia. *Water*, *10*(11), 1507. https://doi.org/10.3390/w10111507

Galloway, J. M., Parsons, M. B., Ardakani, O. H., Falck, H., Fewster, R. E., Swindles, G. T., Sanei, H., Palmer, M. J., Nasser, N. A., & Patterson, R. T. (2024). Organic matter is a predominant control on total mercury concentration of near-surface lake sediments across a boreal to low Arctic tundra transect in northern Canada. *Science of the Total Environment*, *954*, 176466. https://doi.org/10.1016/j.scitotenv.2024.176466

Garbisu, C., & Alkorta, I. (2001). Phytoextraction: a cost-effective plant-based technology for the removal of metals from the environment. *Bioresource Technology*, *77*(3), 229–236. https://doi.org/10.1016/s0960-8524(00)00108-5

Gardham, S., Chariton, A. A., & Hose, G. C. (2015). Direct and indirect effects of copper-contaminated sediments on the functions of model freshwater ecosystems. *Ecotoxicology*, *24*, 61–70. https://doi.org/10.1007/s10646-014-1355-y

Gawryluk, A., Stępniowska, A., & Lipińska, H. (2022). Effect of soil contamination with polycyclic aromatic hydrocarbons from drilling waste on germination and growth of lawn grasses. *Ecotoxicology and Environmental Safety*, *236*, 113492. https://doi.org/10.1016/j.ecoenv.2022.113492

Gerson, J. R., Szponar, N., Agostini, A., Alotaibi, R., Bergquist, B., Chen, A., Fernandez, L. E., Lansdale, K. N., Lee, A. H., Machicao, M. F., Marchese, M. J., Topp, S. N., Vega, C., & Bernhardt, E. S. (2022). Chemistry of surface water, precipitation, throughfall, leaves, sediment, soil, and air near a gold mining region in Peru. *Ecology*, *103*(5), e3666. https://doi.org/10.1002/ecy.3666

Gerson, Jacqueline R., Szponar, N., Zambrano, A. A., Bergquist, B., Broadbent, E., Driscoll, C. T., Erkenswick, G., Evers, D. C., Fernandez, L. E., Hsu-Kim, H., Inga, G., Lansdale, K. N., Marchese, M. J., Martinez, A., Moore, C., Pan, W. K., Purizaca, R. P., Sánchez, V., Silman, M., … Bernhardt, E. S. (2022). Amazon forests capture high levels of atmospheric mercury pollution from artisanal gold mining. *Nature Communications*, *13*, 559. https://doi.org/10.1038/s41467-022-27997-3

Gibb, H., & O'Leary, K. G. (2014). Mercury exposure and health impacts among

individuals in the artisanal and small-scale gold mining community: A comprehensive review. *Environmental Health Perspectives, 122*(7), 667–672. https://doi.org/10.1289/ehp.1307864

Giordano, S., Adamo, P., Monaci, F., Pittao, E., Tretiach, M., & Bargagli, R. (2009). Bags with oven-dried moss for the active monitoring of airborne trace elements in urban areas. *Environmental Pollution, 157*, 2798–2805. https://doi.org/10.1016/j.envpol.2009.04.020

GLSC. (2013). *Guyana national land use plan*. https://glsc.gov.gy/wp-content/uploads/2017/05/National-Land-Use-Plan-Final-Oct-2013.pdf

GLSC. (2017). *The Cooperative Republic of Guyana national land degradation neutrality target setting programme report 2017-2030*.

Gómez-Armesto, A., Méndez-López, M., Pérez-Rodríguez, P., Fernández-Calviño, D., Arias-Estévez, M., & Nóvoa-Muñoz, J. C. (2020). Litterfall Hg deposition to an oak forest soil from southwestern Europe. *Journal of Environmental Management, 269*, 110858. https://doi.org/10.1016/j.jenvman.2020.110858

Gómez-Armesto, Antía, Méndez-López, M., Pontevedra-Pombal, X., García-Rodeja, E., Moretto, A., Estévez-Arias, M., & Nóvoa-Muñoz, J. C. (2020). Mercury accumulation in soil fractions of podzols from two contrasted geographical temperate areas: southwest Europe and southernmost America. *Geoderma, 362*, 114120. https://doi.org/10.1016/j.geoderma.2019.114120

Gong, C., Shao, Y., Luo, M., Xu, D., & Ma, L. (2023). Distribution characteristics of heavy metals in different particle size fractions of chinese paddy soil aggregates. *Processes, 11*, 1873. https://doi.org/10.3390/pr11071873

González-Carrasco, V., Velasquez-Lopez, P. C., Olivero-Verbel, J., & Pájaro-Castro, N. (2011). Air mercury contamination in the gold mining town of Portovelo, Ecuador. *Bulletin of Environmental Contamination and Toxicology, 87*, 250–253. https://doi.org/10.1007/s00128-011-0345-5

González-Merizalde, M. V., Menezes-Filho, J. A., Cruz-Erazo, C. T., Bermeo-Flores, S. A., Sánchez-Castillo, M. O., Hernández-Bonilla, D., & Mora, A. (2016). Manganese and mercury levels in water, sediments, and children living near gold-mining areas of the Nangaritza river basin, Ecuadorian Amazon. *Archives of Environmental Contamination and Toxicology, 71*, 171–182. https://doi.org/10.1007/s00244-016-0285-5

Google. (2024). *Google Earth Pro for desktop* (7.3.6.9796). Google LLC. https://earth.google.com/web/@0.24053023,0.19949377,3660.74729736a,19436775.06386519d,35y,-0h,0t,0r/data=OgMKATA

Government of Suriname. (2023). *First national action plan on artisanal and small-scale gold mining in Suriname*.

Gray, J. E., Theodorakos, P. M., Fey, D. L., & Krabbenhoft, D. P. (2015). Mercury concentrations and distribution in soil, water, mine waste leachates, and air in and around mercury mines in the Big Bend region, Texas, USA. *Environmental Geochemistry and Health, 37*, 35–48. https://doi.org/10.1007/s10653-014-9628-1

Green, C. S., Lewis, P. J., Wozniak, J. R., Drevnick, P. E., & Thies, M. L. (2019). A comparison of factors affecting the small-scale distribution of mercury from artisanal small-scale gold mining in a Zimbabwean stream system. *Science of the Total Environment, 647*, 400–410. https://doi.org/10.1016/j.scitotenv.2018.07.418

Grigal, D. F. (2002). Inputs and outputs of mercury from terrestrial watersheds: A review. *Environmental Reviews*, *10*(1), 1–39. https://doi.org/10.1139/a01-013

Grigal, D. F. (2003). Mercury sequestration in forests and peatlands: A review. *Journal of Environmental Quality*, *32*, 393–405. https://doi.org/10.2134/jeq2003.3930

Gruba, P., Socha, J., Pietrzykowski, M., & Pasychnyk, D. (2019). Tree species affects the concentration of total mercury (Hg) in forest soils: Evidence from a forest soil inventory in Poland. *Science of the Total Environment*, *647*, 141–148. https://doi.org/10.1016/j.scitotenv.2018.07.452

Guédron, S., Amouroux, D., Tessier, E., Grimaldi, C., Barre, J., Berail, S., Perrot, V., & Grimaldi, M. (2018). Mercury isotopic fractionation during pedogenesis in a tropical forest soil catena (French Guiana): Deciphering the impact of historical gold mining. *Environmental Science and Technology*, *52*, 11573–11582. https://doi.org/10.1021/acs.est.8b02186

Guédron, Stéphane, Grangeon, S., Jouravel, G., Charlet, L., & Sarret, G. (2013). Atmospheric mercury incorporation in soils of an area impacted by a chlor-alkali plant (Grenoble, France): Contribution of canopy uptake. *Science of the Total Environment*, *445–446*, 356–364. https://doi.org/10.1016/j.scitotenv.2012.12.084

Guo, D., Ali, A., Ren, C., Du, J., Li, R., Lahori, A., Xiao, R., Zhang, Z., & Zhang, Z. (2019). EDTA and organic acids assisted phytoextraction of Cd and Zn from a smelter contaminated soil by potherb mustard (*Brassica juncea*, Coss) and evaluation of its bioindicators. *Ecotoxicology and Environmental Safety*, *167*, 396–403. https://doi.org/10.1016/j.ecoenv.2018.10.038.

Guo, M. (2020). The 3r principles for applying biochar to improve soil health. *Soil Systems*, *4*(1), 9. https://doi.org/10.3390/soilsystems4010009

Gupta, A., Dubey, P., Kumar, M., Roy, A., Sharma, D., Khan, M. M., Bajpai, A. B., Shukla, R. P., Pathak, N., & Hasanuzzaman, M. (2022). Consequences of arsenic contamination on plants and mycoremediation-mediated arsenic stress tolerance for sustainable agriculture. *Plants*, *11*, 3220. https://doi.org/10.3390/plants11233220

Gusmini, Adrinal, Yaherwandi, Putri, E. L., & Panji, R. (2021). Improvement of nutrient status in ex-gold mining land with the application of rice terra preta biochar technology. *IOP Conference Series: Earth and Environmental Science*, *741*, 012031. https://doi.org/10.1088/1755-1315/741/1/012031

Mining (Amendment) Regulation, (2005) (testimony of Guyana Geology and Mines Commission).

Gworek, B., Dmuchowski, W., & Baczewska-Dąbrowska, A. H. (2020). Mercury in the terrestrial environment: a review. *Environmental Sciences Europe*, *32*, 128. https://doi.org/10.1186/s12302-020-00401-x

Gyamfi, O., Sørensen, P. B., Darko, G., Ansah, E., Vorkamp, K., & Bak, J. L. (2021). Contamination, exposure and risk assessment of mercury in the soils of an artisanal gold mining community in Ghana. *Chemosphere*, *267*, 128910. https://doi.org/10.1016/j.chemosphere.2020.128910

Hadzi, G. Y., Ayoko, G. A., Essumang, D. K., & Osae, S. K. D. (2019). Contamination impact and human health risk assessment of heavy metals in surface soils from selected major mining areas in Ghana. *Environmental Geochemistry and Health*, *41*, 2821–2843. https://doi.org/10.1007/s10653-019-00332-4

Haghighizadeh, A., Rajabi, O., Nezarat, A., Hajyani, Z., Haghmohammadi, M.,

Hedayatikhah, S., Asl, S. D., & Beni, A. A. (2024). Comprehensive analysis of heavy metal soil contamination in mining environments: Impacts, monitoring techniques, and remediation strategies. *Arabian Journal of Chemistry*, *17*, 105777. https://doi.org/10.1016/j.arabjc.2024.105777

Hall, B. D., & St Louis, V. L. (2004). Methylmercury and total mercury in plant litter decomposing in upland forests and flooded landscapes. *Environmental Science & Technology*, *38*(19), 5010–5021. https://doi.org/10.1021/es049800q

Hammond, D. S., Gond, V., Thoisy, B. de, Forget, P.-M., & DeDijn, B. P. E. (2007). Causes and consequences of a tropical forest gold rush in the Guiana Shield, South America. *Ambio*, *36*(8), 661–670. https://doi.org/10.1579/0044-7447(2007)36[661:CACOAT]2.0.CO;2

Han, D., Cheng, J., Hu, X., Jiang, Z., Mo, L., Xu, H., Ma, Y., Chen, X., & Wang, H. (2017). Spatial distribution, risk assessment and source identification of heavy metals in sediments of the Yangtze River Estuary, China. *Marine Pollution Bulletin*, *115*, 141–148. https://doi.org/10.1016/j.marpolbul.2016.11.062

Han, S., Niu, X., Wang, B., Wang, Z., Zhang, X., Wang, Q., Du, J., Liu, P., Liu, D., Pan, F., & Xu, T. (2025). Spatial-temporal patterns of litterfall mercury concentration and flux in typical vegetation in China. *Ecosystem Health and Sustainability*, *11*, 0288. https://doi.org/10.34133/ehs.0288

Harlow, E., Hurley, K., Fox, A., Vargas-Guerra, A., & Gibson, J. (2019). *Small-scale and artisanal mining impacts on biodiversity in Latin America*.

He, M., Tian, L., Braaten, H. F. V., Wu, Q., Luo, J., Cai, L. M., Meng, J. H., & Lin, Y. (2019). Mercury–organic matter interactions in soils and sediments: Angel or devil? *Bulletin of Environmental Contamination and Toxicology*, *102*, 621–627. https://doi.org/10.1007/s00128-018-2523-1

Heiri, O., Lotter, A. F., & Lemcke, G. (2001). Loss on ignition as a method for estimating organic and carbonate content in sediments: reproducibility and comparability of results. *Journal of Paleolimnology*, *25*, 101–110. https://doi.org/10.1023/A:1008119611481

Hellal, J., Schäfer, J., Vigouroux, R., Lanceleur, L., & Laperche, V. (2020). Impact of old and recent gold mining sites on mercury fluxes in suspended particulate matter, water and sediment in French Guiana. *Applied Sciences*, *10*, 7829. https://doi.org/10.3390/app10217829

Helmrich, S., Vlassopoulos, D., Alpers, C. N., & O'Day, P. A. (2021). Critical review of mercury methylation and methylmercury demethylation rate constants in aquatic sediments for biogeochemical modeling. *Critical Reviews in Environmental Science and Technology*. https://doi.org/10.1080/10643389.2021.2013073

Higgins, J. P. T., & Thompson, S. G. (2002). Quantifying heterogeneity in a meta-analysis. *Statistics in Medicine*, *21*(11), 1539–1558. https://doi.org/10.1002/sim.1186

Hilson, G., & Vieira, R. (2007). Challenges with minimising mercury pollution in the small-scale gold mining sector: Experiences from the Guianas. *International Journal Of Environmental Health Research*, *17*(6), 429–441. https://doi.org/10.1080/09603120701633396

Hintelmann, H., Harris, R., Heyes, A., Hurley, J., Kelly, C., Krabbenhoft, D., Lindberg, S., Rudd, J., Scott, K., & St Louis, V. (2002). Reactivity and mobility of new and

old mercury deposition in a boreal forest ecosystem during the first year of the METAALICUS study. *Environmental Science Technology*, *36*(23), 5034–5040. https://doi.org/10.1021/es025572t

Hojdová, M., Rohovec, J., Chrastný, V., Penížek, V., & Navrátil, T. (2015). The influence of sample drying procedures on mercury concentrations analyzed in soils. *Bulletin of Environmental Contamination and Toxicology*, *94*, 570–576. https://doi.org/10.1007/s00128-015-1521-9

Hong, S. H., Kang, B. H., Kang, M. H., Chung, J. W., Jun, W. J., Chung, J. I., Kim, M. C., & Shim, S. I. (2009). Responses of wild plant species to polycyclic aromatic hydrocarbons in soil. *Journal of Environmental Monitoring*, *11*, 1664–1672. https://doi.org/10.1039/b906560a

Hou, Y., Zhao, Y., Lu, J., Wei, Q., Zang, L., & Zhao, X. (2023). Environmental contamination and health risk assessment of potentially toxic trace metal elements in soils near gold mines – A global meta-analysis. *Environmental Pollution*, *330*, 121803. https://doi.org/10.1016/j.envpol.2023.121803

Howard, J. A. (2006). *Gold mining in a tropical rainforest: Mercury sorption to soils in the mining region of Arakaka-Mathew's Ridge, Guyana* [University of South Florida]. http://scholarcommons.usf.edu/etd/2564/

Howard, J., Trotz, M. A., Thomas, K., Omisca, E., Chiu, H. T., Halfhide, T., Akiwumi, F., Michael, R., & Stuart, A. L. (2011). Total mercury loadings in sediment from gold mining and conservation areas in Guyana. *Environmental Monitoring and Assessment*, *179*, 555–573. https://doi.org/10.1007/s10661-010-1762-3

Hu, X. F., Lowe, M., & Chan, H. M. (2021). Mercury exposure, cardiovascular disease, and mortality: A systematic review and dose-response meta-analysis. *Environmental Research*, *193*, 110538. https://doi.org/10.1016/j.envres.2020.110538

Huang, J., Lyman, S. N., Hartman, J. S., & Gustin, M. S. (2014). A review of passive sampling systems for ambient air mercury measurements. *Environmental Science: Processes & Impacts*, *16*(3), 374–392. https://doi.org/10.1039/c3em0 0501a

Huang, Jiaoyan, & Gustin, M. S. (2015). Use of passive sampling methods and models to understand sources of mercury deposition to high elevation sites in the western United States. *Environmental Science and Technology*, *49*, 432–441. https://doi.org/10.1021/es502836w

Iatan, E.-L. (2021). Gold mining industry influence on the environment and possible phytoremediation applications. In *Phytorestoration of Abandoned Mining and Oil Drilling Sites* (pp. 373–408). Elsevier Inc. https://doi.org/10.1016/b978-0-12-821200-4.00007-8

Ibrahim, A., & Horton, R. (2021). Biochar and compost amendment impacts on soil water and pore size distribution of a loamy sand soil. *Soil Science Society of America Journal*, *85*, 1021–1036. https://doi.org/10.1002/saj2.20242

International Biochar Initiative. (2015). IBI Biochar standards - Standardized product definition and product testing guidelines for biochar that is used in soil version 2.1. In *International Biochar Initiative*. http://www.biochar-international.org/characterizationstandard

Islam, M. S., Ahmed, M. K., Raknuzzaman, M., Habibullah -Al- Mamun, M., & Islam, M. K. (2015). Heavy metal pollution in surface water and sediment: A preliminary assessment of an urban river in a developing country. *Ecological Indicators*, *48*,

282–291. https://doi.org/10.1016/j.ecolind.2014.08.016
Jaganmohan, M. (2024). *South America's mine production of gold 2022, by country*. Statista. https://www.statista.com/statistics/1426390/south-america-gold-mine-production-by-country/
Jeffery, S., Verheijen, F. G. A., van der Velde, M., & Bastos, A. C. (2011). A quantitative review of the effects of biochar application to soils on crop productivity using meta-analysis. *Agriculture, Ecosystems and Environment*, *144*, 175–187. https://doi.org/10.1016/j.agee.2011.08.015
Jensen, J. L., Christensen, B. T., Schjønning, P., Watts, C. W., & Munkholm, L. J. (2018). Converting loss-on-ignition to organic carbon content in arable topsoil: pitfalls and proposed procedure. *European Journal of Soil Science*, *69*, 604–612. https://doi.org/10.1111/ejss.12558
Jeon, B., Cizdziel, J. V., Brewer, J. S., Luke, W. T., Cohen, M. D., Ren, X., & Kelley, P. (2020). Gaseous elemental mercury concentrations along the northern gulf of mexico using passive air sampling, with a comparison to active sampling. *Atmosphere*, *11*, 1034. https://doi.org/10.3390/atmos11101034
Jiang, M., Zeng, G., Zhang, C., Ma, X., Chen, M., Zhang, J., Lu, L., Yu, Q., Hu, L., & Liu, L. (2013). Assessment of heavy metal contamination in the surrounding soils and surface sediments in Xiawangang River, Qingshuitang District. *PLoS ONE*, *8*(8), e71176. https://doi.org/10.1371/journal.pone.0071176
Josse, J., & Husson, F. (2016). missMDA: A package for handling missing values in multivariate data analysis. *Journal of Statistical Software*, *70*(1), 1–31. https://doi.org/10.18637/jss.v070.i01
Josse, J., Pagès, J., & Husson, F. (2011). Multiple imputation in principal component analysis. *Advances in Data Analysis and Classification*, *5*, 231–246. https://doi.org/10.1007/s11634-011-0086-7
Juillerat, J. I., Ross, D. S., & Bank, M. S. (2012). Mercury in litterfall and upper soil horizons in forested ecosystems in Vermont, USA. *Environmental Toxicology and Chemistry*, *31*(8), 1720–1729. https://doi.org/10.1002/etc.1896
Kabir, E., Ray, S., Kim, K. H., Yoon, H. O., Jeon, E. C., Kim, Y. S., Cho, Y. S., Yun, S. T., & Brown, R. J. C. (2012). Current status of trace metal pollution in soils affected by industrial activities. *The Scientific World Journal*, *2012*. https://doi.org/10.1100/2012/916705
Kadir Salam, A. (2023). The potential roles of biochar in restoring heavy-metal-polluted tropical soils and plant growth. In M. Bartoli, M. Giorcelli, & A. Tagliaferro (Eds.), *Biochar - Productive Technologies, Properties and Applications*. IntechOpen. https://doi.org/10.5772/intechopen.105791
Kalamandeen, M., Gloor, E., Johnson, I., Agard, S., Katow, M., Vanbrooke, A., Ashley, D., Batterman, S. A., Ziv, G., Holder-Collins, K., Phillips, O. L., Brondizio, E. S., Vieira, I., & Galbraith, D. (2020). Limited biomass recovery from gold mining in Amazonian forests. *Journal of Applied Ecology*, *57*, 1730–1740. https://doi.org/10.1111/1365-2664.13669
Karberg, N. J., Scott, N. A., & Giardina, C. P. (2008). Methods for estimating litter decomposition. In C. M. Hoover (Ed.), *Field measurements for forest carbon monitoring: A landscape-scale approach* (pp. 103–111). Springer Science + Business Media.

Keesstra, S., Mol, G., de Leeuw, J., Okx, J., Molenaar, C., de Cleen, M., & Visser, S. (2018). Soil-related sustainable development goals: Four concepts to make land degradation neutrality and restoration work. *Land*, *7*. https://doi.org/10.3390/land7040133

Kekem, A. J. Van, Pulles, J. H. M., & Khan, Z. (1996). *Soils of the rainforest in Central Guyana*. Tropenbos-Guyana programme.

Khwaja, A. R., Bloom, P. R., & Brezonik, P. L. (2006). Binding constants of divalent mercury (Hg2+) in soil humic acids and soil organic matter. *Environmental Science and Technology*, *40*(3), 844–849. https://doi.org/10.1021/es051085c

Kögel-Knabner, I. (2017). The macromolecular organic composition of plant and microbial residues as inputs to soil organic matter: Fourteen years on. *Soil Biology and Biochemistry*, *105*, A3–A8. https://doi.org/10.1016/j.soilbio.2016.08.011

Kongchum, M., Hudnall, W. H., & Delaune, R. D. (2011). Relationship between sediment clay minerals and total mercury. *Journal of Environmental Science and Health Part A*, *46*(5), 534–539. https://doi.org/10.1080/10934529.2011.551745

Koskey, J. C., Ogendi, G. M., M'Erimba, C. M., & Tamba, C. L. (2020). Influence of particle size and total organic carbon on heavy metal concentrations in sediments of Lake Baringo, Kenya. *African Journal of Environmental Science and Technology*, *14*(12), 394–399. https://doi.org/10.5897/AJEST2019.2796

Kroonenberg, S., Wong, T., Bijnaar, G., Finkie, R., Goenopawiro, K., Asneel, S., Lin-Tsung, M., Nanan, R., Ramdas, K., & Sitaram, P. (2022). Mercury background values in soils and saprolites in the gold-rich greenstone belt of Suriname, Guiana Shield: The role of parent rock and residual enrichment. *Science of the Total Environment*, *848*, 157631. https://doi.org/10.1016/j.scitotenv.2022.157631

Küçükyumuk, Z., Erdal, İ., Coşkan, A., Göktaş, M., & Sırça, E. (2017). Influence of biochar on growth and mineral concentrations of pepper. *Infrastructure and Ecology of Rural Areas*, *2*, 793–802. https://doi.org/10.14597/infraeco.2017.2.2.061

Kuhry, P., & Vitt, D. H. (1996). Fossil carbon/nitrogen ratios as a measure of peat decomposition. *Ecology*, *77*(1), 271–275. https://doi.org/10.2307/2265676

Kumar, B., Smita, K., & Cumbal Flores, L. (2017). Plant mediated detoxification of mercury and lead. *Arabian Journal of Chemistry*, *10*, S2335–S2342. https://doi.org/10.1016/j.arabjc.2013.08.010

Kumar, S., Islam, A. R. M. T., Hasanuzzaman, M., Salam, R., Khan, R., & Islam, M. S. (2021). Preliminary assessment of heavy metals in surface water and sediment in Nakuvadra-Rakiraki River, Fiji using indexical and chemometric approaches. *Journal of Environmental Management*, *298*, 113517. https://doi.org/10.1016/j.jenvman.2021.113517

Lacerda, L. D. de, Marins, R. V., & Dias, F. J. da S. (2020). An Arctic paradox: Response of fluvial Hg inputs and bioavailability to global climate change in an extreme coastal environment. *Frontiers in Earth Science*, *8*, 1–12. https://doi.org/10.3389/feart.2020.00093

Laing, T., Edwards, R., Yusuf, S., & Sparman, C. (2023). Assessing the economics and finances of artisanal and small-scale gold mining in Guyana. *Journal of Rural Studies*, *97*, 438–448. https://doi.org/10.1016/j.jrurstud.2022.11.009

Laker, M. C. (2023). Environmental impacts of gold mining—with special reference to South Africa. *Mining*, *3*, 205–220. https://doi.org/10.3390/mining3020012

Laperche, V., Hellal, J., Maury-Brachet, R., Joseph, B., Laporte, P., Breeze, D., & Blanchard, F. (2014). Regional distribution of mercury in sediments of the main rivers of French Guiana (Amazonian basin). *SpringerPlus*, *3*, 322. https://doi.org/10.1186/2193-1801-3-322

Larney, F. J., & Angers, D. A. (2012). The role of organic amendments in soil reclamation: A review. *Canadian Journal of Soil Science*, *92*, 19–38. https://doi.org/10.4141/CJSS2010-064

Lavoie, R. A., Amyot, M., & Lapierre, J. F. (2019). Global meta-analysis on the relationship between mercury and dissolved organic carbon in freshwater environments. *Journal of Geophysical Research: Biogeosciences*, *124*, 1508–1523. https://doi.org/10.1029/2018JG004896

Lecerf, A., Cébron, A., Gilbert, F., Danger, M., Roussel, H., & Maunoury-Danger, F. (2021). Using plant litter decomposition as an indicator of ecosystem response to soil contamination. *Ecological Indicators*, *125*, 107554. https://doi.org/10.1016/j.ecolind.2021.107554

Lehmann, J., Rillig, M. C., Thies, J., Masiello, C. A., Hockaday, W. C., & Crowley, D. (2011). Biochar effects on soil biota - A review. *Soil Biology and Biochemistry*, *43*, 1812–1836. https://doi.org/10.1016/j.soilbio.2011.04.022

Leiva G., M. A., & Morales, S. (2013). Environmental assessment of mercury pollution in urban tailings from gold mining. *Ecotoxicology and Environmental Safety*, *90*, 167–173. https://doi.org/10.1016/j.ecoenv.2012.12.026

Lewis, L., Hossain, M., & Killur, R. R. B. (2022). The planting density of Acacia mangium influences the rehabilitation of a waste rock dump in Papua New Guinea. *Arabian Journal of Geosciences*, *15*, 216. https://doi.org/10.1007/s12517-022-09522-4

Lewis, L., Hossain, M., & Rao, B. K. R. (2020). Physicochemical assessment of a waste rock dump in the hidden valley gold mine: a case study for bioremediation in Papua New Guinea. *Environmental Earth Sciences*, *79*. https://doi.org/10.1007/s12665-020-8841-8

Li, W., Deng, Y., Wang, H., Hu, Y., & Cheng, H. (2024). Potential risk, leaching behavior and mechanism of heavy metals from mine tailings under acid rain. *Chemosphere*, *350*, 140995. https://doi.org/10.1016/j.chemosphere.2023.140995

Li, X., Wang, X., Yuan, W., Lu, Z., & Wang, D. (2022). Increase of litterfall mercury input and sequestration during decomposition with a montane elevation in Southwest China. *Environmental Pollution*, *292*, 118449. https://doi.org/10.1016/j.envpol.2021.118449

Liu, L., Tan, Z., Gong, H., & Huang, Q. (2019). Migration and transformation mechanisms of nutrient elements (N, P, K) within biochar in straw-biochar-soil-plant systems: A review. *ACS Sustainable Chemistry and Engineering*, *7*, 22–32. https://doi.org/10.1021/acssuschemeng.8b04253

Lodenius, M. (1998). Dry and wet deposition of mercury near a chlor-alkali plant. *The Science of the Total Environment*, *213*, 53–56. https://doi.org/10.1016/S0048-9697(98)00073-4

Lodenius, Martin. (2013). Use of plants for biomonitoring of airborne mercury in contaminated areas. *Environmental Research*, *125*, 113–123. https://doi.org/10.1016/j.envres.2012.10.014

López-Blanco, C., Collahuazo, L., Torres, S., Chinchay, L., Ayala, D., & Benítez, P. (2015). Mercury pollution in soils from the Yacuambi river (Ecuadorian Amazon) as a result of gold placer mining. *Bulletin of Environmental Contamination and Toxicology*, *95*, 311–316. https://doi.org/10.1007/s00128-015-1604-7

Luo, Y., Duan, L., Wang, L., Xu, G., Wang, S., & Hao, J. (2014). Mercury concentrations in forest soils and stream waters in northeast and south China. *Science of the Total Environment*, *496*, 714–720. https://doi.org/10.1016/j.scitotenv.2014.07.036

Lyman, S. N., Gustin, M. S., & Prestbo, E. M. (2010). A passive sampler for ambient gaseous oxidized mercury concentrations. *Atmospheric Environment*, *44*, 246–252. https://doi.org/10.1016/j.atmosenv.2009.10.008

Ma, H., Cheng, H., Guo, F., Zhang, L., Tang, S., Yang, Z., & Peng, M. (2022). Distribution of mercury in foliage, litter and soil profiles in forests of the Qinling Mountains, China. *Environmental Research*, *211*, 113017. https://doi.org/10.1016/j.envres.2022.113017

Macdonald, K., Lund, M., & Blanchette, M. (2015). Impacts of artisanal small-scale gold mining on water quality of a tropical river (Surow River, Ghana). *10th International Conference on Acid Rock Drainage & IMWA Annual Conference*, 1–12. http://www.imwa.info/docs/imwa_2015/IMWA2015_Macdonald_283.pdf

Macháček, J. (2020). Alluvial artisanal and small-scale mining in a river stream-Rutsiro case study (Rwanda). *Forests*, *11*, 762. https://doi.org/10.3390/F11070762

Majid, N. M., Islam, M. M., & Mathew, L. (2012). Heavy metal uptake and translocation by mangium (*Acacia mangium*) from sewage sludge contaminated soil. *Australian Journal of Crop Science*, *6*(8), 1228–1235.

Marrugo-Negrete, J., Durango-Hernández, J., Pinedo-Hernández, J., Enamorado-Montes, G., & Díez, S. (2016). Mercury uptake and effects on growth in Jatropha curcas. *Journal of Environmental Sciences*, *48*, 120–125. https://doi.org/10.1016/j.jes.2015.10.036

Marrugo-Negrete, J., Durango-Hernández, J., Pinedo-Hernández, J., Olivero-Verbel, J., & Díez, S. (2015). Phytoremediation of mercury-contaminated soils by *Jatropha curcas*. *Chemosphere*, *127*, 58–63. https://doi.org/10.1016/j.chemosphere.2014.12.073

Marrugo-Negrete, J., Pinedo-Hernández, J., Marrugo-Madrid, S., & Díez, S. (2021). Assessment of trace element pollution and ecological risks in a river basin impacted by mining in Colombia. *Environmental Science and Pollution Research*, *28*, 201–210. https://doi.org/10.1007/s11356-020-10356-4

Martín, A., Arias, J., López, J., Santos, L., Venegas, C., Duarte, M., Ortíz-Ardila, A., de Parra, N., Campos, C., & Zambrano, C. C. (2020). Evaluation of the effect of gold mining on the water quality in Monterrey, Bolívar (Colombia). *Water*, *12*, 2523. https://doi.org/10.3390/w12092523

Maslennikova, S., Larina, N., & Larin, S. (2012). The effect of sediment grain size on heavy metal content. *Lakes, Reservoirs and Ponds*, *6*(1), 43–54.

McCormack, M. L., Dickie, I. A., Eissenstat, D. M., Fahey, T. J., Fernandez, C. W., Guo, D., Helmisaari, H. S., Hobbie, E. A., Iversen, C. M., Jackson, R. B., Leppälammi-Kujansuu, J., Norby, R. J., Phillips, R. P., Pregitzer, K. S., Pritchard, S. G., Rewald, B., & Zadworny, M. (2015). Redefining fine roots improves understanding of

below-ground contributions to terrestrial biosphere processes. *New Phytologist*, *207*, 505–518. https://doi.org/10.1111/nph.13363

McLagan, D. S., Hussain, B. A., Huang, H., Lei, Y. D., Wania, F., & Mitchell, C. P. J. (2018). Identifying and evaluating urban mercury emission sources through passive sampler-based mapping of atmospheric concentrations. *Environmental Research Letters*, *13*, 074008. https://doi.org/10.1088/1748-9326/aac8e6

McLagan, D. S., Mazur, M. E. E., Mitchell, C. P. J., & Wania, F. (2016). Passive air sampling of gaseous elemental mercury: A critical review. *Atmospheric Chemistry and Physics*, *16*, 3061–3076. https://doi.org/10.5194/acp-16-3061-2016

McLagan, D. S., Mitchell, C. P. J., Huang, H., Abdul Hussain, B., Duan Lei, Y., & Wania, F. (2017). The effects of meteorological parameters and diffusive barrier reuse on the sampling rate of a passive air sampler for gaseous mercury. *Atmospheric Measurement Techniques*, *10*, 3651–3660. https://doi.org/10.5194/amt-10-3651-2017

McLagan, D. S., Mitchell, C. P. J., Huang, H., Lei, Y. D., Cole, A. S., Steffen, A., Hung, H., & Wania, F. (2016). A high-precision passive air sampler for gaseous mercury. *Environmental Science and Technology Letters*, *3*, 24–29. https://doi.org/10.1021/acs.estlett.5b00319

Mclagan, D. S., Mitchell, C. P. J., Steffen, A., Hung, H., Shin, C., Stupple, G. W., Olson, M. L., Luke, W. T., Kelley, P., Howard, D., Edwards, G. C., Nelson, P. F., Xiao, H., Sheu, G., Dreyer, A., Huang, H., Hussain, B. A., Lei, Y. D., Tavshunsky, I., & Wania, F. (2018). Global evaluation and calibration of a passive air sampler for gaseous mercury. *Atmospheric Chemistry and Physics*, *18*, 5905–5919. https://doi.org/10.5194/acp-18-5905-2018

McLagan, D. S., Monaci, F., Huang, H., Lei, Y. D., Mitchell, C. P. J., & Wania, F. (2019). Characterization and quantification of atmospheric mercury sources using passive air samplers. *Journal of Geophysical Research: Atmospheres*, *124*, 2351–2362. https://doi.org/10.1029/2018JD029373

McLagan, D. S., Osterwalder, S., & Biester, H. (2021). Temporal and spatial assessment of gaseous elemental mercury concentrations and emissions at contaminated sites using active and passive measurements. *Environmental Research Communications*, *3*, 051004. https://doi.org/10.1088/2515-7620/abfe02

Meloni, F., Calabrese, S., Vaselli, O., Capecchiacci, F., Ciani, F., Brusca, L., Bellomo, S., D'Alessandro, W., Daskalopoulou, K., Venturi, S., Nisi, B., Rappuoli, D., Tassi, F., & Cabassi, J. (2025). Active moss biomonitoring of mercury in the mine-polluted area of Abbadia San Salvatore (Mt. Amiata, Central Italy). *Toxics*, *13*, 2. https://doi.org/10.3390/toxics13010002

Mencho, B. B. (2022). Assessing the effects of gold mining on environment: A case study of Shekiso district, Guji zone, Ethiopia. *Heliyon*, *8*, e11882. https://doi.org/10.1016/j.heliyon.2022.e11882

Mendes, L. A., de Lena, J. C., do Valle, C. M., Fleming, P. M., & Windmöller, C. C. (2016). Quantification of methylmercury and geochemistry of mercury in sediments from a contaminated area of Descoberto (MG), Brazil. *Applied Geochemistry*, *75*, 32–43. https://doi.org/10.1016/j.apgeochem.2016.10.011

Mensah, A. K., Marschner, B., Shaheen, S. M., Wang, J., Wang, S. L., & Rinklebe, J. (2020). Arsenic contamination in abandoned and active gold mine spoils in Ghana:

Geochemical fractionation, speciation, and assessment of the potential human health risk. *Environmental Pollution*, *261*, 114116. https://doi.org/10.1016/j.envpol.2020.114116

Mensah, M. K., Drebenstedt, C., Hoth, N., Ola, I. M., Okoroafor, P. U., & Wiafe, E. D. (2023). Artisanal gold mine spoil types within a common geological area and their variations in contaminant loads and human health risks. *Environmental Monitoring and Assessment*, *195*, 312. https://doi.org/10.1007/s10661-023-10932-4

Miller, E. K., Vanarsdale, A., Keeler, G. J., Chalmers, A., Poissant, L., Kamman, N. C., & Brulotte, R. (2005). Estimation and mapping of wet and dry mercury deposition across northeastern North America. *Ecotoxicology*, *14*, 53–70. https://doi.org/10.1007/s10646-004-6259-9

Mimba, M. E., Mbafor, P. U. T., Nguemhe Fils, S. C., & Nforba, M. T. (2023). Environmental impact of artisanal and small-scale gold mining in East Cameroon, Sub-Saharan Africa: An overview. *Ore and Energy Resource Geology*, *15*, 100031. https://doi.org/10.1016/j.oreoa.2023.100031

Mining Act, 65:01, 3 (1989).

Mining Information Toolkit for Guyana. (2012). *A mining information toolkit for Guyana*.

Miserendino, R. A., Guimarães, J. R. D., Schudel, G., Ghosh, S., Godoy, J. M., Silbergeld, E. K., Lees, P. S. J., & Bergquist, B. A. (2018). Mercury pollution in Amapá, Brazil: Mercury amalgamation in artisanal and small-scale gold mining or land-cover and land-use changes? *ACS Earth and Space Chemistry*, *2*, 441–450. https://doi.org/10.1021/acsearthspacechem.7b00089

Monaci, F., Ancora, S., Paoli, L., Loppi, S., & Wania, F. (2022). Lichen transplants as indicators of gaseous elemental mercury concentrations. *Environmental Pollution*, *313*, 120189. https://doi.org/10.1016/j.envpol.2022.120189

Moonilall, N. I., Homenauth, O., & Lal, R. (2020). Emergy analysis for maize fields under different amendment applications in Guyana. *Journal of Cleaner Production*, *258*, 120761. https://doi.org/10.1016/j.jclepro.2020.120761

Moreno-Brush, M., McLagan, D. S., & Biester, H. (2020). Fate of mercury from artisanal and small-scale gold mining in tropical rivers: Hydrological and biogeochemical controls. A critical review. *Critical Reviews in Environmental Science and Technology*, *50*(5), 437–475. https://doi.org/10.1080/10643389.2019.1629793

Morosini, C., Terzaghi, E., Raspa, G., Zanardini, E., Anelli, S., Armiraglio, S., Petranich, E., Covelli, S., & Di Guardo, A. (2021). Mercury vertical and horizontal concentrations in agricultural soils of a historically contaminated site: Role of soil properties, chemical loading, and cultivated plant species in driving its mobility. *Environmental Pollution*, *285*, 117467. https://doi.org/10.1016/j.envpol.2021.117467

Mousavi, A. (2015). Are thiolate anions the only natural organic matter ligands for which mercury(II) has an exceptionally high affinity in aquatic ecosystems? *Revista de Chimie*, *66*(5), 774–777.

Muddarisna, N., & Siahaan, B. C. (2014). Application of organic matter to enhance phytoremediation of mercury contaminated soils using local plant species: a case study on small-scale gold mining locations in Banyuwangi of East Java. *Journal of Degraded and Mining Lands Management*, *2*(1), 251–258.

https://doi.org/10.15243/jdmlm.2014.021.251
Mulholland, D. S., Boaventura, G. R., & Araújo, D. F. (2012). Geological and anthropogenic influences on sediment metal composition in the upper Paracatu River Basin, Brazil. *Environmental Earth Sciences*, *67*, 1307–1317. https://doi.org/10.1007/s12665-012-1574-6
Musei, S. K., Kuyah, S., Nyawira, S., Ng'ang'a, S. K., Karugu, W. N., Smucker, A., & Nkurunziza, L. (2024). Sandy soil reclamation technologies to improve crop productivity and soil health: a review. *Frontiers in Soil Science*, *4*, 1345895. https://doi.org/10.3389/fsoil.2024.1345895
Naccarato, A., Tassone, A., Martino, M., Moretti, S., Macagnano, A., Zampetti, E., Papa, P., Avossa, J., Pirrone, N., Nerentorp, M., Munthe, J., Wängberg, I., Stupple, G. W., Mitchell, C. P. J., Martin, A. R., Steffen, A., Babi, D., Prestbo, E. M., Sprovieri, F., & Wania, F. (2021). A field intercomparison of three passive air samplers for gaseous mercury in ambient air. *Atmospheric Measurement Techniques*, *14*, 3657–3672. https://doi.org/10.5194/amt-14-3657-2021
Nacishali Nteranya, J., & Mukulia, P. M. (2023). Restoration of degraded lands and alternatives in artisanal mining areas: Sustainable development perspectives from Democratic Republic of Congo. In W. Leal Filho, I. R. Abubakar, I. da Silva, R. Pretorius, & K. Tarabieh (Eds.), *SDGs in Africa and the Middle East Region*.
Nakazawa, K., Nagafuchi, O., Kawakami, T., Inoue, T., Yokota, K., Serikawa, Y., Basir-Cyio, M., & Elvince, R. (2016). Human health risk assessment of mercury vapor around artisanal small-scale gold mining area, Palu city, Central Sulawesi, Indonesia. *Ecotoxicology and Environmental Safety*, *124*, 155–162. https://doi.org/10.1016/j.ecoenv.2015.09.042
Navarro, M. C., Pérez-Sirvent, C., Martínez-Sánchez, M. J., Vidal, J., Tovar, P. J., & Bech, J. (2008). Abandoned mine sites as a source of contamination by heavy metals: A case study in a semi-arid zone. *Journal of Geochemical Exploration*, *96*, 183–193. https://doi.org/10.1016/j.gexplo.2007.04.011
Nazeri, A., Jusoh, I., & Wasli, M. E. (2021). Growth of *Acacia mangium* at different stand ages and soil physicochemical properties in Sarawak, Malaysia. *Pertanika Journal of Tropical Agricultural Science*, *44*(4), 773–793. https://doi.org/10.47836/pjtas.44.4.02
Ndungu, K., Schaanning, M., & Braaten, H. F. V. (2016). Effects of organic matter addition on methylmercury formation in capped and uncapped marine sediments. *Water Research*, *103*, 401–407. https://doi.org/10.1016/j.watres.2016.07.055
Niane, B., Guédron, S., Feder, F., Legros, S., Ngom, P. M., & Moritz, R. (2019). Impact of recent artisanal small-scale gold mining in Senegal: Mercury and methylmercury contamination of terrestrial and aquatic ecosystems. *Science of the Total Environment*, *669*, 185–193. https://doi.org/10.1016/j.scitotenv.2019.03.108
Nkuba, B., Bervoets, L., & Geenen, S. (2019). Invisible and ignored? Local perspectives on mercury in Congolese gold mining. *Journal of Cleaner Production*, *221*, 795–804. https://doi.org/10.1016/j.jclepro.2019.01.174
O'Connor, D., Hou, D., Ok, Y. S., Mulder, J., Duan, L., Wu, Q., Wang, S., Tack, F. M. G., & Rinklebe, J. (2019). Mercury speciation, transformation, and transportation in soils, atmospheric flux, and implications for risk management: A critical review. *Environment International*, *126*, 747–761.

https://doi.org/10.1016/j.envint.2019.03.019
Obrist, D., Johnson, D. W., & Lindberg, S. E. (2009). Mercury concentrations and pools in four Sierra Nevada forest sites, and relationships to organic carbon and nitrogen. *Biogeosciences*, *6*, 765–777. https://doi.org/10.5194/bg-6-765-2009
Obrist, D., Johnson, D. W., Lindberg, S. E., Luo, Y., Hararuk, O., Bracho, R., Battles, J. J., Dail, D. B., Edmonds, R. L., Monson, R. K., Ollinger, S. V., Pallardy, S. G., Pregitzer, K. S., & Todd, D. E. (2011). Mercury distribution across 14 U.S. Forests. Part I: Spatial patterns of concentrations in biomass, litter, and soils. *Environmental Science and Technology*, *45*, 3974–3981. https://doi.org/10.1021/es104384m
Obrist, Daniel, Faïn, X., & Berger, C. (2010). Gaseous elemental mercury emissions and CO2 respiration rates in terrestrial soils under controlled aerobic and anaerobic laboratory conditions. *Science of the Total Environment*, *408*, 1691–1700. https://doi.org/10.1016/j.scitotenv.2009.12.008
Obrist, Daniel, Kirk, J. L., Zhang, L., Sunderland, E. M., Jiskra, M., & Selin, N. E. (2018). A review of global environmental mercury processes in response to human and natural perturbations: Changes of emissions, climate, and land use. *Ambio*, *47*, 116–140. https://doi.org/10.1007/s13280-017-1004-9
Occupational Safety and Health Act, 3 (1997).
Odukoya, A. M., Uruowhe, B., Watts, M. J., Hamilton, E. M., Marriott, A. L., Alo, B., & Anene, N. C. (2022). Assessment of bioaccessibility and health risk of mercury within soil of artisanal gold mine sites, Niger, North-central part of Nigeria. *Environmental Geochemistry and Health*, *44*(6), 893–909. https://doi.org/10.1007/s10653-021-00991-2
Ogola, J. S., Mitullah, W. V., & Omulo, M. A. (2002). Impact of gold mining on the environment and human health: A case study in the Migori Gold Belt, Kenya. *Environmental Geochemistry and Health*, *24*, 141–157. https://doi.org/10.1023/A:1014207832471
Olowoyo, J. O., Lion, N., Unathi, T., & Oladeji, O. M. (2022). Concentrations of Pb and other associated elements in soil dust 15 years after the introduction of unleaded fuel and the human health implications in Pretoria, South Africa. *International Journal of Environmental Research and Public Health*, *19*, 10238. https://doi.org/10.3390/ijerph191610238
Olson, C., Jiskra, M., Biester, H., Chow, J., & Obrist, D. (2018). Mercury in active-layer Tundra soils of Alaska: Concentrations, pools, origins, and spatial distribution. *Global Biogeochemical Cycles*. https://doi.org/10.1029/2017GB005840
Osborne, C., Gilbert-Parkes, S., Graeme, S., Lamit, L. J., Lilleskov, E. A., Basiliko, N., Watmough, S., & Global Peatland Microbiome Project. (2024). Global patterns of metal and other element enrichment in bog and fen peatlands. *Archives of Environmental Contamination and Toxicology*, *86*, 125–139. https://doi.org/10.1007/s00244-024-01051-3
Osborne, C., Gilbert-Parkes, S., Spiers, G., Lamit, L. J., Lilleskov, E. A., Basiliko, N., & Watmough, S. (2024). Global patterns of metal and other element enrichment in bog and fen peatlands. *Archives of Environmental Contamination and Toxicology*, *86*, 125–139. https://doi.org/10.1007/s00244-024-01051-3
Ott, N. (2021). *The influence of tree species litterfall on soil chemistry and implications for modelling soil recovery from acidification*. Trent University.

Ouboter, P. E., Landburg, G. A., Quik, J. H. M., Mol, J. H. A., & Van Der Lugt, F. (2012). Mercury levels in pristine and gold mining impacted aquatic ecosystems of Suriname, South America. *Ambio*, *41*, 873–882. https://doi.org/10.1007/s13280-012-0299-9

Oyarzún, J., Castillo, D., Maturana, H., Kretschmer, N., Soto, G., Amezaga, J. M., Rötting, T. S., Younger, P. L., & Oyarzún, R. (2012). Abandoned tailings deposits, acid drainage and alluvial sediments geochemistry, in the arid Elqui River Basin, North-Central Chile. *Journal of Geochemical Exploration*, *115*, 47–58. https://doi.org/10.1016/j.gexplo.2012.02.008

Pacyna, E. G., Pacyna, J. M., Sundseth, K., Munthe, J., Kindbom, K., Wilson, S., Steenhuisen, F., & Maxson, P. (2010). Global emission of mercury to the atmosphere from anthropogenic sources in 2005 and projections to 2020. *Atmospheric Environment*, *44*, 2487–2499. https://doi.org/10.1016/j.atmosenv.2009.06.009

Palacios-Torres, Y., de la Rosa, J. D., & Olivero-Verbel, J. (2020). Trace elements in sediments and fish from Atrato River: an ecosystem with legal rights impacted by gold mining at the Colombian Pacific. *Environmental Pollution*, *256*, 113290. https://doi.org/10.1016/j.envpol.2019.113290

Palomino, D. (2019). Peru. In E. R. La Flèche (Ed.), *The mining law review* (8th ed., pp. 156–166). Law Business Research Ltd. www.TheLawReviews.co.uk

Pan, J., Chen, M., Zhang, Z., Zhang, H., Zong, J., Wang, Z., & Zhang, G. (2023). Risk assessments of plant leaf and soil mercury pollution in different functional areas of Changchun city. *Forests*, *14*, 1108. https://doi.org/10.3390/f14061108

Pasha, S., Wenner, M. D., & Clarke, D. (2017). *Toward the greening of the gold mining sector of Guyana transition issues and challenges*. http://www.iadb.org

Pavilonis, B., Grassman, J., Johnson, G., Diaz, Y., & Caravanos, J. (2017). Characterization and risk of exposure to elements from artisanal gold mining operations in the Bolivian Andes. *Environmental Research*, *154*, 1–9. https://doi.org/10.1016/j.envres.2016.12.010

Pejman, A., Nabi Bidhendi, G., Ardestani, M., Saeedi, M., & Baghvand, A. (2015). A new index for assessing heavy metals contamination in sediments: A case study. *Ecological Indicators*, *58*, 365–373. https://doi.org/10.1016/j.ecolind.2015.06.012

Persaud, T., Homenauth, O., Fredericks, D., & Hamer, S. (2018). Effect of rice husk biochar as an amendment on a marginal soil in Guyana. *World Environment*, *8*(1), 20–25. https://doi.org/10.5923/j.env.20180801.03

Pinedo-Hernández, J., Marrugo-Negrete, J., & Díez, S. (2015). Speciation and bioavailability of mercury in sediments impacted by gold mining in Colombia. *Chemosphere*, *119*, 1289–1295. https://doi.org/10.1016/j.chemosphere.2014.09.044

Pirrone, N., Aas, W., Cinnirella, S., Ebinghaus, R., Hedgecock, I. M., Pacyna, J., Sprovieri, F., & Sunderland, E. M. (2013). Toward the next generation of air quality monitoring: Mercury. *Atmospheric Environment*, *80*, 599–611. https://doi.org/10.1016/j.atmosenv.2013.06.053

Law No. 535: Mining and metallurgy law, (2014) (testimony of Plurinational State of Bolivia).

Poikolainen, J., Kubin, E., Piispanen, J., & Karhu, J. (2004). Estimation of the long-range transport of mercury, cadmium, and lead to northern Finland on the basis of moss

surveys. *Arctic, Antarctic, and Alpine Research*, *36*(3), 292–297. https://doi.org/10.1657/1523-0430(2004)036[0292:EOTLTO]2.0.CO;2
Pokharel, A. K., & Obrist, D. (2011). Fate of mercury in tree litter during decomposition. *Biogeosciences*, *8*, 2507–2521. https://doi.org/10.5194/bg-8-2507-2011
Pratte, S., Mucci, A., & Garneau, M. (2013). Historical records of atmospheric metal deposition along the St. Lawrence Valley (eastern Canada) based on peat bog cores. *Atmospheric Environment*, *79*, 831–840. https://doi.org/10.1016/j.atmosenv.2013.07.063
Prendergast-Miller, M. T., Duvall, M., & Sohi, S. P. (2014). Biochar – root interactions are mediated by biochar nutrient content and impacts on soil nutrient availability. *European Journal of Soil Science*, *65*, 173–185. https://doi.org/10.1111/ejss.12079
Qian, Y., Ralescu, D. A., & Zhang, B. (2019). The analysis of factors affecting global gold price. *Resources Policy*, *64*, 101478. https://doi.org/10.1016/j.resourpol.2019.101478
Qin, A., Ran, S., He, T., Yin, D., & Xu, Y. (2023). The Effects of different soil component couplings on the methylation and bioavailability of mercury in soil. *Toxics*, *11*, 942. https://doi.org/10.3390/toxics11110942
R Core Team. (2021). *R: A language and environment for statistical computing* (4.0.4). R Foundation for Statistical Computing. https://www.r-project.org/
Rajaee, M., Obiri, S., Green, A., Long, R., Cobbina, S. J., Nartey, V., Buck, D., Antwi, E., & Basu, N. (2015). Integrated assessment of artisinal and small-scale gold mining in Ghana-Part 2: Natural sciences review. *International Journal of Environmental Research and Public Health*, *12*, 8971–9011.
Rakotondrabe, F., Ndam Ngoupayou, J. R., Mfonka, Z., Rasolomanana, E. H., Nyangono Abolo, A. J., & Ako Ako, A. (2018). Water quality assessment in the Bétaré-Oya gold mining area (East-Cameroon): Multivariate statistical analysis approach. *Science of the Total Environment*, *610–611*, 831–844. https://doi.org/10.1016/j.scitotenv.2017.08.080
Rea, A. W., Lindberg, S. E., & Keeler, G. J. (2001). Dry deposition and foliar leaching of mercury and selected trace elements in deciduous forest throughfall. *Atmospheric Environment*, *35*, 3453–3462. https://doi.org/10.1016/S1352-2310(01)00133-9
Reid, C., & Watmough, S. A. (2014). Evaluating the effects of liming and wood-ash treatment on forest ecosystems through systematic meta-analysis. *Canadian Journal of Forest Research*, *44*, 867–885. https://doi.org/10.1139/cjfr-2013-0488
Reis, A. T., Lopes, C. B., Davidson, C. M., Duarte, A. C., & Pereira, E. (2015). Extraction of available and labile fractions of mercury from contaminated soils: The role of operational parameters. *Geoderma*, *259–260*, 213–223. https://doi.org/10.1016/j.geoderma.2015.06.004
Riscassi, A. L., & Scanlon, T. M. (2011). Controls on stream water dissolved mercury in three mid-Appalachian forested headwater catchments. *Water Resources Research*, *47*, W12512. https://doi.org/10.1029/2011WR010977
Różański, S. Ł., Castejón, J. M. P., & Fernández, G. G. (2016). Bioavailability and mobility of mercury in selected soil profiles. *Environmental Earth Sciences*, *75*, 1065. https://doi.org/10.1007/s12665-016-5863-3
Rudd, J. W. M., Bodaly, R. A., Fisher, N. S., Kelly, C. A., Kopec, D., & Whipple, C. (2018). Fifty years after its discharge, methylation of legacy mercury trapped in the

Penobscot Estuary sustains high mercury in biota. *Science of the Total Environment, 642*, 1340–1352. https://doi.org/10.1016/j.scitotenv.2018.06.060

Sądej, W., Żołnowski, A. C., Ciećko, Z., Grzybowski, Ł., & Szostek, R. (2020). Evaluation of the impact of soil contamination with mercury and application of soil amendments on the yield and chemical composition of Avena sativa L. *Journal of Environmental Science and Health, Part A, 55*(1), 82–96. https://doi.org/10.1080/10934529.2019.1667671

Salas-Moreno, M., & Marrugo-Negrete, J. (2020). Phytoremediation potential of Cd and Pb-contaminated soils by *Paspalum fasciculatum* Willd. ex Flüggé. *International Journal of Phytoremediation, 22*(1), 87–97. https://doi.org/10.1080/15226514.2019.1644291

Salazar, M., Bosch-Serra, À., Estudillos, G., & Poch, R. M. (2009). Rehabilitation of semi-arid coal mine spoil bank soils with mine residues and farm organic by-products. *Arid Land Research and Management, 23*, 327–341. https://doi.org/10.1080/15324980903231934

Sanei, H., & Goodarzi, F. (2006). Relationship between organic matter and mercury in recent lake sediment: The physical-geochemical aspects. *Applied Geochemistry, 21*, 1900–1912. https://doi.org/10.1016/j.apgeochem.2006.08.015

Santos-Francés, F., García-Sánchez, A., Alonso-Rojo, P., Contreras, F., & Adams, M. (2011). Distribution and mobility of mercury in soils of a gold mining region, Cuyuni river basin, Venezuela. *Journal of Environmental Management, 92*, 1268–1276. https://doi.org/10.1016/j.jenvman.2010.12.003

Santos-Francés, Fernando, Martínez-Graña, A., Rojo, P. A., & Sánchez, A. G. (2017). Geochemical background and baseline values determination and spatial distribution of heavy metal pollution in soils of the andes mountain range (Cajamarca-Huancavelica, Peru). *International Journal of Environmental Research and Public Health, 14*, 859. https://doi.org/10.3390/ijerph14080859

Santos-Lima, C. dos, Mourão, D. de S., Carvalho, C. F. de, Souza-Marques, B., Vega, C. M., Gonçalves, R. A., Argollo, N., Menezes-Filho, J. A., Abreu, N., & Hacon, S. de S. (2020). Neuropsychological effects of mercury exposure in children and adolescents of the Amazon Region, Brazil. *Neurotoxicology, 79*, 48–57. https://doi.org/10.1016/j.neuro.2020.04.004

Scammacca, O., Gunzburger, Y., & Mehdizadeh, R. (2021). Gold mining in French Guiana: A multi-criteria classification of mining projects for risk assessment at the territorial scale. *Extractive Industries and Society, 8*, 32–43. https://doi.org/10.1016/j.exis.2020.06.020

Scheid, S., Günthardt-Goerg, M. S., Schulin, R., & Nowack, B. (2009). Accumulation and solubility of metals during leaf litter decomposition in non-polluted and polluted soil. *European Journal of Soil Science, 60*, 613–621. https://doi.org/10.1111/j.1365-2389.2009.01153.x

Schröder, W., Holy, M., Pesch, R., Harmens, H., Ilyin, I., Steinnes, E., Alber, R., Aleksiayenak, Y., Blum, O., Coşkun, M., Dam, M., De Temmerman, L., Frolova, M., Frontasyeva, M., Miqueo, L. G., Grodzińska, K., Jeran, Z., Korzekwa, S., Krmar, M., … Zechmeister, H. G. (2010). Are cadmium, lead and mercury concentrations in mosses across Europe primarily determined by atmospheric deposition of these metals? *Journal of Soils and Sediments, 10*, 1572–1584.

https://doi.org/10.1007/s11368-010-0254-y
Seki, H. A., Thorn, J. P. R., Platts, P. J., Shirima, D. D., Marchant, R. A., Abeid, Y., Baker, N., Annandale, M., & Marshall, A. R. (2022). Indirect impacts of commercial gold mining on adjacent ecosystems. *Biological Conservation*, *275*, 109782. https://doi.org/10.1016/j.biocon.2022.109782
Selvendiran, P., Driscoll, C. T., Bushey, J. T., & Montesdeoca, M. R. (2008). Wetland influence on mercury fate and transport in a temperate forested watershed. *Environmental Pollution*, *154*, 46–55. https://doi.org/10.1016/j.envpol.2007.12.005
Seshadri, B., Bolan, N. S., & Naidu, R. (2015). Rhizosphere-induced heavy metal(loid) transformation in relation to bioavailability and remediation. *Journal of Soil Science and Plant Nutrition*, *15*(2), 524–548. https://doi.org/10.4067/s0718-95162015005000043
Shipitalo, M. J., & Bonta, J. V. (2008). Impact of using paper mill sludge for surface-mine reclamation on runoff water quality and plant growth. *Journal of Environmental Quality*, *37*, 2351–2359. https://doi.org/10.2134/jeq2007.0648
Skyllberg, U., Xia, K., Bloom, P. ., Nater, E. A., & Bleam, W. F. (2000). Binding of mercury to reduced sulfur in soil organic matter along upland-peat soil transects. *Journal of Environmental Quality*, *29*(3), 855–865. https://doi.org/10.2134/jeq2000.00472425002900030022x
Slemr, F., Brunke, E. G., Ebinghaus, R., & Kuss, J. (2011). Worldwide trend of atmospheric mercury since 1995. *Atmospheric Chemistry and Physics*, *11*, 4779–4787. https://doi.org/10.5194/acp-11-4779-2011
Snow, M. A., Darko, G., Gyamfi, O., Ansah, E., Breivik, K., Hoang, C., Lei, Y. D., & Wania, F. (2021). Characterization of inhalation exposure to gaseous elemental mercury during artisanal gold mining and e-waste recycling through combined stationary and personal passive sampling. *Environmental Science: Processes and Impacts*, *23*, 569–579. https://doi.org/10.1039/d0em00494d
Soe, P. S., Kyaw, W. T., Arizono, K., Ishibashi, Y., & Agusa, T. (2022). Mercury pollution from artisanal and small-scale gold mining in Myanmar and other Southeast Asian countries. *International Journal of Environmental Research and Public Health*, *19*, 6290. https://doi.org/10.3390/ijerph19106290
Soinne, H., Keskinen, R., Tähtikarhu, M., Kuva, J., & Hyväluoma, J. (2023). Effects of organic carbon and clay contents on structure-related properties of arable soils with high clay content. *European Journal of Soil Science*, *74*, e134224. https://doi.org/10.1111/ejss.13424
Sokol, N. W., & Bradford, M. A. (2019). Microbial formation of stable soil carbon is more efficient from belowground than aboveground input. *Nature Geoscience*, *12*, 46–53. https://doi.org/10.1038/s41561-018-0258-6
Sokol, N. W., Sanderman, J., & Bradford, M. A. (2019). Pathways of mineral-associated soil organic matter formation: Integrating the role of plant carbon source, chemistry, and point of entry. *Global Change Biology*, *25*, 12–24. https://doi.org/10.1111/gcb.14482
Sousa, R., Veiga, M., Van Zyl, D., Telmer, K., Spiegel, S., & Selder, J. (2011). Policies and regulations for Brazil's artisanal gold mining sector: Analysis and recommendations. *Journal of Cleaner Production*, *19*, 742–750. https://doi.org/10.1016/j.jclepro.2010.12.001

Spokas, K. A., Novak, J. M., Stewart, C. E., Cantrell, K. B., Uchimiya, M., DuSaire, M. G., & Ro, K. S. (2011). Qualitative analysis of volatile organic compounds on biochar. *Chemosphere*, *85*, 869–882. https://doi.org/10.1016/j.chemosphere.2011.06.108

Sprovieri, F., Pirrone, N., Bencardino, M., D'Amore, F., Carbone, F., Cinnirella, S., Mannarino, V., Landis, M., Ebinghaus, R., Weigelt, A., Brunke, E.-G., Labuschagne, C., Martin, L., Munthe, J., Wängberg, I., Artaxo, P., Morais, F., Barbosa, H. de M. J., Brito, J., … Norstrom, C. (2016). Atmospheric mercury concentrations observed at ground-based monitoring sites globally distributed in the framework of the GMOS network. *Atmospheric Chemistry and Physics*, *16*(18), 11915–11935. https://doi.org/10.5194/acp-16-11915-2016.

Ssenku, J. E., Naziriwo, B., Kutesakwe, J., Mustafa, A. S., Kayeera, D., & Tebandeke, E. (2023). Mercury accumulation in food crops and phytoremediation potential of wild plants thriving in artisanal and small-scale gold mining areas in Uganda. *Pollutants*, *3*, 181–196. https://doi.org/10.3390/pollutants3020014

Stefanowicz, A. M., Kapusta, P., Zubek, S., Stanek, M., & Woch, M. W. (2020). Soil organic matter prevails over heavy metal pollution and vegetation as a factor shaping soil microbial communities at historical Zn–Pb mining sites. *Chemosphere*, *240*, 124922. https://doi.org/10.1016/j.chemosphere.2019.124922

Sun, N., Sarkar, B., Li, S., Tian, Y., Sha, L., Gao, Y., Luo, X., & Yang, X. (2024). Biochar addition increased soil carbon storage but did not exacerbate soil carbon emission in young subtropical plantation forest. *Forests*, *15*(6), 917. https://doi.org/10.3390/f15060917

Sutton, K. T., Cohen, R. A., & Vives, S. P. (2014). Evaluating relationships between mercury concentrations in air and in Spanish moss (*Tillandsia usneoides* L.). *Ecological Indicators*, *36*, 392–399. https://doi.org/10.1016/j.ecolind.2013.08.011

Syuhada, A. B., Shamshuddin, J., Fauziah, C. I., Rosenani, A. B., & Arifin, A. (2016). Biochar as soil amendment: Impact on chemical properties and corn nutrient uptake in a Podzol. *Canadian Journal of Soil Science*, *96*, 400–412. https://doi.org/10.1139/cjss-2015-0044

Tabaja, N., Amouroux, D., Chalak, L., Fourel, F., Tessier, E., Jomaa, I., El Riachy, M., & Bentaleb, I. (2023). Seasonal variation of mercury concentration of ancient olive groves of Lebanon. *Biogeosciences*, *20*, 619–633. https://doi.org/10.5194/bg-20-619-2023

Tang, L., Zhang, Y., Ma, S., Yan, C., Geng, H., Yu, G., Ji, H., & Wang, F. (2021). Potentially toxic element contaminations and lead isotopic fingerprinting in soils and sediments from a historical gold mining site. *International Journal of Environmental Research and Public Health*, *18*, 10925. https://doi.org/10.3390/ijerph182010925

Tankari Dan-Badjo, A., Ibrahim, O. Z., Guéro, Y., Morel, J. L., Feidt, C., & Echevarria, G. (2019). Impacts of artisanal gold mining on soil, water and plant contamination by trace elements at Komabangou, Western Niger. *Journal of Geochemical Exploration*, *205*, 106328. https://doi.org/10.1016/j.gexplo.2019.06.010

Taux, K., Kraus, T., & Kaifie, A. (2022). Mercury exposure and its health effects in workers in the artisanal and small-scale gold mining (ASGM) sector—A systematic review. *International Journal of Environmental Research and Public Health*, *19*, 2081. https://doi.org/10.3390/ijerph19042081

Teixeira, R. A., Fernandes, A. R., Ferreira, J. R., Vasconcelos, S. S., & de Souza Braz, A. M. (2018). Contamination and soil biological properties in the Serra Pelada mine - Amazonia, Brazil. *Revista Brasileira de Ciencia Do Solo*, *42*, e0160354. https://doi.org/10.1590/18069657rbcs20160354

Tian, H. Z., Zhu, C. Y., Gao, J. J., Cheng, K., Hao, J. M., Wang, K., Hua, S. B., Wang, Y., & Zhou, J. R. (2015). Quantitative assessment of atmospheric emissions of toxic heavy metals from anthropogenic sources in China: historical trend, spatial distribution, uncertainties, and control policies. *Atmospheric Chemistry and Physics*, *15*, 10127–10147. https://doi.org/10.5194/acp-15-10127-2015

Tibane, L. V., & Mamba, D. (2022). Ecological risk of trace metals in soil from gold mining region in South Africa. *Journal of Hazardous Materials Advances*, *7*, 100118. https://doi.org/10.1016/j.hazadv.2022.100118

Timsina, S., Hardy, N. G., Woodbury, D. J., Ashton, M. S., Cook-Patton, S. C., Pasternack, R., & Martin, M. P. (2022). Tropical surface gold mining: A review of ecological impacts and restoration strategies. *Land Degradation and Development*, *33*, 3661–3674. https://doi.org/10.1002/ldr.4430

Tomiyasu, T., Baransano, C., Hamada, Y. K., Kodamatani, H., Kanzaki, R., Hidayati, N., & Rahajoe, J. S. (2020). Distribution of total and organic mercury in soils around an artisanal and small-scale gold mining area in West Java, Indonesia. *SN Applied Sciences*, *2*, 1213. https://doi.org/10.1007/s42452-020-3008-5

Toy, T. J., & Griffith, J. J. (2001). Changing surface-mine reclamation practices in Minas Gerais, Brazil. *International Journal of Surface Mining, Reclamation and Environment*, *15*(1), 33–51. https://doi.org/10.1076/ijsm.15.1.33.3425

Tsui, M. T. K., Finlay, J. C., & Nater, E. A. (2008). Effects of stream water chemistry and tree species on release and methylation of mercury during litter decomposition. *Environmental Science and Technology*, *42*, 8692–8697. https://doi.org/10.1021/es800956q

Tume, P., Roca, N., Rubio, R., King, R., & Bech, J. (2018). An assessment of the potentially hazardous element contamination in urban soils of Arica, Chile. *Journal of Geochemical Exploration*, *184*, 345–357. https://doi.org/10.1016/j.gexplo.2016.09.011

UN Environment. (2019). *Global mercury assessment 2018*.

UNCCD. (2018). *Preliminary analysis – strategic objective 1: To improve the condition of affected ecosystems, combat desertification/land degradation, promote sustainable land management and contribute to land degradation neutrality*. https://www.unccd.int/official-documents/cric-17-georgetown-guyana-2019

UNEP. (2013). *Minamata convention on mercury – text and annexes*.

UNIDO, & Green Industry. (2011). *UNIDO green industry initiative for sustainable industrial development*.

US EPA. (2000). *Draft implementation framework for the use of equilibrium partitioning sediment guidelines: Guidance for using equilibrium partitioning sediment guidelines (ESGs) in water quality programs*.

US EPA. (2002). *Supplemental guidance for developing soil screening levels for superfund sites*.

van Straaten, P. (2000). Mercury contamination associated with small-scale gold mining in Tanzania and Zimbabwe. *The Science of the Total Environment*, *259*, 105–113.

https://doi.org/10.1016/s0048-9697(00)00553-2
Vardè, M., Barbante, C., Barbaro, E., Becherini, F., Bonasoni, P., Busetto, M., Calzolari, F., Cozzi, G., Cristofanelli, P., Dallo, F., De Blasi, F., Feltracco, M., Gabrieli, J., Gambaro, A., Maffezzoli, N., Morabito, E., Putero, D., Spolaor, A., & Cairns, W. R. L. (2022). Characterization of atmospheric total gaseous mercury at a remote high-elevation site (Col Margherita Observatory, 2543 m a.s.l.) in the Italian Alps. *Atmospheric Environment*, *271*, 118917. https://doi.org/10.1016/j.atmosenv.2021.118917
Vaselli, O., Higueras, P., Nisi, B., María Esbrí, J., Cabassi, J., Martínez-Coronado, A., Tassi, F., & Rappuoli, D. (2013). Distribution of gaseous Hg in the mercury mining district of Mt. Amiata (central Italy): A geochemical survey prior the reclamation project. *Environmental Research*, *125*, 179–187. https://doi.org/10.1016/j.envres.2012.12.010
Veiga, M. M., Tarra A, J. A., Restrepo-Baena, O. J., & De Tomi, G. (2022). Coexistence of artisanal gold mining with companies in Latin America. *The Extractive Industries and Society*, *12*, 101177. https://doi.org/10.1016/j.exis.2022.101177
Velásquez-López, P. C., Veiga, M. M., & Hall, K. (2010). Mercury balance in amalgamation in artisanal and small-scale gold mining: Identifying strategies for reducing environmental pollution in Portovelo-Zaruma, Ecuador. *Journal of Cleaner Production*, *18*, 226–232. https://doi.org/10.1016/j.jclepro.2009.10.010
Velásquez Ramírez, M. G., Vega Ruiz, C. M., Gomringer, R. C., Pillaca, M., Thomas, E., Stewart, P. M., Gamarra Miranda, L. A., Dañobeytia, F. R., Guerrero Barrantes, J. A., Gushiken, M. C., Bardales, J. V., Silman, M., Fernandez, L., Ascorra, C., & Torres, D. del C. (2021). Mercury in soils impacted by alluvial gold mining in the Peruvian Amazon. *Journal of Environmental Management*, *288*, 112364. https://doi.org/10.1016/j.jenvman.2021.112364
Veroniki, A. A., Jackson, D., Viechtbauer, W., Bender, R., Bowden, J., Knapp, G., Kuss, O., Higgins, J. P., Langan, D., & Salanti, G. (2016). Methods to estimate the between-study variance and its uncertainty in meta-analysis. *Research Synthesis Methods*, *7*, 55–79. https://doi.org/10.1002/jrsm.1164
Vijayanathan, J., Yahya, A. Z., Yaacob, A., Kassim, A. S., & Chik, S. W. (2011). Impact of thinning of Acacia mangium plantation on soil chemical properties. *Malaysian Journal of Soil Science*, *15*, 75–85.
Walter, M., & Wagner, L. (2021). Mining struggles in Argentina. The keys of a successful story of mobilisation. *Extractive Industries and Society*, *8*, 100940. https://doi.org/10.1016/j.exis.2021.100940
Wang, J., Xie, Q., Xiang, Y., Xue, J., Jiang, T., Zhang, C., Li, J., Wang, Y., & Wang, D. (2024). Anthropogenic activities enhance mercury methylation in sediments of a multifunctional lake: Evidence from dissolved organic matter and mercury-methylating microorganisms. *Journal of Hazardous Materials*, *466*, 133505. https://doi.org/10.1016/j.jhazmat.2024.133505
Wang, P., Sun, Z., Hu, Y., & Cheng, H. (2019). Leaching of heavy metals from abandoned mine tailings brought by precipitation and the associated environmental impact. *Science of the Total Environment*, *695*, 133893. https://doi.org/10.1016/j.scitotenv.2019.133893
Wang, X., Yuan, W., Lu, Z., Lin, C. J., Yin, R., Li, F., & Feng, X. (2019). Effects of

precipitation on mercury accumulation on subtropical montane forest floor: Implications on climate forcing. *Journal of Geophysical Research: Biogeosciences*, *124*, 959–972. https://doi.org/10.1029/2018JG004809

Wang, Yechun, Ao, L., Lei, B., & Zhang, S. (2015). Assessment of heavy metal contamination from sediment and soil in the riparian zone China's Three Gorges Reservoir. *Polish Journal of Environmental Studies*, *24*(5), 2253–2259. https://doi.org/10.15244/pjoes/44473

Wang, Yongjie, Shi, G., Wang, D., Zhao, Q., Jiang, S., Li, Y., Wang, D., Li, C., Chen, Z., & Bargagli, R. (2023). Relationships between concentrations of mercury and organic carbon in soils allow the identification of Antarctic ice-free areas with enhanced deposition of the metal. *Catena*, *220*, 106718. https://doi.org/10.1016/j.catena.2022.106718

Watmough, S. A., Whitfield, C. J., & Baker, S. (2019). An assessment of traditional chemical indicators of atmospheric pollution in northern Saskatchewan forest soils. *Soil Science Society of America Journal*, *83*, 49–58. https://doi.org/10.2136/sssaj2018.07.0281

Watmough, S., Gilbert-Parkes, S., Basiliko, N., Lamit, L. J., Lilleskov, E. A., Andersen, R., del Aguila-Pasquel, J., Artz, R. E., Benscoter, B. W., Borken, W., Bragazza, L., Brandt, S. M., Bräuer, S. L., Carson, M. A., Chen, X., Chimner, R. A., Clarkson, B. R., Cobb, A. R., Enriquez, A. S., … Zahn, G. (2022). Variation in carbon and nitrogen concentrations among peatland categories at the global scale. *PLoS ONE*, *17*(11), e0275149. https://doi.org/10.1371/journal.pone.0275149

Weleabzgi, B., Alemayehu, T., & Estifanos, S. (2021). Assessing the environmental impact of artisanal gold mining activities on the waters and sediments around Meli, Northwestern Tigray, Ethiopia. *Momona Ethiopian Journal of Science*, *13*(2), 281–299. https://doi.org/10.4314/mejs.v13i2.6

Whyte, D., Simpson, L., & Osborne, C. (2024). Response of lettuce (*Lactuca sativa* L .) inoculated with Rhizophagus irregularis to charcoal amended tabela sand. *Journal of Academic Research and Essays*.

Wijitkosum, S. (2021). Factor influencing land degradation sensitivity and desertification in a drought prone watershed in Thailand. *International Soil and Water Conservation Research*, *9*, 217–228. https://doi.org/10.1016/j.iswcr.2020.10.005

Wongsasuluk, P., Tun, A. Z., Chotpantarat, S., & Siriwong, W. (2021). Related health risk assessment of exposure to arsenic and some heavy metals in gold mines in Banmauk Township, Myanmar. *Scientific Reports*, *11*, 22843. https://doi.org/10.1038/s41598-021-02171-9

Wu, M., Luo, Q., Liu, S., Zhao, Y., Long, Y., & Pan, Y. (2018). Screening ornamental plants to identify potential Cd hyperaccumulators for bioremediation. *Ecotoxicology and Environmental Safety*, *162*, 35–41. https://doi.org/10.1016/j.ecoenv.2018.06.049

Xiao, R., Wang, S., Li, R., Wang, J. J., & Zhang, Z. (2017). Soil heavy metal contamination and health risks associated with artisanal gold mining in Tongguan, Shaanxi, China. *Ecotoxicology and Environmental Safety*, *141*, 17–24. https://doi.org/10.1016/j.ecoenv.2017.03.002

Xu, D., Shen, Z., Dou, C., Dou, Z., Li, Y., Gao, Y., & Sun, Q. (2022). Effects of soil properties on heavy metal bioavailability and accumulation in crop grains under different farmland use patterns. *Scientific Reports*, *12*, 9211.

https://doi.org/10.1038/s41598-022-13140-1
Xu, Y., Wu, Y., Han, J., & Li, P. (2017). The current status of heavy metal in lake sediments from China: Pollution and ecological risk assessment. *Ecology and Evolution*, *7*, 5454–5466. https://doi.org/10.1002/ece3.3124
Xue, W., Kwon, S. Y., Grasby, S. E., Sunderland, E. M., Pan, X., Sun, R., Zhou, T., Yan, H., & Yin, R. (2019). Anthropogenic influences on mercury in Chinese soil and sediment revealed by relationships with total organic carbon. *Environmental Pollution*, *255*, 113186. https://doi.org/10.1016/j.envpol.2019.113186
Yan, J., Wang, C., Wang, Z., Yang, S., & Li, P. (2019). Mercury concentration and speciation in mine wastes in Tongren mercury mining area, southwest China and environmental effects. *Applied Geochemistry*, *106*, 112–119. https://doi.org/10.1016/j.apgeochem.2019.05.008
Yang, Yang, Yanai, R. D., Driscoll, C. T., Montesdeoca, M., & Smith, K. T. (2018). Concentrations and content of mercury in bark, wood, and leaves in hardwoods and conifers in four forested sites in the northeastern USA. *PLoS ONE*, *13*(4), e0196293. https://doi.org/10.1371/journal.pone.0196293
Yang, Yong-kui, Zhang, C., Shi, X., Lin, T., & Wang, D. (2007). Effect of organic matter and pH on mercury release from soils. *Journal of Environmental Sciences*, *19*, 1349–1354. https://doi.org/10.1016/S1001-0742(07)60220-4
Yao, Q., Wang, X., Jian, H., Chen, H., & Yu, Z. (2015). Characterization of the particle size fraction associated with heavy metals in suspended sediments of the yellow river. *International Journal of Environmental Research and Public Health*, *12*(6), 6725–6744. https://doi.org/10.3390/ijerph120606725
Yu, X., Driscoll, C. T., Warby, R. A. F., Montesdeoca, M., & Johnson, C. E. (2014). Soil mercury and its response to atmospheric mercury deposition across the northeastern United States. *Ecological Applications*, *24*(4), 812–822. https://doi.org/10.1890/13-0212.1
Yuan, W., Wang, X., Lin, C.-J., Wu, C., Zhang, L., Wang, B., Sommar, J., Lu, Z., & Feng, X. (2020). Stable mercury isotope transition during postdepositional decomposition of biomass in a forest ecosystem over five centuries. *Environmental Science & Technology*, *54*(14), 8739–8749. https://doi.org/10.1021/acs.est.0c00950
Zapata, J. V., Fajardo, D., & Cabrera, M. A. (2017). Colombia. In E. R. La Flèche (Ed.), *The mining law review* (6th ed., pp. 60–70). Law Business Research Ltd. www.TheLawReviews.co.uk
Zar, J. H. (2010). *Biostatistical analysis* (5th ed.). Pearson Prentice Hall: Upper Saddle River.
Zhang, A., Bian, R., Pan, G., Cui, L., Hussain, Q., Li, L., Zheng, J., Zheng, J., Zhang, X., Han, X., & Yu, X. (2012). Effects of biochar amendment on soil quality, crop yield and greenhouse gas emission in a Chinese rice paddy: A field study of 2 consecutive rice growing cycles. *Field Crops Research*, *127*, 153–160. https://doi.org/10.1016/j.fcr.2011.11.020
Zhao, D., Chen, Y., Zhang, W., Chen, X., Chen, X., & Zhang, F. (2021). Concentration, spatial distribution and potential ecological risk of heavy metals in stream sediments of the misiones province, Argentina. *Minerals*, *11*, 1112. https://doi.org/10.3390/min11101112
Zhao, Z., & Xing, Z. (2024). Gold mining, corporate business management, and green

growth in Asia. *Resources Policy*, *89*, 104677. https://doi.org/10.1016/j.resourpol.2024.104677

Zheng, Y., Luo, X., Zhang, W., Wu, X., Zhang, J., & Han, F. (2016). Transport mechanisms of soil-bound mercury in the erosion process during rainfall-runoff events. *Environmental Pollution*, *215*, 10–17. https://doi.org/10.1016/j.envpol.2016.04.101

Zhou, J., Wang, Z., & Zhang, X. (2018). Deposition and fate of mercury in litterfall, litter, and soil in coniferous and broad-leaved forests. *Journal of Geophysical Research: Biogeosciences*, *123*, 2590–2603. https://doi.org/10.1029/2018JG004415

Zhou, X., Chen, Q., Liu, C., & Fang, Y. (2017). Using moss to assess airborne heavy metal pollution in Taizhou, China. *International Journal of Environmental Research and Public Health*, *14*, 430. https://doi.org/10.3390/ijerph14040430

Appendix

Table S2. 1. Literature search according to environmental media across South America for the period 2008 to 2023.

Study	Country	Soil	Sediment
López-Blanco et al. (2015)	Ecuador	√	
Guédron et al. (2018)	French Guiana	√	
Calabró et al. (2022)	Argentina	√	
Tume et al. (2018)	Chile	√	
Leiva G. & Morales (2013)	Chile	√	
Santos-Francés et al. (2017)	Peru	√	
Velásquez Ramírez et al. (2021)	Peru	√	
Marrugo-Negrete et al. (2021)	Colombia	√	
Carranza-Lopez et al. (2019)	Colombia	√	
Kroonenberg et al. (2022)	Suriname	√	
Pavilonis et al. (2017)	Bolivia	√	
Acosta et al. (2011)	Bolivia	√	√
Dias et al. (2022)	Brazil	√	
Covre et al. (2022)	Brazil	√	√
Teixeira et al. (2018)	Brazil	√	√
Miserendino et al. (2018)	Brazil	√	√
Osborne and Watmough (unpublished, 2023)	Guyana	√	√
Santos-Francés et al. (2011)	Venezuela	√	√

Study	Country	Soil	Sediment
Carling et al. (2013)	Ecuador		√
González-Merizalde et al. (2016)	Ecuador		√
Palacios-Torres et al. (2020)	Colombia		√
Marrugo-Negrete et al. (2021)	Colombia		√
Pinedo-Hernández et al. (2015)	Colombia		√
Moreno-Brush et al. (2020)	Peru		√
Beal et al. (2013)	Peru		√
da Penha Rhodes et al. (2018)	Brazil		√
Mendes et al. (2016)	Brazil		√
Mulholland et al. (2012)	Brazil		√
Zhao et al. (2021)	Argentina		√
Aguilar et al. (2021)	Chile		√
Oyarzún et al. (2012)	Chile		√
Laperche et al. (2014)	French Guiana		√
Hellal et al. (2020)	French Guiana		√
Howard et al. (2011)	Guyana		√

Table S2. 2. Primary policy instruments for the regulation of artisanal gold mines across South America.

Country	Policy instrument	Purpose	Source
Argentina	*Glaciers Law*	Catalogues and protects glaciers from mining activities.	Walter & Wagner (2021)
	Native Forest Law	Halt deforestation and displacement of peasant and indigenous communities.	
	National Mining Code	Outline the rules for mining through exploration and development.	Dentons (2022)
	General Environmental Law No. 25,675	Protection of the environment.	
Bolivia	*Law No 535: Mining and Metallurgy Law*	Framework regulation for mining activities in terms of mining rights and mining in a responsible, planned, and sustainable manner.	(*Law No. 535: Mining and Metallurgy Law*, 2014)
Brazil	*National Environmental Protection Act*	Foundation of a strict liability standard for environmental damages.	Sousa et al. (2011)

Country	Policy instrument	Purpose	Source
	Mining Code	Utilization of mineral resources, definition of mineral and mine research, rights of miners and landowners, priority rights and areas available for mining.	
	Law 7.805, Resolution no. 178	Regulates artisanal and small-scale gold mining through a permit system.	
	Law 11.685, Decree 97.632	Artisanal miners are required to reclaim areas degraded.	
	Decree no. 97.634, Resolution IBAMA no.32	Controls the production, importation, and commercialization of metallic mercury.	
	Decree no. 97.507	Prohibits the use of mercury and cyanide in garimpos unless it is permitted by the legal authority.	
	Resolution IBAMA no. 435	Determines the use of retorts when mercury is authorized	

Country	Policy instrument	Purpose	Source
		to be used for gold amalgamation and requires that the minimum efficiency of 96% (mercury recovery) is achieved.	
Chile	*Mining Code, Mining Safety Regulation*	Granting mining concessions for exploration and exploitation. Regulation of mining safety related issues.	
	General Environmental Framework Law	Regulates environmental matters and responsibilities.	Bertrand-Galindo et al. (2022)
	Law No. 20,551 and its Regulation	Regulate the closure of mining operations, installations, and remediation.	
Colombia	*Mining Code*	Regulate the legal relationships between the state and individuals at all stages of mining (exploration, construction and assembly, exploitation,	Zapata et al. (2017)

Country	Policy instrument	Purpose	Source
		processing, transport, and marketing of minerals in the soil or subsoil).	
	Environmental Law	Regulates the issuance of environmental authorization in the form of an environmental licence.	
Ecuador	*Mining Law*	Regulates mining activities through the exploration and exploitation phase.	
	Mining Activities Health and Safety Regulation	Ensure the safety and health at work in all phases of the mining activity and includes the general guidelines to prevent the labour risks under the mining special regimes	Calisto (2019)
	Mining Activities Environmental Regulation	Establishes the requirements and procedures for the application of the environmental permits.	

Country	Policy instrument	Purpose	Source
Guyana	*Mining Act*	Make provisions with respect to prospecting for and mining of metals, minerals, and precious stones and regulating their conveyance.	*Mining Act* (1989)
	Environmental Protection (Amendment) Act	Provide for the management, conservation, protection and improvement of the environment and sustainable use of natural resources.	*Environmental Protection (Amendment) Act* (2005)
	Mining (Amendment) Regulation	Outlines code of practice for use of mercury, mine effluents, tailings management, waste management and disposal, and mine reclamation and closure to provide environmental management guidance and promote related best management practices.	*Mining (Amendment) Regulation* (2005)

Country	Policy instrument	Purpose	Source
	Occupational Health and Safety Act	Provide for the registration and regulation of industrial establishments, for occupational safety and health of persons at work.	*Occupational Safety and Health Act* (1997)
French Guiana	*Mining Code*	Establishes the size and the duration of the mining permit depending on the phase of mining.	Scammacca et al. (2021)
	Departmental Mining Plan	Stipulates where mining can and cannot take place.	
Peru	*General Mining Law*	Dictates mining activities at the level of search, prospection, commercialization, exploration, exploitation, beneficiation, mining transportation and general work.	Palomino (2019)
	Organic Law for Sustainable Development of Natural Resources	Dictates sustainable development of mining activities.	

Country	Policy instrument	Purpose	Source
	Law No. 28090	Regulates mine closure.	
	Law No. 28611	Regulates the protection of the general environment.	
	Law No. 27446	National environmental impact evaluation system.	
	Law No. 29785	Right to prior consultation of indigenous or native peoples.	
	Supreme Decree No. 042-2017-EM	Environmental regulations for activities of mining exploration.	
	Supreme Decree No. 024-2016-EM	Prevent incidents, occupational diseases and occupational accidents in mining activities.	
Suriname	*Mining Decree*	Stipulates good practices in mining, health and safety of workers, protection of ecosystems, and local content.	Government of Suriname (2023)
	Decree Negative List	Special license for importation of elemental mercury.	

Country	Policy instrument	Purpose	Source
Venezuela	*Environmental Framework Act*	Determine what substances are considered contaminants and permissible concentrations and establish norms for production or release of contaminants into the environment.	Fong-Sam (2022)
	Safety Law, Labour Inspection Decree, Occupational Accidents Regulation	Protecting the safety and health of mine workers.	
	Decree of Rank, Value and Force of the Organic Law	Grant right to explore for and mine strategic minerals.	
	Tax Regime for the Development of the Orinoco Mining Region	Diversify the economy of the region by allowing mining activities, while ensuring environmental and indigenous communities protection.	

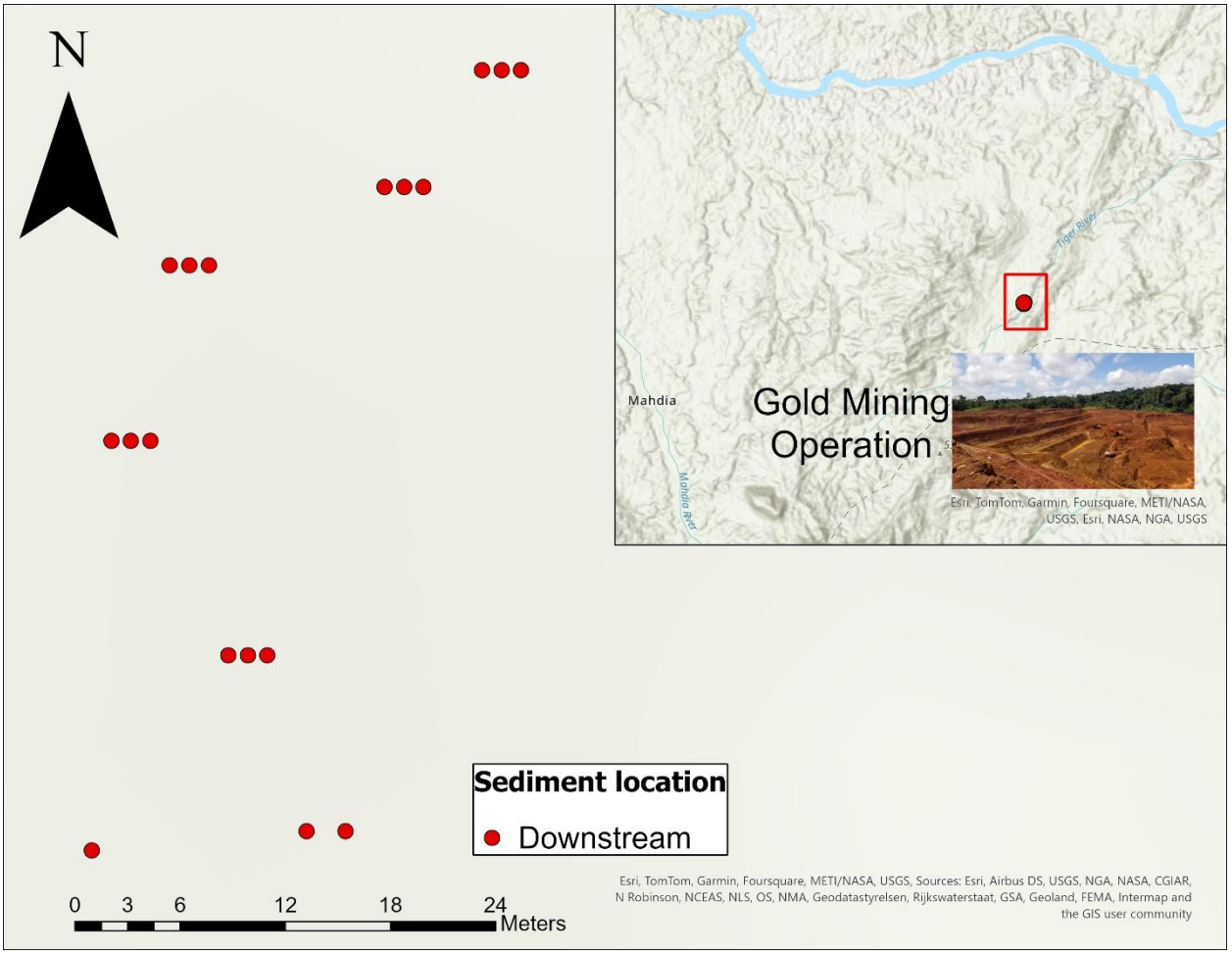

Figure S3. 1. Spatial distribution of sediment downstream of sampled gold mine in Mahdia.

Table S4. 1. Summary of mean (± SE) and range metal concentrations (mg kg^{-1}) in moss at Mahdia. Different letters indicate statistically significant differences ($p < 0.05$) using Dunn's test between sample zones.

Metal	Distant		Adjacent		Mining Operation	
	Mean ± SE	Range	Mean ± SE	Range	Mean ± SE	Range
			Mahdia (n = 24)			
As	-	-	-	-	-	-
Cd	-	-	-	-	-	-
Co	0.19^{a} ± 0.02	0.16 – 0.24	0.21^{a} ± 0.01	0.19 – 0.24	0.25^{a} ± 0.02	0.16 – 0.40
Cu	11.02^{a} ± 0.48	9.51 – 12.48	11.56^{a} ± 1.49	8.55 – 17.12	9.57^{a} ± 0.63	6.43 – 14.03
Mn	70.08^{a} ± 3.20	59.76 – 76.80	69.43^{a} ± 6.03	52.00 – 79.71	70.48^{a} ± 4.65	38.23 – 104.01
Ni	2.15^{a} ± 0.16	1.80 – 2.70	6.73^{a} ± 4.82	1.60 – 26.01	2.19^{a} ± 0.22	1.50 – 4.89
Pb	4.00^{a} ± 0.29	3.28 – 4.85	4.70^{a} ± 1.12	3.18 – 9.10	4.75^{a} ± 0.62	2.41 – 9.00
Zn	61.42^{a} ± 4.68	51.87 – 77.41	56.63^{a} ± 4.38	48.55 – 67.43	85.45^{a} ± 13.54	42.44 – 196.48

SE = standard error, - not detected

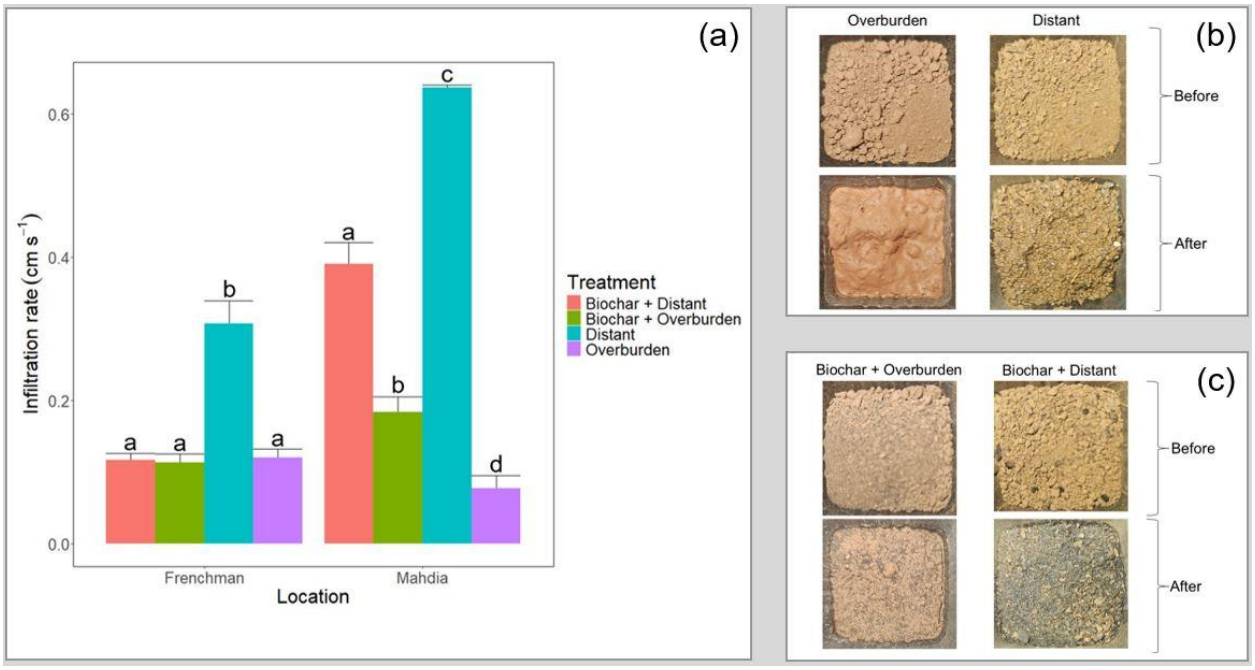

Figure S6. 1. Soil physical properties based on (a) infiltration rate in treated and untreated soil and appearance before and after water application in (b) untreated and (c) treated soil.